Microbial Degradation of RDX and HMX

SERDP Project CU1213

Performing Organizations

Biotechnology Research Institute, National Research Council of Canada,

6100 Royalmount Ave., Montreal (Quebec) H4P 2R2, Canada.

Defense Research and Development Canada, Valcartier (Quebec) G3J 1X5, Canada

US Air Force Research Laboratory, 139 Barnes Dr, Tyndall AFB, Fl 32403

Final Report

(December 2001 - December 2003)

Submitted to

Andrea Leeson,

901 North Stuart St., Suite 303

Arlington, Virginia, 22203

February 2004

Report Documentation Page

Form Approved
OMB No. 0704-0188

1. REPORT DATE	2. REPORT TYPE	3. DATES COVERED
FEB 2004		**00-00-2004 to 00-00-2004**

4. TITLE AND SUBTITLE	5a. CONTRACT NUMBER
Microbial Degradation of RDX and HMX	5b. GRANT NUMBER
	5c. PROGRAM ELEMENT NUMBER
6. AUTHOR(S)	5d. PROJECT NUMBER
	5e. TASK NUMBER
	5f. WORK UNIT NUMBER
7. PERFORMING ORGANIZATION NAME(S) AND ADDRESS(ES) **US Air Force Research Laboratory,139 Barnes Dr,Tyndall AFB,FL,32403**	8. PERFORMING ORGANIZATION REPORT NUMBER
9. SPONSORING/MONITORING AGENCY NAME(S) AND ADDRESS(ES)	10. SPONSOR/MONITOR'S ACRONYM(S)
	11. SPONSOR/MONITOR'S REPORT NUMBER(S)

12. DISTRIBUTION/AVAILABILITY STATEMENT
Approved for public release; distribution unlimited

13. SUPPLEMENTARY NOTES

14. ABSTRACT

15. SUBJECT TERMS

16. SECURITY CLASSIFICATION OF:			17. LIMITATION OF ABSTRACT	18. NUMBER OF PAGES	19a. NAME OF RESPONSIBLE PERSON
a. REPORT	b. ABSTRACT	c. THIS PAGE			
unclassified	**unclassified**	**unclassified**	**Same as Report (SAR)**	**221**	

Project Participants

BRI, Canada:

Jalal Hawari, Ph.D. Chemistry, *PI*

Jian-Shen Zhao, Ph.D. Microbiology

Bharat Bhushan, Ph.D. Biochemistry

Vimal Balakrishnan, Ph.D. Chemistry

Diane Fournier, Ph.D. Microbiology

Annamaria Halasz, M.Sc. Analytical Chemistry

Carl Groom, M.Sc. Eng. Chemical Engineering

Tara Hooper, B.Sc. Biochemistry

Louise Paquet, B.Sc. Chemistry

AFRL, USA:

Jim Spain, Ph.D. Biochemistry, *Co-PI*

Sandra Trott, Ph.D. Microbiology

DRDC, Canada

Guy Ampleman, Ph.D. Chemistry

Sonia Thiboutot, Ph.D. Chemistry

TABLE OF CONTENTS

Project Overview

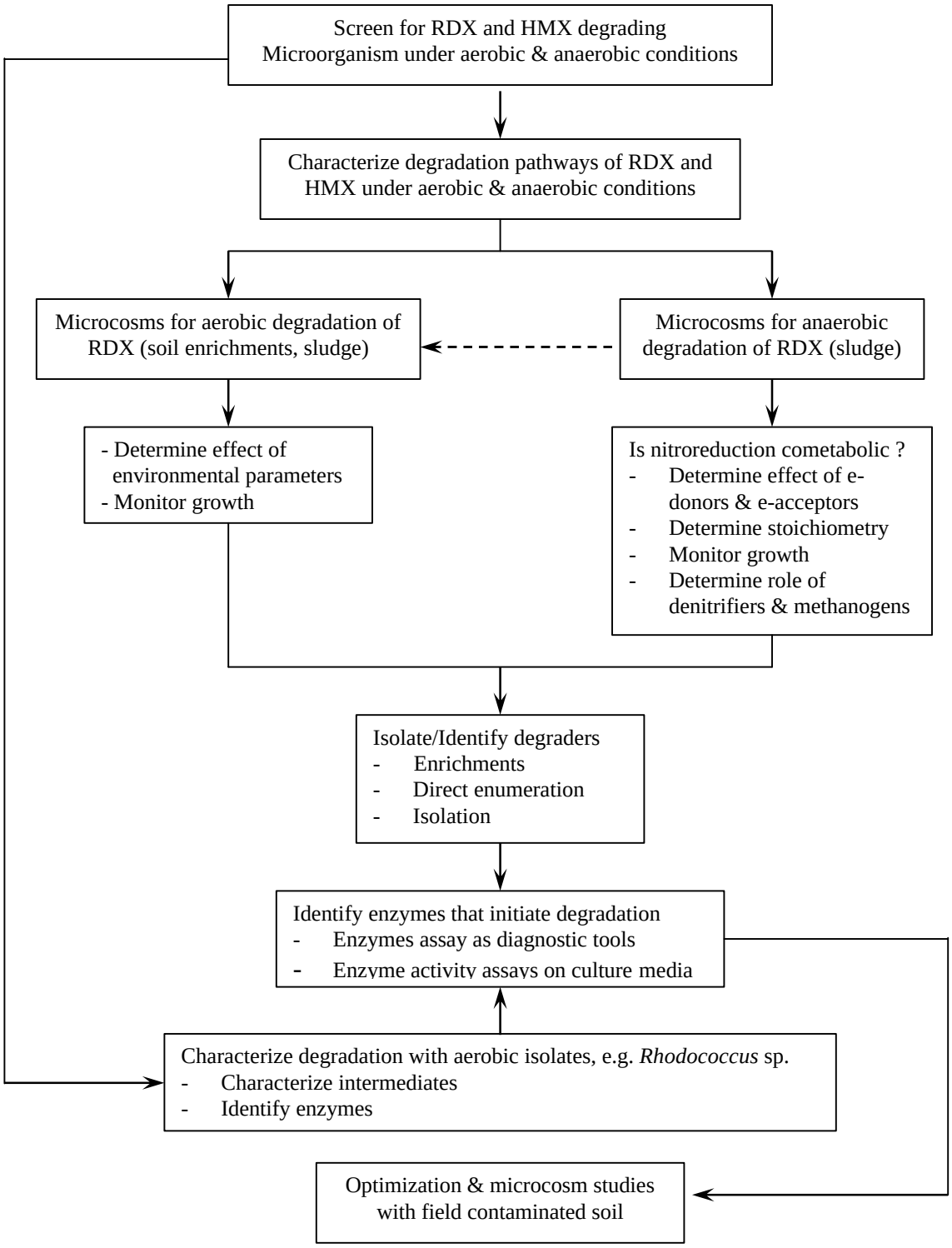

I PROJECT BACKGROUND

The present SERDP funded project (CU1213) responds directly to the original SERDP statement of need (CUSON-01-05) to address the cleanup of the two powerful and widely used explosives hexahydro-1,3,5-trinitro-1,3,5-triazine (RDX) and octahydro-1,3,5,7-tetranitro-1,3,5,7-tetrazocine (HMX). Both of these cyclic nitramine explosives are used extensively by the military and they are released to the environment during manufacturing, testing and training, demilitarization and open burning/open detonation (OB/OD). Such activities lead to the contamination of surface and subsurface soil. Also, because of their solubility (50 mg/L and 5 mg/L for RDX and HMX at 25 °C, respectively) in water and their weak binding affinity for soil, both RDX and HMX migrate through subsurface soil and cause groundwater contamination. One of the most recent examples is the well-publicized contamination of the aquifer at the Massachusetts Military Reservation on Cape Cod.

Cyclic nitramine explosives are toxic to aquatic organisms (Sunahara et al., 1999; Talmage et al., 1999), earthworms (Robidoux et al., 2000, 2001), mammals (Talmage et al., 1999) and human monocytes (Bruns-Nagel et al., 1999), and above all, they are also carcinogenic. The toxicity of cyclic nitramines necessitates that contaminated soil and groundwater be remediated using cost effective and environmentally safe processes such as bioremediation. Incineration is not a desirable remediation option because of high costs and hazardous emissions. Several studies reported biodegradation of RDX and HMX under both anaerobic and aerobic conditions using anaerobic sludge (McCormick et al., 1981), consortia (Funk et al., 1993), or specific isolates (Kitts et al., 1994; Binks et al., 1995**;** Young et al., 1997a; Coleman et al., 1998; and Boopathy et al., 1998). Despite these early efforts, there is little existing information regarding ring cleavage products and the enzymes that lead to their formation. Until recently, the only reported pathway for the degradation of RDX was that of McCormick et al. (1981) who postulated a pathway based on the sequential reduction of RDX to hexahydro-1-nitroso-3,5-dinitro-1,3,5-triazine (MNX), hexahydro-1,3-dinitroso-5-nitro-1,3,5-triazine (DNX), and hexahydro-1,3,5-trinitroso-1,3,5-triazine (TNX), followed by ring cleavage to produce formaldehyde (HCHO), methanol (MeOH) and the undesirable

compounds hydrazine (NH_2NH_2) and dimethylhydrazine (Me_2NNH_2).

More recent work in our laboratory demonstrated that initial enzymatic attack by anaerobic bacteria (from a municipal sludge) leads to complete destruction of the two cyclic nitramines (Hawari, 2000). Again, the details of the initial reactions are unknown and therefore cannot be predicted or enhanced. Therefore, we proposed to SERDP a research plan to biodegrade both RDX and HMX under aerobic and anaerobic conditions using domestic sludge and soil isolates. In our proposal, we worked out a research plan to screen microorganisms, to identify degradation products and to determine the kinetics and stoichiometry of their formation, and finally to identify initial microbial (enzymatic) processes leading to decomposition.

Our hypothesis is based on the understanding that RDX and HMX lack the aromatic stability enjoyed by TNT (Figure 1), and as soon as either compound is subjected to an initial chemical attack (thermal cleavage of a N-NO_2 or a C-H bond), the molecule is destabilized (inner C-N bonds are < 2 kcal/mol) (Melius, 1990; Hawari, 2000) and completely decomposes to give HCHO, N_2O, NH_3 and CO_2. Therefore, a successful initial enzymatic attack on its nitro (-NO_2) and methylene (-CH_2-) group(s) might destabilize the molecule and lead to ring cleavage and spontaneous decomposition, as demonstrated during its photochemical degradation (Peyton et al., 1999), alkaline hydrolysis (Hoffsommer et al., 1977) and thermal decomposition (Melius, 1990).

In an earlier study we found that biodegradation of RDX in cultures from municipal anaerobic sludge yielded MNX and traces of DNX, resulting from the reduction of the –NO_2 group(s), a well as several ring cleavage metabolites that were tentatively identified as methylenedinitramine ($(O_2NNH)_2CH_2$) and bis(hydroxymethyl)nitramine ($(HOCH_2)_2NNO_2$). None of the above metabolites seemed to accumulate in the system and they disappeared to eventually produce HCHO, NH_3, N_2O and CO_2 (Hawari et al., 2000a).

The formation of RDX-nitroso compounds under anaerobic conditions has been recently reported by Adrian and Chow (2001) and Beller (2002). Once again, no details on the occurrence of a ring cleavage were reported in either study, although Beller (2002) reported negligible amounts (< 2 %) of RDX mineralization ($^{14}CO_2$). Subsequent work conducted by Oh et al. (2001) confirmed our earlier observation (Hawari et al., 2000a) of the formation of

RDX-nitroso metabolites in addition to the ring cleavage products methylenedinitramine, HCHO, CO_2, and N_2O during degradation of the energetic chemical with anaerobic sludge in the presence of Fe(0).

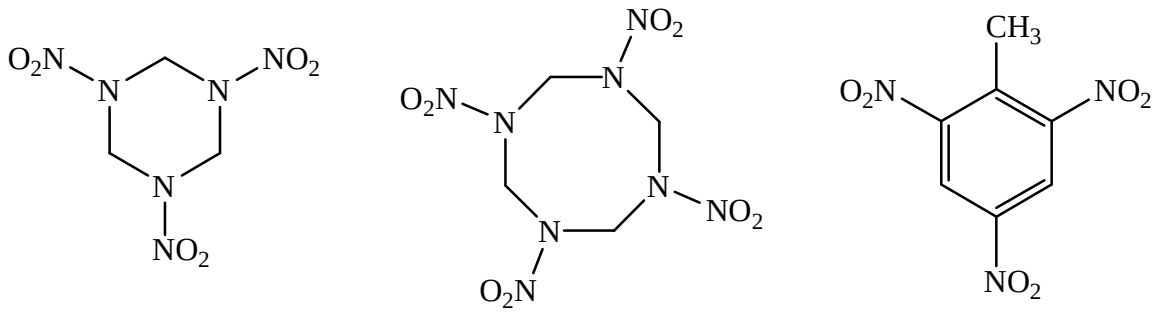

RDX **HMX** **TNT**

Figure 1. Structures of the cyclic nitramine explosives RDX and HMX, and the aromatic explosive TNT.

To gain further insight into the microbial and enzymatic processes and degradation products involved in the biodegradation of RDX and HMX we designed a work plan comprising a multidisciplinary expertise of microbiology, biochemistry and analytical chemistry as shown in the enclosed Project Overview (page 5). The proposed research is intended to provide SERDP with the fundamental knowledge of the microbial processes and enzymes that initiate the attack on the two explosives. Once these mechanisms are understood, it will be possible to use the acquired knowledge to enhance the bioremediation process and to develop strategies for scale up and future field applications.

II GLOBAL OBJECTIVES

The primary objective of the proposed research is to determine the enzymatic and microbial processes involved in the initial attack on RDX and HMX that lead to their rapid autodecomposition. The mechanism leading to mineralization is unknown, however we have several hypotheses based on our belief that any successful initial attack on these molecules would lead to ring cleavage and spontaneous decomposition in water (Hawari, 2000). First we designed experiments to identify the degradation products, particularly early intermediates, and to determine the kinetics and mechanisms of their formation. Second, similar experiments were designed to determine the types of enzymes and microorganisms that initiate the degradation of RDX and HMX in liquid culture media. Subsequently, experiments were conducted to determine how these biochemical processes function in natural and representative model soil systems. This information will provide insight to enhance bioremediation of both cyclic nitramines and to scale up the developed processes for future field applications.

With the discovery of the two intermediates $O_2NNHCH_2NHNO_2$ (MEDINA) and O_2NNHCH_2NHCHO (4-NDAB) we conducted experiments to understand the role of bacterial isolates and the initial enzymatic steps involved in the degradation process. Therefore we designed experiments to isolate and characterize specific degraders from the sludge and from soils and to determine their degradation potential for the above energetic chemicals. Parallel experiments were also conducted to determine the initial enzymatic steps involved in the degradation process. Finally, alternative methods including photolysis and hydrolysis were applied to degrade RDX and HMX in an attempt to generate sufficient amounts of other suspected enzymatic intermediates, that might have escaped detection during biodegradation, particularly early products. Intermediates of particular interest are those expected to be formed following initial denitration of RDX and HMX. Our hypothesis is based on the understanding that initial denitration of the two cyclic nitramines in water, chemically or enzymatically, will produce the same initial intermediate whose subsequent decomposition will lead to similar product distributions.

III SUMMARY OF ACCOMPLISHMENTS

We successfully characterized and identified bacteria from domestic sludge (anaerobic) and soil (aerobic) that can effectively degrade RDX and HMX. Several strains of anaerobic bacteria (*Clostridium, Klebsiella* and *Biofermentants*) were isolated from the sludge and employed to degrade RDX and HMX. We obtained closely related product distributions (MeOH, HCHO, NO_2^-, NH_3, CO_2) with some variation in their relative yields.

Under anaerobic conditions in liquid cultures we detected, for the first time the key ring cleavage product methylenedinitramine (MEDINA) (Halasz et al., 2002) that shed insight into the initial steps (denitration followed by ring cleavage or reduction to the mononitroso derivatives prior to denitration and ring cleavage) involved in degradation of the two cyclic nitramines. Subsequently we tested several commercial enzymes (nitrate reductase and diaphorase) and obtained similar product distributions to those obtained by *Klebsiella* and *Clostridium*.

Also we obtained three aerobic Rhodococci (strain A from Canadian soil, strain 11Y from UK and strain DN22 from Australia) and found that all degraded RDX but that none were able to degrade HMX. The three strains produced the same product distribution (HCHO, CO_2, N_2O). Here we detected for the first time the ring cleavage product 4-nitro-2,4-diazabutanal, (4-NDAB) (Fournier et al., 2002), that also provided deep insight into the initial steps involved in the degradation of RDX in liquid cultures under aerobic conditions. Later cytochrome P450 was identified as the enzyme responsible for initiating denitration on RDX, which led to ring cleavage and spontaneous decomposition. We found that the aerobic dead end product NDAB could be further degraded under anaerobic conditions, or by the fungus *P. chrysosporium* (Fournier et al., 2003) or by alkaline hydrolysis (> pH 10) (Balakrishnan et al., 2003).

Interestingly, we found that denitration of RDX by photolysis, hydrolysis or electrolysis led to product distributions similar to those obtained by degradation under aerobic and anaerobic conditions. These experimental findings suggested that once a successful initial attack, preferably denitration, takes place on the two cyclic nitramines the resulting intermediates

undergo spontaneous hydrolytic decomposition in water. The main difference between the biotic and the abiotic reactions is the ultimate use of carbon (HCHO) by the microorganisms to produce CO_2.

In soil, we found that both RDX and HMX can be degraded and mineralized under anaerobic conditions. However, we found that both chemicals also undergo sequential reduction of the N-NO_2 to form the corresponding N-NO groups eventually producing trinitroso-RDX (TNX) and tetranitroso-HMX (4NO-HMX), both of which ultimately degraded. Occasional analysis of real soils contaminated with RDX and HMX showed the presence of these nitroso products.

IV TECHNICAL APPROACH

Experimental procedures common to all studies in the report are presented in this chapter while more specific ones are described later in subsequent chapters.

The following chapter thus describes general procedures used to prepare microcosms for the microbial degradation of RDX and HMX and also the analytical methods developed to determine degradation products, mass balances, reaction stoichiometries, and degradation pathways.

Further details on experimental protocols can also be found in publications arising from this project (see appendix for listings).

IV.1 Chemicals and reagents.

Commercial grade RDX (purity > 99 %) and HMX (98 % purity) were provided by the Defence Research Establishment Valcartier, Quebec, Canada (DREV). MNX with 98 % purity was obtained from R. Spanggord (SRI, Menlo Park, CA) and TNX (99 %) was obtained from G. Ampleman (DRDC, Quebec, Canada). Acetone, formamide and formaldehyde were from Aldrich, Ca. Nitrous oxide was purchased from Scott specialty gases (Sarnia, ON, Canada). Carbon monoxide was purchased from Aldrich chemical company (Milwaukee, WI, US).

Uniformly labeled [UL-^{14}C]-RDX (chemical purity, >98%; radiochemical purity, 96%; specific radioactivity, 28.7 $\mu Ci \cdot mmol^{-1}$) and [UL-^{14}C]-HMX (chemical and radiochemical purity reached 94 % and 91%, respectively, specific radioactivity, 93.4 $\mu Ci \cdot mmol^{-1}$) were provided by Defense Research and Development Canada (DRDC), Quebec, Canada (Ampleman et al., 1995,1999b). The ring-labeled [^{15}N]-RDX and labeled [^{15}N]-HMX were provided by Defense Research and Development Canada (DRDC), Valcartier, Canada (Ampleman et al., 1999a). All other chemicals were reagent grade. D_2O (99 % purity) and [^{14}C]-HCHO (53 $mCi \cdot mmol^{-1}$ specific activity as provided by the supplier) were from Aldrich, Canada. ^{18}O-labeled water (enrichment 95 atom %) and ^{18}O-labeled molecular oxygen (min 99 atom %) were purchased from Isotec Inc. (Miamisburg, OH, US).

IV.2 Synthesis of Methylenedinitramine (MEDINA).

Methylenedinitramine was synthesized as described in the literature (Miksovsky et al., 1993; Brian and Lamberton, 1949). Briefly, acetic anhydride (11.16 mL, 12.075 g) was introduced into a 50-mL three-neck roundbottom flask and cooled to 10 ^{o}C. Methylene-bis-formamide (MBF) (3 g) was added into the flask followed by dropwise addition of nitric acid (11.16 mL, 16.86 g) for ca. 40 min. The solution was then stirred for 2.5 h at 8-12 °C and heated to 21 °C over 30 min. The solution was poured in a mixture of ice (75 g) and water (15 mL), stirred for 5 min., filtered through sintered glass, and washed with water (8.7 g of wet product are

recovered). The precipitate is hydrolyzed by washing with 80 mL of 2M HCl in a 100-mL flask, at 0 °C, for 1h, and filtered on a sintered glass M. The filtrate was kept and the solid (5.6 g) stirred again with 80 mL of 2M HCl at ^{0}C, for 1h. A second filtration was performed and the filtrates were combined. The remaining solid (1.6 g) was washed a third time with 60 mL of 2M HCl at 0 C for 45 min. The filtrate was combined with the above filtrates and evaporated under vacuum with a water-pump. The resulting solid (5.49 g) was recrystallized with a mixture of 1,2-dichloroethane: isopropanol (9:1, v:v) (5mL/g). 5.49 g of crude product was isolated which after crystallization gave only 2.40 g with a M.P. range of 100-102 °C. LC/MS (ES-) of the isolated product was similar (chromatographic and mass data) to a commercial sample that was obtained at the Rare Chemical Department at Aldrich. Both the commercial product and the synthesized one showed a deprotonated molecular mass $[M-H]^-$ ion at 135 Da.

IV.3 Synthesis of 4-nitro-2,4-diazabutanal (NDAB).

4-Nitro-2,4-diazabutanal was synthesized at SRI, Menlo Park, Ca., using the following procedure. Methylene(bis)formamide was prepared using the method of Sauer and Follett (1955). Acetyl nitrate was prepared by adding 7 g (100 mmol) nitric acid (90%) to 15 g of acetic anhydride in 15 mL of acetic acid with ice cooling. Methylene(bis)formamide, 6.1 g (50 mmol), was added and the mixture was stirred at room temperature for 24 hours. Chlorobenzene (100 mL) was added and the solution was concentrated carefully (>40ºC) *in vacuo* to remove excess nitric acid, acetic acid, and acetyl nitrate. The residue was dissolved in 100 mL of ethanol and the solution was kept at 45-50ºC for 24 hours to achieve ethanolysis of the initially formed mononitromethylene(bis)formamide by cleaving the undesired formyl group. The concentrate was flash chromatographed using a 4×1 inch silica gel column. The compound that eluted at R_f=0.4 ($EtOAc/SiO_2$) was collected and crystallized from EtOAc/toluene to yield 1.5 g of crystalline product (40%). Both elemental analysis and ^{1}H NMR were performed at University of Montreal, QC, Canada. The structure of the product was determined by ^{1}H NMR (Bruker AV-400) in d_6-dimethyl sulfoxide (d 12.45 (s, 1H, N**H**NO_2); d 8.93 (s, 1H, N**H**CHO); d 8.06 (d, 1H, C**H**O); d 4.70 (d, 2H, C**H**$_2$)), ^{13}C NMR

(d 165.05 (**C**HO); d 47.73 (**C**H_2)), and elemental analysis ($C_2H_5N_3O_3$; calc.: %C = 20.17, %N = 35.28, % H = 4.23; found: % C = 20.48, % N = 34.25, % H = 4.19).

IV.4 Enzymes and inhibitors.

Commercial enzymes including nitrate reductase, diaphorase, cytochrome P450 2B4 (EC 1.14.14.1) and cytochrome P450 reductase (EC 1.6.2.4) from rabbit liver were obtained from Sigma Chemicals, Canada. Pentoxyresorufin, cytochrome c, NADPH, 1-aminobenzotriazole (ABT) and ellipticine were also purchased from Sigma chemicals, Canada. 2-Methyl-1,2-di-3-pyridyl-1-propanone (metyrapone) and phenylhydrazine were obtained from Aldrich, Canada.

IV.5 Anaerobic sludge.

Anaerobic sludge was obtained from the biological waste treatment section of a nutrient factory (Sensient Flavors Canada) in Cornwall, Ontario. The sludge was always obtained fresh and stored at 4 ^{o}C when not in use. The viability of the sludge was measured using a glucose activity test (Guiot et al., 1995). On average the biomass concentration of the sludge was 8 g VSS/L (volatile suspended solid) with a zero mV reduction potential (E_h) before incubation that dropped down to a range of -250 to -300 mV during the biodegradation of RDX or HMX. The drop in E_h is possibly related to several fermentative processes such as those leading to the production of hydrogen from other co-substrates. The sludge was also found to contain several heavy metals [mg/kg dry weight] including iron, copper, nickel and manganese. A BBL dry anaerobic indicator (VWR, Canlab, ON, Canada) was placed inside the microcosm to be used to detect air leaks and to ensure anaerobic conditions.

IV.6 Aerobic degraders.

Three Rhodococci strains were used in the present study: strain A from BRI, NRC, Canada (Jones et al., 1995); strain DN22 (Coleman et al., 1998) from N.Coleman, Australia and

strain 11Y from N. Bruce (Cambridge University) (Binks et al., 1995). The fungus *P. chrysosporium* ATCC 24725 was provided by Ian Reid (Paprican, Canada, Montreal) and was maintained on YPD (per liter: yeast extract, 5 g; peptone, 10 g; dextrose, 20 g; agar, 20 g; at pH 5.5 adjusted with H_2SO_4) at 37ºC. Conidiospores were harvested from 10 day-old cultures in a sterile aqueous solution with 0.2% Tween 80 and kept at 4ºC.

IV.7 Soil and isolates.

A contaminated soil was obtained form a Canadian RDX manufacturing facility and used to isolate *Rhodococcus* sp. strain A. A farm soil was also used to determine soil sorption–desorption and their effect on degradation kinetics of RDX and HMX (see later sections). When needed, especially in certain sorption experiments, the soil was sterilized by gamma-irradiation using a cobalt-60 source at the Canadian Irradiation Centre in Laval, Quebec (Sheremata et al., 2001). Also, the farm soil was used to isolate two other bacteria that were identified, using cellular fatty acids and 16s-rRNA gene analyses, as *Pseudomonas* sp. FA1 and *Bacillus* sp. FA2. Both isolates degraded RDX and HMX (see later sections for details).

IV.8 Biotransformation and mineralization of RDX and HMX with anaerobic sludge: identification of initial intermediates and products.

- Hawari, J., A. Halasz, S. Beaudet, L. Paquet, G. Ampleman, and S. Thiboutot. 2001. Biotransformation routes of octahydro-1,3,5,7-tetranitro-1,3,5,7-tetrazocine by municipal anaerobic sludge. Environ. Sci. Technol. 35: 70-75.
- Halasz, A., Spain, J., Paquet, L., Beaulieu, C. and Hawari, J. 2002. Insights into the Formation and Degradation Mechanisms of Methylenedinitramine during the Incubation of RDX with Anaerobic Sludge. Environ. Sci. Technol., 36: 633-638.

IV.8.1 Biotransformation of RDX and HMX.

Biodegradation experiments were prepared in serum bottles (100 mL) containing anaerobic sludge (5 mL) and a 45 mL mineral salt medium containing NaH_2PO_4 (0.15 g/L), K_2HPO_4 (0.45 g/L) and of Na_2SO_4 (0.24 g/L) (Figure 2). Glucose (2.1 g/L) was added as a C source

and RDX (200 mg/L) or HMX (100 mg/L) as a N source. We used high concentrations of RDX and HMX in an attempt to generate sufficient amounts of metabolites for detection. To account for insoluble or suspended RDX and HMX (water solubility *ca* 60 mg/L and 5 mg/L, respectively (Talmage et al., 1999)) all the content of the microcosm was extracted in acetonitrile. However, we expect that the sludge itself contained other organic nitrogenous compounds that could also serve as a nitrogen source to the degrading microorganisms.

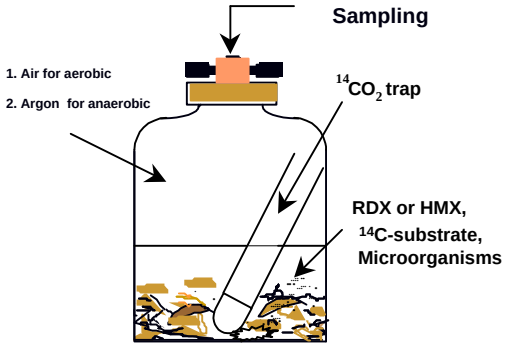

Figure 2. A typical drawing of a microcosm to conduct biotransformation studies of RDX and HMX under both anaerobic and aerobic conditions.

Two controls, one containing RDX or HMX and buffer without the sludge and the second containing sludge in buffer without RDX or HMX were present during the tests. Some serum bottles (microcosms) were supplemented with [UL-^{14}C]-RDX (0.038 μCi) or [UL-^{14}C]-HMX (0.04 μCi) and then fitted with a small test tube containing 1.0 mL of 0.5 M KOH to trap liberated carbon dioxide ($^{14}CO_2$) for subsequent measurement using a Packard, Tri-Carb 4530 liquid scintillation counter (Model 2100 TR, Packard Instrument Company, Meriden, CT). Ring labeled [^{15}N]-RDX was added to certain RDX incubation mixtures in order to determine which nitrogen atoms were incorporated into the metabolites, particularly in N_2O. The headspace in each serum bottle was sparged with nitrogen or argon gas to maintain anaerobic conditions. The bottles were closed with Teflon coated butyl rubber septa and aluminum crimp seals to prevent the loss of gaseous products such as CO_2, N_2O, N_2 and other volatile metabolites. Each microcosm was wrapped with aluminum foil to protect the

mixture against photolysis. For the analysis of N_2 and N_2O, sampling of the gaseous products from the headspace was performed using a gas tight syringe.

IV.8.2 Formation and decomposition of methylenedinitramine, a suspected RDX ring cleavage product.

To gain insight into the mechanisms of formation of methylenedinitramine, $O_2NNHCH_2NHNO_2$, we incubated RDX in the presence of water (D_2O) under the same conditions described above. In experiments with D_2O, we added sludge (1.5 mL) diluted with the proper volume of D_2O to produce different D_2O / H_2O solutions (90, 50 and 0 %, v/v). The incubation mixtures were each supplemented with RDX (200 mg/L). The total volume of incubation mixture was kept at 15 mL in order to maintain the final concentration of sludge at 10 % v/v throughout the study. We omitted glucose from the experiments with D_2O to be able to monitor the formation of the metabolite methylenedinitramine without the interference of volatile fatty acids metabolites. Two control microcosms without sludge and containing D_2O were present during the tests. One control bottle was supplemented with RDX and the other with methylenedinitramine. The stability of methylenedinitramine and its autodecompostion in water and in the sludge was determined by dissolving a predetermined weight (20 mg/L) of the amine in H_2O in one case and in the sludge in the second followed by monitoring its concentration and the concentration of its products (HCHO and N_2O) as discussed below. Once again the headspace in each microcosm was sparged with either nitrogen or argon gas to maintain anaerobic conditions. The bottles were then closed with Teflon coated butyl rubber septa and aluminum crimp seals.

IV.8.3 Analysis of RDX and HMX and their intermediate products.

RDX and HMX concentrations were determined by HPLC equipped with a photodiode array (PDA) detector as described in ref. (Hawari et al., 2001). Briefly, samples (50 μL) were injected into a Supelcosil LC-CN column (4.6 mm ID × 25 cm) (Supelco, Oakville, ON, Canada) and the analytes were eluted using a methanol/water gradient at a flow rate of 1.5

mL/min. RDX, HMX and their metabolites including the nitroso derivatives and the ring cleavage product, methylenedinitramine, were analyzed using a Micromass Platform bench top single quadrupole mass detector connected to a Hewlett Packard 1100 Series HPLC system equipped with a photodiode array detector. Acetonitrile (50 mL) was added to the above treated culture medium and mixed for few min. at room temperature. Aliquots (1 mL) from the above treated culture medium were filtered through a 0.45-μm-pore-size Millex-HV filter. Aliquot (50 μL) from the filtered culture medium were analyzed with HPLC at 25ºC. A Synergi Polar - RP column (15 cm x 4.6 mm, particle size 4 μm) was used for separation with a solvent system consisting of a gradient of methanol/water and HCOOH (200 μM) at a flow rate of 0.75 mL/min at 25°C. An initial MeOH - H_2O composition of 10 % v/v was used for 10 minutes, which was subsequently changed to 90 % v/v and was kept for 5 minutes. The composition of eluent was changed to its original value (10 % v/v) over a period of 10 minutes. Detection was done with a photodiode array detector at 230 nm. Whereas for mass analysis, ionization was done in a negative electrospray ionization mode ES(-) producing mainly the deprotonated mass ions $[M-H]^-$.

Analysis of nitrogen end products. Nitrite (NO_2^-) and nitrate (NO_3^-) were performed by capillary electrophoresis using sodium borate (25 mM) and hexamethonium bromide (25 mM) electrolytic solution at pH 9.2 (Okemgbo et al., 1999). The voltage was –20 kV, and the temperature was 25 °C. Samples were injected by applying 50 mbar pressure to the capillary inlet for 10 s. UV detection was at 215 nm. Ammonium cation (NH_4^+) was analyzed in the aqueous phase of the culture medium using an SP 8100 HPLC system equipped with a Waters 431 conductivity detector and a Hamilton PRP-X200 (250 mm x 4.1 mm x 10 μm) analytical cation exchange column using 30% methanol in 4 mM nitric acid at a flow rate of 0.75 mL/min.

For N_2O detection and quantification, gas samples (500 μL) taken from the headspace of the microcosms using a gas-tight syringe were injected into a GC (SRI 8610, INSUS Systems Inc.) connected to a Supelco Porapack Q column (2 m) coupled to an electron capture detector (ECD) (330 °C). Helium was used as the carrier gas (21 mL/min) at 60 °C. In the case of the ring-labeled [^{15}N]-RDX analysis of $^{15}N^{14}NO$ (45 Da) and $^{14}N^{14}NO$ (44 Da) was carried out with a GC /MS system. Gaseous nitrogen was analyzed with an HP GC connected

to SupelcoChomosorb 102 column coupled with a thermal conductivity detector (TCD).

***Analysis of hydrazine and dimethyl hydrazine*.** Ion chromatography (Dionex model DX-500 ion chromatograph system) consisting of a GP40 gradient pump and coupled with electrochemical detector (pulsed detection mode) was used to analyze hydrazines as described by Larson and Strong (1996)**.** Samples (25µL) from the culture medium were injected into a Hamilton PRP-X200 (250 mm x 4.1 mm x 10 µm) analytical cation exchange column using 30 % methanol in 4 mM nitric acid at a flow rate of 1 mL/min. Standards of hydrazine and dimethyl hydrazine were employed for confirmation. Solid Phase Microextraction (SPME)/ GC-MS, a more sensitive technique with a pg detection limit was also employed to confirm the absence of hydrazines as products of the two cyclic nitramines RDX and HMX.

Analysis of carbon end products. Formaldehyde was detected as its oxime derivative using an SPME fiber coated with poly-(dimethylsiloxane)/divinylbenzene (Supelco) and the derivatizing agent O-(2,3,4,5,6-pentafluorobenzyl)hydroxylamine as described by Martos and Pawliszyn (1998). Alternatively, HCHO was analyzed as described by Summers (1990) with a few modifications. Samples were derivatized with 2,4-pentanedione in the presence of ammonium acetate and glacial acetic acid for one hour at pH 6.0 and 40 °C. The derivatives were then analyzed by HPLC using a 5 µm Supelcosil LC-8 column (4.6 mm ID x 25 cm) (Supelco, Bellafonte, PA) maintained at 40°C. The mobile phase consisted of an acetonitrile gradient of 15% to 27%, at a flow rate of 1.5 mL/min for 6 min. The derivatives were detected and quantified by a Fluorescence detector (excitation at 430 nm and emission at 520 nm). Meanwhile formic acid, HCOOH, was analyzed by capillary electrophoresis (CE) and UV detection using a Hewlett-Packard ^{3D}HPCE system consisting of a photodiode array detector following the procedure that was described by Chen et al. (1997) and developed later for the analysis of RDX metabolites (Groom et al., 2003). Formic acid was initially detected and quantified at 340 nm (210 nm reference) with a limit of detection of 200 µg/L. The identity of HCOOH as a degradation product of RDX and HMX was confirmed using [UL-^{14}C] HMX and by collecting the product by HPLC fractionation for subsequent radioactivity measurement.

Another potential intermediate from the two explosives is formic hydrazine ($H_2N–NH–$

CHO), which may form as a result of the reaction between hydrazine and formaldehyde or formic acid. We thus derivatized formic hydrazine with salicylaldehyde, and detected the product by LC-MS- ES(-) as its deprotonated molecular mass ion [M-H]. The product was detected at 163 Da. Once again, we were unable to detect this product when the same analytical method was applied to the RDX treated sludge. So far, the results demonstrate the absence of hydrazine as metabolite of RDX and HMX during their incubation with the domestic anaerobic sludge.

Methane including $^{14}CH_4$ was analyzed using an SRI 8610 GC (INSUS Systems Inc.) connected to a Supelco Porapack Q column (2 m) and coupled with a radio activity detector (RAM). The gaseous products from the head space of the culture medium were sampled using a gas tight syringe for subsequent injection inside the GC using helium as a carrier gas (21 ml/min) at 60 ºC. Gas identification was confirmed by comparison with reference materials. The detection limit for RAM was 150 dpm.

IV.9 Biotransformation and mineralization of RDX and HMX by *Rhodococcus* sp. strain DN22: identification of initial intermediates and products.

- Fournier, D., Halasz, A., Spain, J., Fiurasek, P., and Hawari, J. 2002. Determination of Key Metabolites during Biodegradation of RDX with Rhodococcus sp. strain DN22. Appl. Environ. Microbiol. 68: 166-172.

IV.9.1 Microbial culture and growth conditions.

Rhodococcus sp. strain DN22, previously isolated from a soil contaminated with RDX, 2,4,6-trinitrotoluene, 2,4-dinitrotoluene and heavy metals, was kindly provided by Nicholas V. Coleman (University of Sydney, Australia). The strain was grown in a mineral salt medium previously described by Coleman et al. (1998). Unless otherwise specified, succinate (2.4 mM) was used as the carbon source and RDX (175 μM) (from a concentrated acetone stock solution) was added as the sole nitrogen source. Excess acetone was removed by evaporation in a biological fume hood under sterile conditions. Growth of the microbial cells was

monitored spectrophotometrically at 530 nm (OD530) (Thermo Spectronic, Rochester, NY). Cultures were protected from light and were agitated at 250 rpm at 25 °C. Mineralization of RDX by growing cultures of *Rhodococcus* sp. DN22 was performed in 120 mL serum bottles containing 10 mL of mineral salt medium and RDX (175 μM) spiked with [UL-^{14}C]-RDX (0.038 μCi) (see section IV.8.3). When the stationary phase was reached, the microcosms were sacrificed to measure the remaining radioactivity in the culture supernatant and in the biomass.

Resting cells assays were performed using mid-log phase culture (OD530 = 0.4-0.5). The cells were washed and were resuspended in the mineral salt medium described above to an OD530 of 1.2 without the addition of any carbon-source or nitrogen-source apart from RDX. As recommended previously, $(NH_4)_2SO_4$ (1 mM) was added to the DN22 cultures to prevent the uptake of NO_2^- produced during RDX degradation (Coleman et al., 1998). In some cell suspensions we added ring labeled [^{15}N]-RDX to DN22 cultures to determine which nitrogen atoms were incorporated into the metabolites. In the case of $^{18}O_2$ labeled experiments, the culture medium was first sparged with nitrogen gas to remove air and then $^{18}O_2$ (97 % pure) was added to the head space of the above mixture using a gas tight syringe followed by the addition of DN22 cells. The final oxygen concentration was approximately 20 % v/v as measured by a GC connected to a thermal conductivity detector (TCD). In the experiments with deuterated water, RDX grown cells were harvested by centrifugation and were then resuspended in pure D_2O (5 mL) in the presence of RDX (175 μM) for subsequent analysis by LC-MS.

IV.9.2 Determination of products.

The concentration of RDX and HMX was monitored using the HPLC method described above with anaerobic sludge. Also N-containing products (N_2, N_2O, NO_2^+, NO_3^+, NH_4^+) and C-containing products (HCHO, HCOOH, $^{14}CO_2$) were in accordance with the methods developed for the analysis of RDX and HMX incubation mixtures with anaerobic sludge (described above). During aerobic degradation of RDX a key dead end product with empirical formula $C_2H_5N_3O_3$ was detected in significant amounts (aprox. 66 %). The

subsequent experiments will describe methods of isolating the dead end product ($C_2H_5N_3O_3$) and of determining its structure using a combination of NMR and MS analyses.

IV.9.3 Production and isolation of RDX dead end product $C_2H_5N_3O_3$ using strain DN22.

The dead end metabolite $C_2H_5N_3O_3$ (MW 119) was produced by transformation of RDX by *Rhodococcus* sp. strain DN22 in a 3 L bioreactor (Applicon Inc., CA) containing 2 L of growth medium. *Rhodococcus* sp. strain DN22 was grown in two liters of medium containing 2.44 g of K_2HPO_4, 1.22 g of KH_2PO_4, 66 mg of $CaCl_2 \cdot 2H_2O$, 0.4 g of $MgCl_2$, 6 mL of trace elements (Owens and Keddie, 1969), 10.8 g of sodium succinate $\cdot$ $6H_2O$ as sole carbon source, and 80 mg of RDX as sole nitrogen source. The bioreactor was constantly aerated and stirred at 800 rpm at 30°C. The RDX was continuously added to the bioreactor. The total amount of RDX added in the bioreactor (including the initial amount) was 1.1 g. Sodium succinate and trace elements were added twice (in total 15.5 g and 8.6 mL, respectively). The bioreactor was operated for 9 days (OD_{530} increased from 0.69 to 5.11) until there was no further increase in the concentration of the dead end metabolite. Cells were filtered out from the broth (Pellicon Cassette System by Millipore, Bedford, MA) and filtrate was passed over C18 (Sep-Pak, 10 g, Waters, Milford, MA) and SAX columns (Mega Bond Elut, 10 g, Varian, Harbor City, CA). The collected aqueous phase was concentrated under reduced pressure by using a rotary evaporator (Buchi, Switzerland). The concentrated residue was washed eight times with 10-20 mL of acetonitrile each time in order to extract the organic metabolite from the inorganic salts. The fractions containing the metabolite were pooled, evaporated to dryness and stored at 4°C for subsequent elemental analysis and structural identification by LC/MS (ES-) and NMR. Both elemental analysis and NMR were performed at University of Montreal, QC, Canada. The [M – H] of the product as determined by LC/MS(ES-) was 118 Da, representing an empirical formula of $C_2H_5N_3O_3$. ^{1}H NMR (Bruker AV-400) in d_6-dimethyl sulfoxide (d 12.45 (s, 1H, N**H**NO_2); d 8.93 (s, 1H, N**H**CHO); d 8.06 (d, 1H, C**H**O); d 4.70 (d, 2H, C**H**$_2$)), ^{13}C NMR (d 165.05 (**C**HO); d 47.73 (**C**H_2)), and elemental analysis ($C_2H_5N_3O_3$; calc.: %C = 20.17, %N = 35.28, % H = 4.23; found: % C = 20.48, % N = 34.25, % H = 4.19). These MS and NMR data were the same as

those obtained with the synthesized 4-nitro-2,4-diazabutanal.

IV.9.4 Kinetics and stoichiometry of degradation.

We conducted time course studies for the removal of RDX (and HMX) and the appearance and disappearance of their intermediate and end products. These compounds were analyzed using chromatographic and mass spectrometric techniques (SPME/GC-MS, LC/MS and capillary electrophoresis/MS). Following these analyses, the carbon and nitrogen mass balances and the stoichiometry of reaction were determined. Product distribution and mass balance data were determined using uniformly labeled compound [UL -^{14}C]-RDX (or [UL -^{14}C]-HMX) and uniformly ring labeled [^{15}N]-RDX (or [^{15}N]-HMX).

IV.10 Screening, identification and isolation of degraders from anaerobic sludge.

- Zhao, J.-S., Halasz, A., Paquet, L., Beaulieu, C., Hawari J. 2002. Biodegradation of RDX and its Mononitroso Derivative MNX by *Klebsiella* sp. Strain SCZ-1 Isolated from an Anaerobic Sludge. Appl. Environ. Microbiol. 68: 5336-5341.
- Zhao, J.-S., Halasz, A., Paquet, L., Hawari J. 2003. Metabolism of hexahydro-1,3,5-trinitro-1,3,5-triazine through initial reduction to hexahydro-1-nitroso-3,5-dinitro-1,3,5-triazine followed by denitration in *Clostridium bifermentans* HAW-1. Appl. Microbiol. Biotechnol. 63 : 187-193.

IV.10.1 Isolation and characterization of Klebsiella pneumoniae sp. strain SCZ-1.

Media. The medium used for the isolation of anaerobic bacteria was 5.8 % Difco Anaerobic agar (Becton Dickinson, Sparks, MD, US). The YPG medium (pH 7.3) used for fermentative bacterial growth and RDX degradation was composed of yeast extract (3.0 g), Bacto peptone (0.6 g) and glucose (1.0 g) in one L of basic salts medium. The basic salts medium was prepared as described previously (Weimer, 1984), but in this case no $(NH_4)_2SO_4$ was added and also $(NH_4)_6Mo_7O_{24}.4H_2O$ was replaced with $NaMoO_4.2H_2O$. YPS agar was prepared as described by Zhao et al. (2000). Liquid media were sterilized either by autoclaving at 120 ºC for 20 min or through filtration by sterile filters (0.22 μm, Millex^{TM} GP, Millipore, Bedford,

MA, US, for trace metals and glucose stock solution). The dry serum bottles were sterilized by autoclaving at 120 ºC for 60 min.

Bacterial isolation and characterization. A methanogenic industrial sludge was obtained from Sensient Flavor Canada (Cornwall, Ontario) and incubated on Difco- Anaerobic Agar plates at 37 ºC under an atmosphere of mixture of H_2 and CO_2 (BBL GasPak Plus^{TM} , Sparks, MD, US). Anaerobic conditions were monitored with a BBL indicator (VWR Canlab, Mississauga, ON, Canada). One strain, SCZ-1, was selected for subsequent characterization due to its highest growth rate under both aerobic and anaerobic conditions, and its capacity to mineralize RDX anaerobically. Using the Sherlock Microbial Identification System (MIDI, Newark, Del. US), strain SCZ-1 was found to be close to *Klebsiella pneumoniae* with a similarity index of 0.9. Using the 16s-rRNA identification method (Johnson, 1994), the gene sequence of a 0.7Kb-long fragment (representing half of the total length of the gene) of 16s-rRNA gene from the isolate, was 99 % similar to that of *Klebsiella pneumoniae*.

Bacterial growth and biodegradation tests. Using a procedure described previously (Hawari et al., 2000a), serum bottles (60 mL), each containing 18.5 mL YPG media and 106 μM of RDX, were made anaerobic by repeatedly degassing under vacuum and charging with filter-sterilized oxygen-free nitrogen or argon. The sealed bottles were then inoculated with 1.5 mL of aerobic liquid culture (initial OD_{600nm}, 0.15) of strain SCZ-1, and incubated in a rotary shaker (200 rpm) at 37 ºC. After 3h of anaerobic incubation, bacterial growth reached a maximum of 0.7 OD_{600nm} {0.91 mg (dry cell weight, dcw)/L}. We measured the redox potential (E_h) with a Pt/Ag/AgCl electrode (Fisher Scientific, Montreal Canada) and found E_h dropped from +200 mV to –300 mV during this incubation period (while pH dropped from 7.3 to 6.3). MNX (100 μM) and TNX (100 μM) biodegradation tests were conducted under the same conditions as those used for RDX degradation. Separate bottles were used for monitoring production of either aqueous metabolites or N_2O. For sampling, sterile syringe and needles washed with reduced buffer were used. Some microcosms were spiked with [UL-^{14}C]-RDX (0.038 μCi) to measure mineralization (see section IV.8.1). When $^{14}CO_2$ ceased to form, the microcosm(s) were sacrificed to measure the remaining radioactivity in the culture supernatant and in the biomass. A similar procedure was used to mineralize HCHO (166 μM) supplemented with ^{14}C-HCHO (0.030 μCi).

RDX and metabolite analyses. The concentration of RDX and its nitroso products MNX, DNX and TNX (in aqueous phase obtained by centrifugation at 9000g for 3 min) were analyzed by HPLC/UV at 230 nm as described previously in the report (Hawari et al., 2000a). Analysis of methylenedinitramine, (methyl)hydrazines, N_2O and HCHO were also conducted as described above (Hawari et al., 2000a; Halasz et al., 2002 and Fournier et al., 2002). CH_3OH was measured by GC/FID (HP 6890) using a Hayesep Q micropacked column (2m x 0.03mm) (Supelco, Bellafonte, PA) (detection limit, 0.25 ppm). Nitrite was analyzed by US EPA method 345.1 (EPA, 1979) with a detection limit of 10 ppb. Ammonia was analyzed by an enzymatic assay using L-glutamate dehydrogenase and NADPH (Sigma, St. Louis, MO). All tests were run in triplicate.

IV.10.2 Isolation and characterization of **Clostridium** *sp. Strain HAW-1.*

Media. The medium used for the isolation and maintenance of anaerobic bacteria was Bacto Brewer Anaerobic agar (5.8%, Becton Dickinson, Sparks, MD, US). The basic salts and vitamins medium were prepared as described previously (Zhao et al., 2002), using a Wolin vitamin solution (5 mL in 1 L) (Wolin et al., 1963) and a trace metal solution (pH 4) (TMS, 10 mL in 1 L) composed of 100 mg/L of each of $FeSO_4 \cdot 7H_2O$, $FeCl_3$, $MnCl_2 \cdot 4H_2O$, $NiCl_2 \cdot 2H_2O$, $ZnCl_2$, 10 mg/L of each of Na_2SeO_3, $CoCl_2 \cdot 6H_2O$, $Na_2MoO_4 \cdot 12H_2O$, and 1 mg/L of each of H_3BO_3, $CuSO_4$, $AlK(SO_4)_2 \cdot 12H_2O$, $Na_2WO_4 \cdot 2H_2O$. The yeast extract (YE) medium was prepared by dissolving 1 gram of YE in 1 L of the above basic salts and vitamins medium. The liquid media were sterilized either by autoclaving at 120 ºC for 20 min or through filtration by sterile filters (0.22 μm, Millex^{TM} GP, Millipore, Bedford, MA, US). The dry serum bottles were sterilized by autoclaving at 120 ºC for 60 min.

Bacterial enrichment, isolation and characterization. The following anaerobic procedure was used for all bacterial enrichment and biodegradation tests unless otherwise noted. The basic salts and vitamins medium (19 mL) containing RDX (100 μM) was added to a serum bottle and degassed using an oil vacuum pump. The headspace was charged with oxygen-free argon after passing the gas through a sterile filter. Sodium sulfide (0.025 %) and L-cysteine·HCl (0.025 %) were then added to the medium to remove final traces of oxygen.

Prior to inoculation, the argon in the headspace of all bottles was replaced with hydrogen to serve as a potential bacterial energy source. One mL of methanogenic industrial sludge suspension from Sensient Flavor Canada (Cornwall, Ontario) was inoculated and incubated statically at 37 ºC. A total of seven serial transfers of this culture to fresh medium were made every 20-30 days. Bacterial growth and RDX degradation was monitored during the serial transfers. Bacterial strains were isolated by spreading the liquid culture on the agar surface prepared inside the serum bottles and incubated for three days at 37 ºC. The anaerobic agar bottle was prepared by solidifying Bacto Brewer Anaerobic agar containing 0.025 % of Na_2S, 0.025 % of L-cysteine·HCl and 0.5 % of $Na_2SO_{3\ onto}$ the inner surface and sealed under an atmosphere of hydrogen gas (Holdeman et al., 1977).

Bacterial isolates were evaluated for their RDX degradation capability in the YE (0.1 %) medium. The YE was added because the isolates were found to grow poorly in its absence in the basic salts and vitamins media when RDX (100 μM) was used as the sole carbon and/or nitrogen source. One strain, HAW-1, was selected for subsequent characterization due to its high growth rate and capability to degrade RDX. Using the 16s-rRNA identification method (Johnson, 1994), the gene sequence, representing 85 % of the total length of the 16s-rRNA gene from the isolate, was 99 % similar to that of *Clostridium bifermentans* and *Clostridium paraputrificum.*

Bacterial growth and biodegradation tests. Serum bottles (microcosms) (60 mL), each containing the YE media (19 mL) and RDX (104 μM), were first made anaerobic and then inoculated with 1 mL of culture (initial OD_{600nm}, 0.02) and incubated statically at 37 ºC. Bacterial spores began to germinate after 5 h, reaching a maximal growth (0.2 OD_{600nm}; 150 mg [wet cell weight] $\cdot$ l^{-1}) after 15 hours. MNX (96 μM) and TNX (100 μM) biodegradation tests were conducted under the same conditions used for RDX. A sterile syringe, washed with argon and reduced buffer, was used for sampling of the liquid culture, and a gas-tight syringe for sampling of the headspace for subsequent analysis (see below). Rates of substrate removal and metabolite formation were measured from the linear phase of degradation, which occurred between 5 and 24 h of incubation. Some microcosms were spiked with [UL-^{14}C]-RDX (0.038 μCi) to measure mineralization (liberated $^{14}CO_2$) using a Tri-Carb 4530 liquid scintillation counter (LSC, model 2100 TR, Packard Instrument Company, Meriden, CT,

US). When $^{14}CO_2$ ceased to form, the microcosm was sacrificed to measure the remaining radioactivity in the culture supernatant and in the biomass.

RDX and metabolites analyses. The concentration of RDX and its nitroso products MNX, DNX and TNX were analyzed by HPLC/UV at 230 nm as described previously in the report and in the literature (Hawari et al., 2000a; Zhao et al., 2002). Methods for the analyses of methylenedinitramine and 1,1-dimethylhydrazines (Hawari et al., 2000a; Zhao et al., 2002), 4-nitro-2,4-diaza-butanal (NDAB) (Hawari et al., 2002), nitrite (EPA, 1979)**,** ammonia (Zhao et al., 2002), formamide, HCHO and MeOH (Zhao et al., 2002) were described above or can be found in more details in the cited publications from the present study. Hexahydro-1,3,5-triamino-1,3,5-triazine was analyzed by LC/MS using positive electrospray ionization (ES+) mode and by searching for the protonated molecular mass ion $[M+H]^+$ at 133 Da or at 136 for ring-labeled [^{15}N]-RDX. All tests were performed in triplicate.

IV.11 Screening and identification of commercial enzymes for their ability to degrade RDX and HMX: insight into initial reactions involved in the degradation.

- Bhushan, B., Halasz, A., Spain, J., Thiboutot, S., Ampleman, G. and Hawari, J. 2002. Biotransformation of Hexahydro-1,3,5-trinitro-1,3,5-triazine (RDX) Catalyzed by a NAD(P)H: Nitrate Oxidoreductase from *Aspergillus niger*. Environ. Sci. Technol. 36: 3104-3108.
- Bhushan, B., Halasz, A. and Hawari J. 2002. Diaphorase catalyzed biotransformation of RDX via N-denitration mechanism. Biochem. Biophys. Res. Comm. 296: 779-784;
- Bhushan, B., Trott, S., Spain, J. C., Halasz, A., Paquet, L. and J. Hawari. 2003. Biotransformation of Hexahydro-1,3,5-trinitro-1,3,5-triazine (RDX) by a rabbit liver Cytochrome P450: Insight into the mechanism of RDX biodegradation by *Rhodococcus* sp. strain DN22. Appl. Environ. Microbiol. 69: 1347-1351.

IV.11.1 Nitrate reductase enzymatic assay.

A lyophilized powder of enzyme *Aspergillus niger* nitrate oxidoreductase (EC 1.6.6.2), NADPH obtained from Sigma chemicals, Canada, was suspended in potassium phosphate buffer (50 mM) at pH 7.0 and was washed three times with 2.5 mL of a buffer solution using Biomax-5K membrane centrifuge filter units (Sigma chemicals) and was finally resuspended in 0.5 mL of the same buffer. The protein concentration was measured by the bicinchoninic

acid (BCA) kit (Sigma chemicals) using bovine serum albumin as the standard. The native enzyme activity was estimated spectrophotometrically at 340 nm as the rate of oxidation of NADPH in presence of nitrate. The nitrate reductase-catalyzed transformation of RDX was carried out under anaerobic conditions in 6 mL glass vials containing one mL reaction mixture and sealed under an atmosphere of argon. One mL assay mixture contained RDX (100 μM), NADPH (300 μM) and one mg enzyme (equivalent to 0.25 native units) was prepared in a potassium phosphate buffer (50 mM) at pH 7.0 and 30 ^{o}C. Three different controls were used to determine the enzyme catalysis of RDX transformation using NADPH as electron donor, as follows: the first control contained RDX, NADPH and buffer without enzyme; the second control contained RDX, enzyme and buffer without NADPH and the third control contained RDX and buffer without enzyme or NADPH. The samples from liquid and gas phases were withdrawn periodically to analyze for RDX and the transformation products as described below. RDX transformation activity of the enzyme was expressed as nmoles RDX transformed $h^{-1}mg^{-1}$protein. Enzymatic assays were also conducted with two potential RDX metabolites, formamide (50 μM) and hydrazine (50 μM), using nitrate reductase under the same conditions described above. Residual RDX, formamide, hydrazines and their degradation products methylenedinitramine, N_2O, NH_3, HCHO were analyzed as described earlier.

IV.11.2 Diaphorase enzymatic assays.

Diaphorase (or lipoyl dehydrogenase, EC 1.8.1.4) from *Clostridium kluyveri* was obtained from Sigma chemicals, Canada, as a lyophilized powder. The enzyme was suspended in 50 mM potassium phosphate buffer (pH 7.0) and washed twice with 2.0 mL of the same buffer solution using Biomax-5K membrane centrifuge filter units (Sigma chemicals) and then it was resuspended in the same buffer. The protein concentration was measured by the bicinchoninic acid (BCA) kit (Sigma chemicals) using bovine serum albumin as the standard. The native enzyme activity was estimated spectrophotometrically at 340 nm as the rate of oxidation of NADH in presence of 2,6-dichlorophenol-indophenol as the electron acceptor.
RDX biotransformation assays with diaphorase were performed under anaerobic conditions

in 6 mL glass vials under an atmosphere of argon. Each vial contained one mL assay mixture containing RDX (100 μM), NADH (150 μM) and 50 μL of the diaphorase (equivalent to 0.5 native units) in a potassium phosphate buffer (50 mM). Three different controls were prepared to determine the enzymatic catalysis of RDX transformation: the first control contained RDX, NADH and buffer without enzyme; the second contained RDX, enzyme and buffer without NADH, and the third contained RDX and buffer without enzyme or NADH. The reaction time was one hour, unless otherwise stated.

The effect of oxygen on enzyme activity was studied by performing the assays under aerobic (in presence of air) and anaerobic conditions (under an atmosphere of argon) at pH 7.0 and 27 ^{o}C. All other reaction conditions were the same as described above. In the time course study, liquid and gas samples were withdrawn from the experimental bottles and were analyzed for their content of RDX and the transformed products as described below. RDX transformation activity of enzyme was expressed as nmoles of RDX transformed $h^{-1}mg^{-1}$protein.

Finally, the deflavo form of enzyme was prepared by using the earlier reported methods (Madigan and Mayhew, 1993; Tedeschi et al., 1995) with some modifications. The holoenzyme was dialyzed for 48 hours at 4^{o}C against a dialysis solution composed of 100 mM potassium phosphate buffer (pH 7.0), EDTA (0.1 mM) and glycerol (10 % v/v) and KBr (3 M). The dialysis buffer was changed every 6 hour. The reconstitution of apoenzyme was carried out in ice-cold potassium phosphate buffer (pH 7.0) in the presence of glycerol (10 % v/v). Flavon mononucleotide (FMN) was added at variable concentrations (0-250 μM) to the apoenzyme preparation. The unbound FMN was removed by washing the enzyme with the same buffer using Biomax-5K membrane centrifuge filter units. The enzyme activity was assayed after each addition of FMN to the apoenzyme, in order to determine the concentration-dependent reconstitution of apoenzyme by the FMN.

The analysis of RDX and the products such as NO_2^-, NH_4^+, HCHO and N_2O were performed as described earlier in the report and as shown in more detail in the annexed manuscripts. Due to the controversy surrounding the potential formation of hydrazine as an RDX metabolite, we developed another method for its detection in addition to the one described earlier in the report based on the use of HPLC connected to an electrochemical detector. Thus we used an HPLC system equipped with a Waters model 600 pump (Waters Associates,

Milford, MA), a 717 plus autosampler, a Hamilton RPX-X200 analytical cation exchange column (250 mm × 4.1 mm), a Waters post column reaction module with a Waters reagent manager pump, a Waters model 464 electrochemical detector with a gold-working electrode and a base resistant Ag/AgCl reference electrode. The eluent was 6 % v/v acetonitrile in 0.005 M KH_2PO_4 solution in deionized water. The eluent was degassed by continuous helium sparging before and during use. The post-column reaction solution was 0.1 M NaOH solution in deionized water. The operating parameters for the system were: eluent flow rate, 1.0 mL/min.; temperature, 30^{o}C; injection volume, 25 µL; flow-rate of post-column reaction solution, 250 µL/min.; working electrode cleaning potential, 500 mV (0.333 sec); pretreatment potential, -350 mV (0.333 sec) and measuring potential, 100 mV in DC mode. Formamide was analyzed by MS (ES+) connected to an HPLC system equipped with a photodiode array detector and a Synergi Polar-RP column (4.6 mm ID × 15 cm) (Phenomenex, Torrance, CA) at 25^{o}C. The solvent system was methanol/water gradient (10-90 % v/v) at a flow rate of 0.75 mL/min. For mass analysis, the ionization was carried out in a positive electrospray ionization mode ES+ producing mainly the [M+H] mass ions. The electrospray probe tip potential was set at 3.5 KV with a cone voltage of 35 V at an ion source temperature of 150^{o}C.

IV.11.3 Cytochrome P450 Enzymatic assays.

Pentoxyresorufin, cytochrome c, NADPH, 1-aminobenzotriazole (ABT) and ellipticine were purchased from Sigma chemicals, Canada. Methylenedinitramine, 2-methyl-1,2-di-3-pyridyl-1-propanone (metyrapone) and phenylhydrazine were obtained from Aldrich, Canada. All other chemicals were of the highest purity commercially available (see section IV.1). Cytochrome P450 2B4 (EC 1.14.14.1) and cytochrome P450 reductase (EC 1.6.2.4) from rabbit liver were obtained from Sigma Chemicals, Canada. The protein concentration was measured with a bicinchoninic acid (BCA) kit (Sigma Chemicals, Canada) using bovine serum albumin as standard. The native enzyme activities were estimated according to the manufacturer's guidelines.

RDX biotransformation assays with cytochrome P450 2B4 and cytochrome P450 reductase

were performed under both aerobic and anaerobic conditions in 6 mL glass vials. Anaerobic conditions were created by purging all the solutions with argon three times (15 min. each time) and replacing the headspace air with argon in a sealed vial. Each vial was charged with one mL of an assay mixture containing RDX (100 μM), NADPH (150 μM), cytochrome P450 2B4 (100 μg) or cytochrome P450 reductase (10 μg) in a potassium phosphate buffer (50 mM), pH 7.2. Reactions were performed at 37 ^{o}C with cytochrome P450 2B4 and 30 ^{o}C with cytochrome P450 reductase. Three different controls were prepared by omitting enzyme, NADPH or both from the assay mixture. Samples from the liquid and gas phases in the vials were withdrawn periodically to analyze for RDX and the transformation products as described in analytical procedures. NADPH was determined as described previously (Bhushan et al., 2002a). RDX transformation activity of the enzyme was expressed as nmoles of RDX transformed min^{-1} mg^{-1} protein unless otherwise stated. To determine the role of oxygen and water in the enzymatic degradation of RDX, enzymatic assays were conducted using $H_2{}^{18}O$ in a potassium phosphate buffer (100 mM), pH 7.2 in a ratio of 7:3. All other assay ingredients and conditions were the same as described above. When the reaction was carried out under anaerobic conditions, reactants were added to the vial through a rubber septum with a syringe and needle. For the labeling experiments with $^{18}O_2$, the headspace and the aqueous phase were flushed with argon and replaced with $^{18}O_2$ (approx. 21 % v/v). Thereafter, the reaction was performed as described above. The concentration of RDX was determined using high performance liquid chromatograph (HPLC) connected to photodiode array (PDA) detector ($\lambda_{254\ nm}$) as described above. LC/MS was performed with a Micromass bench-top single quadrupole mass detector attached to a Hewlett Packard 1100 series HPLC system equipped with a photodiode array detector (Fournier et al., 2002). The RDX metabolite was detected at 118 Da. Other RDX metabolites including methylenedinitramine, 4-nitro-2,4-diazabutanal, MNX, formaldehyde (HCHO), formamide, ammonium (NH_4^+), nitrite (NO_2^-), and nitrous oxide (N_2O) were analyzed as described earlier in the report.

IV.12 Identification of intermediate and end products during alkaline hydrolysis of RDX: insight into biodegradation pathways.

- Balakrishnan, V. K., Halasz, A., and Hawari, J. 2003. The alkaline hydrolysis of the cyclic nitramine explosives RDX, HMX and CL-20: New insights into degradation pathways obtained by the observation of novel intermediates. Environ. Sci. Technol. 37: 1838-1843.

Hydrolysis of RDX, MNX and HMX in aqueous solution at pH 10. To a series of dry 20 mL vials (each wrapped in Aluminum foil) was added an aliquot of cyclic nitramine stock solution prepared in acetone. The acetone was evaporated in a fume hood, followed by the addition of 10 mL of a NaOH solution (pH 10) to give the following concentrations 215, 180 and 110 ppm for RDX, MNX and HMX, respectively. The initial concentrations were kept well in excess of the maximum water solubility of each nitramine (ca. 65 ppm for RDX and 6 ppm for HMX at 30 °C (Lynch et al., 2001) in an attempt to generate sufficient amounts of intermediates to allow detection. The vials were sealed with Teflon coated serum caps and placed in a thermostated benchtop shaker at 30 ^{0}C and 200 rpm. Some vials were sparged with Argon for 2 hours to allow analysis for N_2. We used a gas-tight syringe to measure gaseous products (N_2O and N_2) in the headspace but for the analysis of the liquid medium we first quenched the reaction by adding HCl taken in a MeCN solution (10 mL) (pH 4.5). MeCN was used to solubilize unreacted starting material for subsequent analysis. The quenched vials were then stored in a refrigerator at 4 ^{0}C until analyzed.

Hydrolysis of RDX in 70% MeCN : 30 % H_2O (v/v) mixture. A predetermined weight of RDX (0.1 g) was placed into a vial to which a 10 mL solution of NaOH (pH 12.3) in 70:30 (v/v) acetonitrile: water was added, giving an initial RDX concentration of 10,000 ppm. MeCN was used to solubilize the high RDX concentration used, while a high pH was used to accelerate the reaction. The vial was sealed with a Teflon coated serum cap and placed in a thermostated benchtop shaker at 30 ^{0}C and 200 rpm. After 22 h, the reaction was quenched by the addition of HCl (1 M) and the volume of the quenched mixture was then reduced under reduced pressure (18 mm Hg). The remaining mixture was passed through a column

containing 3-aminopropyl-functionalized silica gel (Aldrich) using a 70 % acetonitrile:30 % water (v/v) mixture to remove chloride and nitrite anions, preventing interference during LC-MS (ES-) analysis (discussed below). This experiment was then repeated using [^{15}N]-RDX.

Hydrolysis of RDX in the presence of Hydroxypropyl-*b*-Cyclodextrin (HP-*b*-CD). HP-β-CD was used in an effort to stabilize putative early intermediates such as pentahydro-3,5-dinitro-1,3,5-triazacyclohex-1-ene and its ring cleavage products 4,6–dinitro-2,4,6-triaza-hexanal ($O_2NNHCH_2NNO_2CH_2NHCHO$), and 5-hydroxy-3-nitro-2,4-diaza-pentanal ($HOCH_2NNO_2CH_2NHCHO$) by forming inclusion complexes. RDX (0.1 g) or [^{15}N]-RDX (0.1 g) was placed in a vial, followed by the addition of 10 mL NaOH (pH 12.3) in 65:35 (v/v) acetonitrile:water containing 3 % (wt/v) HP-β–CD. Hydrolysis and sample preparation for subsequent analysis was conducted as discussed above.

Product analysis. The concentration of RDX, MNX and HMX was determined using a reversed-phase HPLC connected to a photodiode array (PDA) detector, as described previously (Fournier et al., 2002). Formaldehyde (HCHO) (Summers, 1990), $^{15}N^{14}NO$ (45 Da) and $^{14}N^{14}NO$ (44 Da) analyses were carried out as described by Sheremata and Hawari (2000). Analyses of nitrite (NO_2^-), nitrate (NO_3^-), formate ($HCOO^-$) and ammonium (NH_4^+) were performed by capillary electrophoresis on a Hewlett-Packard 3D-CE equipped with a Model 1600 photodiode array detector and a HP capillary part number 1600-61232. The total capillary length was 64.5 cm, with an effective length of 56 cm and an internal diameter of 50 μm. For nitrite, nitrate and formate, analyses were performed using sodium borate (25 mM) and hexamethonium bromide (25 mM) electrolytic solution at pH 9.2 (Okemgbo et al., 1999). The ammonium cation was analyzed using a formic acid (5 mM), imidazole (10 mM) and 18-crown-6 (50 mM) electrolytic solution at pH 5. In all cases, UV detection was performed at 215 nm.

A Micromass bench-top single quadrupole mass detector attached to a Hewlett Packard 1100 Series HPLC system equipped with a DAD detector was used to analyze for RDX ring cleavage intermediates (Hawari et al., 2000a).

IV.13 Identification of intermediates during photolysis of RDX in aqueous solutions at 350 nm: insight into biodegradation pathways.

- Hawari, J., Halasz, A., Groom, C., Deschamps, S., Paquet, L., Beaulieu, C., and Corriveau, A. 2002. Photodegradation of RDX in aqueous solution: a mechanistic probe for biodegradation with *Rhodococcus* sp. Environ. Sci. Technol. 36: 5117-5123.

***Irradiation experiments and products formation*.** A Rayonet photoreactor RPR-100 fitted with a merry-go-round apparatus (Southern New England Co, Hamden, CT) equipped with sixteen 350 nm lamps were used as light sources. Photolysis was conducted in 20 mL tubes made of quartz. Each tube was charged with 10 mL of an aqueous solution of RDX (10 mg/L) in the presence and absence of acetone (250 ppm, v/v). Photolysis was carried out in non-degassed quartz tubes sealed with Teflon coated mininert valves. Controls containing RDX were kept in the dark during the course of the experiment. The temperature of the reactor was maintained at 25 ^{o}C by maintaining the apparatus in a cold room at 10 ^{o}C during irradiation. Light intensities, λ 350 = 3.0 10^{-6} einstein $mL^{-1}s^{-1}$ (RPR-350 nm lamp tubes emitting > 90 % of their energy at 350 nm) were measured using ferrioxalate actinometry.

Product analysis. Analysis of 3,5-dinitro-1,3,5-triaza-cyclohex-1-ene was carried out on a Hewlett Packard 6890 gas chromatograph coupled to a 5973 quadrupole mass spectrometer in the positive chemical ionization (PCI) mode using methane. Five μL ethyl acetate extracts of the photolyzed mixture were injected in the solvent vent mode i.e. at 10 ^{o}C maintained 0.15 min. then fast heated to 200^{o}C under splitless condition on a 15 m x 250 um x 0.5 um RTX-5 amine capillary column from Restek. Helium was used as the carrier gas with an average velocity of 27 cm/sec. The column was heated at 55^{o}C for 3 min. then raised to 200^{o}C at a rate of 10^{o}C/min, which was held for 2 min. The detector interface was maintained at 200^{o}C. The quadrupole and the source were held at 106 and 150 ^{o}C, respectively. The product was detected as its protonated molecular mass ion [M + H]. The cyclic carbinol intermediate 4,6-dinitro-2,4,6-triaza-*c*-hexanol ($C_3H_8N_5O_5$), its ring cleavage product 4,6-dinitro-2,4,6-triaza-hexanal ($C_3H_8N_5O_5$) and their subsequent hydrolyzed products including methylenedinitramine and 4-nitro-2,4-diazabutanal were also analyzed using LC/MS (ES-) and reference standards when available.

Formamide was derivatized with O-(2,3,4,5,6-pentafluorobenzyl)hydroxylamine.HCl (PFBHA) for 30 min. at 80 ^{o}C, and analyzed by LC/MS (ES-) using a 5 µm Supelcosil LC-8 column (4.6 mm ID x 25 cm) (Supelco, Oakville, ON) maintained at 35 ^{o}C. The solvent system consisted of acetonitrile / water gradient (50 to 90 % v/v) at a flow rate of 1 mL/min. Detection was done by monitoring its [M-H] mass ions. Nitrous oxide (N_2O) and formaldehyde (HCHO) were analyzed as described above. Formic acid, NO_2^- and NO_3^- and $NH4^+$ were analyzed using an SP 8100 HPLC system equipped with a Waters 431 conductivity detector and a Hamilton PRP-X200 (250 mm x 4.6 mm x 10 µm) analytical cation exchange column as described earlier in the report (Hawari et al., 2001). For trace concentrations, NH_4^+ was measured by capillary electrophoresis using a HP^{3D} CE instrument model 1600 equipped with a diode array detector. The system was fitted with an Agilent G16006132 fused silica capillary with a total length of 64.5 cm (56 cm effective length) and an internal diameter of 50 µm. The voltage was set at 15 kV (positive polarity) and the temperature at 25^{o}C. Samples were injected by applying 50 mbar pressure to the capillary inlet for 50 s. The electrolyte solution was prefiltered and buffered with lactic acid at pH 3.5. 18-crown-6 was added as an anion flow modifier. Separation time was 15 minutes. Indirect detection at 350 nm was used with imidazole as the background absorbing ion. The detection limit was 50 ppb. Measurement of methanol was made on a Hewlett Packard 6890 gas chromatograph coupled to a FID. 1 µL of water sample was injected on a 2 m x 0.03 mm Hayesep Q micropacked column from Supelco. The column was heated at 60^{o}C for one minute then raised to 180^{o}C at a rate of 20^{o}C/min. Helium was used as the carrier gas. The injector and detector were maintained at 150 ^{o}C and 250 ^{o}C respectively. Standards were prepared from neat compounds from J.T. Baker. The detection limit was 0.25 ppm.

IV.14 Biodegradation of RDX and HMX in Soil under Anaerobic Conditions

Microcosm preparation. Soil contaminated with high levels of RDX (1075 mg kg^{-1}, 8.8 % RSD) and HMX (385 mg kg^{-1}, 7.7 % RSD) was obtained from Valleyfield, Quebec. The soil was air dried and passed through a 10-mesh sieve prior to use. The soil was kept out of contact with light to avoid photodecomposition of RDX. Two grams of soil was incubated

with 8 mL of either deionized water or 0.2 % glucose (filter sterilized). All microcosms were prepared in sterile 20 mL headspace vials, capped with sterile Teflon coated septa and sealed with aluminum crimps. Microcosms were subsequently flushed with argon for 15 minutes and incubated at 37°C (200 rpm). All vials were placed horizontally to enable maximum agitation of the soil slurry. Microcosms with anaerobic sludge were prepared as described previously (Halasz et al., 2002) using 20 % w/v of soil, 2 g/l of glucose or 8 g/l of nutrient broth and 10 % v/v of sludge. Microcosms were subsequently opened and the redox potential (E_h) and pH were measured using an Accumet Basic AB15 meter (Fisher Scientific). No attempts were made to control either of these parameters during incubation.

Product analysis. Anaerobic microcosms were sacrificed at regular intervals over a 27day period. Prior to sacrifice, nitrous oxide (N_2O) was analyzed as described previously (Fournier et al., 2002). Three mL of the soil slurry was removed, centrifuged (13,000 rpm, 5 minutes) and 2.3 mL of the supernatant was filtered through a 0.45 μm Millipore filter and saved for further analysis. The solid fraction was frozen and lyophilized overnight. The dried soil was then resuspended in 10 mL of acetonitrile and sonicated for two hours. Five mL of the supernatant was mixed with an equal volume of $CaCl_2$ (5 g/L), filtered and the filtrate was analyzed for RDX and HMX as described below. The concentrations of RDX, MNX, TNX and HMX were determined with a reverse-phase high-pressure liquid chromatograph connected to a photodiode array detector (PDA), as described previously (see section IV.8.3). DNX concentrations were estimated based on the linear relationship of peak area and UV-230 nm absorbance of RDX, MNX and TNX. Methylenedinitramine and 4-nitro-2,4-diazabutanal were analyzed with a Micromass benchtop single quadrupole mass detector connected to a Hewlett-Packard 1100 series HPLC system equipped with a photodiode array detector. Ionization was carried out in the negative electrospray mode ES(-), and the target was detected as its $[M–H]^-$ molecular mass ion as described previously (Halasz et al., 2002). Formaldehyde was analyzed as described by Fournier et al. (2002).

V PROJECT ACCOMPLISHMENTS

The following chapters are intended to provide the reader with an overview of our laboratory experimental findings that led to the discovery of the microbial degradation pathways of RDX and HMX under both aerobic (*Rhodococcus*) and anaerobic conditions (sludge and several of its isolates: *Klebsiella, Clostridium*). Sections 1 and 2 will highlight the discovery of two key ring cleavage products, namely, methylenedinitramine and 4-nitro-2,4-diazabutanal, considered crucial for the discovery of the degradation pathways. Later the two key products were produced by several commercial enzymes (Cytochrome P450, Nitrate reductase, Diaphorase), indicating that once a microbial or enzymatic attack occurs on these cyclic compounds the respective molecule undergoes a spontaneous ring cleavage and decomposition in water. We tested our hypothesis by conducting initial attacks, most notably denitration, by photolysis, hydrolysis and electrolysis and in all cases we were able to reproduce the degradation pathways observed for these nitramines under both aerobic and anaerobic conditions. The discovery of these pathways will undoubtedly help engineers optimize processes for the remediation of contaminated sites.

V.1 Biodegradation of RDX and HMX with anaerobic sludge: Discovery of methylenedinitramine. " The removal of the first bottleneck in the understanding of the degradation pathways of RDX and HMX".

We used a combination of chemical and biochemical techniques to identify, for the first time, methylenedinitramine as a key ring cleavage product of RDX and HMX.

Using LC/MS and ^{15}N-[RDX] we initially identified the chemical as methylenedinitramine ($CH_4N_4O_4$). Later we synthesized the chemical and thus were able to confirm our identification of the metabolite as methylenedinitramine ($O_2NNHCH_2NHNO_2$, MEDINA). The discovery of MEDINA allowed us to understand the reactions(s) that led to its formation and the secondary reactions that led to its spontaneous decomposition in water, thus providing new insight into our understanding of the biodegradation pathways of cyclic nitramines. Details are found in the subsequent sections.

V.1.1 Biodegradation of RDX and HMX with anaerobic sludge: discovery of methylenedinitramine.

- Halasz, A., Spain J., Paquet L., Beaulieu C. and Hawari J. **2002**. Insights into the Formation and Degradation Mechanisms of Methylenedinitramine during the Incubation of RDX with Anaerobic Sludge. Environ. Sci. Technol., **36**: 633-638.

Cleavage of RDX in sludge and the formation of methylenedinitramine. Incubation of either RDX or HMX with anaerobic sludge produced an intermediate whose LC/MS(ES-) produced a $[M–H]^-$ at 135 Da, matching an empirical formula of $CH_4N_4O_4$. The intermediate was tentatively identified as methylenedinitramine, $O_2NNHCH_2NHNO_2$ (Hawari et al. 2000a). Later we were able to synthesize methylenedinitramine in collaboration with Dr. Spanggord (SRI, Menlo Park, Ca.), and thus we were able to confirm the product as methylenedinitramine by comparing their deprotonated molecular mass ions $[M-H]^-$ and chromatographic retention times, r.t.

Figure 1A is a typical LC/MS(ES-) spectrum of the metabolite obtained after incubating RDX in the anaerobic sludge for 20 h at pH 7.0 while Figure 1B is the LC/MS(ES-) spectrum of a standard sample of methylenedinitramine. Both the product from RDX biodegradation (Figure 1A) and the standard (Figure 1 B) showed their $[M-H]^-$ and r.t. at 135 Da and 4.3 min, respectively. We found that methylenedinitramine itself is unstable and decomposed spontaneously in water to give N_2O and HCHO in the presence and absence of sludge (Figure 2a,b).

Interestingly, we found that methylenedinitramine (7.5 μmoles) decomposed much faster in pure water (> 90 %) than in the incubation mixture with sludge (< 5 %) (Figures 2a,b). It has been reported that methylenedinitramine undergoes spontaneous decomposition in water, but can be stabilized at highly acidic conditions by forming its salt (McDonnell, 1978; Sauer and Follett, 1955; and Urbanski, 1967).

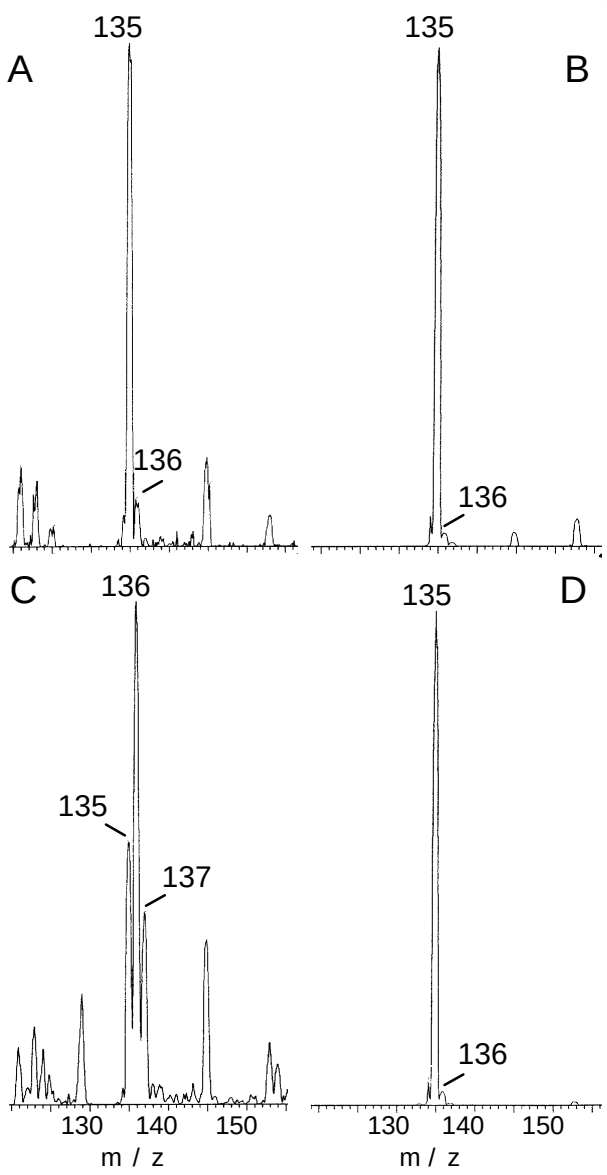

Figure 1. Mass spectra of methylenedinitramine obtained using LC/MS (ES-). A: during biodegradation of RDX with anaerobic sludge in H_2O, B: as standard in H_2O, C: during biodegradation of RDX with anaerobic sludge in D_2O, and D: as standard in D_2O. The trace amounts of the 136 Da observed in (A, B and D) are caused by the natural abundance of the ^{13}C-isotope (1.1 %) in the molecule.

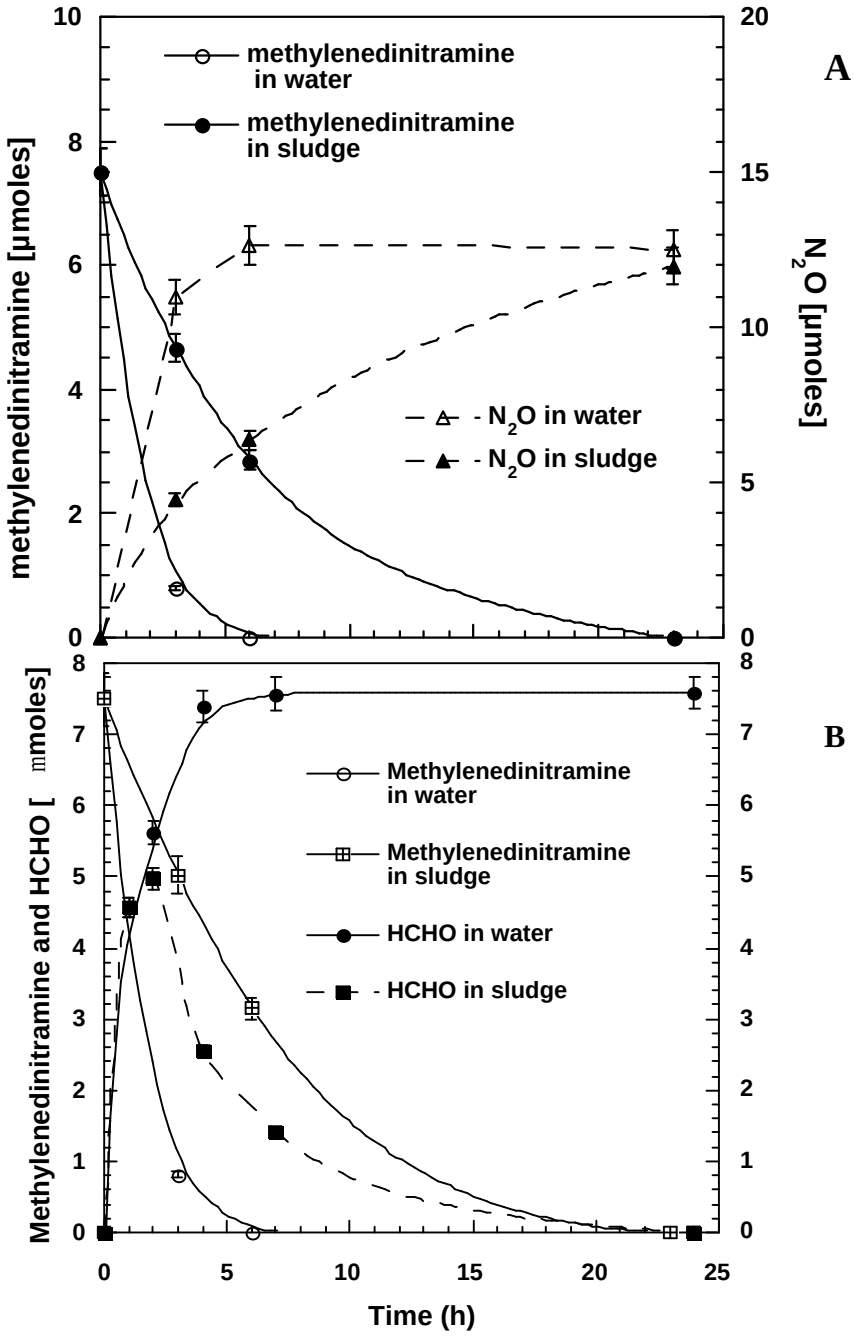

Figure 2. Decomposition of methylenedinitramine in water and sludge shows the formation of (**A**) nitrous oxide and (**B**) formaldehyde.

Despite differences in the rates of decomposition of methylenedinitramine in the above solutions we found that its decomposition patterns in water or sludge were similar and both produced N_2O (Figure 2a) and HCHO (Figure 2 b). The yield of N_2O was 83 % in both sludge and water whereas the yield of HCHO in water was 100 %. Only in incubation mixtures containing sludge was HCHO bioconverted to CO_2. The above observation was confirmed by incubating HCHO (30 mg/L) spiked with $H^{14}CHO$ (0.06 μCi) in anaerobic sludge. More than 60 % of HCHO (30 mg/L) mineralized (liberated $^{14}CO_2$) in 24 h. We did not observe mineralization in controls containing autoclaved sludge and the aldehyde, suggesting that RDX mineralization occurred *via* HCHO produced from autodecomposition of methylenedinitramine.

Cleavage of RDX with sludge in the presence of D_2O. In an attempt to study the role of water in the biodegradation of RDX and the formation of methylenedinitramine we allowed the compound to biodegrade in the presence of several aqueous solutions that contained different amounts of heavy water, D_2O (90, 50 and 0 % v/v). In the presence of water RDX biodegradation lead to the appearance of the deprotonated mass ion 135 Da which was attributed to methylenedinitramine by comparison with a standard material, whereas in the presence of D_2O (90 % v/v in water) the incubation mixture degraded RDX and produced mass ions at 135, 136 and 137 Da (Figure 1C). We found that the relative distribution of the detected mass ions depended on the amount of D_2O in the solvent mixture used during RDX incubation with sludge (Table 1). In the absence of D_2O we only detected the 135 Da mass ion whereas in the presence of 90 and 50 % D_2O/H_2O, the abundance of the mass ion 135 Da decreased and those of the other two mass ions 136 and 137 Da increased (Table 1).

Since we employed negative electrospray ionization (ES-) during mass analysis, the detected mass ions should represent the deprotonated $[M\text{-}H]^-$ (or dedeuterated [M-D]) ions. Accordingly, the mass ions detected at m/z 135, 136 and 137 Da can best be explained as due to the formation of nondeuterated, H-methylenedinitramine (MW 136 Da), monodeuterated, D_1-methylene dinitramine (MW 137 Da) and dideuterated, D_2-methylenedinitramine (MW 138 Da) methylenedinitramine, based on the loss of either H (1 Da) or D (2 Da) from the corresponding parent molecule (Figure 3).

Table 1. Incubation of RDX with anaerobic sludge in the presence of D_2O.

% of D_2O	Mass distribution (%)		
	135 Da	136 Da	137 Da
0	100	0	0
50	47	43	10
90	27	52	21

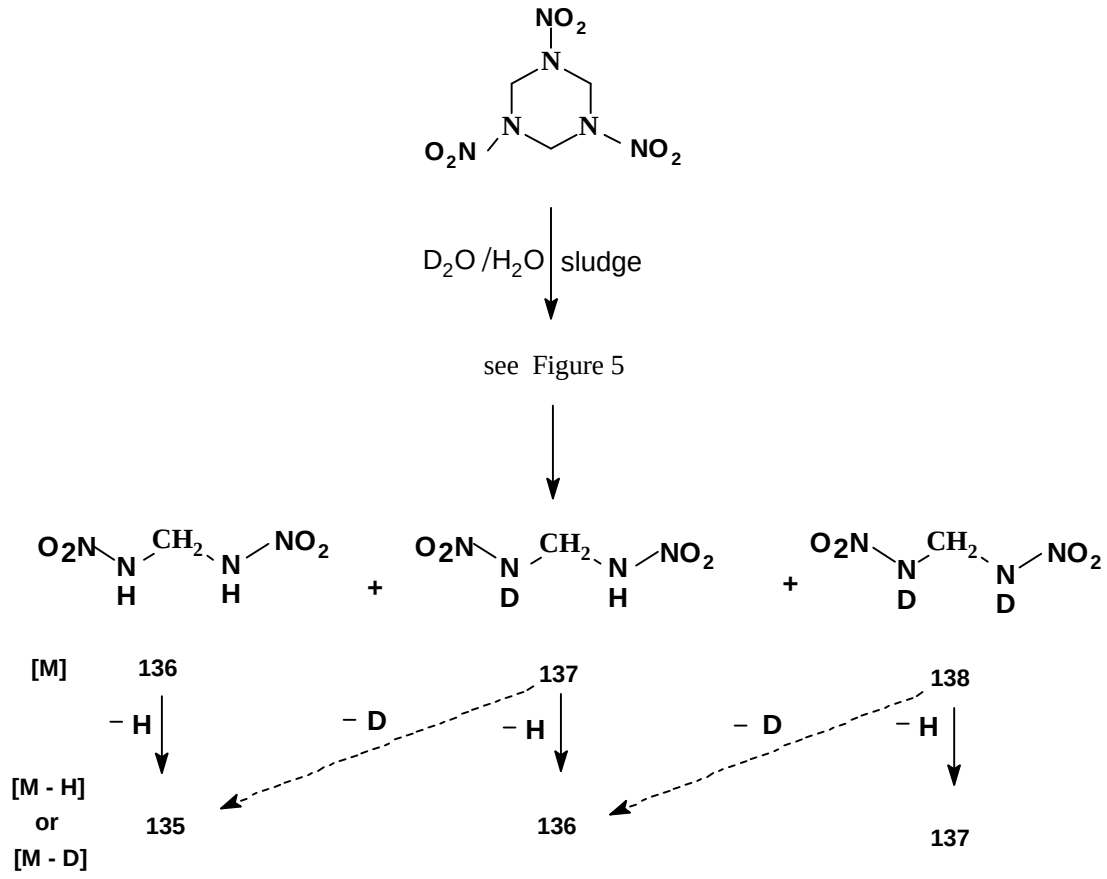

Figure 3. Deuterium distribution in methylenedinitramine metabolite produced during RDX incubation with anaerobic sludge. The Figure explains the loss of either H (or D) from methylenedinitramine during negative electrospray ionization.

As Figure 3 shows, the loss of either H from H-methylenedinitramine or D from D-methylenedinitramine would give the detected mass ion at 135 Da, whereas the loss of either H from D_1-methylenedinitramine or D from D_2-methylenedinitramine would give the mass ion detected at 136 Da. It is only the loss of H from D_2-methylenedinitramine that could give the mass ion at 137 Da. During mass ionization (ES-), each of the two amino nitrogen atoms ($\underline{N}$-NO_2) in methylenedinitramine, originally the inner amino N atoms in RDX, could lose its acquired H or D (Figure 3). The possibility of losing H from the methylene group, CH_2, during ionization of methylenedinitramine in the mass detector should not be excluded.

When we introduced methylenedinitramine into buffered D_2O we were unable to observe either the 136 Da or the 137 Da mass ions, eliminating the possibility of the occurrence of any H-D exchange between methylenedinitramine and the solvent D_2O (Figure 1 D). Also we were unable to observe any deuterated methylenedinitramine when we mixed RDX with D_2O in the absence of the sludge and thus were able to confirm the absence of H-D exchange between RDX and the solvent D_2O. The complex distribution of the above non-deuterated and deuterated methylenedinitramine products (Figure 3) confirmed the direct involvement of water, but not stoichiometry, in the formation of methylenedinitramine.

Insights into the Formation Mechanisms of Methylenedinitramine. The above experiments provided clear evidence on the formation of methylenedinitramine and its decomposition routes during RDX incubation with sludge, but whether methylenedinitramine was formed *via* direct enzymatic hydrolysis of RDX (Figure 4, *path a*) or through the subsequent spontaneous hydrolysis of another, as yet unidentified initial enzymatic product (Figure 4, *path b, c*) is unclear.

We hypothesize that water might participate in the enzymatic cleavage of the inner C-N bonds in RDX *via* a hydroxylase to give the hydroxyalkylnitramine ring cleavage product (I) (Figure 4, *path a*) (Hawari et al 2001). Alternatively, water might abiotically hydrolyze another initial enzymatic RDX product such as the ring cleavage intermediate (III) of the carbinol (II) (Figure 4, *path b*) or the hydroxylamino derivative (IV) of MNX (Figure 4, *path c*).

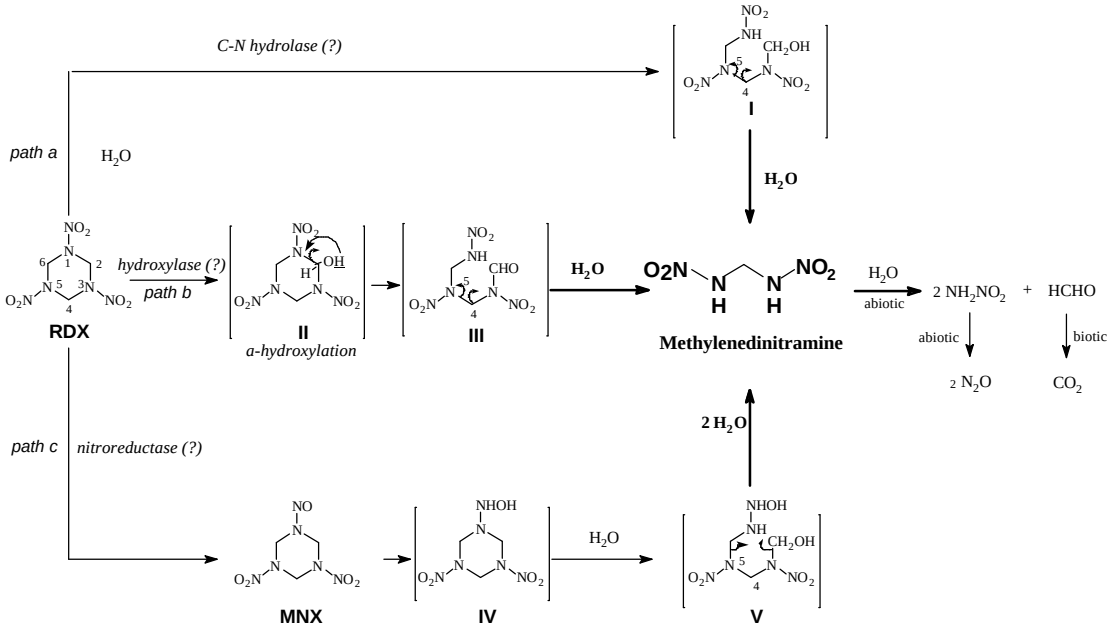

Figure 4. Postulated routes for the production of methylenedinitramine during RDX incubation with anaerobic sludge.
a: direct enzymatic hydrolysis to the hydroxyalkyl nitramine derivative (I).
b: enzymatic hydroxylation to carbinol (II) with subsequent rearrangement to intermediate III.
c: formation of mononitroso-RDX (MNX) which upon reduction to the hydroxylamine derivative (IV) would cleave to produce an unstable hydroxylamine (V). Small inverted arrows symbolize bonds that are hydrolyzed by water to produce methylenedinitramine. Square brackets for undetected compounds. Biotic and abiotic steps are shown on the respective arrows.

We have no solid evidence on the formation of metabolite (I) to prove the occurrence of a direct enzymatic ring cleavage of RDX (Figure 4, *path a*). Also, the closest literature precedent we could find in support of the carbinol (II) mechanism (Figure 4, *path b*) is the aerobic metabolism and alkaline hydrolysis of cyclic and acyclic nitrosamines (Roller et al., 1975; Okada et al., 1980; Druckrey, 1973). For instance, it has been reported that nitrosamines biotransform *via* a mixed function oxidase to produce first the unstable carbinol

products *via* α-hydroxylation. These carbinols then decompose to produce nitrogen and cationic alkyl groups, R^+ (Druckrey, 1973). However, our present process is anaerobic and enzymatic hydroxylation is often aerobic.

Previously McCormick et al. (1981) proposed a pathway for the anaerobic biodegradation of RDX based on the formation of the three nitroso products MNX, DNX and TNX which in turn reduce to the corresponding hydroxylamine derivatives. The end products in the published pathway of McCormick et al. are HCHO, MeOH, hydrazine and 1,2- and 1,1-dimethylhydrazine (McCormick et al., 1981). In our case we did not detect any hydrazine but rather we observed nitrous oxide as a major nitrogen-containing product. The production of nitroso derivatives during anaerobic degradation of RDX has frequently been observed (Adrian and Chow, 2001; Kitts et al., 2000), but initial enzymatic reactions that take place on RDX are still not known.

In an attempt to gain more insight about the mechanisms of formation of methylenedinitramine we determined the stoichiometry of its formation during RDX biodegradation with the sludge. Figure 2a shows that 83 % of the methylenedinitramine converted to N_2O during incubation with sludge within 24 h (assuming that each mole of methylenedinitramine decomposed to give two moles of N_2O). Meanwhile, data in Figure 5 show that 60 μmoles of RDX biodegraded to give 97 μmoles of N_2O during incubation with sludge, suggesting that a 48.5 μmoles of methylenedinitramine were produced. Taking into account that only 83 % of converted methylenedinitramine lead to the production of N_2O, the actual amount of methylenedinitramine would be 58.4 μmoles, implying that for each mole of reacted RDX roughly one mole of methylenedinitramine produced. The above measured stoichiometry did not favor one route over the other in Figure 4 since each route gives 1 molar equivalent of methylenedinitramine for each mole of reacted RDX.

As long as the initial enzyme(s) and / or the specific isolate(s) that lead to initial RDX ring cleavage remain unknown, it may not be possible to resolve which route in Figure 4 was responsible for the formation of stoichiometric amounts of methylenedinitramine.

Generally speaking, alkylnitramine and hydroxyalkylnitramines are both unstable in water and hydrolyze readily with no apparent selectivity on which C-N bond should cleave first to produce HCHO and NH_2NO_2**,** (Urbanski, 1967; Lamberton et al., 1949a,b; Croce and

Okamoto,1979). We thus hypothesize that once the RDX ring is cleaved during incubation with sludge the resulting products, including methylenedinitramine and other initial RDX ring cleavage products, could also hydrolyze spontaneously at any C-N bond. Figure 4 only shows the reactions that can lead to methylenedinitramine, but as discussed above, other products should also be expected depending on which C-N bond in the postulated RDX initial products (I, III or V) is hydrolyzed first. In fact, in addition to methylenedinitramine we detected traces of another transient product with $[M-H]^-$ at 121 Da and tentatively identified it as dimethanol nitramine, $(HOCH_2)_2NNO_2$ using uniformly ring labeled ^{15}N-RDX (Hawari et al., 2000a).

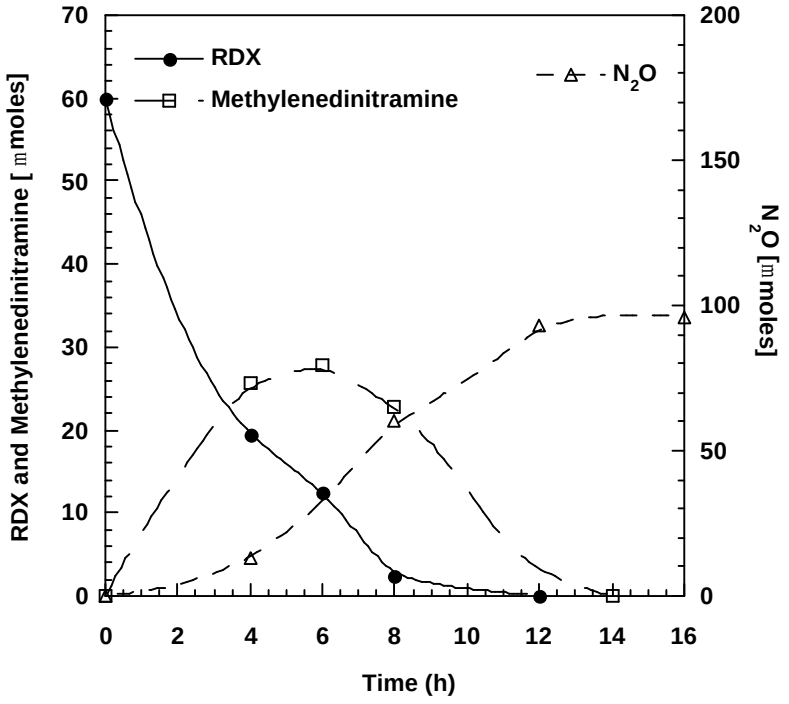

Figure 5. A time course study for the disappearance of RDX (200 mg/L) and the appearance and disappearance of methylenedinitramine and N_2O during treatment with anaerobic sludge.

RDX is characterized by the presence of several functional groups including the -N-NO_2, the inner C-N and the methylene C- H bonds, all of which can act as potential targets for initial enzymatic attack. Also, the sludge used in the present study is expected to contain a complex microbial community that can provide a wide range of enzymes such as hydrolases (Figure 4,

path a), hydroxylases (Figure 4, *path a*), and nitroreductases (Figure 4, *path a*). Therefore it should not be surprising to have (predict) more than one degradation route during RDX incubation with sludge.

The detection of the MNX, although in trace amounts, might support the nitroso route for the production of methylenedinitramine (Figure 4, *path c*). These pathways will become more clear when bacterial isolates from sludge are used (see Section 5.2).

The present study provided the first experimental evidence on the formation of methylenedinitramine, as a key RDX ring cleavage metabolite. Also we found that methylenedinitramine was unstable in water and decomposed spontaneously to N_2O and HCHO. The routes to methylenedinitramine are still controversial, but, they provided insight into most of the secondary steps involved during RDX biodegradation, and thus brought us one step closer to understand the primary step(s) involved in the initial enzymatic reactions on RDX. Therefore the subsequent chapters will focus on the enzyme(s) responsible for initiating the attack on RDX and on the determination of their initial intermediates, particularly MNX, and their subsequent degradation products.

V.1.2 Biotransformation of Octahydro-1,3,5,7-tetranitro-1,3,5,7-tetrazocine (HMX) by Municipal Anaerobic Sludge.

- Hawari, J., A. Halasz, S. Beaudet, L. Paquet, G. Ampleman, and S. Thiboutot. **2001**, Biotransformation of Octahydro-1,3,5,7-tetranitro-1,3,5,7-tetrazine (HMX) to Nitrous Oxide by Municipal Anaerobic Sludge. Environ. Sci. Technol. **35**: 70-75.

The LC/MS ES(-) of HMX after treatment with domestic anaerobic sludge over a period of 6 days (Figure 1) showed several peaks with deprotonated molecular mass ions [M-H] appearing at m/z 279, 263 and 263 Da, matching molecular mass formulas of $C_4H_8N_8O_7$, $C_4H_8N_8O_6$ and $C_4H_8N_8O_6$, respectively. Using the above obtained deprotonated molecular mass ions [M-H], the peaks are tentatively identified as mononitroso (octahydro-1-nitroso-3,5,7-trinitro-1,3,5,7-tetrazocine) [279 Da], mNs-HMX, and two isomers of the dinitroso derivative (octahydro-1,3-dinitroso-5,7-dinitro-1,3,5,7-tetrazocine) [263 Da], and (octahydro-1,5-dinitroso-3,7-dinitro-1,3,5,7-tetrazocine) [263 Da], dNs-HMX. We did not detect any of

the trinitroso derivative, although this compound was formed as a major product during biodegradation of HMX in soil slurry (30 % w/v) using the same type of sludge (Shen et al., 2000).

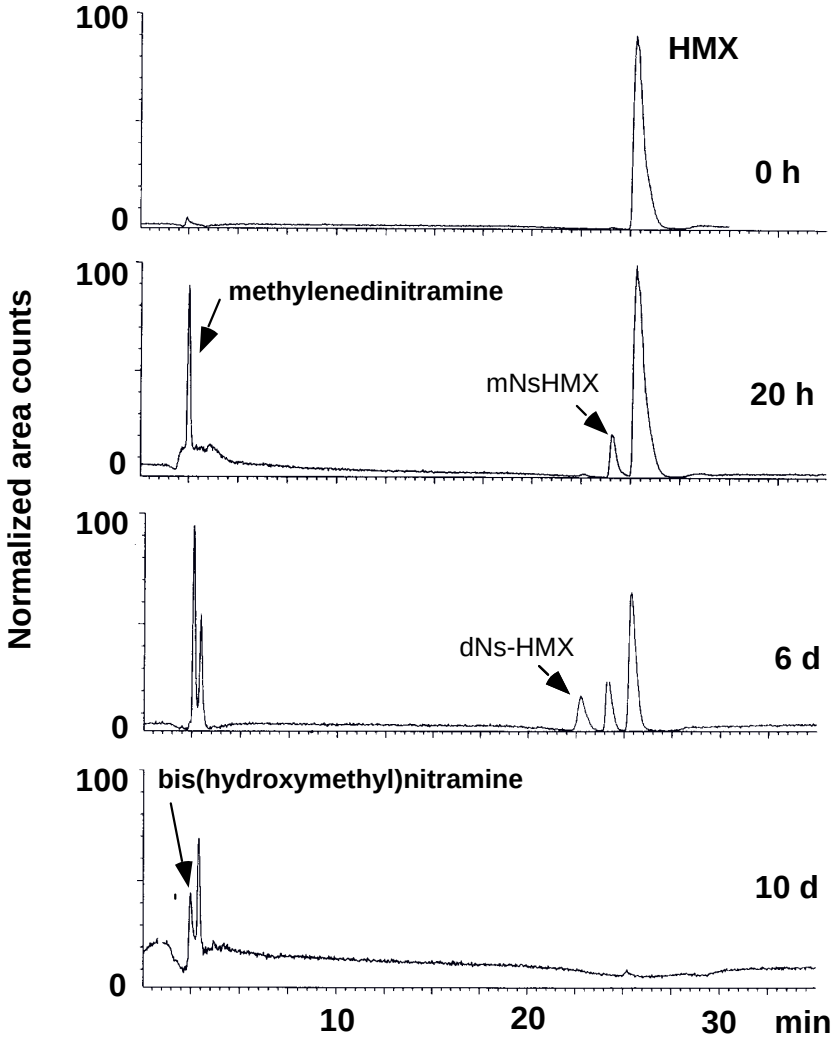

Figure 1. An LC/MS (ES-) time course of biotransformation of HMX (100 mg/L) with a domestic anaerobic sludge in the presence of glucose as a carbon source at pH 7.0. The y-axis represents normalized area counts.

None of the above nitroso derivatives accumulated in the system indefinitely. They disappeared with no clear indication of their actual fate. We did not observe any

hydroxylamino derivatives, HOHN-HMX, described earlier during biodegradation of RDX with anaerobic sludge by McCormick et al. (1981).

Other studies reported the formation of nitroso derivatives during biodegradation of RDX and/or HMX with either soil isolates (*Providencia rettgeri, Citrobacter freundii*, *Morganella morganii*) of the *Enterobacteriaceae* family (Kitts et al., 1994) or consortia of a horse manure under O_2-depleting conditions (Young et al., 1997a,b).

Ring cleavage intermediates. The LC/MS chromatogram of the sludge treated HMX also showed the initial presence of several other peaks and presumed to be ring cleavage products of the original HMX molecule (Figure 1). For instance, one LC/MS peak showed a deprotonated molecular mass ion $[M\text{-}H]^-$ at 135 Da, matching a molecular mass formula of $CH_4N_4O_4$ (MW 136 Da). Another characteristic mass ion was detected at m/z 61 Da, representing the fragment mass ion $-HNNO_2$. The LC/MS (ES-) of this metabolite matched perfectly with a standard material of methylenedinitramine detected earlier during incubation of RDX with sludge from the same source (previous chapter). Meanwhile, another LC/MS peak showed a deprotonated molecular mass ion $[M\text{-}H]^-$ at 121 Da matching a molecular mass formula of $C_2H_6N_2O_4$ (MW 122 Da). Other relevant mass ions included one at m/z 139 Da representing $[M\text{-}H+H_2O]$. We idenfied the peak by comparing its chromatographic and mass data (retention time and mass ion) with those obtained earlier from the degradation of RDX with sludge taken from the same source (Hawari et al., 2000a). Both RDX and HMX gave the same product at the same retention time (3.09 min). In the case of RDX the peak was tentatively identified using ring labeled [^{15}N]-RDX as the ring cleavage product bis(hydroxymethyl)nitramine, $(HOCH_2)_2NNO_2$. Likewise, we tentatively identified the 3.09 min LC/MS peak observed during treatment of HMX with the sludge as the ring cleavage product bis(hydroxymethyl)nitramine. This is not surprising in view of the fact that the two cyclic nitramines RDX and HMX are structurally similar. Both compounds are cyclic oligomers (trimer and tetramer, respectively) of the same chemical unit methylenenitramine, $CH_2\text{–}N\text{–}NO_2$, [$(CH_2NNO_2)_3$ and $(CH_2NNO_2)_4$].

Furthermore, we detected several other LC/MS peaks including one that showed a $[M\text{-}H]^-$ at m/z 121 Da, matching a molecular mass formula of $CH_6N_4O_3$ (MW 122). Other relevant

mass ions in this peak included one at m/z 139 Da representing the solvent adduct [M-H+H_2O] and another at m/z 46 Da, representing the fragment mass ion -NO_2 (m/z 46 Da). The peak was tentatively identified as N-nitro-N'-hydroxylamino-methylenediamine, $O_2NHNCH_2NHNHOH$. We are not sure at the present time whether the product is a reduced form of the previously formed methylenedinitramine, $O_2NHNCH_2NHNO_2$, or is a ring cleavage product of the hydroxylamine-derivative of HMX, HOHN-HMX. McCormick et al. (1981) postulated the presence of HOHN-RDX during biotreatment of RDX with anaerobic sludge, but did not observe them.

None of the above HMX ring cleavage products accumulated indefinitely. They all disappeared and produced predominantly formaldehyde (HCHO) and nitrous oxide (N_2O). The presence of formaldehyde as HMX degradation product was confirmed by the detection of $H^{14}CHO$ using [UL-^{14}C]-HMX. We were also able to detect formic acid and confirmed this by the detection of $H^{14}COOH$. Eventually HCHO (bio)transformed to carbon dioxide (detected as $^{14}CO_2$).

Neither N_2O nor $^{14}CO_2$ was observed in controls containing either the buffer and HMX or HMX and dead biomass. Roughly 40 % of total HMX initial concentration (100 mg/L) was attributed to mineralization ($^{14}CO_2$) after 40 days of incubation. Furthermore, methane ($^{14}CH_4$) was detected and confirmed by the use of uniformly labeled [UL-^{14}C]HMX. Neither hydrazine (NH_2NH_2), nor dimethylhydrazine ($(CH_3)_2NNH_2$), reported earlier by McCormick et al. (1981) was observed in either the present study or the previously described RDX study (Hawari et al., 2000a).

On the other hand we detected nitrogen when HMX was treated with the sludge under a blanket of argon. The two gases were also observed during RDX biodegradation with the same sludge whose formation was confirmed by the detection of $^{15}N^{14}NO$ (m/z 45 Da) and $^{15}N^{14}N$ (m/z 29 Da). Using ring labeled ^{15}N-[RDX] and ^{15}N-[HMX] neither gas was detected in controls that contained neither RDX nor HMX.

Time course study and the degradation pathway. Figures 2a and b represent time course studies for the disappearance of HMX and the appearance of N_2O, N_2 and CO_2 in the

presence and absence of glucose, respectively. Roughly 50% of the total nitrogen content of reacted HMX (90 %) was detected as gaseous nitrogen and nitrous oxide. Using solubility data another 4 % of N_2O could be accounted for as a dissolved fraction in the aqueous phase (Weis and Price, 1980). Formaldehyde did not accumulate and its disappearance was accompanied by the formation of formic acid, HCOOH, methane, CH_4 and carbon dioxide, CO_2.

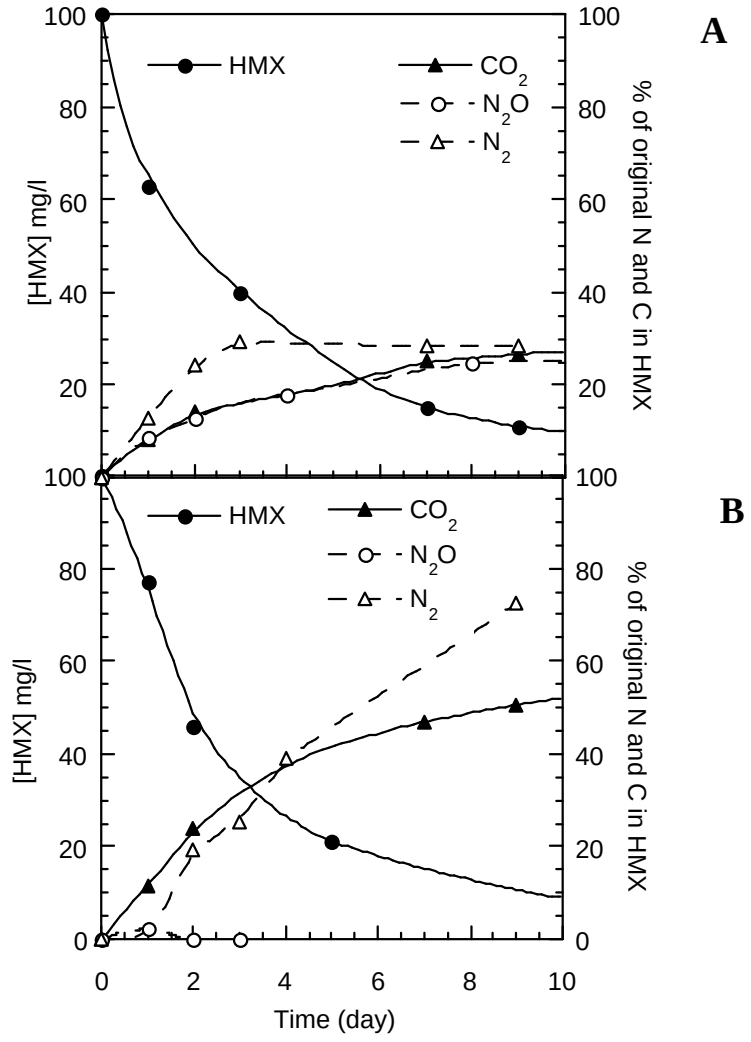

Figure 2. A time course study for the biotransformation of HMX with the domestic anaerobic sludge. **A** (top): in the presence of glucose and **B** (bottom): in the absence of glucose.

The concentrations of HCHO and HCOOH were not high enough and thus are excluded from

Figure 2. This is in contrast to RDX where we successfully measured HCHO and the ring cleavage product methylendinitramine with time (Hawari et al., 2000a). This is possibly caused by a lower biological reactivity of HMX as compared to RDX. It is known that HMX is less water soluble (5 mg/L) than RDX (40 mg/L) (Talmage, 1999) and is chemically more stable (Akhavan, 1998).

Furthermore, controls containing either HMX in a phosphate buffer (pH 7) in the absence of the sludge or HMX in a killed biomass did not give any of the previously described nitroso or ring cleavage products, indicating the essential role of enzymatic reactions on HMX. We expect the domestic sludge used in the present study to contain a microbial community capable of producing several enzymes including nitroreductases and hydrolases. Recently Kitts et al. (2000) reported degradation of RDX by the enteric bacteria *Morganella morganii via* the oxygen insensitive type I nitroreductase. Subsequent reduction by the same type of nitroreductase would produce nitroso-HMX products (Figure 3, *path a*) and the corresponding HOHN-HMX products which were implicated as prerequisite entities prior to ring cleavage in the pathway described for RDX by McCormick et al. (1981). Neither the present study nor the earlier study on RDX revealed the presence of these hydroxylamino derivatives (Hawari et al., 2000a).

We have no evidence at the present time of the direct involvement of any of the above-mentioned enzyme in the degradation process. However, we speculate that the presence of a hydrolase enzyme in the sludge (or an enzyme leading to α-hydroxylation of a CH_2 group) might cleave a C-N bond in HMX to give the primary nitramine product $HOCH_2$-$[CH_2NNO_2]_3$-$NHNO_2$ containing two reactive terminal functional groups, a -CH_2OH and -$NHNO_2$ (Figure 3, *path b*).

Such compounds are not stable in water and their spontaneous decomposition (enzymatic or chemical) in water would eventually produce nitramine, NH_2NO_2, and HCHO (Figure 3, *path b*).

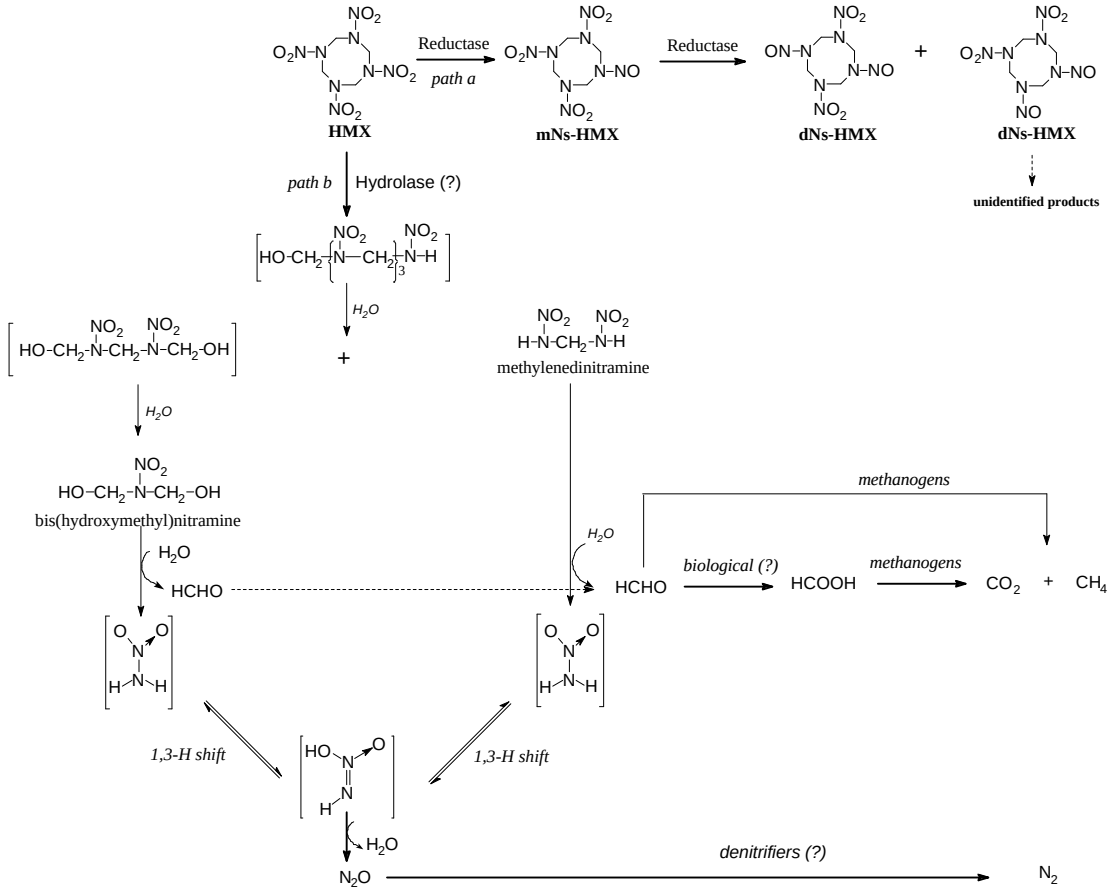

Figure 3. Potential biodegradation routes of HMX during treatment with anaerobic sludge. *Path a*: reduction *via* nitroso route who were later removed from the system without identifying their products. *Path b*: ring cleavage followed by competing chemical and biochemical transformations. A square bracket indicates unidentified product whereas a question mark indicates potential presence that requires further experimental verification. Italicized products on the right hand side are those detected earlier by McCormick et al. (1981) but are not detected in the present study.

Hydroxyalkylnitramines are known to be unstable in water and exist as equilibrated mixtures with their dissociated products HCHO and NH_2NO_2 (Lamberton et al., 1949a,b; Urbanski, 1967). The two metabolites methylenedinitramine and bis(hydroxymethyl)-nitramine do not represent the only HMX ring cleavage products in our study.

There are possibly other undetected products that were produced in trace amounts or as

transients that underwent rapid transformation. However the detection of the above two products are particularly important because we were able to identify them using the chromatographic and mass data obtained in our earlier study with RDX (Hawari et al., 2000a).

Once formed, NH_2NO_2, can undergo spontaneous hydrolytic decomposition to produce nitrous oxide, N_2O (Lamberton et al., 1949a,b; Urbanski, 1967) (Figure 3, *path b*). Decomposition of the nitramide to N_2O is well established and is suggested to initially involve a 1,3-H shift from nitrogen to oxygen followed by hydrolysis as shown in Figure 3 (Melius, 1990). Using ring labeled ^{15}N-[RDX] we previously found that one nitrogen atom in N_2O originated from the $-NO_2$ group and the second one from the ring (Hawari et al., 2000a), while the formation of nitrogen during degradation of HMX was considered to be biological because the gas only appeared in microcosms that contained HMX and live sludge (incubated under an atmosphere of argon). It is possible that unidentified denitrifiers in the sludge caused the transformation of nitrous oxide to nitrogen gas. St. John and Hollocher (1977) and Garber and Hollocher (1982) reported the formation of nitrogen as a metabolite from N_2O under anaerobic conditions using *Pseudomonas aeruginosa*. Also it has been reported that facultative and obligate anaerobic bacteria can reduce N_2O to nitrogen (Matsubara and Mori, 1968). Also we found that microcosms that contained glucose as a carbon substrate during HMX treatment with the anaerobic sludge showed both nitrous oxide and nitrogen gas as major products (Figure 2a), whereas in microcosms that did not receive glucose, nitrogen concentrations increased drastically and nitrous oxide was below the detection limit (Figure 2b). One may expect to observe more reduction of N_2O to N_2 by denitrifiers in the presence of excess e-donors such as glucose. However, we found relatively high amounts of hydrogen sulfide in microcosms that received glucose and only trace amounts in the absence of glucose. It has been reported that sulfides are inhibitory to denitrification processes and thus their presence might have contributed to the inhibition of denitrification thus leading to the accumulation of N_2O (Tam and Knowles, 1979; Sorensen et al., 1980) (Figure 2a). Furthermore, VSS and the heavy metals (Fe, Zn, Cd, Ni and Cu) in the sludge might have served as source of electron donors for the denitrification observed in the absence of glucose

(Figure 2b). Formic acid (detected as ^{14}CHOOH) was detected only in trace amounts. HCOOH is considered as a ring cleavage product following hydrolysis of cyclic nitramines (Canizarro reaction) (Hoffsommer et al., 1977; Heilmann et al., 1996). On the other hand, we speculate that methanogens in the sludge biotransformed formic acid into methane and carbon dioxide (Figure 2). Previously, a sludge of the same origin as the one used here proved to contain several consortia including methanogens (Rocheleau et al., 1999).

Presently we are unable to determine the extent of the nitroso route (Figure 3, *path a*) relative to the ring cleavage one (Figure 3, *path b*) for HMX degradation. Also we do not have any direct evidence of other degradative mechanisms such as reductive denitration. In the case of RDX, non biological reductive denitration *via* a bimolecular elimination (E_2) of HNO_2 yields the unstable intermediate 3,5-dinitro-1,3,5-triazacyclohex-1-ene which undergoes spontaneous decomposition with a rate constant that is 10^5 times higher than that of RDX itself (Croce and Okamoto, 1979). On the other hand, the initial cleavage of an external N-NO_2 or C-H bonds of HMX would destabilize inner C-N chemical bonds (< 5 Kcal/mole), forcing the molecule to undergo rapid autodecomposition to N_2, N_2O, HCHO and HCOOH (Melius, 1990). The above analysis might help explain why most reported biodegradation studies of cyclic nitramines did not describe more than the removal of the explosive and in more specific cases the initial denitration processes as diagnostic tools to describe biodegradation. Often poor knowledge of intermediate metabolites is described and without such knowledge the degradation pathways of RDX and HMX will remain unknown.

Thus far we were able to prove that unidentified anaerobic microorganisms from a domestic sludge can convert HMX *via* at least two mechanisms; one involved sequential reduction of -NO_2 groups to the corresponding nitroso derivatives and the other involved ring cleavage. The present observation confirms our earlier findings with RDX using sludge from the same source. Furthermore we were able to confirm that both RDX and HMX biodegrade anaerobically to produce similar product distribution, but specific isolates and the enzymes responsible for initiating degradation are unknown yet. The coming sections will thus attempt to identify early intermediate products of both RDX and HMX and the degraders and enzymes that produce them.

V.2 Identification of Bacterial Isolates from Sludge and the enzymes that initiate degradation.

In the previous experiments we found that undefined bacteria in anaerobic sludge efficiently degraded RDX and HMX, but the role of isolates in the degradation process was unknown. To have further insight into the role of specific isolates in the degradation pathways of the two chemicals, we isolated and characterized several bacterial strains from the sludge (*Klebsiella* strain SCZ-1 and *Clostridium* HAW-1) and employed each to degrade RDX and HMX under different physiological and environmental conditions. To gain an insight into the degradation pathways involved in initiating the degradation of the two cyclic nitramines RDX and HMX we must first understand which bacterial strain is initiating degradation and by what enzyme(s). The following chapters will attempt to provide answers to these questions.

V.2.1 **Klebsiella pneumoniae** ***Strain SCZ-1: Biodegradation of RDX through denitration or reduction to MNX followed by denitration.***

- Zhao, J.-S., Halasz, A., Paquet, L., Beaulieu, C. and J. Hawari. **2002**. Biodegradation of hexahydro-1,3,5-trinitro-1,3,5-triazine (RDX) and its Mononitroso Derivative hexahydro-1-nitroso-3,5-dinitro-1,3,5-triazine (MNX) by *Klebsiella pneumoniae* Strain SCZ-1 Isolated from an Anaerobic Sludge. Appl. Environ. Microbiol. 68: 5336-5341.

Isolation of strains SCZ-1. An anaerobic RDX-mineralizing bacterium, strain SCZ-1, was isolated from the anaerobic sludge that we previously used to degrade RDX (Halasz et al., 2002; Hawari et al., 2000a). Strain SCZ-1 was characterized as a non-motile, non-spore-forming, gram negative and rod shaped facultative anaerobic bacterium. Under aerobic and anaerobic conditions, strain SCZ-1 grew on glucose and peptone, but did not grow when RDX was used as a sole source of carbon or nitrogen. Based on MIDI and 16s-rRNA methods we identified the strain SCZ-1 as *Klebsiella pneumoniae*.

RDX degradation with strains SCZ-1. We found that strain SCZ-1 grew better aerobically but degraded RDX only under anaerobic conditions in the presence of glucose and peptone. *Klebsiella pneumoniae* strain SCZ-1 degraded RDX at a rate of 0.41 μmol . h^{-1} . $g(dcw)^{-1}$, which was lower than that {10 μmol . h^{-1} . $g(dcw)^{-1}$}(Zhao et al., 2002) of the mixed anaerobic culture. On the other hand, the removal rate of RDX with strain SCZ-1 (9.0 μM · d^{-1}) (biomass: OD_{600nm}, 0.7) is comparable to removal rates previously reported for other facultative isolates such as *M. morganii* (12.1μM · d^{-1}), *P. rettgeri* (12.1μM · d^{-1}), *Citrobacter freundii* (7.3μM · d^{-1}) (Kitts et al. 1994) (biomass: OD_{580nm}, 1.6-1.8) and *Serratia marcescenes* (20.4μM · d^{-1}) (Young et al., 1997a) (biomass: unknown). These previously described pure anaerobic cultures mineralized RDX poorly (Table 1). In contrast, strain SCZ-1 mineralized 72% of RDX (Fig. 1A).

Removal of RDX by strain SCZ-1, was accompanied by formation of several products including N_2O (60 %), HCHO, CO_2 (72 %) and CH_3OH (12 %) (Fig. 1A). In controls containing RDX with killed cells, approximately 10 % of RDX was degraded (hydrolyzed) with the accumulation of nitrite (Fig. 1B). Nitrite was not seen in RDX degradation using

live strain SCZ-1, and this is attributed to the bacterial conversion of nitrite to ammonia. For instance, when we incubated a standard solution of sodium nitrite (130 μM) with strain SCZ-1, the anion disappeared at a rate of 128 $\mu mol \cdot h^{-1} \cdot g\ (dcw)^{-1}$, which was more than 300 times higher than the rate of RDX removal {0.41 $\mu mol \cdot h^{-1} \cdot g\ (dcw)^{-1}$}. Unfortunately we were unable to quantify ammonia because of its release in relatively large amounts from the YPG medium

TABLE 1. Comparison of RDX mineralization and the maximal nitroso metabolites yields by pure anaerobic bacterial isolates.

Bacterial strains (ref.)	Mineralization %, as $^{14}CO_2$ (SD)	Nitroso metabolites % (SD)		
		MNX	DNX	TNX
Klebsiella pneumoniae SCZ-1 [a]	72.3 (0.8)	2 (0.5)	0	0
Morganella morganii B2 [b,c]	5 (1)	25	2.5	0
Providencia rettgeri B1 [b,c]	8 (2)	35	15	0
Citrobacter freundii NS2 [b,c]	9 (2)	50	15	5
Clostridium bifermentans [d]	no data	no metabolite data		
Desulfovibrio sp. [e]	no data	no metabolite data		
Serratia marcescens [f]	no data	50	30	1

[a] This work. The values shown are averages of triplicate samples with standard deviation (SD) in parentheses. Maximal bacterial growth was 0.70 OD_{600nm}. [b] Mineralization values were averages of duplicate samples with SD in parentheses. Maximal bacterial growth (OD_{560nm}) for B2, B1, NS2 was 1.8, 1.8, and 1.6, respectively. [c] Yields of metabolites were calculated from data provided in reference (Kitts et al. 1994). [d] from ref Regan et Crawford (1994). [e] from Boopathy et al., (1998). [f] Biomass was not given. Yields of nitroso metabolites were also estimated from the figures provided in reference Young et al. (1997)

Strain SCZ-1 did not degrade RDX in basic salts medium with RDX supplemented as the carbon or nitrogen source, thus we were unable to quantify ammonia production from RDX degradation. Other potential N-containing products such as hydrazine and dimethyl hydrazines that were reported by McCormick et al. (1981) were not detected in the present study.

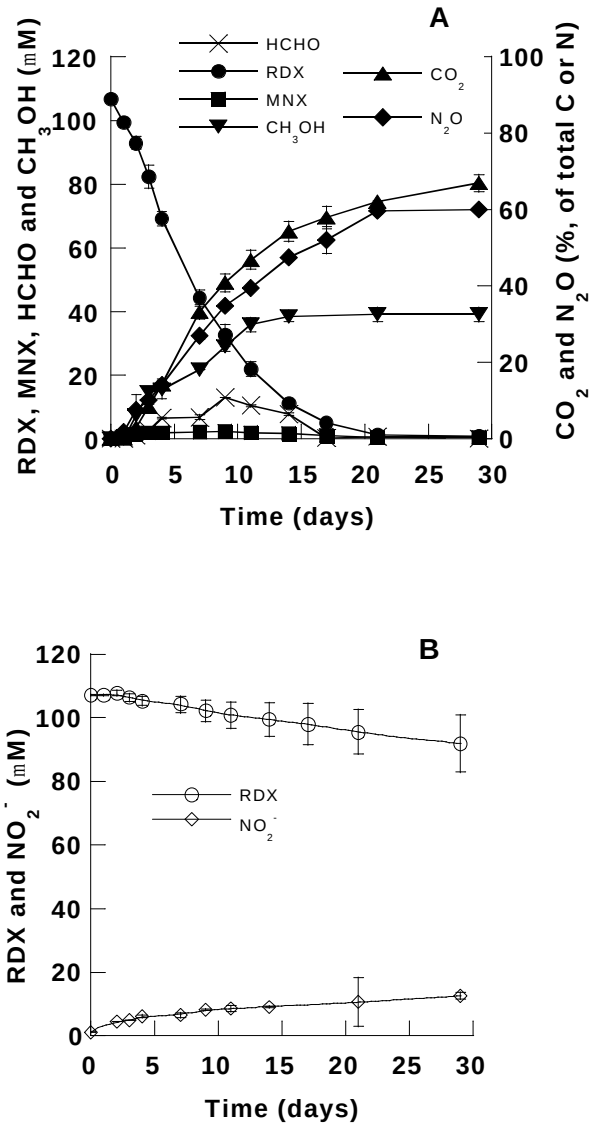

Figure. 1. Anaerobic degradation of 106 μM of RDX with *Klebsiella pneumoniae* strain SCZ-1. A: live cells {initial biomass, 0.15 OD_{600nm}; maximal growth, 0.7 OD_{600nm} or 0.9 g (dcw) · L^{-1}}; B: killed cells (initial biomass, same as A).

HCHO did not accumulate and was mineralized. For instance, when we incubated a reference standard of HCHO spiked with ^{14}C-HCHO with strain SCZ-1, we obtained more

than 85 % mineralization ($^{14}CO_2$) in less than 20h (Fig. 2). Figure 2 clearly shows that long after the removal of the aldehyde, CO_2 continued to form slowly. Using LC/MS (ES-) we were able to identify methylenedinitramine as a key ring cleavage intermediate, which decomposed to N_2O and HCHO. Furthermore we detected trace amounts of MNX, but were unable to detect DNX or TNX.

The above product distribution is strikingly similar to that obtained during RDX incubation with the sludge, indicating similarities between the degradation pathways in both cases (discussed below).

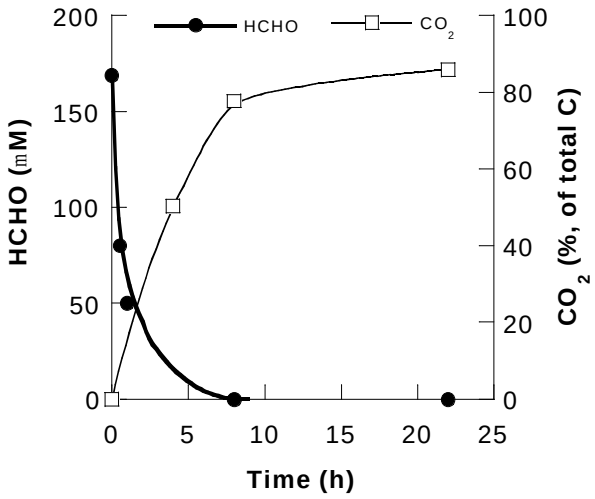

Figure 2. Anaerobic mineralization of 169 μM of HCHO with *Klebsiella pneumoniae* strain SCZ-1 supplemented with 0.03 μCi of ^{14}C-HCHO. Biomass was the same as those in Fig. 1.

Stoichiometry of RDX degradation. The conversion of 2.1 μmole of RDX (106 μM) produced 3.8 μmole of N_2O, representing 60 % of the total N-content in RDX (4 N atoms) (Fig. 1A). Methylenedinitramine, $O_2NNHCH_2NHNNO_2$, a detected key RDX intermediate of strain SCZ-1, is the main source for N_2O. We have previously demonstrated that one mole of $O_2NNHCH_2NHNNO_2$ decomposes quantitatively in water at pH 7 and 30 ºC to produce two moles of N_2O and one mole of HCHO (Halasz et al., 2002). The stoichiometry of N_2O formation supports our belief that methylenedinitramine, with two -NH-NO_2 groups, was

responsible for the quantitative formation of N_2O from RDX in strain SCZ-1.

Conversion of 106 μM of RDX also produced 39 μM of CH_3OH, representing 12% of total carbon in transformed RDX (Fig. 1A). Using UL-^{14}C-RDX as substrate, we found that strain SCZ-1 mineralized 72% of the total carbon in RDX (liberated ^{14}C-CO_2) over 36 days (Fig. 1A). Most of the remaining radioactivity (27 %) was in the aqueous phase of the culture medium and only less than 0.5% of RDX carbon was in biomass, leaving as unaccounted roughly 15% of its carbon content. However, slow release of CO_2 was still occurring long after the complete disappearance of RDX (Fig. 1A).

MNX and TNX degradation. When we incubated MNX (100 μM) with live cells of strain SCZ-1, the compound degraded at an initial rate of 0.39μmol · h^{-1} · g $(dcw)^{-1}$ (Fig. 3A), close to that {0.41 μmol · h^{-1} · g $(dcw)^{-1}$}of RDX degradation under the same conditions. The MNX transformation products were N_2O, CH_3OH and HCHO (Fig. 3A), similar to those of RDX. However, removal of 2 μmoles of MNX only produced 1.0 μmole of N_2O (17% of the total N-content in MNX) (Fig. 3A) as compared to production of 3.8 μmoles of N_2O (60% of total N-content in RDX) from 2.1 μmoles of RDX (Fig. 1A). Another notable observation is the detection of a small amount of DNX from MNX, but not TNX. In MNX degradation we did not observe formation of $O_2NHNCH_2NHNO_2$, the key intermediate during RDX degradation with strain SCZ-1.

In controls containing killed cells (Fig. 3B), MNX decomposed at a rate of 0.16 μmol · h^{-1} · g $(dcw)^{-1}$, almost half that of its removal rate in the presence of live cells {0.39 μmol · h^{-1} · g $(dcw)^{-1}$}, indicating that MNX was not a stable compound and underwent hydrolysis in water (Fig. 3B). Abiotic degradation of each mole of MNX released approximately one mole of nitrite.

When we incubated the trinitroso derivative TNX (100 μM) under the same conditions, we found that the compound was converted much more slowly than either RDX or MNX. The removal rate of TNX {0.07 μmol · h^{-1} · g $(dcw)^{-1}$} was six times lower than that of MNX {0.39 μmol · h^{-1} · g $(dcw)^{-1}$} and RDX {0.41 μmol · h^{-1} · g $(dcw)^{-1}$}.

In controls with killed cells, TNX was not degraded. It has been frequently reported that TNX tends to accumulate during RDX biodegradation (Kitts et al., 1994; McCormick et al., 1981;

Oh et al., 2001; Sheremata et al., 2001; Young et al., 1997a,b).

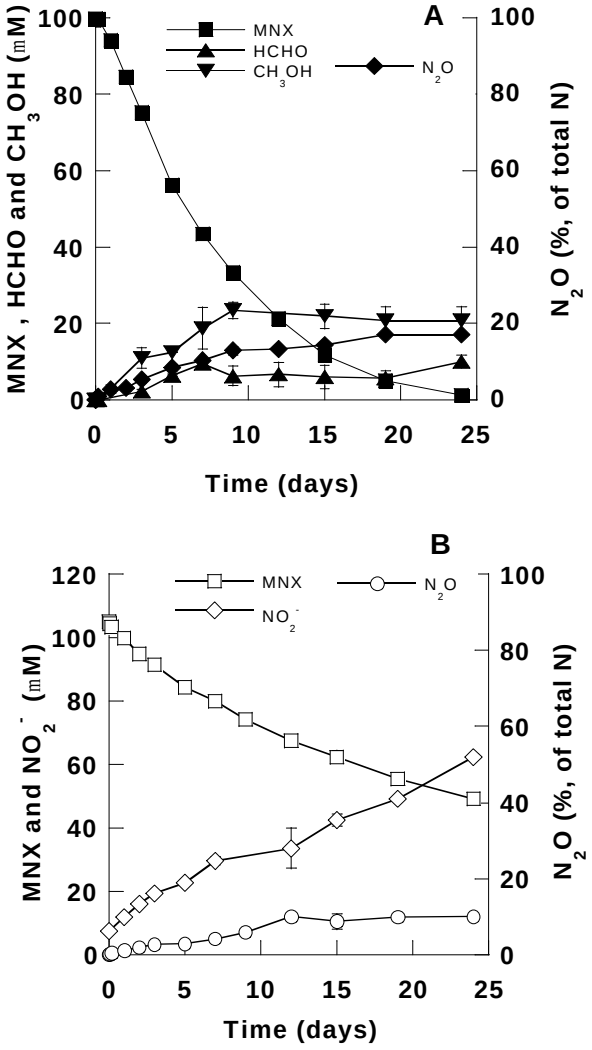

Figure 3. Anaerobic degradation of MNX (2.0 μmole in 20 ml) with *Klebsiella pneumoniae* strain SCZ-1. A: live cells; B: killed cells. Biomass was the same as those in Fig.1.

Degradation pathway(s) of RDX: initial denitration <u>vs</u> nitroso formation. Based on the product distribution described above we propose a RDX degradation pathway in *Klebsiella pneumoniae* strain SCZ-1 (Fig 4). The RDX degradation pathway in this isolate is similar to the one(s) described earlier for the anaerobic sludge in that both involve methylenedinitramine as a ring cleavage intermediate (Halasz et al., 2002; Hawari et al.,

2000a). In the present study we suggest the involvement of an important initial denitration step during RDX degradation that lead to ring cleavage and decomposition (Fig. 4, *path a*). The fact that oxygen completely quenched RDX removals in strain SCZ-1 supports the belief that an O_2-sensitive reaction involving transfer of one electron to NO_2 group in RDX might have initiated degradation. Such a process would produce an unstable radical anion $RDX^{\cdot -}$ (I) whose denitration could produce the unstable radical RDX (II). Subsequent reaction of II *via* either abstraction or elimination of a H atom would give either the amine (III) or the mono unsaturated RDX intermediate (MUX, IV) (Bose et al., 1998; Hoffsommer et al., 1977; Peyton et al., 1999), respectively. Methylenedinitramine is one of the expected products from decomposition of III or IV. The suggested N-denitration mechanism in the present RDX study is similar to the N-denitration mechanism reported earlier for nitramines by dihydronicotinamide (Chapman et al., 1996). In the latter case, the cleavage of a N-NO_2 bond proceeds *via* a one-electron transfer process (Chapman et al 1996). Also N-denitration of RDX to IV has been frequently reported during alkaline hydrolysis (Croce and Okamoto, 1979; Hoffsommer et al., 1977) where the latter compound is found to decompose with a rate constant (k) 10^5 times larger than that of RDX (Hoffsommer et al., 1977).

Sequential reduction of the nitro group(s) (-NO_2) in RDX to the corresponding nitroso (-NO) derivative(s) did not seem to be a major degradation route for strain SCZ-1. If the sequential reduction of -NO_2 to -NO is an important degradation pathway for RDX, then one might expect the accumulation of TNX (Fig. 4, *path b*) which we did not observe in the present study. As discussed above TNX was degraded at a rate much slower than that of MNX and RDX with strain SCZ-1. In addition we observed only traces of MNX during RDX degradation and traces of DNX during MNX degradation. Likewise we suggest that MNX also degraded mainly by initial denitration prior to ring cleavage (Fig. 4, *path a*). The absence of methylenedinitramine from MNX degradation supports the hypothesis that one of the two nitro functional groups (-NO_2) in MNX might have been removed prior to ring cleavage, leaving the compound unable to act as a precursor to methylenedinitramine.

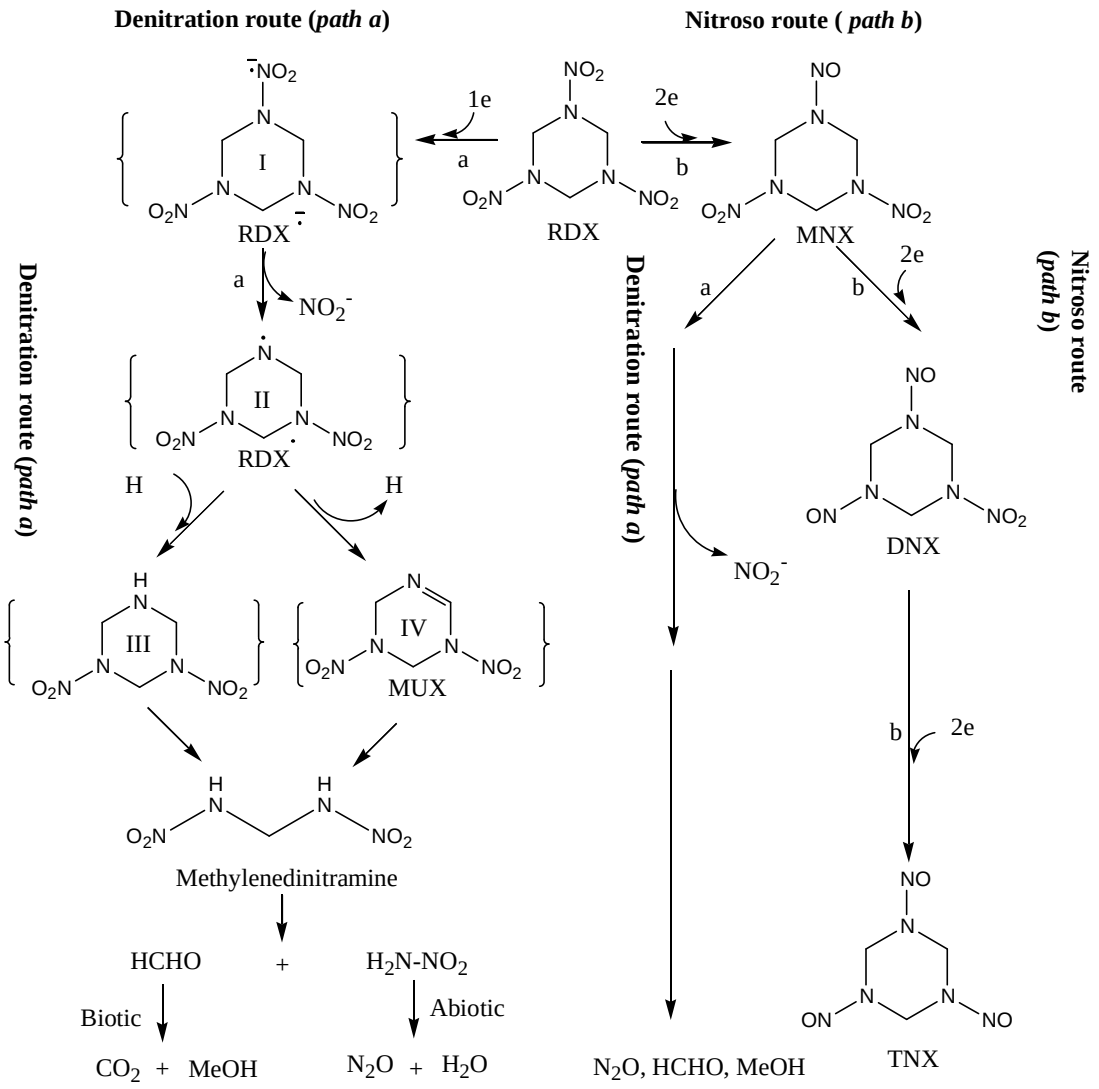

FIG. 4. Postulated routes for anaerobic degradation of RDX and MNX by *Klebsiella pneumoniae* strain SCZ-1 (Compounds in brackets were not detected in this study).

In conclusion, we found that a facultative anaerobic bacterium isolated from an anaerobic sludge mineralized RDX predominantly *via* initial denitration, whereas the reduction of the nitro group of RDX to the corresponding nitroso products was a minor secondary reaction. Although the isolated strain improved our understanding of the pathways involved in the degradation of cyclic nitramines, its application in remedial application might not be practical because of a slow rate of degradation. However, the high mineralization observed during RDX degradation should encourage us to optimize various physiological parameters to enhance rates of degradation of RDX, and thus to search for others more robust degraders. The following chapters will thus attempt to discuss these issues and also to provide insight into the initial enzymatic processes involved in biodegradation.

V.2.2 Clostridium bifermentans HAW-1: Metabolism of RDX through initial reduction to MNX followed by denitration.

- Zhao, J.-S., Halasz, A., Paquet, L. and J. Hawari. **2002**. Biodegradation of hexahydro-1,3,5-trinitro-1,3,5-triazine through initial reduction to hexahydro-1-nitroso-3,5-dinitro-1,3,5-triazine followed by denitration in *Clostridium bifermentans* HAW-1. Appl. Microbiol. Biotechnol. 63 : 187-193.

In the previous section we reported that *Klebsiella pneumoniae* SCZ-1, a facultative bacterium, degraded RDX rather slowly through a one electron transfer-induced initial denitration step followed by subsequent ring cleavage (Zhao et al., 2002). Although strain SCZ-1 degraded RDX with high mineralization amount, the degradation rate was slow. Our objective in the present work is to investigate the metabolism of RDX by attempting to obtain more robust degraders from the anaerobic sludge. In the present study, we thus isolated a fast RDX-degrading (28.1 $\mu molh^{-1}g$[dry weight] of $cells^{-1}$) (biomass, 0.16 g[dry weight] of $cells^{-1}$) and strictly anaerobic bacterial strain HAW-1, identified as *Clostridium bifermentans* using a 16S rRNA based method. Based on initial rates, we found that strain HAW-1 transformed RDX to MNX, DNX and TNX with yields of 56, 7.3 and 0.2%, respectively**.** Complete removal of RDX and its nitroso metabolites produced (%, of total C or N) methanol (MeOH, 23%), formaldehyde (HCHO, 7.4%), carbon dioxide (CO_2, 3.0%) and nitrous oxide (N_2O, 29.5%) as end products. Under the same conditions strain HAW-1 transformed MNX separately at a rate of 16.9 $\mu molh^{-1}g$[dry weight] of $cells^{-1}$ and produced DNX (25%) and TNX (0.4%) as transient products. Final MNX transformation products were (%, of total C or N) MeOH (21%), HCHO (2.9%) and N_2O (17%). Likewise strain HAW-1 degraded TNX at a rate of 7.5 $\mu molh^{-1}g$[dry weight] of $cells^{-1}$ to MeOH and HCHO. Furthermore, removal of both RDX and MNX produced nitrite (NO_2^-) as a transient product, but the nitrite release rate from MNX was quicker than from RDX. We proposed a predominant pathway for RDX degradation based on initial reduction to MNX followed by denitration and decomposition, whereas continued sequential reduction to DNX and TNX was only a minor route.

Isolation and characterization of strain HAW-1. Strain HAW-1, a strictly anaerobic and fast

RDX-degrading bacterium, was isolated from an anaerobic sludge enrichment culture using RDX (100 μM) as the sole carbon and nitrogen source and hydrogen as energy source. Strain HAW-1 is a gram positive, rod-shaped, spore-forming, catalase-negative bacterium. The length of the rods was from 1.5 μm to 11 μm and the diameter ranged from 0.5μm to 1 μm. Its spores grew well on yeast extract, glucose and peptone. Although strain HAW-1 was isolated from the mixed culture that was enriched on RDX as the sole carbon and nitrogen source, it grew poorly in the vitamin-rich basic salts medium when the energetic chemical was used as the sole carbon and/or nitrogen source. On the basis of above features and its 16S rRNA sequence, we identified strain HAW-1 as *Clostridium bifermentans* (Sneath, 1986).

RDX metabolism by strains HAW-1. Strain HAW-1 spores grew rapidly in the YE (0.1%) medium containing RDX (104 μM) as observed by the increase in the OD_{600nm} from 0.02 to 0.2 (0.16 g [dry weight] of cells liter^{-1}) in 15 hours. RDX degradation was accompanied by the formation of the three nitroso compounds MNX, DNX and TNX (Fig. 1A). However, none of the nitroso products persisted, rather they all disappeared at different rates (MNX > DNX > TNX) producing MeOH, HCHO and N_2O as final ring cleavage products (Fig. 2A).

Concurrent to the formation of MNX, DNX (2.1 μmol · h^{-1} · g [dry weight] of cells^{-1}) and TNX (0.06 μmol · h^{-1} · g [dry weight] of cells^{-1}) were also formed with rates equivalent to 7.3% and 0.2% of that of the RDX removal rate, respectively.

MNX was a major intermediate, formed at a rate of 15.6 μmol · h^{-1} · g [dry weight] of cells^{-1}, about 56% of the RDX removal rate (28.1 μmol · h^{-1} · g [dry weight] of cells^{-1}). A rapid disappearance of MNX was observed and its removal was accompanied by the immediate release of HCHO (9.4 μmol · h^{-1} · g [dry weight] of cells^{-1}) and MeOH (11.3 μmol · h^{-1} · g [dry weight] of cells^{-1}) (Fig. 2A). N_2O was only slowly released (6.2 μmol · h^{-1} · g [dry weight] of cells^{-1}) following MNX disappearance. When N_2O was added to the growing strain HAW-1, no removal of the gas was observed. Additionally, we found that RDX (50 μM) removal was accompanied by the formation of nitrite at a rate of 6.3 μmol · h^{-1} · g [dry weight] of cells^{-1}. Nitrite did not accumulate. Instead we found that strain HAW-1 rapidly removed nitrite (added as sodium nitrite) at a rate (187 μmol · h^{-1} · g [dry weight] of cells^{-1}) that was seven times the rate of RDX removal (Fig. 3B). The most likely product of nitrite

biotransformation is ammonia, but we were unable to quantify it due to a severe interference from the medium. Nitrite was not transformed to N_2O by strain HAW-1.

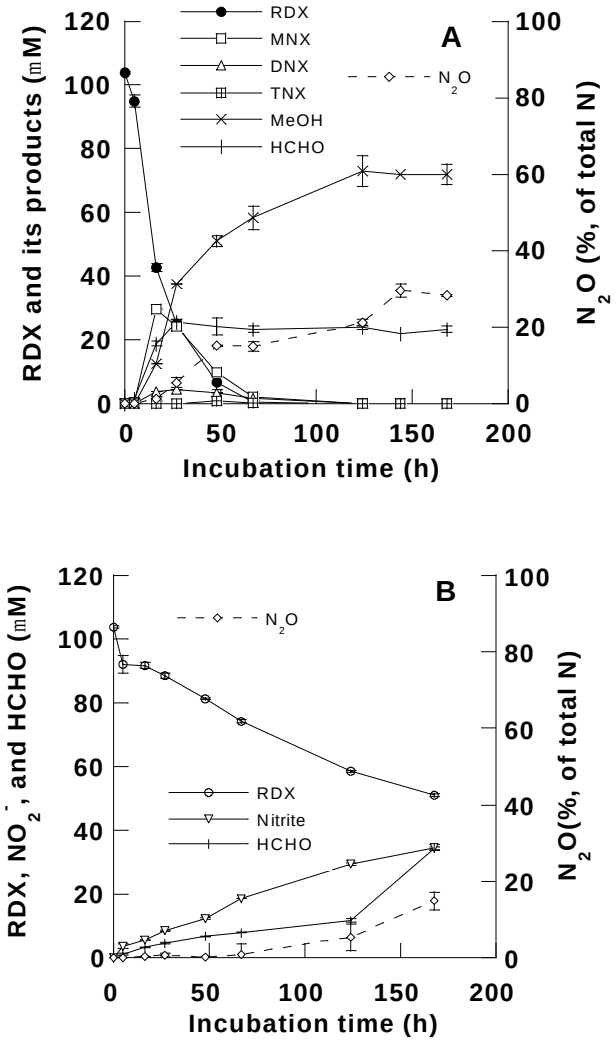

Figure 1. Anaerobic degradation of RDX (104 μM) by *Clostridium bifermentans* HAW-1. A: live cells {final biomass, 0.16 g [dry weight] of cells · liter^{-1}}; B: control without bacterium.

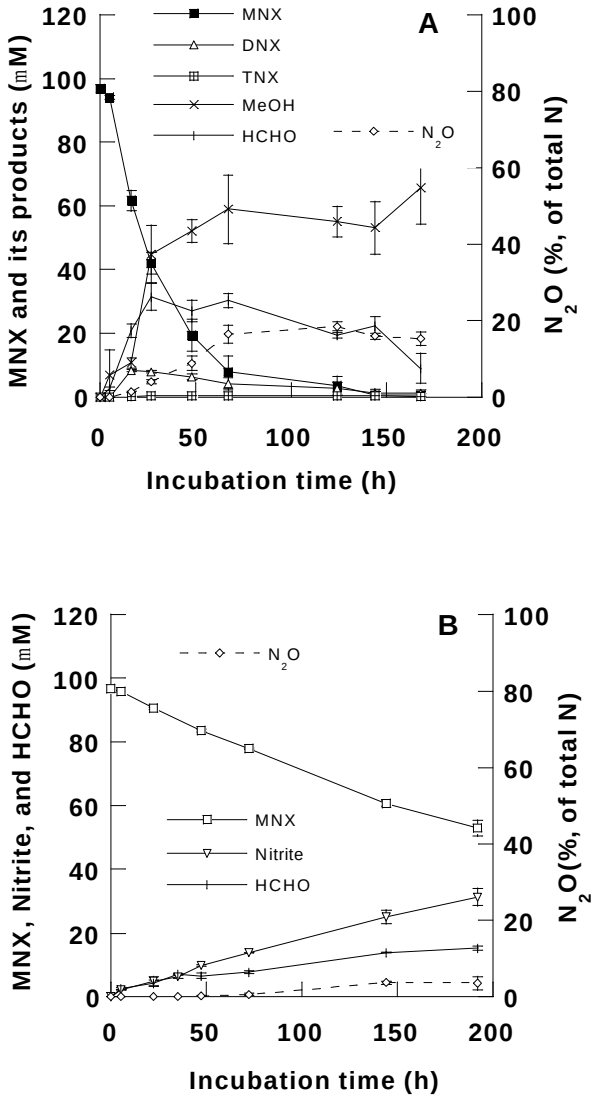

Figure 2. Anaerobic degradation of MNX (96 μM) by *Clostridium bifermentans* HAW-1. A: live cells; B: control without bacterium. The biomass was the same as that in Fig. 1.

Controls containing RDX without strain HAW-1 also showed some degradation (Fig. 1B), but at a rate approximately 7% that of RDX biodegradation by strain HAW-1. The removal of RDX in this control was accompanied by the stoichiometric formation of NO_2^- (one NO_2^- formed for each molecule of RDX transformed), similar to what was normally observed during alkaline hydrolysis (Hoffsommer et al., 1977). The presence of strong reducing condition (E_h -300 mV) in the controls might have contributed to the reductive denitration of RDX. Denitration of RDX in the control also led to the formation of HCHO, but no MeOH

was detected (Fig. 1B).

When we incubated both RDX and the uniformly ring-labeled [^{15}N]-RDX at a relatively high initial concentration (250 μM), we were unable to observe the hexahydro-1,3,5-triamino-1,3,5-triazine product as recently reported by Zhang and Hughes (2003). We also did not observe any hydrazine or dimethyl hydrazine as reported earlier by McCormick et al (1981).

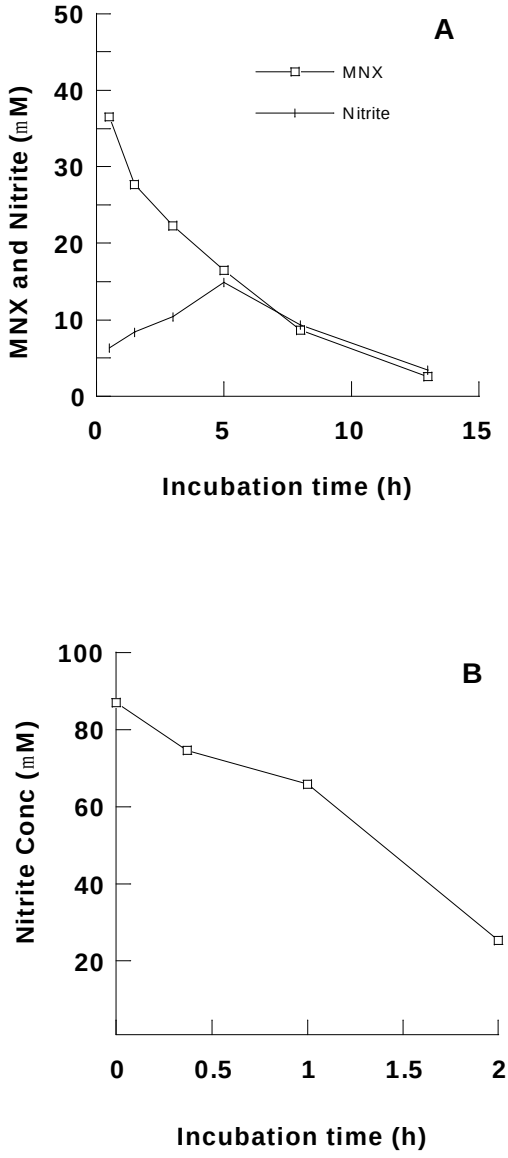

Figure 3. Nitrite production (A) during MNX (48 μM) biodegradation and nitrite removal (B) during incubation of sodium nitrite with strain HAW-1 culture pregrown on YE (0.1%) (biomass was the same as that in Fig. 1).

MNX metabolism by strains HAW-1. The bacterial biomass obtained when strain HAW-1 was grown in the presence of MNX was similar to that (0.16 g [dry weight] of cells · liter^{-1}) obtained when grown in the presence of RDX. MNX (96 μM) was degraded at a rate of 16.9 μmol · h^{-1} · g [dry weight] of cells^{-1}(Fig. 2A), slower than that (28.1 μmol · h^{-1} · g [dry weight] of cells^{-1}) of RDX degradation. MNX removal was immediately followed by the release of HCHO and MeOH (Fig. 2A). The rates of HCHO (9.4 μmol · h^{-1} · g [dry weight] of cells^{-1}) and MeOH (11.3 μmol · h^{-1} · g [dry weight] of cells^{-1}) formation during MNX degradation were similar to the rates of their formation during RDX incubation with strain HAW-1 (Fig. 1A). N_2O was released at a rate of 4.7 μmol · h^{-1} · g [dry weight] of cells^{-1}, slightly lower than the rate (6.2 μmol · h^{-1} · g [dry weight] of cells^{-1}) observed in the case of RDX. In addition, we found that incubation of MNX (48 μM) with strain HAW-1 pre-grown on YE (14 h), resulted in the production of nitrite at an initial rate of 11.3 μmol · h^{-1} · g [dry weight] of cells^{-1} (Fig. 3A), which was almost twice the rate (6.3 μmol · h^{-1} · g [dry weight] of cells^{-1}) of nitrite release from RDX (50 μM) (biomass, 0.16 g [dry weight] of cells · liter^{-1}). The nitrite release rate accounted for 67% of MNX removal rate.

The disappearance of MNX was accompanied by the formation of small amounts of the dinitroso (DNX) (4.3 μmol · h^{-1} · g [dry weight] of cells^{-1}) and the trinitroso (TNX) (0.06 μmol · h^{-1} · g [dry weight] of cells^{-1}) derivatives (Fig. 2A). Based on MNX removal and DNX formation rates, we estimated that approximately 25% of MNX were transformed through reduction to DNX.

In a control containing YE and the reducing medium without strain HAW-1, MNX was found to degrade (hydrolyze) slowly at a rate of 0.25 μM · h^{-1} (Fig. 2B), approximately 10% the rate of its removal by strain HAW-1. In addition, the disappearance of MNX was accompanied by the release of nitrite at a rate of 0.16 μM · h^{-1} together with a trace amount of N_2O. In controls containing water alone (pH 6.5) or a phosphate buffer (25 mM; pH 7.2), MNX degraded (hydrolyzed) more slowly at rates of 0.07 and 0.12 μM · h^{-1}, respectively (Fig. 4). In the latter case, we observed the stoichiometric formation of the ring cleavage product O_2NNHCH_2NHCHO (NDAB) (Fig. 4). We were unable to detect NDAB during MNX incubation with strain HAW-1 or in a control containing YE and the reducing medium.

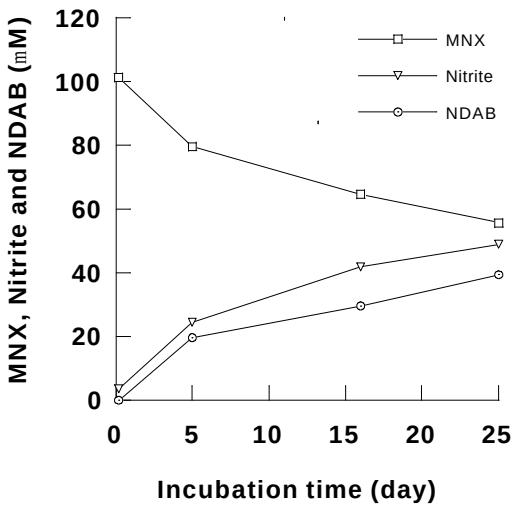

Figure 4. MNX denitration and production of 4-nitro-2,4-diazabutanal (NDAB) in water.

TNX removal by strains HAW-1. We found that incubation of TNX with strain HAW-1 led to the removal of the chemical more slowly than either RDX or MNX (Fig. 5). For instance, the initial removal rate (7.5 μmol · h^{-1} · g [dry weight] of $cells^{-1}$) of TNX (100 μM) was only half that of MNX and one quarter that of RDX biodegradation rates. TNX degradation ceased after 50 h of incubation, probably due to the depletion of nutrients. TNX degradation also produced MeOH and HCHO, but neither NO_2^- nor N_2O were detected. In a control containing TNX without strain HAW-1, the chemical hydrolyzed at a rate of 0.10 μM · h^{-1} which was ten times smaller than its biodegradation rate (1.0 μM · h^{-1}) during incubation with strain HAW-1. Abiotic hydrolysis of TNX in the controls led to the formation of HCHO, but not MeOH.

Mass balances of RDX and MNX degradation. Carbon mass balance measurements showed that conversion of 104 μM (2.1 μmole) of RDX produced 23.3 μM of HCHO and 73 μM of MeOH as final products, representing 7.4% and 23% of total carbon in transformed RDX, respectively (Fig. 1A). Using [UL-^{14}C]-RDX, we found that strain HAW-1 mineralized 3% of total carbon in RDX to CO_2 over 20 days. Of the total radioactivity we found 0.39 % of

RDX associated with biomass and 96.4% soluble in the aqueous phase. Methanol and HCHO represent 30.4% of measured radioactivity in solution, leaving unaccounted about 66% of total C in RDX. Nitrogen mass balances showed that conversion of 2.1 μmoles of RDX in strain HAW-1 produced 1.82 μmoles of N_2O, representing 29.5% of total nitrogen (Fig. 1A).

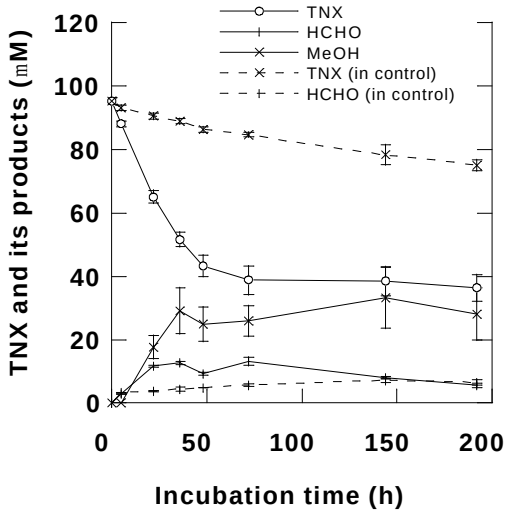

Figure 5. Anaerobic degradation of TNX (100 μM) by *Clostridium bifermentans* HAW-1 (solid line, live cells; broken line, control without bacterium). The biomass was the same as that in Fig. 1.

Part of the unaccounted nitrogen was presumed to be associated with the unidentified organic products described above. For MNX, N_2O accounted for 17% of total nitrogen, whereas HCHO and MeOH accounted for 2.9% and 21% of total carbon, respectively (Fig. 2A).

The formation of MNX, DNX and TNX during incubation of RDX with *Clostridium bifermentans* HAW-1 under strictly anaerobic conditions clearly indicates the occurrence of sequential reduction of the nitro (NO_2) groups in the energetic chemical to the corresponding nitroso (NO) groups (Fig.1), whereas the formation of MeOH, HCHO, CO_2 and N_2O demonstrated the occurrence of ring cleavage. As discussed above, neither the triamino derivative of RDX that was observed by Zhang and Hughes (2003) nor hydrazines that were reported by McCormick et al. (1981) were detected in the present study. The present product distribution was close to that observed during degradation of RDX with the facultative microorganism *K. pneumoniae* strain SCZ-1, but with different yields. Mineralization (3 %)

in the case of HAW-1 was much lower than that obtained (72 %) with SCZ-1, but the rate of RDX removal in the former case (28.1 μmol · h^{-1} · g [dry weight] of $cells^{-1}$) was seventy times higher than the latter case (0.39 μmol · h^{-1} · g [dry weight] of $cells^{-1}$) (Zhao et al., 2002). In the case of SCZ-1 we suggested that denitration of RDX was responsible for initiating ring cleavage and decomposition (Zhao et al., 2002).

Kinetic studies demonstrated that the degradation rates of RDX and its nitroso derivatives (MNX and TNX) in strain HAW-1 followed the order RDX>MNX>TNX (Fig. 1A; Fig. 2A and Fig. 5) which was similar to that reported with *Serratia marcescens* by Young et al. (1997a). The observed low yield of TNX during RDX (Fig. 1A) and MNX (Fig. 2A) incubation combined with a slow rate of degradation (Fig. 5), suggested that the nitroso route was not significant. The high yield of MNX during RDX degradation and the striking similarity between its product distribution and that of RDX suggested that the latter degraded through MNX. Since the rate of MNX removal was close to that of its denitration and the rate of nitrite release from MNX was twice that obtained from RDX, we suggest that the dominant initial step for MNX degradation is denitration. MNX was also found to be reactive towards denitration during hydrolysis in the abiotic control (bimolecular elimination of HNO_2) (Fig. 4).

Following MNX denitration, the molecule underwent an apparent rapid decomposition as demonstrated by the formation of HCHO and N_2O (Fig. 2A). Previously we demonstrated that the nitramine group (N-NO_2) was the part responsible for the formation of N_2O during degradation of RDX and HMX (Hawari et al., 2000a; Halasz et al., 2002). Interestingly, the 29.5 % yield of N_2O from RDX degradation by strain HAW-1 represents approximately one N-NO_2 bond. The above scenario can only occur following denitration of MNX, a process which should leave the molecule with only one N-NO_2 bond, whereas in the case of RDX, denitration would yield close to 66 % of N_2O (2 N-NO_2 moieties) as was the case with the facultative strain SCZ-1 (Zhao et al., 2002).

Degradation pathways. In view of the above experimental findings we propose that following RDX reduction to MNX in strain HAW-1, decomposition can proceed *via* two primary routes. One route involves continued sequential reduction to DNX and TNX (Fig.

6a) and the second involves denitration prior to ring cleavage and decomposition (Fig. 6b). For MNX, we postulate that the occurrence of a one-electron transfer step lead to the radical anion, $MNX^{\cdot -}$ (**I**) whose subsequent denitration (loss of NO_2^-) produces the free radical $MNX^{\cdot}$ (**II**).

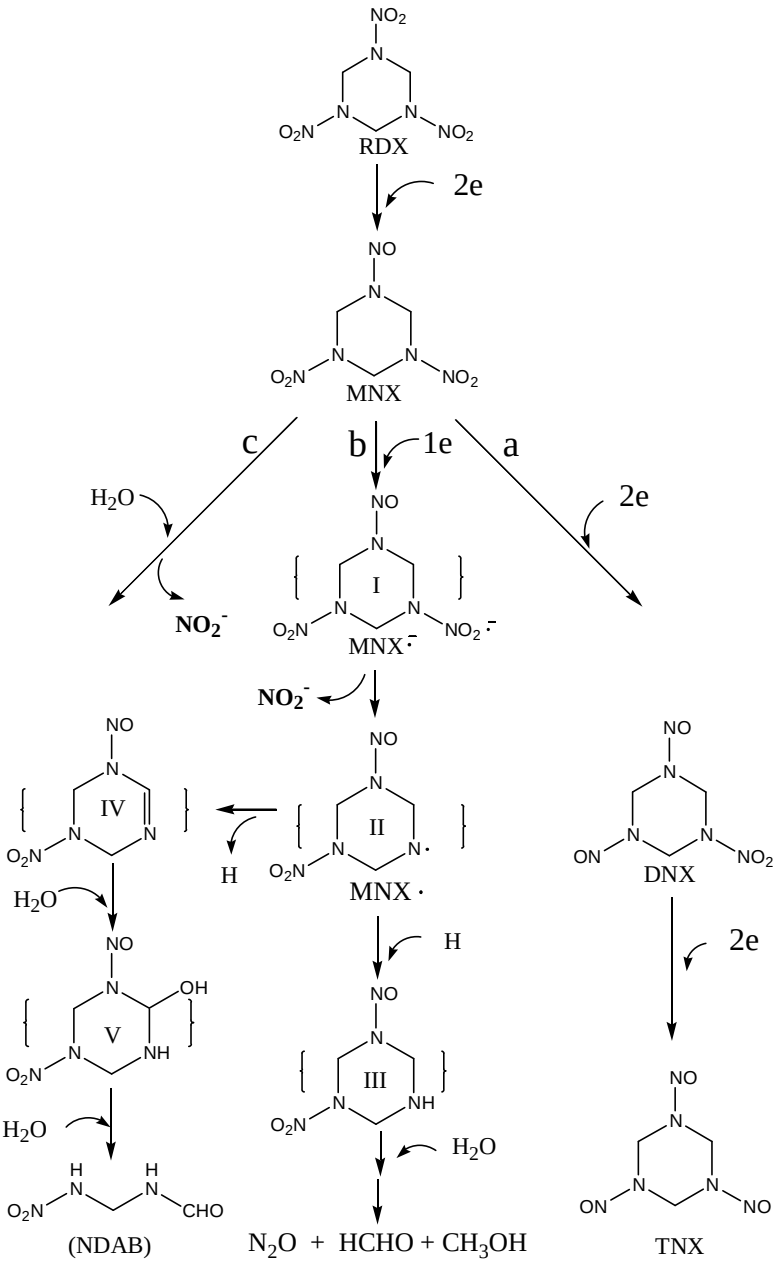

Figure 6. Routes proposed for RDX degradation by *Clostridium bifermentans* HAW-1. Compounds in brackets were not detected.

The radical **II** can either produce the amine (**III)** (H-abstraction) or the enamine (**IV)** (H removal) (Fig. 6b). A denitration mechanism similar to that shown in Fig. 6b was reported during degradation of RDX with a commercial diaphorase enzyme as shown in the report (Bhushan et al., 2002b). Alternatively, bimolecular elimination of HNO_2, as normally observed during the alkaline hydrolysis of RDX (Hoffsommer et al. 1977; Balakrishnan et al. 2003), can easily lead to the production of the enamine (**IV**) from MNX (Fig. 6c).

Reaction of the enamine **IV** with a water molecule would produce the α-hydroxynitrosamine intermediate (**V**). α-Hydroxynitrosamine was unstable (Okada et al., 1980) and should undergo spontaneous decomposition (Balakrishnan et al. 2003) to give O_2NNHCH_2NHCHO (NDAB) (Fig. 4).

In summary, *Clostridium bifermentans* HAW-1 mainly degraded RDX through initial reduction to MNX followed by denitration and decomposition. The removal rate of RDX by strain HAW-1 was high but mineralization was poor (3%). This is in contrast to the previous facultative isolate, *K. pneumoniae* SCZ-1, which exhibited a low rate of degradation but with high mineralization (72% of total C) (previous section and Zhao et al., 2002). Therefore, a joint process combining the two degraders might constitute the basis for the development of a bioprocess that can rapidly and effectively mineralize cyclic nitramine explosives to N_2O and CO_2.

In the following chapter we will discuss in more details the phylogenic and metabolic diversity of RDX biotransforming bacteria in sludge using the energetic chemical RDX as a N-source.

V.2.3 Phylogenetic and metabolic diversity of hexahydro-1,3,5-trinitro-1,3,5-triazine (RDX)-transforming bacteria in strictly anaerobic mixed cultures enriched on RDX as nitrogen source.

- Zhao, J.-S., J. Spain, and J. Hawari**. 2003.** Phylogenetic and metabolic diversity of hexahydro-1,3,5-trinitro-1,3,5-triazine (RDX)-transforming bacteria in strictly anaerobic mixed cultures enriched on RDX as nitrogen source. FEMS Microbiol. Ecol. 46: 189-196.

Most reported RDX-degrading anaerobic bacteria are facultative including members of the *Enterobacteriaceae* family (*Klebsiella pneumoniae, Serratia marcescens, Morganella morganii, Citrobacter freundii,* and *Escherichia coli*) (Kitts et al., 1994; Young et al., 1997a). None of above bacteria was reported to grow on RDX as nitrogen source. Although obligate anaerobes always exist in RDX-degrading anaerobic consortia, little is known about the role of obligate anaerobes in degradation of the energetic chemical. Adrian and Lowder (1999), Adrian and Sutherland (1998), Adrian and Chow (2001) and Beller (2002) proposed that acetogens are responsible for RDX removal in anaerobic consortia, but no acetogenic species were isolated. Boopathy et al. (1998) described degradation of RDX by a sulfate-reducing consortium from creek sediment, but degradation of RDX by individual sulfate-reducing bacterium was not reported. Thus far only one obligate anaerobe, *Clostridium bifermentans*, isolated from a contaminated soil, was reported to remove RDX in a complex brain-heart-infusion medium (Regan and Crawford, 1994).

One major concern regarding anaerobic degradation of RDX is the potential accumulation of toxic nitroso derivatives (McCormick et al., 1981; Adrian and Lowder, 1999; Adrian and Sutherland, 1998; Adrian and Chow, 2001; Young et al., 1997a,b, Kitts et al., 1994;). We previously found that an anaerobic sludge (Halasz et al., 2002, Hawari et al., 2000a,b) and a facultative anaerobic isolate, *Klebsiella pneumoniae* strain SCZ-1 (Zhao et al., 2002), was able to cleave the RDX ring to ultimately give nitrous oxide (N_2O), formaldehyde (HCHO) and methanol (CH_3OH). In the present study, we investigated the phylogenetic and metabolic diversity of RDX-transforming bacterial isolates in the strictly anaerobic mixed cultures enriched on RDX as nitrogen source.

In all we isolated five obligate anaerobes that according to their 16S rRNA genes sequences were most closely related to *Clostridium bifermentans, Clostridium celerecrescens,*

Clostridium saccharolyticum, *Clostridium butyricum* and *Desulfovibrio desulfuricans*. There were isolated from enrichment cultures using RDX as a nitrogen source. The above isolates transformed RDX at rates of 24.0, 5.4, 6.2, 2.5, 5.5 micromol $\cdot h^{-1} \cdot$ g [dry weight] of cells^{-1}, respectively, to nitrite (NO_2^-), formaldehyde (HCHO), methanol (CH_3OH), and nitrous oxide (N_2O). The present results indicate that clostridia are major strains responsible for RDX removal, and all isolates seemed to mainly transform RDX *via* its initial reduction to MNX and subsequent denitration. Since clostridia are commonly present in soil, we suggest that they may contribute to the removal of RDX in the subsurface (anoxic) soil.

Chemicals and media. The basic salts and vitamins medium were prepared as described previously using a Wolin vitamin solution (5 ml in 1 liter) and a trace metal solution (Wolin et al., 1963). The nutrient broth was composed of ($g \cdot l^{-1}$) 3 of beef extract and 5 of peptone. Yeast extract (1 $g \cdot l^{-1}$), or bacto peptone (1 $g \cdot l^{-1}$) or glucose (1 $g \cdot l^{-1}$) was added to improve growth of bacterial isolates when necessary. The medium used for the isolation and maintenance of anaerobic bacteria was Bacto Brewer Anaerobic agar (58 $g \cdot l^{-1}$) (Becton Dickinson, Sparks, MD, US). Other chemicals used in the present study were discussed in previous chapters.

Enrichment of anaerobic bacteria on RDX. The original anaerobic sludge was from a continuous upflow anaerobic sludge blanket digester (Biothane) (pH 6.5-7.5, 36-38 ºC), located in Sensient Flavor Canada (Cornwall, Ontario). It was used to convert nutrients in the food processing wastewater to methane (70% of the total gas released). The following compounds were added to the basic salts and vitamins medium to enrich bacteria using RDX (0.1 mM) as nitrogen source: hydrogen, formate and carbonate, ethanol, glucose and lactate (Table 1). Where applicable, sulfate (3.5 mM) was added to enrich sulfate-reducing bacteria. Prior to inoculation, the liquid medium in sealed serum bottles was degassed and charged with oxygen-free argon, followed by addition of sodium sulfide (0.025 %) and L-cysteine $\cdot$ HCl (0.025 %). When RDX was used as the sole carbon and nitrogen source, the headspace was charged with hydrogen gas (1 atmosphere). When formate and carbonate was used, the headspace gas was a mixture of carbon dioxide (CO_2, 20 %) and hydrogen gas (H_2, 80 %).

Nutrient broth was used as a rich medium to preserve all RDX-degrading bacteria in the anaerobic sludge.

Table 1. Growth of the anaerobic sludge enrichment cultures and biotransformation of RDX (0.2 mM) as nitrogen source in the presence of different carbon and energy sources after 8 days of incubation under argon (measurement were done in triplicates with standard deviations in bracket).

Carbon or energy sources	Biomass increase (OD_{600nm})		RDX removal (%)	RDX products (%, of total C or N)	
	without RDX	with RDX		TNX	N_2O
H_2 (1atm) (RDX as C source) [a]	0.01 (0.0)	0.07 (0.00)	94 (57)	0.1 (0.02)	31 (3)
Glucose (3.2 mM)[a]	0.05 (0.04)	0.55 (0.1)	98 (9)	0.4 (0.1)	0
Ethanol (11 mM)[a,c]	0.02 (0.01)	0.2 (0.1)	91 (8)	0.2 (0.05)	0.7 (0.8)
Ethanol (11 mM) and sodium sulfate (3.5 mM)[b,c]	0.03 (0.02)	1.0 (0.1)	78 (10)	0	21 (9)
Sodium formate (7.3 mM) sodium carbonate (4.7 mM), H_2 (0.8atm) and CO_2 (0.2atm)[a]	0.01 (0.01)	0.06 (0.02)	59 (41)	0	2 (3)
Sodium lactate (13.5 mM)[b,c]	0.2 (0.1)	1.1 (0.1)	83 (0.6)	0	4.2 (5.8)
Sodium lactate (13.5 mM) and sodium sulfate (3.5 mM)[b,c]	0.3 (0.1)	1.3 (0.0)	93 (24)	0	0.2 (0.2)
Beef extract (3 g l^{-1}) and peptone (5 g l^{-1})[a,c,d]	0.6 (0.1)	0.6 (0.1)	98 (32)	0.9 (0.3)	0.08 (0.08)

[a]: Initial biomass (OD_{600nm}) ranged from 0.02 to 0.06. [b]: Initial biomass (OD_{600nm}) ranged from 0.1 to 0.15 [c]: These enrichment cultures produced methane. [d]: The low biomass was probably due to conversion of carbon to methane.

One mL of the original anaerobic sludge was added to 19 mL of anaerobic liquid medium containing RDX (0.1 mM) and incubated statically at 37 ºC. After RDX disappearance, a fresh amount of RDX was added and the microcosm was incubated for two weeks. The

cultures were subcultured (5% transfer) consecutively seven times over a period of six months. The final enrichment cultures did not show any growth in the basic salts media in the absence of RDX (Table 1). The enrichment cultures were plated on Bacto Brewer Anaerobic agar prepared inside sealed serum bottles. Following incubation at 37 ºC (3-7 days), colonies with different morphologies were picked and were re-plated on the same agar media. The latter process was repeated three times for the purification of isolates. Growth of the bacterial isolates on RDX, sodium nitrite ($NaNO_2$, 0.5 mM) and ammonium chloride (NH_4Cl, 0.5 mM) as nitrogen source was evaluated by measuring increase in OD_{600nm} and by microscopic examination.

Phylogenetic analysis of 16S rRNA gene sequences of bacterial isolates. Colonies grown on pre-reduced PY agar (Smibert and Krieg, 1981) were picked for extraction of total DNA and PCR amplification of 16S rRNA genes according to standard molecular biology methods (Johnson, 1994; Sambrook and Russel, 2001). Sequences, with a length ranging from 1236 to 1314 bases, of 16S rRNA were compared to published sequences by BLAST. The 16S rRNA gene sequences of the isolates and those of closely related standard strains were aligned by ClustalX(1.81). The neighbor-joining method (in the MEGA2 package (Kumar et al., 2001)) based on the pair wise nucleotide distance of Kimura 2-parameter was used to build the phylogenetic tree. The number of bootstrap repetitions was 1000.

Anaerobic transformation of RDX. General RDX biotransformation conditions were described in the above enrichment tests. The carbon and energy sources used for RDX transformation by enrichment cultures and their isolates were described in Table 1. For selected isolates, the headspace of serum bottles used for growth was charged with argon unless otherwise noted. Yeast extract ($1\ g \cdot l^{-1}$), bacto peptone ($1\ g \cdot l^{-1}$) or glucose ($1\ g \cdot l^{-1}$) was added to improve growth of bacterial isolates when indicated. One mL of liquid culture was inoculated to 19 mL of liquid biotransformation media (initial OD_{600nm} of the 20 ml media after inoculation, 0.05-0.15). Microcosms were sampled under strictly anaerobic conditions for subsequent analyses as described below.

Enrichment of RDX-degrading bacteria from anaerobic sludge. In the enrichment cultures, optimal growth and RDX transformation was observed when glucose, ethanol, or lactate was added as a carbon source (Table 1). Addition of sulfate further improved growth on ethanol and lactate. The enriched mixed cultures removed 60-99% of 0.2 mM of RDX within 8 days, whereas in the abiotic controls with nitrogen in the headspace, RDX removal was less than 10%. Growth of bacteria on RDX in the presence of hydrogen gas or formate was poor. The entire final enriched mixed cultures showed little growth in the basic salts media in the absence of RDX (Table 1), indicating that the energetic chemical acted as a nitrogen source for growth.

All enriched mixed cultures transformed RDX with production of the transient nitroso derivatives MNX, DNX and TNX (Fig. 1).

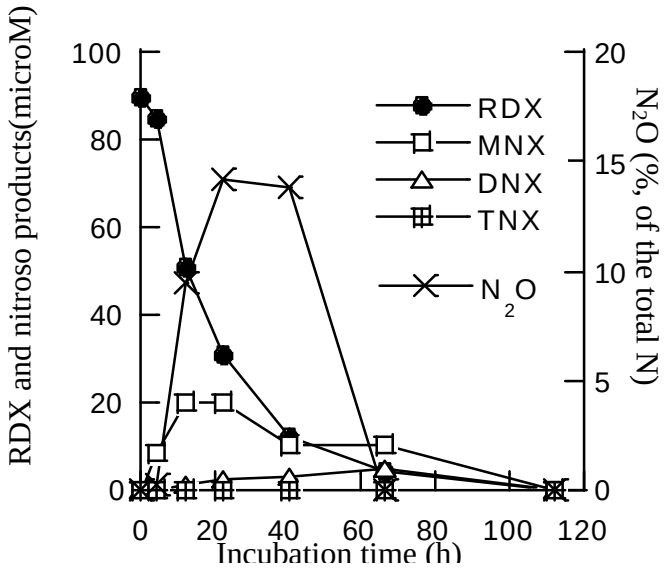

Figure 1. N_2O production and removal during RDX biotransformation by the mixed cultures enriched on RDX and nutrient broth.

Their disappearance was accompanied by the formation of HCHO, CH_3OH (data not shown) and N_2O (Table 1). The final yields of N_2O from RDX by five of the eight enrichment mixed cultures were very low (Table 1). Fig. 1 shows that N_2O was only formed as a transient product. During RDX transformation with ethanol or lactate enriched mixed cultures, CH_4

was produced, but not in RDX transformation with glucose enriched culture.

Phylogenetic diversity of RDX-transforming isolates in the enrichment cultures. Pure cultures were isolated and characterized from five of the above enrichment cultures using hydrogen, formate, glucose, ethanol or ethanol plus sulfate as co-substrate(s). Out of the 16 morphologically different colonies chosen, 15 exhibited RDX-removal activity. By comparing the partial 16S rRNA gene sequences of the isolates to genes in the GeneBank, we found that the 15 colonies belonged to six genetically distinguishable bacterial species: HAW-1, HAW-G3, HAW-G4, HAW-E3, HAW-HC1, and HAW-ES2, isolated from enrichment culture fed with hydrogen, glucose, ethanol, formate, and ethanol plus sulfate, respectively.

All the isolates were catalase and oxidase negative, obligate anaerobes, five of which (HAW-1, HAW-G3, HAW-G4, HAW-E3, HAW-HC1) were gram-positive, spore-forming, straight rods. The phylogenetic tree of 16S rRNA genes of the six isolates and those closely related standard bacterial strains is shown in Figure 2. The sequences of 16S rRNA genes of the five gram-positive isolate (HAW-1, HAW-G3, HAW-G4, HAW-E3, HAW-HC1) fell within the clusters of *Clostridium* genus. Collins et al. found that all the known species of *Clostridium* genus were very heterogeneous by their 16S rRNA gene sequences, and could be separated into 19 clusters (Collins et al., 1994). HAW-1 was a long rod (1.5-11 μm long with a diameter of 0.5-1 μm) and had an opaque round colony. Its partial 16S rRNA gene sequences fell within the cluster XI of *Clostridium* genus as described by Collins et al. (1994), with *Clostridium bifermentans* as the most closely related species (Fig. 2). HAW-G3 and HAW-G4 were short rods (1.5-3.0 μm long with a diameter of 0.5 μm) and their colonies were transparent and colorless. The 16S rRNA gene sequences of both isolates (HAW-G3 and HAW-G4) fell within the cluster XIVa of *Clostridium* genus (Collins et al., 1994) and were very closely related to *Clostridium celerecrescens* (ATCC 19403) and *Clostridium sphenoides* (DSM 5628) (Fig. 2). Highest similarity was found between the two isolates (99.8% for HAW-G4; 99.5% for HAW-G3) and *Clostridium celerecrescens.* HAW-E3 (or ES1) was also short rod (1.5 to 3.0 μm long with a diameter of 0.5 μm) and its colony was early white and flat.

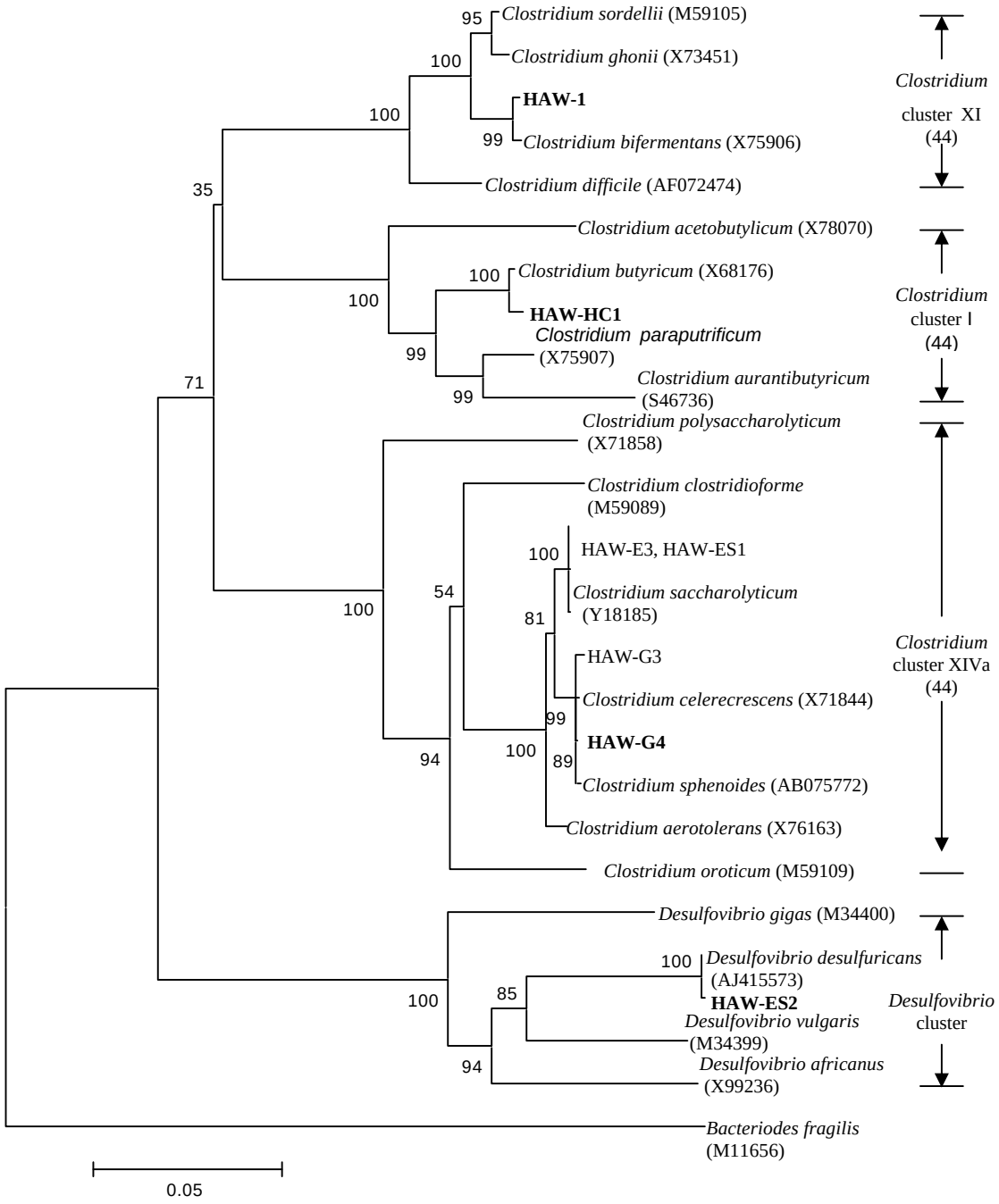

Fig. 2. Phylogeny of anaerobic bacterial isolates. The phylogenetic tree was generated based on pair wise nucleotide distance of Kimura 2-parameter using the neighbor-joining method included in MEGA2 software package. The bar indicates the difference of 2 nucleotides per 100. The number beside the node is the statistical bootstrap value.

Its partial 16S rRNA gene sequences fell within the cluster XIVa of *Clostridium* genus with the *Clostridium saccharolyticum* as the most closely related species (Fig. 2). HAW-HC1 was

a long rod (2.5-10 μm long with a diameter of 0.5-1.0 μm) and had an opaque and slightly yellowish colony. Its 16S rRNA gene sequence fell within the cluster I of *Clostridium* genus (Collins et al., 1994). Its most closely related species was *Clostridium butyricum* (Fig. 2). The spores in the liquid cultures of the above five clostridial isolates (in yeast extract and peptone medium) could not be killed by heating at 95ºC for 10 minutes. They all fermented glucose and peptone to produce hydrogen gas. The isolate HAW-ES2 was a gram-negative, non-spore forming bacterium. Its 16S rRNA gene sequence fell within the cluster of *Desulfovibrio* genus with *Desulfovibrio desulfuricans* as the closest match (Fig. 2). In general, *Clostridia* were found to be the major RDX-removing bacteria.

Beller (2002) proposed that homoacetogens are responsible for removal of RDX (at a rate of 0.5 $\mu M \cdot day^{-1}$) in an aquifer bacterial mixture using hydrogen gas as the electron donor and RDX as nitrogen source in the presence of carbonate. In the present study, a similar mixed culture removed RDX at a rate of 25 $\mu M \cdot day^{-1}$, and contained a fast RDX-removing clostridial bacterium HAW-1.

A similar clostridial RDX-removing strain identified as *Clostridium bifermentans* was previously isolated by Regan and Crawford (1994) from soils contaminated white explosives, it latter appeared to remove RDX at a rate (180 $\mu M \cdot day^{-1}$, 1.2 OD_{600nm} of biomass) slower that that (330 $\mu M \cdot day^{-1}$, 0.8 OD_{600nm} of biomass) of isolate HAW-1.

To the best of our knowledge, isolate HAW-ES2 is the first RDX-degrading sulfate-reducing bacterium, although a consortium has been reported to remove the energetic chemical under sulfate-reducing condition (Boopathy et al., 1998).

Although the presence of methanogenic bacteria in the ethanol enriched mixed cultures was demonstrated by the formation of CH_4, we did not obtain any methanogenic isolate from the above ethanol enrichment culture. This could be attributed to the employment of isolation medium that favored the growth of fermentative rather than methanogenic bacteria. The present results and the previous reports (Kitts et al., 1994; Young et al., 1997b; Zhao et al., 2002; Regan and Crawford, 1994, Pudge et al., 2003; Zhang and Hughes, 2003) showed that most known RDX-removing anaerobic (facultative or obligate) isolates are fermentative bacteria.

Bacterial diversity on RDX metabolic kinetics. When either glucose (for isolate HAW-G4) or ethanol (for isolate HAW-E3) was used as a carbon source, isolate HAW-G4 and isolate HAW-E3 used RDX as a nitrogen source for growth. Growth of the two isolates on RDX as nitrogen source was confirmed by an obvious increase in the OD_{600nm} in the presence of RDX and a negligible increase in controls that did not contain RDX or any other nitrogen source (Table 2). The two isolates were also found to grow when RDX in the above media was replaced with ammonium ion. Addition of yeast extract and peptone improved growth of both isolate HAW-G4 and isolate HAW-E3, and enhanced RDX transformation (data not shown). The specific rate for RDX removal for both isolates (HAW-G4 and E3) was 5.2 and 6.2 $\mu mol \cdot h^{-1} \cdot g$ [dry weight] of $cells^{-1}$, respectively. As shown in Table 2, isolate HAW-ES2 also seemed to grow on RDX as nitrogen source in the basic medium containing ethanol and sulfate (Table 2). The specific RDX-removal rate (5.5 $\mu mol \cdot h^{-1} \cdot g$ [dry weight] of $cells^{-1}$) of HAW-ES2 was close to that of isolate HAW-G4 and E3.

Table 2. Growth of bacterial isolates on RDX (0.1mM) as nitrogen source and yields of RDX products (measurement were done in triplicates with standard deviations in bracket).

Isolates	Bacterial growth (OD_{600nm} increase)[a]		Yields of final products (%, of total C or N in RDX removed)		
	Without RDX	With RDX	C-products CH_3OH	HCHO	N-product N_2O
HAW-G4[b]	0.03 (0.02)	0.24 (0.05)	80(6)	0.47(0.06)	27(0.8)
HAW-E3[c]	0.02 (0.01)	0.12 (0.02)	8.7(0.1)	8.0(0.4)	33(2)
HAW-ES2[d]	0.03(0.01)	0.10 (0.02)	7.5(0.5)	0.4(0.1)	35(2)

[a]: Initial biomass (OD_{600nm}): HAW-G4, 0.1; HAW-E3, 0.11; HAW-ES2, 0.07. [b]:Glucose (1 g l^{-1}) was used as carbon source. [c]: Ethanol (1 g l^{-1}) was used as carbon source. [d]: Ethanol (1 g l^{-1}) was used as carbon source and sodium sulfate (3.5 mM) as electron acceptor.

Although the enrichment culture was able to grow on RDX and H_2 (Table 1), its isolate HAW-1 did not show any appreciable growth under the same conditions. However, addition of yeast extract greatly improved its growth and the removal rate of the energetic chemical (data not shown). Isolate HAW-1 showed the highest specific RDX-removal rate (24.0

μmol·h^{-1}·g [dry weight] of $cells^{-1}$) among all isolates, suggesting that this strain might possess a high RDX-transformation activity.

Similarly, the isolate HAW-HC1 that was able to grow on RDX as nitrogen source and formate as carbon source (Table 1) did not show any obvious growth on RDX under the same conditions. Addition of yeast extract, peptone and glucose moderately improved the growth of strain HAW-HC1 and enhanced RDX removal. Isolate HAW-HC1 exhibited the lowest specific rate (2.5 μmol·h^{-1}·g [dry weight] of $cells^{-1}$) for RDX removal amongst all the isolates. All the above four clostridial isolates are strictly anaerobic fermentative bacteria, exhibiting faster RDX-removal rates than any previously reported facultative anaerobic bacteria belonging to the fermentative *Enterobacteriaceae* family (Kitts et al., 1994; Young et al., 1997; Zhao et al., 2002; Pudge et al., 2003). For example, the RDX removal rates (2.4 - 24.0 μmol·h^{-1}·g [dry weight] of $cells^{-1}$) of the present isolates were approximately six to sixty times higher than the rate (0.41 μmol·h^{-1}·g [dry weight] of $cells^{-1}$) of the previously isolated *Klebsiella pneumoniae* strain SCZ-1 (Zhao et al., 2002). This suggests that obligate fermentative anaerobes are faster in removing RDX than facultative ones.

RDX metabolic products by bacterial isolates. Like the enrichment cultures, bacterial isolates also transformed RDX to initially produce the nitroso derivatives MNX, DNX and TNX prior to ring cleavage to HCHO and CH_3OH. After 5 days of incubation in the basic salts media containing either glucose or ethanol as carbon source, isolate E3 and G4 removed 83-99% of 0.1 mM RDX , with production of 8-17% of nitroso derivatives and 3-9.6 % of nitrite (relative to the total nitrogen in RDX removed). The yields of TNX of the latter two isolates were less than 1%. During transformation of RDX by isolate ES2, the yields of DNX and TNX were negligible. All the nitroso derivatives were not persistent. Complete removal of RDX and its nitroso derivatives produced HCHO and methanol. In one case, isolate HAW-G4 transformed RDX to produce mainly CH_3OH, accounting for 80% of total carbon of RDX removed.

Although we did not detect NO_2^- during RDX incubation with the mixed cultures, we were able to detect it with all isolates with the highest yield (9.6% of total N in RDX removed) observed with isolate HAW-E3, indicating that in addition to nitroso routes, RDX

degradation also involved denitration. Previously we showed that *Rhodococcus* sp. Strain DN22 aerobically degraded RDX via initial denitration to the dead end product 4-nitro-2,4-diazabutanal (Fournier et al., 2002), the absence of 4-NDAB in this case is attributed to its degradation under anaerobic conditions.

All isolates produced N_2O as final products, which accounted for approximately one third of the total nitrogen content of RDX removed. The pure cultures fed with NO_2^- in the absence of RDX, did not produce N_2O. In contrast to the enriched mixed cultures (Table 1), none of the five isolates removed N_2O, suggesting that other unidentified bacteria in the mixed cultures were responsible for N_2O removal.

The formation of the secondary product N_2O was suggested to be derived from one of the -N-NO_2 groups originally present in RDX (Hawari et al., 2000a). In the present study, all isolates gave N_2O with yields close to 30% of the total nitrogen in RDX (Table 2), suggesting the involvement of only one -N-NO_2 group (representing one third of the total nitrogen content of RDX) in its formation. As reported previously, RDX can transform anaerobically *via* sequential reduction to MNX, DNX and TNX or *via* initial denitration followed by ring cleavage to produce HCHO, CH_3OH and N_2O (Johnson, 1994; Boopathy et al., 1998). In all tested isolates, formation of MNX was found, but TNX and DNX were only detected in low amounts, indicating that denitration of MNX, was a dominant route to RDX ring cleavage and secondary decomposition.

All RDX-removing facultative bacteria of the *Enterobacteriaceae* family (Kitts et al., 1994; Young et al., 1997, Zhao et al., 2002; Pudge et al., 2003) and strictly anaerobic bacteria (Regan and Crawford, 1994; Zhang and Hughes, 2003) including the present isolates are known to contain hydrogenase enzyme (Wu and Mandrand, 1993; Zehnder, 1988; Schlegel and Schneider, 1978; Widdel and Hanson, 1991; Fritz et al., 2001). Most of the RDX-removing anaerobic bacterial isolates known thus far are fermentative H_2-producers. Also a rapid H_2-dependent RDX transformation activity was previously described in the crude extract of *Clostridium acetobutylicum* (Zhang and Hughes, 2003).

Finally, the *Enterobacteriaceae* family only exhibited hydrogenase and RDX-removing activity under anaerobic conditions (Zhao et al., 2002; Pudge et al., 2003; Kitts et al., 1994; Young et al., 1997). Experimental evidence gathered thus far suggest that RDX

transformation was initiated by hydrogenase activity. *Clostridia,* which seemingly play a major role in the rapid removal of RDX under strictly anaerobic conditions, are also present in soils contaminated with RDX (Regan and Crawford, 1994). Therefore our observations suggest that *clostridia* in the anoxic environment of soil may also use RDX as a N source without accumulating nitroso derivatives. On the other hand, aerobic bacteria such as *Stenotrophomonas maltophilia* (Binks et al., 1995) and species of *Rhodococcus* (Coleman et al., 1998; Seth-Smith et al., 2002) in soil have been reported to degrade RDX. Since both aerobic (surface soil) and anaerobic (subsurface soil) environment are present in soils, both aerobic and anaerobic bacteria will compete for RDX at the oxic/anoxic boundary. Further study on this ecological aspect would be useful to help understand how RDX is degraded in field soil environment, which will be discussed latter in the report. In the previous chapters we successfully employed sludge to degrade RDX and HMX. Also we isolated several isolates and used them to degrade the two cyclic nitramines. In the following chapters, we will discuss the role of enzymes in the initial steps of degradation under anaerobic conditions.

V.3 Role of Enzymes in the Degradation of RDX and HMX.

The previous discussion demonstrated that it is possible to degrade RDX and HMX by consortia in anaerobic sludge. Facultative and strict anaerobes were also isolated and employed to biodegrade the two energetic chemicals. Although we were able to provide experimental evidence for the degradation and mineralization of RDX and HMX, the initial enzymatic processes involved in their transformation were still unknown. To test the hypothesis that the initial reaction involves either reduction of a nitro group(s) or denitration we designed experiments to test the ability of several enzymes that are known for their reducing activities such as nitrate reductase, xanthine oxidase and diaphorase to catalyze the initial reaction(s) leading to ring cleavage of the two energetic chemicals and subsequent decomposition. Enzymology of RDX and HMX is not well known and hence more work is needed in this area in order to understand and optimize the bioremediation process of these compounds.

V.3.1 Biotransformation of RDX Catalyzed by a NAD(P)H: Nitrate Oxidoreductase from **Aspergillus niger.**

- Bhushan, B., A. Halasz, J. Spain, S. Thiboutot, G. Ampleman, and J. Hawari. **2002.** Biotransformation of hexahydro-1,3,5-trinitro-1,3,5-triazine catalyzed by a NAD(P)H: nitrate oxidoreductase from *Aspergillus niger*. *Environ. Sci. Technol***.** 36: 3104-3108.

KEY FINDINGS:

A nitrate reductase from *Aspergillus niger* catalyzed biotransformation of RDX most effectively at pH 7.0 and 30^{o}C under anaerobic conditions using NADPH as the electron donor. LC/MS (ES-) chromatograms showed the formation of MNX and methylenedinitramine (MEDINA) as key initial products of RDX, but neither the dinitroso (DNX) nor the trinitroso (TNX) derivatives were observed. None of the initially detected products accumulated and their disappearance was accompanied by the accumulation of nitrous oxide (N_2O), formaldehyde (HCHO) and ammonium ion (NH_4^+). Stoichiometric studies showed that three NADPH molecules were consumed and one molecule of methylenedinitramine was produced per RDX molecule. The carbon and nitrogen mass balances were 96.14 % and 82.10 %, respectively. The stoichiometries and mass balance measurements supported a mechanism involving initial transformation of RDX to MNX *via* a two electron reduction mechanism. We assume that MNX undergoes further reduction to produce hydroxylamine (RDX-NHOH) and amine (RDX-NH_2) derivatives, which lead to a rapid ring cleavage to form methylenedinitramine. The latter underwent quantitative decomposition to produce two molecules of N_2O and one HCHO molecule. The results clearly indicate that an initial reduction of a nitro group(s) to the corresponding MNX is necessary and sufficient for the continued decomposition of RDX.

Biotransformation conditions and product identification. We found that *A. niger* nitrate reductase catalyzed the transformation of RDX in the presence of NADPH as the electron donor. The transformation was optimal under anaerobic conditions at pH 7.0 and 30^{o}C (data not shown). The disappearance of RDX was accompanied by the formation of MNX and the ring cleavage product methylenedinitramine (MEDINA). In control experiments, no RDX

degradation was observed in second and third control (see experimental section IV.11.1). However, in the first control a negligible RDX loss (< 3 % of total RDX degradation) was observed due to direct interaction of NADPH and RDX. In order to strengthen our hypothesis that RDX is first reduced to MNX, which them undergoes further reduction to finally produce methylenedinitramine, we incubated the standard MNX with nitrate reductase under similar reaction conditions as those of RDX biotransformation. As a result, we observed the formation of methylenedinitramine from MNX (Figure 1, blocks C and D). Figure 1 is a typical LC/MS (ES-) chromatogram obtained after incubating RDX and MNX in separate vials with nitrate reductase for 60 minutes under the optimal reaction conditions. MNX and methylenedinitramine were identified by their chromatographic retention times and UV spectra as compared with that of standards. In mass-spectrometric (MS) studies using negative electrospray ionization mode (ES-), MNX produced from RDX and the standard MNX exhibited characteristic mass fragment at 46 Da and a characteristic mass of an adduct product at 251 Da, while, MEDINA exhibited a deprotonated molecular mass ion [M-H] at 135 Da and a characteristic mass fragment at 61 Da consistent with the standard as we have reported previously (Halasz et al., 2002).

A significant observation in Figure 1 is the absence of the dinitroso (DNX) and trinitroso (TNX) products of RDX. None of the products in Figure 1 accumulated and their disappearance was accompanied by the accumulation of formaldehyde (HCHO) and nitrous oxide (N_2O).

The product distribution was similar to that obtained during biodegradation of RDX with domestic anaerobic sludge (Halasz et al., 2002). The main difference between the two systems is the subsequent mineralization of HCHO in the presence of sludge (Halasz et al., 2002). The latter is expected to contain a complex consortium of microbes with enzyme(s) for the biodegradation of HCHO.

Stoichiometry and pathway. In the time course study, methylenedinitramine was observed as the prime intermediate and N_2O and HCHO were the major end products (Figure 2). Throughout the course of reaction, the concentration of methylenedinitramine was low and did not exceed 10 μmoles because it is quite unstable at pH 7.0 and rapidly decomposed into

N_2O and HCHO. The time-course and stoichiometry of the abiotic decomposition of methylenedinitramine in water has been studied earlier and reported in one of our previous work (Halasz et al., 2002).

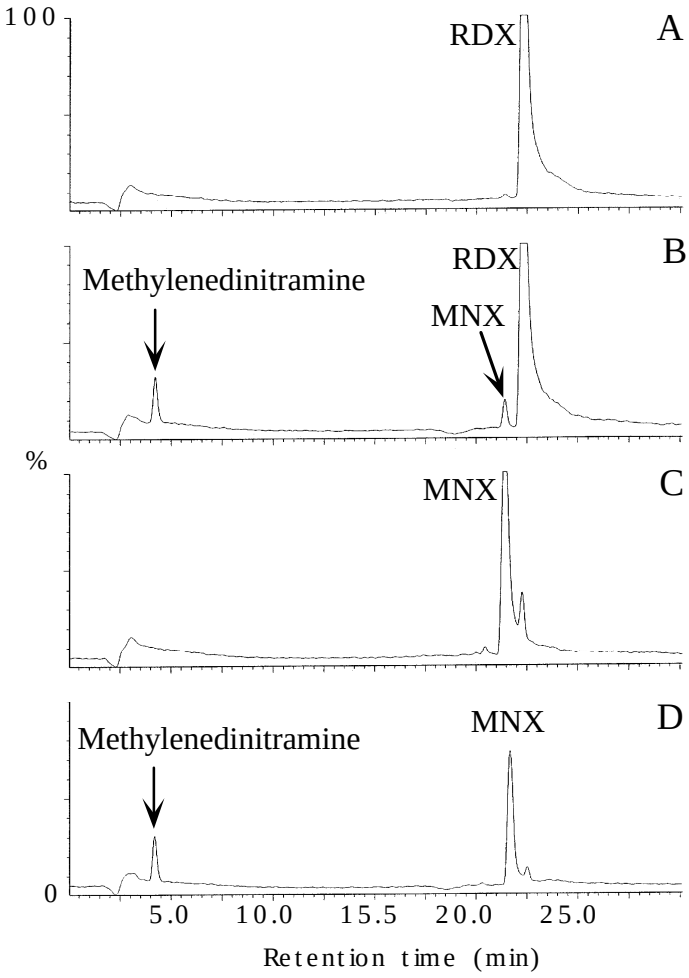

Figure 1. LC/MS (ES-) chromatogram of nitrate reductase catalyzed transformation of RDX and MNX showing methylenedinitramine as the prime intermediate. Block A and B are 0 minute and 60 minutes reaction, respectively, between RDX and nitrate reductase; C and D are 0 minute and 60 minutes reaction, respectively, between MNX and nitrate reductase.

The quantitative decomposition of methylenedinitramine into two molecules of N_2O and one molecule of HCHO (Halasz et al., 2002) was used in the present study to calculate the stoichiometry of RDX biotransformation with the enzyme. Table 1 shows that 86 μmoles of RDX produced 148 μmoles N_2O and 10 μmoles methylenedinitramine (equivalent to 20

μmoles N_2O). Hence we concluded that for each reacted molecule of RDX only one molecule of methylenedinitramine, representing two third of N-NO_2 groups, was produced.A part of the remaining one third of the N-NO_2 groups in RDX apparently leads to the formation of ammonium ion (88 μmoles). The total nitrogen mass balance was 82.10 % and was distributed between N2O (57.37 %), methylenedinitramine (7.75 %), and ammonium ion (16.98 %) (Table 1). The carbon mass balance was 96.13 % and was distributed between HCHO (92.27 %) and methylenedinitramine (3.87 %) which indicated that all the recovered carbon was in form of HCHO. As a result, it was concluded that one RDX molecule produced three HCHO molecules (Figure 3).

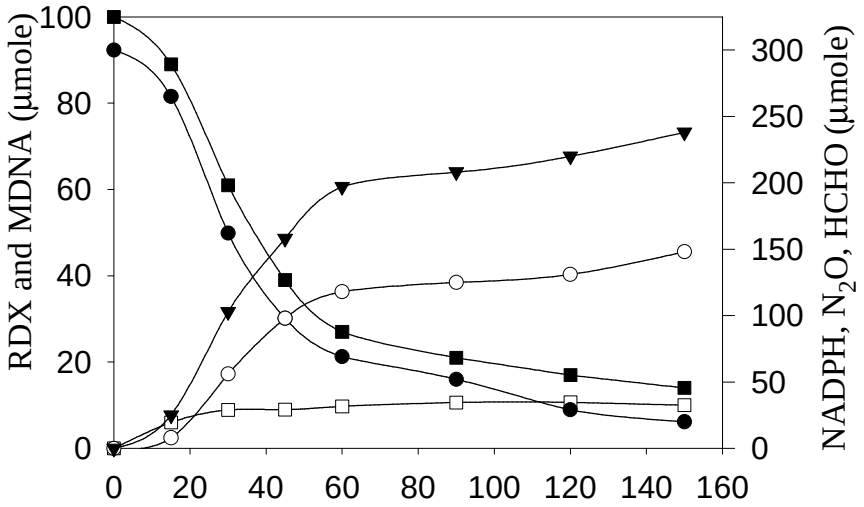

Figure 2. Time course curves of nitrate reductase catalyzed RDX transformation with simultaneous production of intermediates and end-products; symbols, ¡ RDX; ? Methylenedinitramine (MDNA); ? N_2O; ? NADPH; ? HCHO. Standard deviations were within 7 % of the mean absolute value (n = 3).

It was difficult to quantify MNX since it existed in trace amount, throughout the reaction because of its continuous further conversion. In another experiment, standard MNX (with two N-NO_2) was bioconverted to methylenedinitramine (with two N-NO_2) by nitrate reductase (Figure 1). Neither DNX (with only one N-NO_2) nor TNX (with no N-NO_2) can act

as a precursor to methylenedinitramine. For each reacted RDX molecule, roughly three molecules of NADPH, representing 6 electrons, were consumed (Table 1).

Table 1. Carbon and nitrogen mass balance and stoichiometry of metabolites produced during RDX transformation catalyzed by nitrate reductase from *Aspergillus niger* after 150 minutes of reaction.

Reactants/Metabolites	Concentration of Reactants/metabolites (μmole)	% Carbon recovery*	% Nitrogen recovery*
1. RDX	86	100	100
2. NADPH	280	NA	NA
3. Methylenedinitramine (MEDINA)	10	3.87	7.75
4. Formaldehyde (HCHO)	238	92.27	NA
5. Nitrous oxide (N_2O)	148	NA	57.37
6. Ammonium ion (NH_4^+)	88	NA	16.98
Total % mass recovery		96.14	82.10

*Calculated from the total absolute mass values of carbon and nitrogen in the transformed RDX (86 μmole); NA, not applicable; Standard deviations were within 7 % of the mean absolute value (n = 3).

Based on the above stoichiometry, we proposed a degradation pathway for RDX as shown in Figure 3. RDX was reduced in three sequential steps to first produce MNX, followed by the formation of the hydroxylamine derivative (I) which then reduced further to the amine metabolite NH_2-RDX (II). Both I and II are expected to be unstable in water and might undergo rapid ring cleavage to produce the unstable hydroxyalkylnitramine product (III). Alkylhydroxylamines are reportedly unstable in water (Corbett and Corbett, 1995) and thus III should undergo rapid decomposition to produce methylenedinitramine, HCHO and another hypothetical compound possibly methanolhydrazine (VI) (NH_2NHCH_2OH).

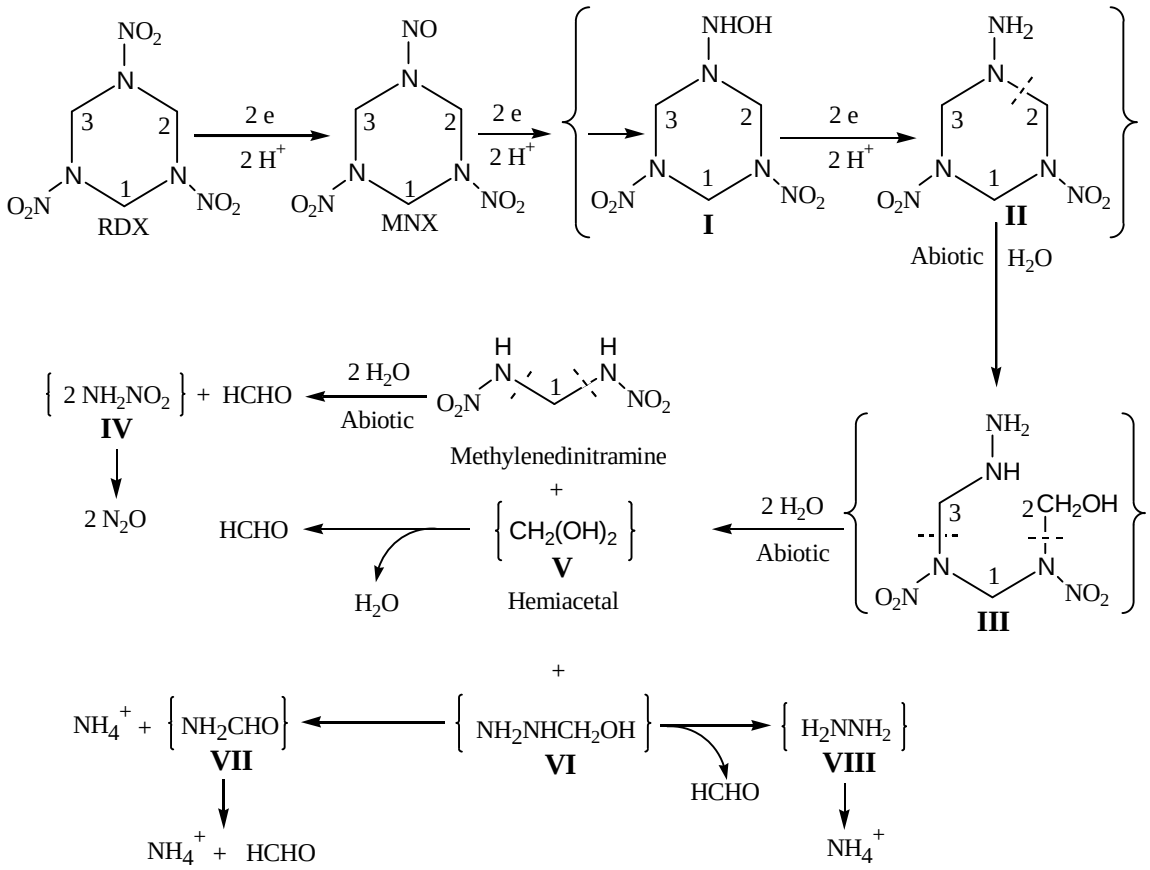

Figure 3. Proposed pathway of nitrate reductase catalyzed RDX transformation on the basis of stoichiometry of metabolites recovered and NADPH consumed. Carbon atoms are numbered as 1, 2, 3 in the RDX ring. Intermediates shown inside brackets were not detected.

VI most likely also decomposes in water since we could not detect it. The decomposition of VI was presumed to produce HCHO and NH_4^+ possibly by two routes *i.e. via* formation of formamide and/or hydrazine (Figure 3). However, we did not detect either of the two compounds probably because they did not accumulate. For instance, when either formamide (50 μM) or hydrazine (50 μM) was incubated with nitrate reductase under similar reaction conditions to those described for RDX, roughly 50 % of the formamide was converted to HCHO and NH_4^+, and 40 % of the hydrazine to NH_4^+. The unaccounted starting materials could not be traced probably because of their reactivity with reaction mixture components like protein, buffer and/or NADPH.

We were able to account for 82.10 % of the total nitrogen mass content of RDX; we

speculated that the missing 18 % nitrogen mass existed in form of an unidentified compound that might have reacted with other components as mentioned above. In particular, hydrazine is a very reactive compound and it is known to polymerize with HCHO (Mashima, 1966; Kamachi and Murahashi, 1974). Hydrazine formation was first proposed by McCormick et al. (1981) during RDX degradation by an anaerobic sludge and since then there has been no other report that describes its formation from biodegradation of cyclic nitramine explosives such as RDX.

We excluded DNX and TNX from the RDX biotransformation pathway (Figure 3) based on our observation that none could be detected by LC/MS (ES-). Furthermore, neither of the two nitroso products can produce methylenedinitramine. In contrast, the stoichiometric formation of methylenedinitramine (one μmole of RDX produced one μmole of methylenedinitramine) confirmed that ring cleavage proceeded *via* MNX (Figure 3). However, DNX and TNX have been reportedly observed during RDX degradation by a consortium containing *Serratia marcescence* (Young et al., 1997a), by anaerobic sludge (McCormick et al., 1981; Adrian and Chow, 2001; Oh et al., 2001) and by soil slurries (Shen et al., 2000; Sheremata et al., 2001; Young et al., 1997b) which further indicate the possibility of some other mechanism(s) operating in the complex environments.

Role of nitrate reductase in the initial transformation of RDX. Eukaryotic nitrate reductases (EC 1.6.6.1-3) contain three redox cofactors *i.e.* FAD, heme-Fe and molybdopterin (Mo-MPT). FAD is the oxidation site for NAD(P)H and the subsequent electron transfer proceeds through heme-Fe center to the molybdopterin which is a reduction site for nitrate (Campbell, 2001). It is known that this enzyme reduces nitrate to nitrite *via* a two electron transfer mechanism and this reaction takes place at Mo-MPT cofactor site (Campbell, 1999, 2001; Brockman et al., 1949). During nitrate reduction, the molybdenum (Mo) present in the Mo-MPT cofactor frequently changes its oxidation states from oxidized (Mo^{VI}) to reduced state (Mo^{IV}) and *vice-versa* by receiving two electrons from the heme-Fe center and transferring them to nitrate. In the present study, nitrate appeared to be a competitive inhibitor of RDX biotransformation as evident by the Lineweaver-Burk plots in the presence of increasing concentration of nitrate in the reaction mixture (Figure 4). This

indicated that nitrate and RDX might be sharing a common binding site on the enzyme (*i.e.* Mo-MPT cofactor).

We found that 86 μmoles of RDX transformation was accompanied by the consumption of 280 μmoles of NADPH, indicating that roughly three NADPH molecules were consumed during transformation of one RDX molecule under anaerobic conditions (Table 1). Therefore, we presume that a total of six electrons (or 3 NADPH) have been utilized in the complete transformation of RDX. Since RDX requires an obligatory two electrons to be transformed to MNX, it is concluded that nitrate reductase might have catalyzed two electron transfer to the RDX in the first reduction step to produce MNX. Thereafter, four additional electrons might have been consumed for the subsequent reduction of MNX to RDX-NHOH (II) (1 NADPH) and RDX-NH_2 (II) (1 NADPH) (Figure 3). However, we can not rule out the possibility that RDX-NHOH, being unstable, may also undergo ring cleavage. Under these circumstances, the last pair of electrons (1 NADPH) may be utilized after the ring cleavage.

As far as we are aware, there are no reports that describe the transformation of cyclic nitramine compound(s) with nitrate reductase(s). However, the enzyme-catalyzed two electron reduction of nitroaromatic compounds to nitroso derivatives by NAD(P)H:quinone reductase (Riley and Workman, 1992; Knox et al., 1993) and bacterial nitroreductases (Peterson et al., 1979; Bryant and DeLuca, 1991; Koder and Miller, 1998, Nivinskas et al., 2001; Wenzhong et al., 1987) have been reported. It has been reported that type 1 oxygen insensitive nitroreductase from *Escherichia coli* catalyze a two electron reduction of nitro groups (Peterson et al., 1979). Kitts et al. (2000) demonstrated the reduction of RDX and TNT by a type I oxygen insensitive nitroreductase from *Enterobacter cloacae* without elaborating on the mechanism or degradation products. It was earlier reported that the prime function of nitroreductases is to reduce only nitro groups of nitroaromatic compounds and they can not reduce inorganic *N*-oxides such as nitrate or nitrite (Bryant and DeLuca, 1991; Kinouchi and Ohnishi, 1983). On the other hand, Averill (1995) reported that nitrate is chemically analogous to organic nitro group (Ar–NO_2) which indirectly indicates that nitrate reductase may function as nitroreductase. In the present study, nitrate reductase from *A. niger* seemed to share the functional similarity (Figure 3) with type I nitroreductase because the latter also catalyze a two electron transfer process (Peterson et al., 1979; Bryant and DeLuca,

1991; Koder and Miller, 1998; Nivinskas et al., 2001).

The results discussed above have clearly demonstrated that MNX is the first reduced product of RDX formed by a two electron reduction catalyzed by the nitrate reductase. MNX most likely underwent further reduction followed by the ring cleavage and subsequent decomposition and finally produced stoichiometric amount of products.

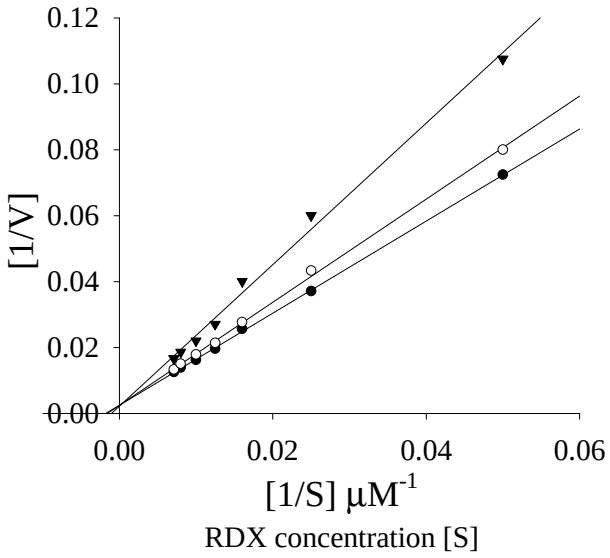

Figure 4. Lineweaver-Burk plots showing nitrate as the competitive inhibitor of nitrate reductase catalyzed RDX transformation. Symbols, (?) without nitrate; (?) in the presence of 20 μM nitrate; (?) in the presence of 100 μM nitrate.

This study strongly supported our previous hypothesis of the involvement of MNX as one of the key initial metabolites formed during RDX incubation with sludge prior to ring cleavage (Halasz et al., 2002). In the following chapter we will explore the degradation of RDX and HMX with other potential reducing enzymes to gain further insight into other initial process, such as denitration and α-hydroxylation, involved in the degradation of these chemicals.

V.3.2 Mechanism of xanthine oxidase catalyzed biotransformation of HMX under anaerobic conditions.

- Bhushan, B., L. Paquet, A. Halasz, J. C. Spain, and J. Hawari. **2003b**. Mechanism of xanthine oxidase catalyzed biotransformation of HMX under anaerobic conditions. *Biochem. Biophys. Res. Commun*. 306: 509-515.

KEY FINDINGS:

Enzyme catalyzed biotransformation of the energetic chemical HMX is not known. The present study describes a xanthine oxidase (XO) catalyzed biotransformation of HMX to provide insight into the biodegradation pathway of this energetic chemical. The rates of biotransformation under aerobic and anaerobic conditions were 1.6 ± 0.2 and 10.5 ± 0.9 nmoles h^{-1} mg $protein^{-1}$, respectively, indicating that anaerobic conditions favored the reaction. The biotransformation rate was about 6-fold higher using NADH as an electron-donor compared to xanthine. During the course of reaction, the products obtained were nitrite (NO_2^-), methylenedinitramine (MEDINA), 4-nitro-2,4-diazabutanal (NDAB), formaldehyde (HCHO), nitrous oxide (N_2O), formic acid (HCOOH) and ammonium (NH_4^+). The product distribution gave carbon and nitrogen mass-balances of 91 and 88 %, respectively. A comparative study with native-, deflavo- and desulfo-XO and the site-specific inhibition studies showed that HMX biotransformation occurred at the FAD-site of XO. Nitrite stoichiometry revealed that an initial single N-denitration step was sufficient for the spontaneous decomposition of HMX.

Enzyme preparation. NADH, xanthine, uric acid, flavin adenine dinucleotide (FAD), allopurinol, diphenyleneiodonium chloride (DPI) were purchased from Sigma chemicals. Xanthine oxidase (EC 1.1.3.22) from buttermilk was obtained from Sigma chemicals, Canada. The enzyme suspension was mixed with five volumes of potassium phosphate buffer (50 mM, pH 7.0) and filtered through a Biomax-5K membrane (Sigma chemicals) twice before resuspending in the same buffer. The protein concentration was measured by bicinchoninic acid (BCA) kit (Sigma chemicals) as per company instructions using bovine serum albumin as standard. The native xanthine oxidase (XO) activity was estimated using

the standard method by measuring the increase in absorbance at 295 nm as a function of rate of oxidation of xanthine to uric acid.

Enzyme modifications and reconstitution. The deflavo- and reconstituted-XO were prepared as described by Komai et al. (1969). Reconstitution was carried out by incubating the deflavo-XO with 200 μM FAD in a potassium phosphate buffer (50 mM, pH 7.0) for 1 h at 30^{o}C. The unbound FAD was removed by washing the enzyme with the same buffer using Biomax-5K membrane centrifuge filter units. Preparation of desulfo-XO and its subsequent reactivation were done by the methods described by Massey and Edmondson (1970). The reactivation of desulfo-XO was performed by incubating it with a 10 mM solution of Na_2S at 30^{o}C in a potassium phosphate buffer (50 mM, pH 7.0) for 90 min. After the incubation period, the free Na_2S was removed as described above.

Biotransformation assays. HMX biotransformation by the native-, desulfo- and deflavo-forms of xanthine oxidase were performed under both aerobic and anaerobic conditions in 6 mL glass vials. Anaerobic conditions were created by purging all the solutions with argon three times (10 min. each time at 10 min. intervals) and replacing the headspace air with argon in a sealed vial. Each assay vial had one mL of an assay mixture containing HMX (40 μM), NADH (150 μM) or xanthine (150 μM) and xanthine oxidase (1 mg/mL) in a potassium phosphate buffer (50 mM), pH 7.0. Reactions were performed at 30^{o}C. Three different controls were prepared by omitting either enzyme, NADH or both from the assay mixture. Samples from the liquid and gas phase in the vials were withdrawn periodically to analyze for HMX and the biotransformed products as described in analytical procedures (discussed below). NADH was determined as described previously Bhushan et al. (2002a). HMX biotransformation activity of the enzyme was expressed as nmoles.h^{-1}.mg protein^{-1} unless otherwise stated.

In order to detect and quantify the HMX metabolites which were produced in trace amounts, the energetic chemical was added to the reaction mixture at a final concentration of 11.8 mg.L^{-1} (above saturation level) from a 10,000 mg.L^{-1} stock solution made in acetone. The aqueous solubility of HMX at 25 ^{o}C has been reported as 6.6 mg.L^{-1} (Groom et al., 2003).

HMX and its nitroso-derivatives *i.e.* octahydro-1-nitroso-3,5,7-trinitro-1,3,5,7-tetrazocine, octahydro-1,3-dinitroso-5,7-dinitro-1,3,5,7- tetrazocine, octahydro-1,5-dinitroso-3,7-dinitro-1,3,5,7- tetrazocine, octahydro-1,3,5-trinitroso-7-nitro-1,3,5,7- tetrazocine, and octahydro-1,3,5,7-tetranitroso-1,3,5,7-tetrazocine were analyzed by LC/MS as described previously in the report. The two ring cleavage products methylenedinitramine and 4-nitro-2,4-diazabutanal were analyzed and quantified by a Waters HPLC as described above and by comparison with reference standards. Nitrite (NO_2^-), ammonium (NH_4^+), formaldehyde (HCHO) and nitrous oxide (N_2O) were analyzed by the previously described methods in the technical approach section. The detection of formic acid was enhanced by reducing the background with an autosuppressor from ALTECH (model DS-Plus) and the detection limit was 100 ppb (parts per billion).

Biotransformation of the intermediates. In order to determine the fate of transient HMX intermediates i.e. methylenedinitramine (40 μM), 4-nitro-2,4-diazabutanal (40 μM) and HCHO (100 μM), the standard intermediates were incubated separately with XO under the same experimental conditions as used for the biotransformation of HMX under anaerobic conditions. Samples from the liquid and gas phase in the vials were withdrawn periodically to analyze for the residual compound and the biotransformed products as described in analytical procedures.

Enzyme inhibition studies. This study was performed by incubating XO with increasing concentrations of site-specific inhibitors i.e. allopurinol or DPI for 30 min at room temperature. Thereafter, HMX biotransformation activity of the treated enzyme was determined by using two different electron-donors i.e. NADH and xanthine. The nitrite mediated inhibition of HMX biotransformation was determined by assaying the XO against HMX in the presence of increasing $NaNO_2$ concentrations. The type of inhibition was inferred from the standard Lineweaver-Burk plots.

Biotransformation, mass-balance and product stoichiometry of HMX. Xanthine oxidase biotransformed HMX, using NADH as electron-donor, under aerobic and anaerobic

conditions at the rates of 1.6 ± 0.2 and 10.5 ± 0.9 nmoles h^{-1} mg $protein^{-1}$, respectively, indicating that anaerobic conditions favored the reaction. Hence the subsequent study was carried out under anaerobic conditions. In a time-course, HMX disappearance was accompanied by the formation of nitrite (NO_2^-), nitrous oxide (N_2O), formaldehyde (HCHO) and formic acid (HCOOH) (Fig. 1).

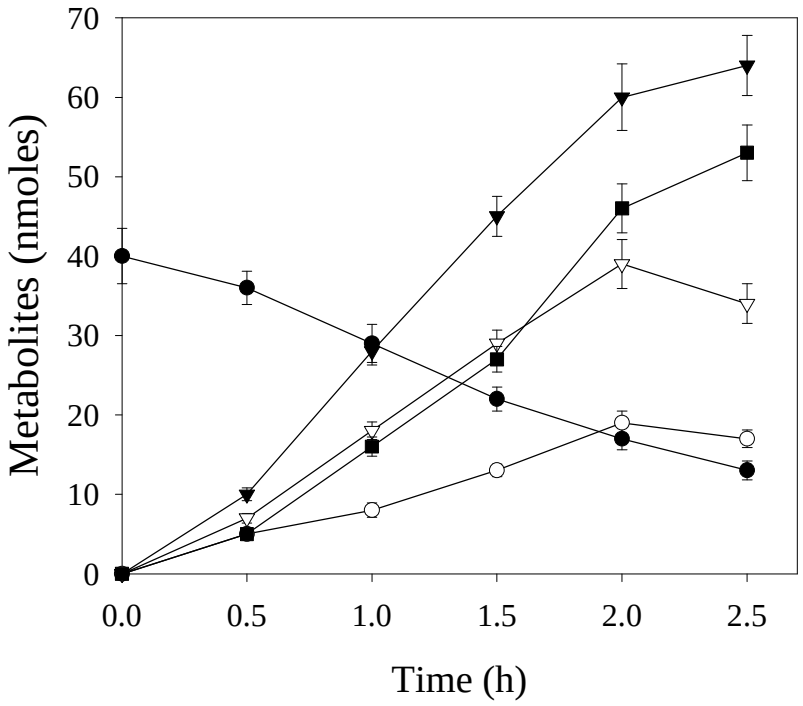

Fig. 1. Time-course of NADH-dependent biotransformation of HMX by xanthine oxidase under anaerobic conditions. HMX (?), nitrite (?), HCHO (∇), HCOOH (¦) and nitrous oxide (?). Data are mean of duplicate experiments (*n* = 2), error bars indicate standard deviation. Some error bars are not visible due to their smaller size.

Methylenedinitramine (MEDINA) and 4-nitro-2,4-diazabutanal (NDAB) were detected as transient metabolites, and ammonium (NH_4^+) was an end product (Table 1).

XO also biotransformed HMX metabolites i.e. NDAB and HCHO. For example, when

standard compounds of NDAB and HCHO were incubated with XO under the same reaction conditions as used for HMX, both compounds were biotransformed at the rates of 8.0 ± 0.6 and 16.5 ± 1.4 nmoles h^{-1} mg $protein^{-1}$, respectively. The NDAB produced N_2O, NH_4^+ and HCOOH whereas utilizes water (H_2O) as a source of oxygen during biotransformation of HCHO to HCOOH (Hille and Nishino, 1995).

On the other hand, standard MEDINA was readily decomposed abiotically at a rate of 9.2 ± 0.7 nmoles h^{-1} under similar reaction conditions. It has previously been reported that MEDINA decomposes abiotically to produce N_2O and HCHO (Halasz et al., 2002). None of the nitroso-derivatives of HMX were observed during the course of reaction.

Some of the HMX products observed in the present study are consistent with those detected in our previous studies with HMX (Hawari et al., 2001; Balakrishnan et al., 2003) and RDX (hexahydro-1,3,5-trinitro-1,3,5-triazine) (Bhushan et al., 2002a,b, 2003a; Fournier et al., 2002). Biodegradation of HMX with anaerobic sludge produced an array of products including nitroso-derivatives of HMX, methylenedinitramine, formaldehyde, nitrous oxide, nitrogen and carbon dioxide (Hawari et al., 2001). Recently, we observed nitrite, nitrous oxide, 4-nitro-2,4-diazabutanal and formaldehyde during alkaline hydrolysis of HMX (Balakrishnan et al., 2003). The 4-nitro-2,4-diazabutanal, besides being a HMX metabolite in the present study, was also a major product during biotransformation of RDX by cytochrome P450 (Bhushan et al., 2003a) and *Rhodococcus* sp. DN22 (Fournier et al., 2002). On the other hand, methylenedinitramine was a major transient metabolite produced during RDX biotransformation by a diaphorase from *Clostridium kluyveri* (Bhushan et al., 2002b) and nitrate reductase from *Aspergillus niger* (Bhushan et al., 2002a).

The total carbon and nitrogen mass-balances in the present study were 91 and 88 %, respectively (Table 1). Numerically, of the 4.0 carbon atoms per HMX molecule, 3.3 were recovered in forms of HCHO and HCOOH. On the other hand, of the 8 nitrogen atoms per HMX molecule, 6 were recovered in forms of NO_2^-, N_2O and NH_4^+ (Table 1). The absence of nitroso-intermediates from HMX and the formation 0.6 mole of NO_2^- (equivalent to one mole) per mole of reacted HMX indicated a single N-denitration of HMX. The remaining 0.4 mole may account for further bioconversion of NO_2^- to nitric oxide (NO) by XO under anaerobic conditions as reported previously (Godber et al., 2000; Li et al., 2001).

Table 1. Stoichiometry and carbon and nitrogen mass balance of metabolites produced during HMX biotransformation catalyzed by xanthine oxidase (1 mg/ml) at pH 7.0 and 30^{o}C for 2.5 h under anaerobic conditions.

Metabolites	Amount (nmoles)	Molar ratio (per mole of HMX)	% Carbon recovery*	% Nitrogen recovery*
1. Methylenedinitramine	3.5	0.1	3	6
2. 4-nitro-2,4-diazabutanal	4.2	0.1	8	6
3. Formaldehyde (HCHO)	34.0	1.3	31	N.A.
4. Formic acid (HCOOH)	53.0	2.0	49	N.A.
5. Nitrous oxide (N_2O)	64.0	2.4	N.A.	59
6. Nitrite (NO_2^-)	17.0	0.6	N.A.	8
7. Ammonium (NH_4^+)	19.0	0.7	N.A.	9
Total % mass recovery			91	88

* Calculated from the total carbon and nitrogen mass in 27 nmoles of biotransformed HMX; N.A., not applicable. Data are mean of duplicate experiments (n = 2). Standard deviations were within 8 % of the mean absolute values.

Involvement of FAD-site in HMX biotransformation. Xanthine oxidase has three redox-cofactors: the FAD-site, the molybdenum-site and the two Fe-S centers (Fig. 2). The molybdenum-site interacts with a variety of substrates such as xanthine, inorganic nitrate and nitrite (Li et al 2003) and aldehydes (Hille and Nishino, 1995) whereas the FAD-site reduces oxygen (Hille and Nishino, 1995) and organic nitrates (Doel et al., 2001). Xanthine and NADH donate electrons at molybdenum-site and FAD-site, respectively (Fig. 2).

Chemically modified XO (deflavo- and desulfo-XO) were used in order to determine the reaction site for HMX biotransformation. In an experiment with deflavo-XO, both NADH and xanthine-dependent HMX biotransformations were inhibited (Table 2) indicating the direct involvement of FAD-site in HMX biotransformation. Furthermore, upon reconstitution of deflavo-XO with a 200 μM of FAD, both NADH and xanthine-dependent HMX biotransformation activities were restored up to 78 % (Table 2) providing an additional support for the involvement of FAD-site in HMX biotransformation. On the other hand, in desulfo-XO, there was no significant change in HMX biotransformation activity when

NADH was used as electron-donor, however, no activity was observed using xanthine as electron-donor (Table 2). This experiment indicated that HMX biotransformation did not occur at molybdenum-site of XO. Previously, Doel et al. (2001) demonstrated that glyceryl trinitrate was biotransformed at the FAD-site of XO with concomitant release of nitrite when the reaction was performed under anaerobic conditions using xanthine as an electron-donor.

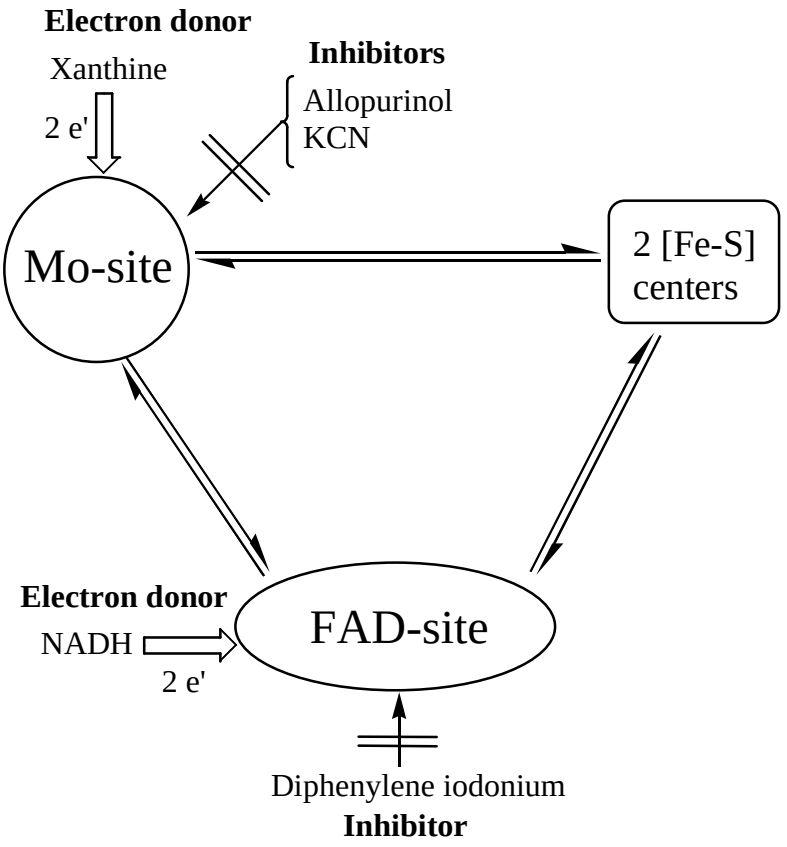

Fig. 2. A schematic representation of redox-cofactors present in xanthine oxidase (modified scheme from Komai et al. (1969)) showing the interaction-sites for various electron-donors and site-specific inhibitors. Mo-site is molybdenum-site. Arrows indicate the direction of flow of electrons.

The rate of HMX biotransformation by the native-XO was about 6-fold higher with NADH compared to xanthine as an electron donor (Table 2). The most plausible reason may be the interaction of NADH and HMX at the same site (i.e. FAD-site) of XO for donating and

accepting electrons, respectively, which led to a higher reaction rate. In contrast, the xanthine donates electron at the molybdenum-site which subsequently transfers them to the FAD-site. The latter finally transfers the electron to HMX. These multi-step electron-transfer processes probably decrease the resultant reaction rate.

Table 2: Biotransformation of HMX by native and modified xanthine oxidase (XO) in the presence of NADH or xanthine as an electron-donor under anaerobic conditions at pH 7.0 and 30^{o}C.

Electron-donor	HMX biotransformation activity (nmoles h^{-1} mg $protein^{-1}$) of:				
	Native-XO	Deflavo-XO	Reconstituted form of deflavo-XO	Desulfo-XO	Reactivated form of desulfo-XO
NADH	10.3 ± 0.8	1.9 ± 0.2	8.2 ± 0.4	9.6 ± 0.6	9.8 ± 0.8
Xanthine	1.8 ± 0.1	0.3 ± 0.04	1.4 ± 0.1	N. D.	1.3 ± 0.1

N.D., not detectable. Data are presented as mean ± S.D. (n = 3).

Site-specific inhibition studies. Diphenylene iodonium (DPI) acts at the FAD-site and prevents NADH from donating electrons at the site (Komai et al., 1969) whereas allopurinol binds at the molybdenum-site and prevent its participation in electron transfer reactions (Ichimori et al., 1999). In the present study, DPI inhibited the XO catalyzed biotransformation of HMX in a concentration-dependent manner (Fig. 3) whereas allopurinol did not inhibit the same reaction using NADH as electron-donor (Fig. 3). This experiment proved that HMX biotransformation occurred at the FAD-site and not the molybdenum-site. On the other hand, when xanthine was used as an electron-donor instead of NADH, both DPI and allopurinol inhibited the HMX biotransformation (data not shown) which additionally supported the idea that FAD-site is the site of reaction.

Lineweaver-Burk plots showed that nitrite was a non-competitive inhibitor of HMX biotransformation (Fig. 4), which indicated that nitrite and HMX bind at different sites on XO, although they share a common electron source, NADH. Since nitrite binds at the

molybdenum-site for its reduction (Godber et al., 2000; Li et al., 2001; 2003), HMX must bind at the FAD-site in order to accept electron.

Several lines of evidence have proven that biotransformation of HMX occurred at the FAD-site. The present study is analogous with a previous report (Doel et al., 2001) which also showed the reduction of organic nitrates at the FAD-site of xanthine oxidoreductase under anaerobic conditions.

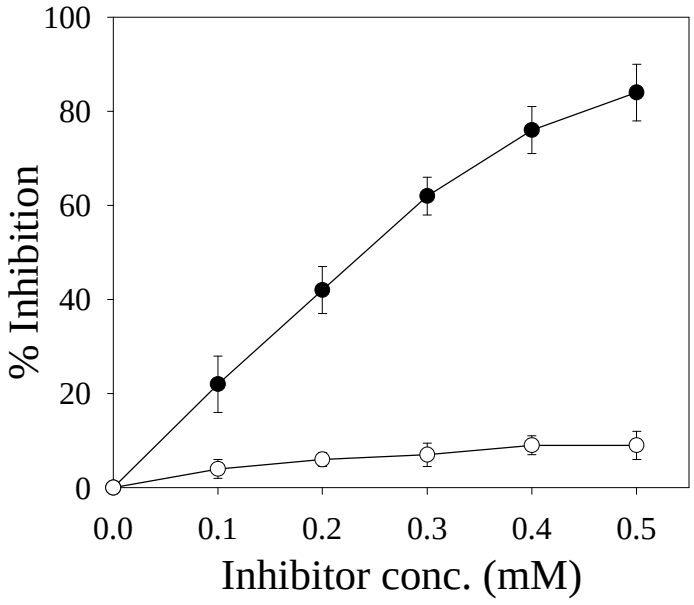

Fig. 3. Effect of site-specific inhibitors on NADH-dependent biotransformation of HMX by the xanthine oxidase. Allopurinol (?), diphenylene iodonium chloride (?). 100 % activity was equivalent to 10.5 ± 0.9 nmoles h^{-1} mg $protein^{-1}$. Data are the mean of triplicate experiments (n = 3), error bars indicate standard deviation.

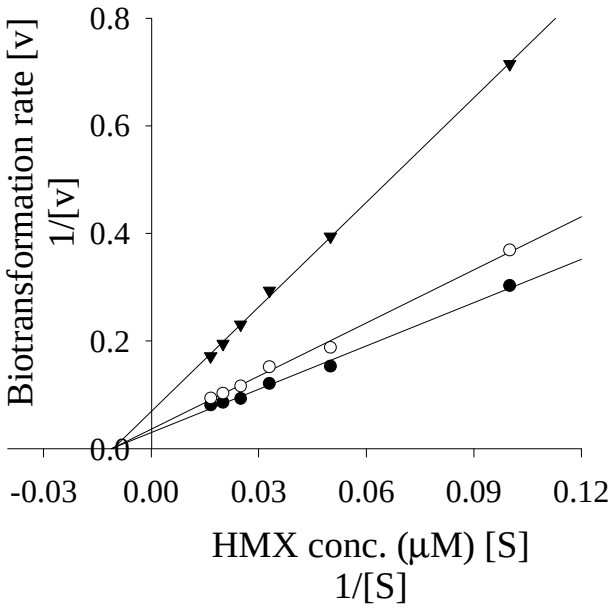

Fig. 4. Lineweaver-Burk plots showing nitrite as a non-competitive inhibitor of NADH-dependent biotransformation of HMX by xanthine oxidase under anaerobic conditions. Nitrite concentrations, 0 mM (?), 0.5 mM (?), 5.0 mM (?). HMX biotransformation rate was expressed as nmoles h^{-1} mg $protein^{-1}$. Data are mean of duplicate experiments.

***Proposed biotransformation mechanism*.** Based on the above data, we propose that HMX undergoes a single N-denitration which requires an initial obligatory one electron transfer step. In the present study, the electron transfer reaction occurred at the FAD-site which is known to catalyze one electron transfer to O_2 (Hille and Nishino, 1995; Komai et al., 1969). Therefore, under aerobic conditions, O_2 and HMX compete for the common binding-site (i.e. the FAD-site) which accounts for the 6.5-fold lower HMX biotransformation rate in the presence of O_2.

On the other hand, under anaerobic conditions, XO could catalyze one electron transfer to HMX followed by a single N-denitration which eventually formed hypothetical structure I (Fig. 5). Structure I is analogous to the one we proposed during RDX biotransformation by

cytochrome P450 (Bhushan et al., 2003a). The hypothetical structure I, being unstable, underwent hydrolytic decomposition to first produce structure II followed by ring cleavage to produce structure III (Fig. 5).

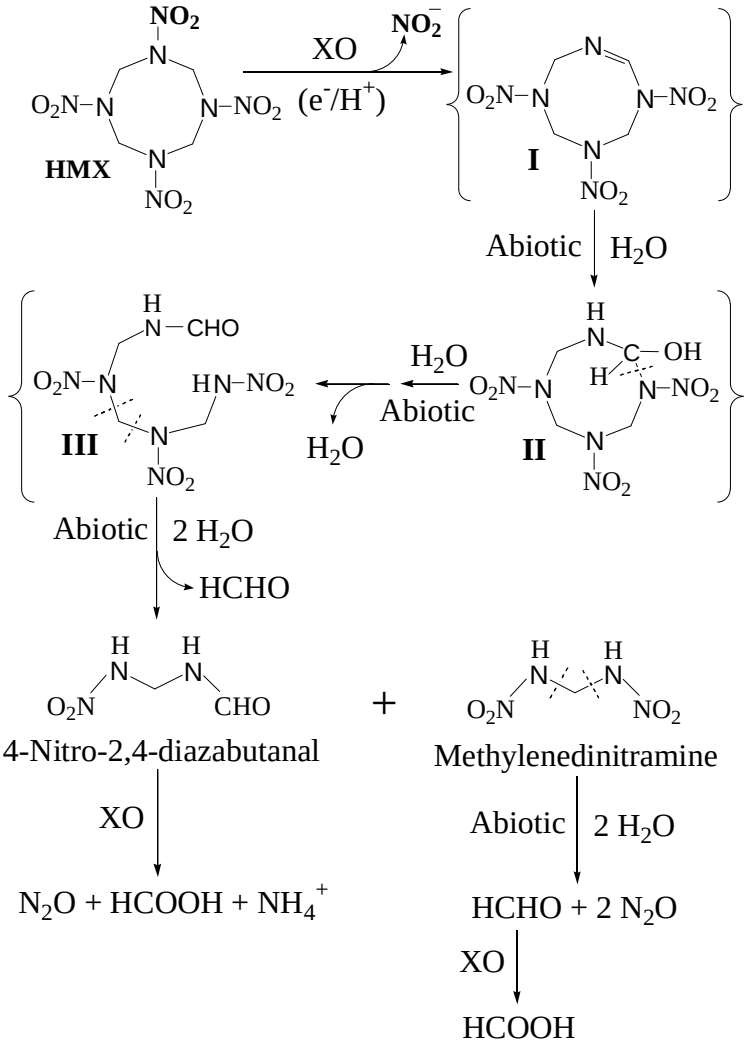

Fig. 5. Proposed pathway of xanthine oxidase (XO) catalyzed biotransformation of octahydro-1,3,5,7-tetranitro-1,3,5,7-tetrazocine (HMX). Products shown inside brackets were not detected.

The spontaneous hydrolysis of III would produce MEDINA and NDAB (Fig. 5). As mentioned above, NDAB was further biotransformed by XO to its respective products (i.e. N_2O, NH_4^+ and HCOOH) whereas MEDINA was abiotically decomposed to N_2O and

HCHO. Since MEDINA is a substrate for XO, it was also partly biotransformed to HCOOH (mentioned above).

In a previous report, Chapman et al. (1996) demonstrated a chemical N-denitration of HMX using a net hydride transfer agent, 1-benzyl-1,4-dihydronicotinamide, in a photochemical reactor having a 200-W tungsten light bulb. They proposed that all the four N-NO_2 bond scissions occurred to produce the corresponding amine (octahydro-1,3,5,7-tetrazocine). The latter was unstable and underwent rearrangement to produce a more stable product hexamethylenetetramine (Chapman et al., 1996). In contrast, we observed a single N-denitration of HMX leading to its spontaneous decomposition (Table 1). Hence, the present study apparently favors the XO catalyzed one electron transfer to HMX instead of a hydride transfer.

A variety of experimental evidence such as the oxygen-sensitivity of the reaction, involvement of the FAD-site in HMX biotransformation and a stoichiometric single N-denitration of HMX have proven that XO catalyzed a one-electron transfer to HMX at FAD-site, necessary to cause a single N-denitration, leading to spontaneous decomposition.

In conclusion, we provided the first biochemical evidence of XO catalyzed biotransformation of HMX under anaerobic conditions. The mechanism described here is consistent with our previous results regarding enzymatic biotransformation of RDX (Bhushan et al., 2002a, 2003a), which also proved that one-electron transfer is necessary and sufficient to cause single N-denitration of RDX. As we will discus in subsequent sections 4-nitro-2,4-diazabutanal (NDAB), is also observed during denitration of RDX under abiotic conditions (photodenitration or bimolecular elimination of HNO_2 at alkaline pHs) (Hawari et al., 2002; Balakrishnan et al., 2003) or with *Rhodococcus* sp. DN22 (Fournier et al., 2002). In the present study NDAB did not accumulate, but instead further biotransforms under anaerobic conditions. This observation encourages the use of microorganisms producing XO or similar enzyme(s) for the complete degradation of RDX and HMX to innocuous products without the accumulation of intermediates. The present study extend the fundamental knowledge of the biotransformation mechanism(s) of energetic cyclic nitramine compounds so as to design and optimize a well-controlled biochemical reaction for their complete mineralization.

V.3.3 Diaphorase catalyzed biotransformation of RDX via N-denitration mechanism.

- Bhushan, B., A. Halasz, J. C. Spain, J. Hawari. **2002**. Diaphorase catalyzed biotransformation of RDX via N-denitration mechanism. *Biochem. Biophys. Res. Commun.* 296: 779-784.

KEY FINDINGS:

Previously, we hypothesized that hexahydro RDX can be biotransformed by anaerobic sludge via three different routes: 1. direct ring cleavage via α-hydroxylation of a -CH_2 group, 2. reduction of one of the –NO_2 groups to –NO, 3. N-denitration prior to ring cleavage (Figure 4, Section V.1.1). The present study describes biotransformation of RDX via route 3 by a diaphorase (EC 1.8.1.4) from *Clostridium kluyveri* using NADH as electron donor. The removal of RDX was accompanied by the formation and accumulation of nitrite ion (NO_2^-), formaldehyde (HCHO), ammonium (NH_4^+) and nitrous oxide (N_2O). None of the RDX-nitroso products were detected. The ring cleavage product methylenedinitramine was detected as the transient intermediate. Product stoichiometry showed that each reacted RDX molecule produced one nitrite ion and the product distribution gave a carbon (C) and nitrogen (N) mass balance of 91 % and 92 %, respectively, supporting the occurrence of a mono-denitration step prior to the ring cleavage and decomposition. Severe oxygen mediated inhibition (92 % inhibition) of RDX biotransformation and superoxide dismutase-sensitive cytochrome c reduction indicated the potential involvement of an anion radical $RDX^{\bullet-}$ prior to denitration. A comparative study between native- and apo- enzymes showed the possible involvement of flavin mononucleotide (FMN) in catalyzing the transfer of a redox equivalent (e/H^+) from NADH to RDX in order to produce $RDX^{\bullet-}$ responsible for secondary decomposition.

RDX biotransformation and product identification. *Clostridium kluyveri* diaphorase was found to transform RDX at pH 7.0 and 27 ^oC under anaerobic conditions using NADH as the electron donor. A typical LC/MS chromatogram of RDX transformation with diaphorase showed the production of methylenedinitramine as a key ring cleavage metabolite at a retention time of 4.2 minute as shown in Figure 1.

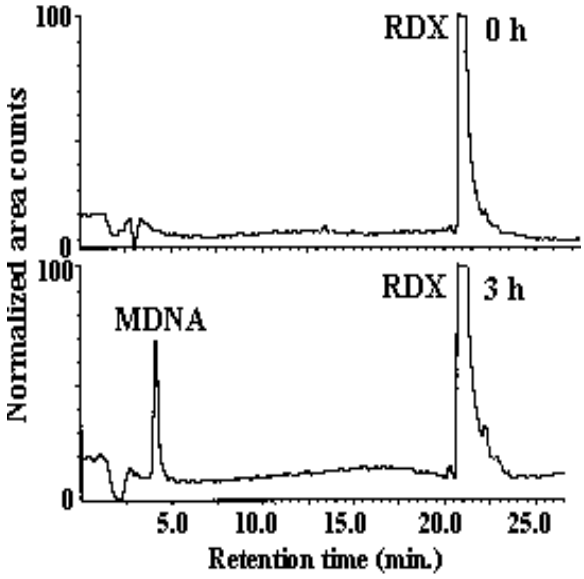

Figure 1. LC/MS (ES-) chromatogram of RDX and diaphorase reaction showing methylenedinitramine as a key RDX intermediate. A, 0 hour reaction; B, 3 hour reaction.

None of the nitroso-RDX intermediates, particularly hexahydro-1-nitroso-3,5-dinitro-1,3,5-triazine (MNX), were detected, although such initial RDX reduced products were frequently observed during RDX degradation by anaerobic sludge (Hawari et al., 2000a; Halasz et al., 2002). No biotransformation of RDX was observed in the control experiments that did not contain enzyme and/or NADH. The time course of the reaction showed that the disappearance of RDX and NADH were accompanied by the formation and accumulation of HCHO, N_2O and NO_2^- (Fig. 2).

Inhibition by oxygen. We found that the presence of oxygen (O_2) inhibited (92 %) the transformation of RDX as shown in Figure 3, clearly supporting the involvement of an oxygen-sensitive step during the initial enzymatic attack on RDX. We observed a negligible oxidation of NADH under aerobic conditions within the assay time of one hour, indicating that O_2 inhibition of RDX biotransformation was not due to the depletion of NADH. In

another experiment, we observed that diaphorase did not catalyze the electron transfer from NADH to O_2 and this observation was similar to the one reported by Kaplan et al. (1969) using the same enzyme.

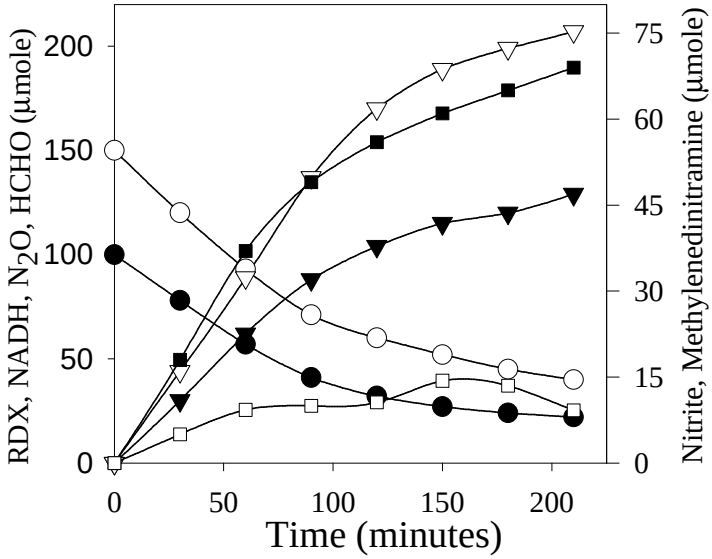

Figure 2. Time course of diaphorase catalyzed RDX transformation with simultaneous production of intermediate and end-products. Symbols; ? RDX; ? NADH; ? N_2O; ∇ HCHO; ¦ Nitrite; ? Methylenedinitramine. Standard deviations were within 6 % of the absolute mean values (n = 3).

Based on these observations, we hypothesized that inhibition of RDX transformation by O_2 is most probably due to quenching of an unpaired electron from the RDX anion radical ($RDX^{\bullet-}$) by the O_2. Such reaction would revert $RDX^{\bullet-}$, an initial transformation product, to its original structure RDX producing instead $O_2^{\bullet-}$ thus preventing the molecule from further decomposition (Fig. 4) as was the case with tetryl (Shah and Spain, 1996; Anusevicius et al., 1998). $RDX^{\bullet-}$ appears to be formed via an initial electron transfer process catalyzed by diaphorase (Fig. 4). Ritter and Malejka-Giganti (1998) also reported the reduction of a nitro group in nitrofluorene compounds via an O_2-sensitive one electron transfer process catalyzed

by a diaphorase from *Clostridium kluyveri*.

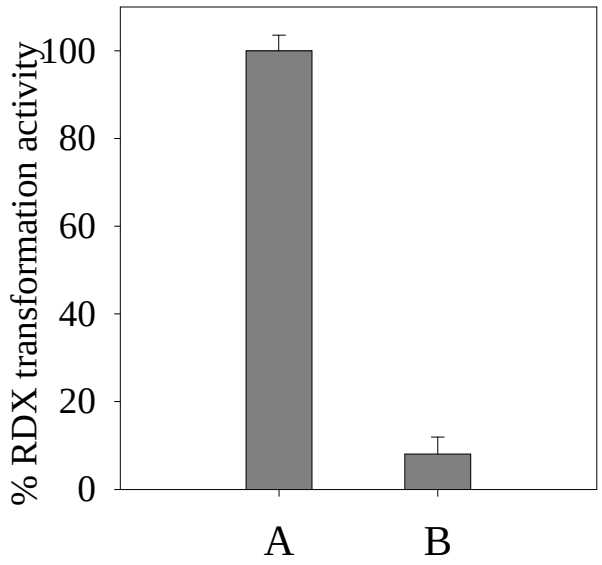

Figure 3. Effect of oxygen on diaphorase catalyzed RDX transformation. A, anaerobic conditions; B, aerobic conditions. 100 % RDX transformation activity was equivalent to 47 μmoles RDX transformed $h^{-1}mg^{-1}$ protein.

In order to test the hypothesis that O_2 inhibited the transformation of RDX by quenching an electron from $RDX^{\bullet-}$, we incubated RDX with diaphorase in the presence of NADH, superoxide dismutase (SOD) and cytochrome c. It was observed that SOD inhibited the reduction of cytochrome c by 37 % thus providing evidence for the potential involvement of redox cycling between $RDX^{\bullet-}$ and RDX through which O_2 was converted to $O_2^{\bullet-}$ (Fig. 4). Control experiments without diaphorase showed that RDX can neither be autooxidized nor it can reduce cytochrome c.

C- and N- mass-balance and stoichiometry of the reaction. The reaction stoichiometry (Table 1) indicated that one nitrite molecule was produced per reacted RDX molecule. On the

other hand, 78 μmoles of the reacted RDX produced 129 μmoles N_2O and 9.2 μmoles of methylenedinitramine. The latter is unstable in water at pH 7.0 and 27 ^oC and decomposes quantitatively to produce stoichiometric amounts of N_2O (two molecules) and HCHO (one molecule) (Halasz et al., 2002). Considering that all of the N_2O produced during the reaction comes from the decomposition of methylenedinitramine, it was concluded that one molecule of methylenedinitramine was produced for each reacted RDX molecule.

Table 1. Carbon and nitrogen mass balance and stoichiometry of reactants consumed and metabolites produced during RDX transformation catalyzed by a diaphorase from *Clostridium kluyveri* at pH 7.0 and 27^oC.

Reactants/Metabolites	Amount of Reactants/Metabolites (μmole)	% Carbon recovery*	% Nitrogen recovery*
Reactants consumed			
1. RDX	78.0	100.0	100.0
2. NADH	110.0	NA	NA
Metabolites produced			
1. Methylenedinitramine	9.2	4.0	8.0
2. Formaldehyde (HCHO)	207.0	88.0	NA
3. Nitrite (NO_2^-)	69.0	NA	15.0
4. Nitrous oxide (N_2O)	129.0	NA	55.0
5. Ammonium (NH_4^+)	62.0	NA	13.0
Total % mass recovery		92.0	91.0

*Calculated from the total carbon and nitrogen mass in the transformed RDX (78 μmoles); Initial RDX and NADH concentrations were 100 and 150 μmoles, respectively; NA, not applicable; The standard deviations were within 6 % of the absolute mean values (n = 3).

The total nitrogen mass recovery was 91 % and was distributed as N_2O (55 %), nitrite (15 %), ammonium (13 %) and methylenedinitramine (8 %). The N mass balance data revealed that of the six nitrogen atoms in one RDX molecule, four atoms were finally recovered as nitrous oxide (2 N_2O molecules) whereas the fifth and sixth atoms were present in nitrite (NO_2^-) and ammonium (NH_4^+), respectively, (Table 1). The total C mass recovery was 92 % and it was distributed as formaldehyde (88 %) and methylenedinitramine (4 %). The latter, as mentioned

above, decomposes quantitatively to HCHO and N_2O, indicating that all the three C atoms in RDX were finally recovered in the form of HCHO.

Numerically, 1.4 μmoles of NADH were consumed in order to biotransform 1.0 μmole of RDX (Table 1). The stoichiometry of NADH consumption vs RDX transformation supports that 1 molecule of NADH ($2e^-/2H^+$) was utilized per RDX molecule for its initial denitration. The remaining 0.4 μmoles were either utilized by other transient intermediates/end-products following the ring cleavage or bound to protein and thus prevented their detection. The other possibility is that some NADH may be consumed during the futile redox cycling in the presence of traces of oxygen in the reaction medium.

Proposed mechanism of biotransformation. Based on the oxygen sensitivity, product identification, C- and N- mass-balance, and stoichiometry of the reaction, we propose that RDX undergoes a mono-denitration process which was responsible and sufficient for the ring cleavage and secondary decomposition. The absence of nitroso products such as MNX, DNX and/or TNX also supported the denitration of RDX as the main reaction step responsible for the ring cleavage.

The oxygen inhibition (92 %) of RDX transformation and SOD-sensitive cytochrome c reduction experiments suggested that the transfer of a net two redox equivalents (2 e/H+) to the RDX, as determined by stoichiometry of NADH, occurred in a stepwise manner. First step produce $RDX^{\bullet-}$ (I) whose spontaneous denitration would generate nitrite and the free radical $RDX^{\bullet}$ (II) (Fig. 4). In the second step, $RDX^{\bullet}$ (II) either undergoes H–abstraction to form the amine derivative (III) by acquiring a second redox equivalent (e^-/H^+) or can lose a hydrogen atom to form the cyclohexene derivative (IV) (Fig. 4). However, the stoichiometry of NADH consumption favors the formation of amine derivative (III). The formation of amine derivative (III) via a H-abstraction by the $RDX^{\bullet}$ (II) during photolysis of RDX has been reported (Peyton et al., 1999) previously, but to the best of our knowledge no similar biological reactions are known. However, Anusevicius et al. (1998) reported two single e-transfer steps during N-denitration of tetryl catalyzed by a mammalian DT-diaphorase (EC 1.6.99.2).

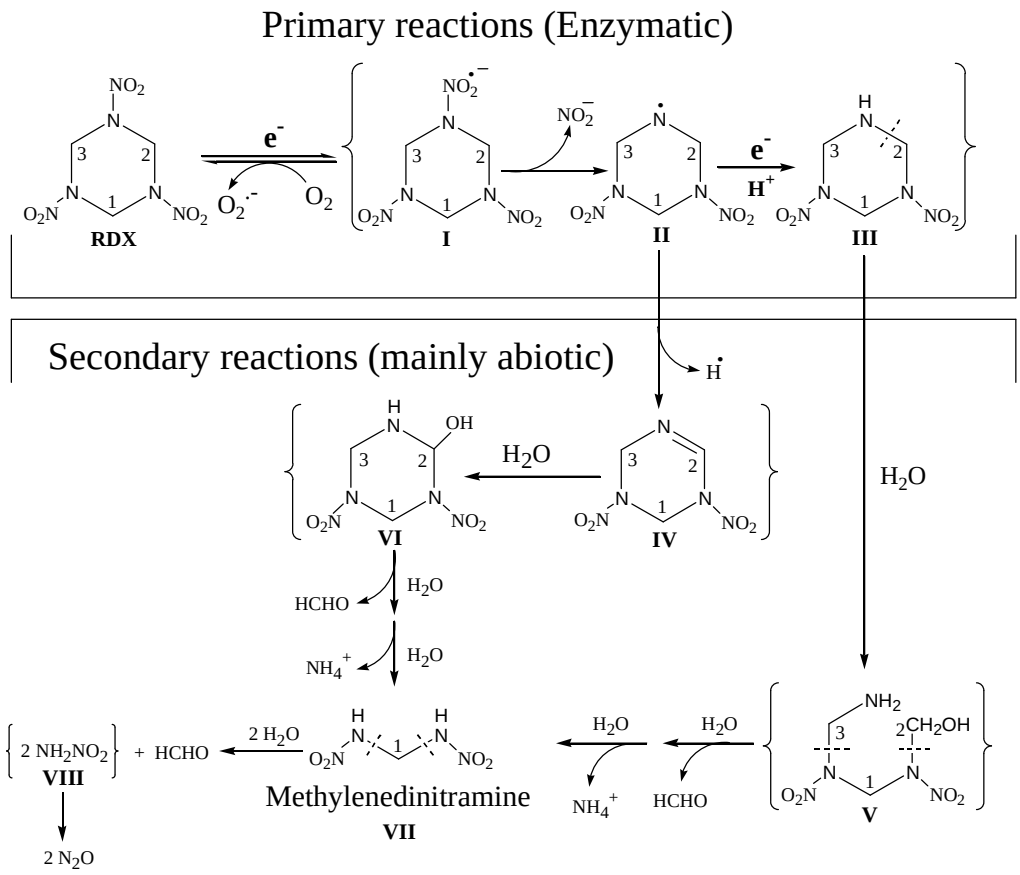

Fig. 4, Hawari

Figure 4. Proposed pathway of diaphorase catalyzed RDX transformation based on stoichiometry of metabolites recovered and NADH consumed. Primary reactions involve RDX reduction to RDX anion radical I that undergoes denitrohydrogenation to produce III. Secondary reactions involve ring cleavage and spontaneous decomposition in water. Intermediates shown inside brackets were not detected.

The hypothetical intermediates III and IV might be unstable in water and therefore underwent hydrolytic ring cleavage. As a result, III would produce V, and IV would give rise to VI. Further, the hypothetical intermediates V and VI decompose in water and stoichiometrically produce methylenedinitramine (VII), HCHO and NH_4^+ (Fig. 4). Methylenedinitramine, being unstable in water also decomposes to produce HCHO and N_2O (Halasz et al., 2002). Although, we detected methylenedinitramine quantitatively but we were unable to detect its hypothetical precursor intermediates V and VI.

The proposed pathway in Fig. 4 is consistent with the experimental mass balance of carbon

and nitrogen (Table 1). Chapman et al. (1996) reported a similar, but non-enzymatic N-denitrohydrogenation of HMX (a cyclic nitramine explosive) using 1-benzyl-1,4-dihydronicotinamide instead of NADH, however, this reaction needed an initiation by sodium dithionite or light. On the other hand, N-denitrohydrogenation of tetryl using a ferredoxin-$NADP^+$ oxidoreductase (EC 1.18.1.2) (Shah and Spain, 1996) and a mammalian DT-diaphorase (EC 1.6.99.2) (Anusevicius et al., 1998) has also been reported.

Possible involvement of FMN in RDX transformation. FMN is a redox cofactor of *Clostridium kluyveri* diaphorase and it is present in the ratio of 1 mole per mole of enzyme (Kaplan et al., 1969). In the present study, the deflavo enzyme (apoenzyme) lost 87.5 % of the RDX transformation activity (Fig. 5), suggesting that FMN is an active redox center that possibly mediates the transfer of electrons from NADH to RDX.

The remaining 12.5 % enzymatic activity may be due to the incomplete removal of FMN from the native enzyme. We found that when the deflavo enzyme was reconstituted with increasing concentration of FMN, there was a gradual increase in RDX transformation activity up to a maximum of 85 % at the FMN concentration of 200 μM (Fig. 6).

In another experiment, we found that a commercially available FMN in free form can transform RDX using NADH as electron donor. However, the transformation rate of the free FMN was comparatively lower than the diaphorase-bound FMN (Fig. 6). These results indicate that FMN plays a crucial role in the reduction of RDX by acting as a possible site of electron transfer reaction. In this context, Khan et al. (2002), showed that reduced FMN in pentaerythritol tetranitrate reductase caused the reduction of nitroester explosives (glycerol trinitrate and pentaerythritol tetranitrate) and nitroaromatic explosives (TNT and picric acid).

Other reports also showed that the flavin moieties (FAD and FMN) in the flavoenzymes play a key role in substrate reduction (Madigan and Mayhew, 1993; Lindsay et al., 2000; Xia et al., 2001).

In conclusion, the present study showed that the diaphorase catalyzed N-denitration of RDX is an oxygen-sensitive reaction which possibly requires a net two redox equivalents. Based on the present experimental data and its analogy with other reported systems (Shah and Spain,

1996; Ritter and Malejka- Giganti, 1998; Anusevicius et al., 1998) we proposed that the first redox equivalent leads to the transformation of RDX to $RDX^{\bullet-}$ whose subsequent denitration leads to $RDX^{\bullet}$. The second redox equivalent possibly causes hydrogenation of $RDX^{\bullet}$ leading to the formation of corresponding amine (III) (Fig. 4). The latter undergoes spontaneous hydrolytic decomposition in water to produce the transient intermediates and end-products. FMN seems to play a key role in transferring the redox equivalents from NADH (donor) to RDX (acceptor).

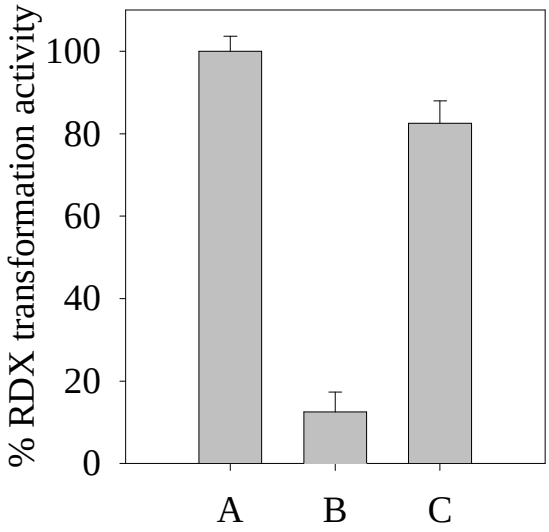

Figure 5. Role of FMN in RDX transformation activity of diaphorase. A, native enzyme; B, apoenzyme (deflavo form); C, apoenzyme reconstituted with 200 μM FMN. 100 % activity was equivalent to 41 μmoles RDX transformed $h^{-1}mg^{-1}$ protein

One significance of the present study is that *Clostridium kluyveri* diaphorase catalyzed the RDX transformation at the expense of a net two redox equivalents per one RDX molecule which is apparently different and more economical than the earlier reported conventional RDX biotransformation route *i.e.* via MNX formation (Hawari et al., 2000a, Halasz et al., 2002; Kitts et al., 2000). In a recent study, the MNX route of RDX transformation utilized a

net six electrons in order to transform one RDX molecule before its ring cleavage and decomposition (Shah and Spain, 1996). This study also revealed that the transformation of at least one nitro group of RDX is necessary and sufficient to initiate the ring cleavage and subsequent decomposition.

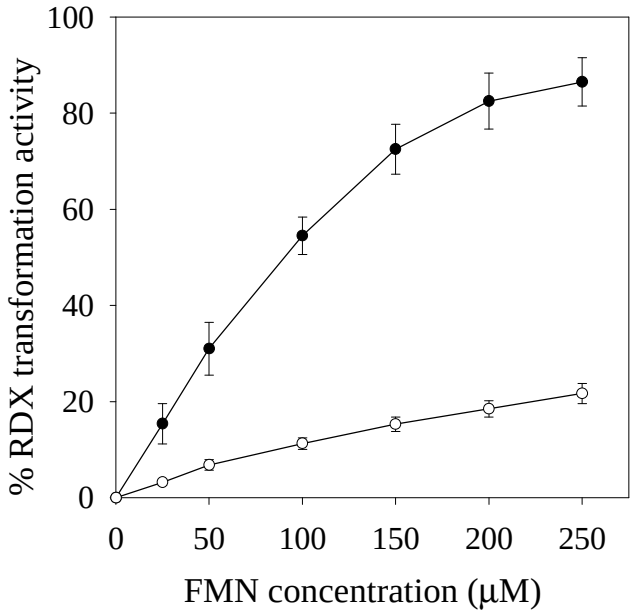

Figure 6. Concentration dependent reconstitution of diaphorase by FMN. Symbols, •, % restored activity of diaphorase; ?, FMN (commercially available) catalyzed RDX transformation. 100 % activity was equivalent to 41 μmoles RDX transformed $h^{-1}mg^{-1}$ protein.

Thus far we were able to successfully degrade RDX and HMX under anaerobic conditions using sludge, isolates and enzymes. In the following chapters we will describe the potential to also degrade this family of chemicals under aerobic conditions using bacteria, fungi and enzymes.

V.4 Biodegradation of RDX and HMX under aerobic conditions.

Summary. We successfully used three Rhodococci strains (A, DN22 and 11Y) to degrade RDX under aerobic conditions. The three strains produced similar products (one carbon atom (C) was utilized and eliminated as CO_2 and the remaining 2 Cs were involved in the formation of a dead end product that was identified as 4-nitro-2, 4-dizabutanal). A degradation pathway was suggested based on initial denitration followed by hydrolytic ring cleavage and decomposition. Later we found that a rabbit liver cytochrome P450 can degrade RDX to produce a product distribution that was similar to that obtained with the three tested *Rhodococcus* strains. Based on several lines of biochemical evidence and the results described in previous work (Coleman et al., 2002; Fournier et al., 2002; Seth-Smith et al., 2002) we concluded that an enzyme(s) belonging to the cytochrome P450 family is responsible for RDX biotransformation by the three strains *Rhodococcus* sp. DN22, *Rhodococcus* sp. A and *Rhodococcus* sp. 11Y.

V.4.1 Biotransformation of RDX with **Rhodococcus** *sp. DN22: discovery of 4-nitro-2,4-diazabutanal and the removal of a second bottleneck in the degradation pathways of cyclic nitramines.*

- Fournier, D., Halasz, A., Spain, J., Fiurasek, P. and J. Hawari. **2002**. Determination of key metabolites during biodegradation of RDX with *Rhodococcus* sp. Strain DN22. Appl. Environ. Microbiol. **68**: 166-172.

KEY FINDINGS:

Nitrogen-containing products. As already shown by Coleman et al. (1998) we found that the growth of strain DN22 in a mineral salt medium containing RDX (35 μmole) as the Nitrogen source and succinate (12 mM) as the carbon source was accompanied by RDX degradation and transient accumulation of nitrite (NO_2^-) (Fig. 1A).

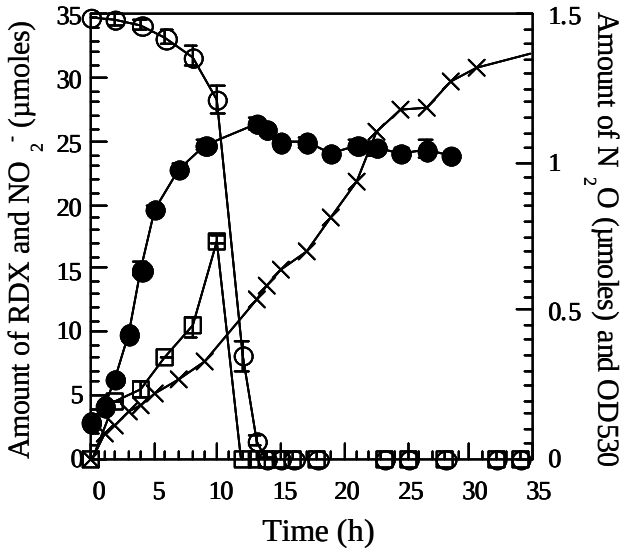

Figure 1A. Time course study of RDX biodegradation with *Rhodococcus* strain DN22. Removal of RDX (○), growth of cells (●), evolution of nitrite (□), and nitrous oxide (X). Values represent the average and standard deviation of duplicate experiments.

There was no lag phase in the degradation of RDX because inocula were prepared with mid-log DN22 pre-cultures grown on RDX. Maximum cell density (A_{530} 1.14) was attained after

14 hours of incubation during which RDX disappeared completely. In the uninoculated controls no RDX removal was observed.

The removal of RDX and the formation NO_2^- was accompanied by the formation of N_2O which continued to accumulate long after the disappearance of NO_2^- (Fig. 1A). After 4 days of incubation the amount of N_2O attained a plateau of 4.5 µmoles (not shown). We did not observe N_2O in controls containing RDX in the absence of *Rhodococcus*. The presence of N_2O was confirmed by comparison with a reference standard material and by measuring its molecular mass ion at 44 Da by GC-MS. Incubation of RDX grown cells with $NaNO_2$ in the presence of succinate also lead to the accumulation of N_2O also in trace amounts. When the above biodegradation experiment was repeated using ring-labeled [^{15}N]-RDX as the nitrogen source for DN22, we detected a molecular mass ion at 45 Da, corresponding to $^{14}N^{15}NO$ and another at 44 Da corresponding to $^{14}N^{14}NO$ almost with the same intensity. The results indicate that trace amounts of N_2O were produced from RDX or from RDX metabolites such as NO_2^-.

We did not detect any of the RDX nitroso derivatives such as MNX, DNX and TNX. Although such products have been frequently observed during biodegradation of RDX with anaerobic sludge (Hawari et al., 2000a; McCormick et al., 1981) and with *P. chrysosporium* (Sheremata and Hawari, 2000).

Carbon-containing products. Incubation of RDX with cultures of strain DN22 led to the disappearance of RDX and the formation of formaldehyde (HCHO) (Fig. 1B). Formaldehyde accumulated during the time of rapid RDX removal and was subsequently mineralized as determined by accumulation of $^{14}CO_2$ from [U-^{14}C]-RDX (Fig. 1B). In a separate experiment incubation of $H^{14}CHO$ with RDX grown cultures under the same conditions led to the degradation of the aldehyde and the accumulation of $^{14}CO_2$ in very high yield (88 %).

Accumulation of a dead end product. During the growth of strain DN22 on RDX (Fig. 2) there was a concurrent formation and accumulation of another soluble metabolite as detected by HPLC/UV and LC-MS(ES-). The early chromatographic elution of the metabolite (retention time of 3.6 min.) implies that the compound was more polar than RDX. The

compound was not degraded by strain DN22. The metabolite gave a deprotonated molecular mass ion $[M\text{-}H]^-$ at 118 Da (MW 119 Da) (Fig. 3A). The fragmentation pattern of the metabolite shows two other relevant mass ions at 61 and 46 Da representing fragments $–NHNO_2$ and $–NO_2$ (Fig. 3A). Values represent the average and standard deviation of duplicate experiments.

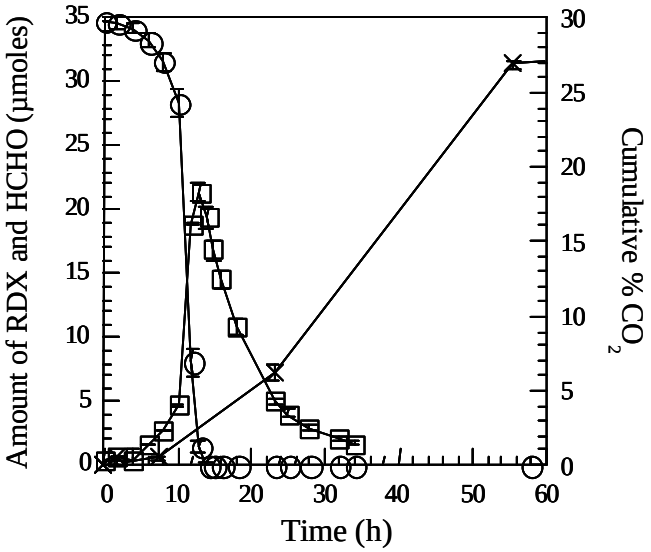

Figure 1B. Time course study of RDX biodegradation with *Rhodococcus* strain DN22. Removal of RDX (○), evolution of formaldehyde (□), and cumulative percentage of $^{14}CO_2$ (X).

When ring-labeled [^{15}N]-RDX was used, the $[M\text{-}H]^-$ of the metabolite shifted to 120 Da (Fig. 3B), indicating that the metabolite contained two of the three ring labeled ^{15}N atoms in RDX.

Also the mass ion fragment $–NHNO_2$ shifted from 61 Da to 62 Da, confirming that the fragment still contains one atom of ^{15}N. High resolution mass spectrometry of the metabolite gave a $[M\text{-}H]^-$ at 118.0331, matching a deprotonated molecular formula of $C_2H_4N_3O_3$. The calculated mass of the deprotonated mass ion was 118.0253, suggesting that the metabolite had a molecular formula of $C_2H_5N_3O_3$ (MW 119 Da) containing 3 N atoms (half of the total N-content of RDX), 2 C atoms (two third of the total C-content of RDX) and 5 H atoms.

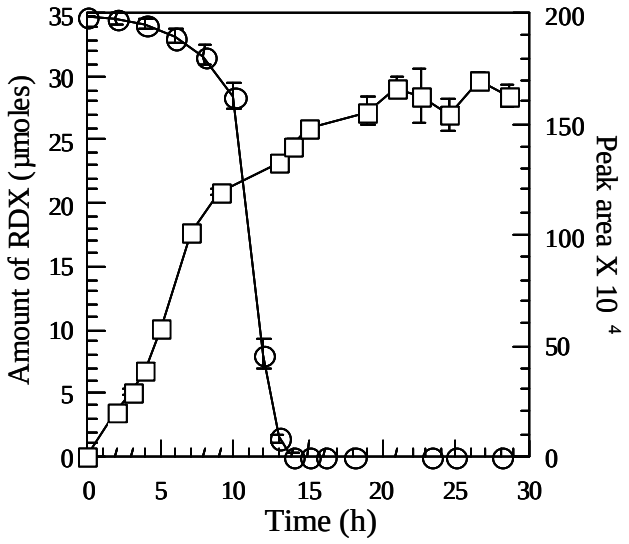

Figure 2. Accumulation of the metabolite MW 119 (□) during RDX biodegradation with *Rhodococcus* strain DN22 (○). Mass area was used to monitor the formation of the metabolite.

Biodegradation of RDX by resting cells resuspended in pure D_2O yielded two products with deprotonated molecular mass ions [M - H] at 118 and 119 Da. The percentage of 119 to 118 Da was 18 % (data not shown). We did not account for water residues that were retained with biomass after centrifugation. The D-labeled experiment indicated the incorporation of only one deuterium in the metabolite based on the assumption that H rather than D was lost during ionization in the mass spectrometer. The suggested molecular formula of the above metabolite would be $C_2H_4DN_3O_3$.

Figure 3C shows that alkaline hydrolysis of RDX with NaOH at pH 12 produced a product, which had the same chromatographic (r.t. at 3.6 min) and mass ($[M-H]^-$ at 118 Da) data as observed earlier for the MW 119 RDX metabolite. Alkaline hydrolysis of RDX (pH 12) in the presence of D_2O also resulted in the formation of a product with $[M-H]^-$ at 119 Da, indicating the inclusion of one D atom in the product.

When RDX was incubated with cells in the presence of $^{18}O_2$ we did not observe any mass change in the MW 119 Da metabolite. It was very difficult to search for ^{18}O in HCHO, but no

^{18}O was detected in carbon dioxide when the latter was trapped in an alkaline medium and analyzed on LC-MS.

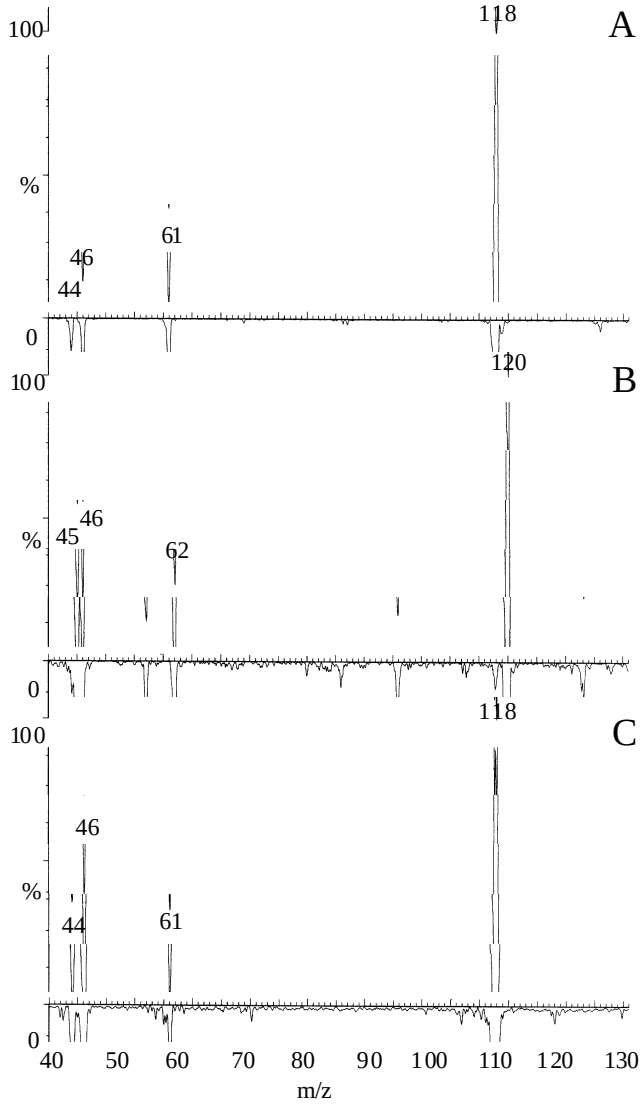

Figure 3. A LC/MS (ES-) spectra of the metabolite MW 119 produced during RDX degradation using: A. resting DN22 cells; B. DN22 cells and ring-labeled [^{15}N]-RDX and C. sodium hydroxide (pH 12).

Stoichiometry. We used resting cell assays to calculate the distribution of nitrogen in RDX metabolites produced during incubation with DN22 in the presence of ammonium sulfate (1

mM). The latter was added to prevent the uptake of NO_2^- produced as an RDX metabolite (Coleman et al., 1998; Ecker et al., 1992). In experiments supplemented with ammonium sulfate, the concentration of ammonia as an RDX product was calculated as the difference between initial and final concentrations of NH_4^+. Table 1 summarizes the percentage of N-containing products produced following RDX removal. We found a N-mass balance of 91.2 % distributed as follows: NO_2^- (30 %), N_2O (3.2 %), NH_3 measured as NH_4^+ (10 %) and metabolite with MW 119 (48 %). Table 1 also summarizes the carbon stoichiometry in a 4 day culture. After 4 days of incubation, 97.6 % of original radioactivity in RDX was found as 30 % CO_2 and 67.6 % in the liquid phase. However, Table 1 shows a 94 % carbon mass balance distributed as follows: CO_2 (30 %) and metabolite with MW 119 (64 %) leaving 3 % of measured radioactivity unidentified.

Table 1 Stoichiometry of nitrogen and carbon during RDX degradation calculated based on % of reacted RDX using total theoretical numbers of N and C atoms.

Total # of N and C atoms	NO_2^-	N_2O	NH_3 [a]	CO_2	MW 119	% recovered
3 C	-	-	-	30.0 [b] (0.8) [e]	64.0 [c]	94.0 [d]
6 N	30.0 (1.7) [e]	1.5(8.5) [e]	10.0	-	48.0f	89.5

a. no ammonium salt was added to the resting cell suspension.
b. based on $^{14}CO_2$ measured using [U-^{14}C]-RDX
c. based on HPLC/radioactivity measurement using [U-^{14}C]-RDX
d. total measured values were 97.6 % distributed as follows 30 % CO_2 and 67.6 % in the liquid phase leaving 3 % unidentified.
e. value in brackets represents RSD of a triplicate
f. calculated based on the empirical formula $C_2H_5N_3O_3$ found by LC/MS (ES-) and high resolution mass spectrometry.

The stoichiometry shown in Table I indicates that following the removal of RDX ($C_3H_6N_6O_6$) 30% of its C-content (1 atom) was used to produce $^{14}CO_2$ and 64% (2 C atoms) were incorporated in the dead end product MW 119 ($C_2H_5N_3O_3$). Controls containing RDX without strain DN22 retained close to 99.5% of the original radioactivity in the form of

unreacted RDX.

The formation of nitrite concurrent with RDX disappearance during incubation with growing DN22 cells (Fig. 1A) clearly indicated the occurrence of an important early enzymatic denitration step in the degradation process (Fig. 4).

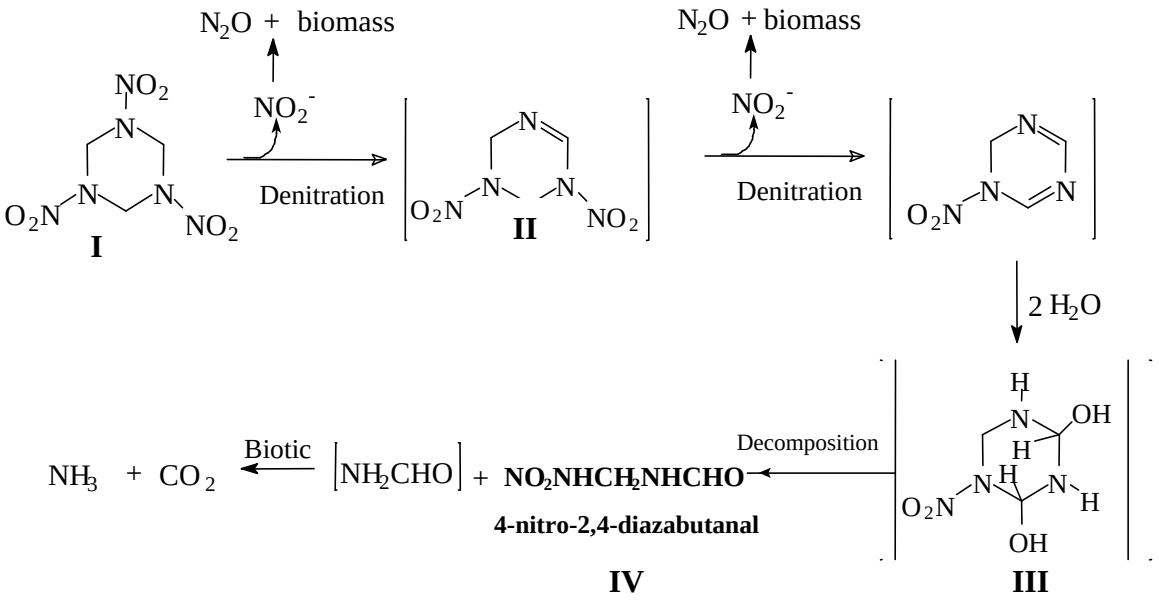

Figure 4. Biotransformation of RDX with *Rhodococcus* sp. strain DN22 (Fournier et al., 2002)

The absence of any of the familiar nitroso products MNX, DNX and TNX also supported the hypothesis that denitration was the most critical initial microbial (enzymatic) step in RDX degradation. Nitrite did not accumulate in the system and its disappearance was accompanied by microbial growth and the formation of N_2O (Fig. 1), suggesting that nitrite was assimilated by the bacteria. Nitrogen assimilation *via* ammonia can be accompanied by the production of N_2O (Zumft, 1997.).

The continued formation of N_2O (total yield 3.6 %) long after the complete removal of RDX and nitrite indicated that in addition to nitrite assimilation by DN22 the presence of other RDX intermediate(s) might have been directly responsible for its formation. Also the

detection of both $^{14}N^{14}NO$ (m/z 44 Da) and $^{15}N^{14}NO$ (m/z 45 Da) during biodegradation of ring labeled [^{15}N]-RDX indicated that in addition to -NO_2^- assimilation there must be another route for its production. The formation of $^{15}N^{14}NO$ requires the direct participation of an RDX nitramine group (^{15}N-$^{14}NO_2$). Earlier we reported the formation of N_2O from the spontaneous decomposition of nitramide, NH_2NO_2, considered as a ring cleavage product of RDX biodegradation with anaerobic sludge (Hawari et al., 2000a). Regardless of which mechanism leads to the production N_2O, its formation as a secondary product in a small yield (3.6 %) does not provide insight about early steps in RDX metabolism.

The formation of two moles of NO_2^- per molecule of RDX that disappeared is consistent with the stoichiometry reported earlier by Coleman et al. (2002). A plausible hypothesis would be that the first loss of NO_2^- produced the cyclohexenyl product (I) whereas the second denitration produced the cyclohexadienyl intermediate (II) (Fig. 4).

The transient accumulation of HCHO and the subsequent formation of CO_2 clearly indicate the cleavage of the RDX ring following its denitration. The concurrent formation of carbon dioxide with the disappearance of HCHO (Fig. 1B) might indicate the direct involvement of the aldehyde in the formation of CO_2. The above conclusion is supported by the rapid and efficient degradation of $H^{14}CHO$ to $^{14}CO_2$ (88 %) under the same conditions. The total yield of CO_2 indicated that roughly one carbon atom in each RDX molecule mineralized.

We tentatively identified the molecular structure of the detected $C_2H_5N_3O_3$ metabolite as the aldehyde (IVA) or the amine (IVB) (Fig. 5).

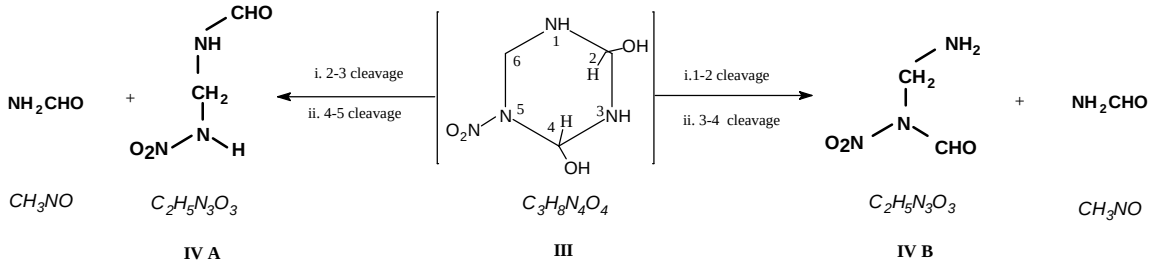

Figure 5. Proposed chemical structures of the MW 119 ($C_2H_5N_3O_3$) metabolite and the hypothetical hydroxylated product (III) that lead to their formation.

We based our conclusion on the assumption that the denitrated intermediate II would first react with water to produce the hypothetical hydroxylated structure III. The subsequent spontaneous decomposition of the resulting α-hydroxylated product (III) would then produce both IV A and IVB (Figure 5).

The autodecomposition of the unstable α-hydroxylated product (III) would also produce NH_3, HCHO in addition to the dead end product IV ($C_2H_5N_3O_3$) (Fig. 4). No nitrite assimilation occurred during resting cell assays. Therefore the formation of ammonia in these assays was presumed to be generated directly through the decomposition of the hydroxylated product III or *via* one of its ring cleavage intermediates possibly formamide (NH_2CHO). *Pseudomonas putida* biodegrades NH_2CHO to NH_3 and CO_2 (Babu et al., 1996). α–Hydroxylation of cyclic and acyclic dialkyl nitrosamines catalyzed by a mixed function oxidase can lead to the production of unstable carbinol products which decompose to nitrogen and cationic alkyl groups, R^+ (Okada et al., 1980; Rowland, 1988). Our hypothesis of the occurrence of a rapid hydrolytic ring cleavage (II to III to IV) following RDX initial denitration (RDX to I to II) was supported by our observation of deuterium in the MW 119 metabolite during RDX biodegradation in the presence of D_2O. The evidence does not support a simple exchange with the solvent because when we added an HPLC purified sample of $C_2H_5N_3O_3$ to D_2O we did not observe any change in the MW. Furthermore, we observed the MW 119 Da product during alkaline hydrolysis of RDX at pH 12. The absence of ^{18}O in the metabolite produced during RDX transformation in the presence of $^{18}O_2$ clearly supports the formation of MW 119 *via* a hydrolytic step. Interestingly we did not observe any ^{18}O incorporation in CO_2. However, further spectroscopic evidence on the identity of the 119 Da metabolites is needed to provide insight about the mechanism of its formation and also its subsequent reactions.

Previously we reported that biodegradation of RDX with another isolated *Rhodococcus* strain produced the cyclohexenyl intermediate (I) which autodecomposed to produce the dead end product MW 119 (IV) that was tentatively identified as the aldehyde IV A (Hawari, 2000). In fact both mono denitration followed by ring cleavage (Hoffsommer et al., 1977) and successive elimination of $2HNO_2$ molecules followed by ring cleavage (Jones, 1954), have been reported for the destruction of RDX under alkaline conditions.

Comparison of the metabolites formed during the degradation of RDX using Rhodococcus rhodochrous 11Y and Rhodococcus sp. DN22. In a previous work we determined key metabolites during incubation of RDX with *Rhodococcus* sp. DN22 (Fournier et al., 2002). In a subsequent study we degraded RDX with *Rhodococcus rhodochrous* 11Y, obtained from Dr. Neil Bruce, Cambridge University (presently York University, UK), and obtained a similar product distribution (Tables 2 and 3).

Table 2. Stoichiometry of carbon during RDX (35 ppm) degradation by the two *Rhodococcus* strains based on percentage of reacted RDX using total theoretical numbers of C atoms.

Carbon (3)	4-NDAB $C_2H_5N_3O_3$	CO_2	MEDINA $CH_4N_4O_4$	% of C recovered
Strain DN22	62.0	31.6	0	93.6
Strain 11Y	62.0	32.6	Traces	94.6

The C mass balance, 93.6 and 94,6 %, respectively, and stoichiometries were strikingly similar for both strains DN22 and 11Y. In both strains DN22 and 11Y, RDX degraded and produced almost equal amounts of $^{14}CO_2$ (31.6 and 32.6 %, respectively).

Table 3. Stoichiometry of nitrogen during RDX (35 ppm) degradation by the two *Rhodococcus* strains. The values represent percentage of reacted RDX using total theoretical numbers of N atoms. In order to allow the detection of NO_2^- 1 mM NH_4Cl was added to the cell suspensions.

Nitrogen (6)	NO_2^-	N_2O	NH_3	4-NDAB $C_2H_5N_3O_3$	MEDINA $CH_4N_4O_4$	% of N recovered
Strain DN22	33.3	2.8	10.0	47.0	0	93.1
Strain Y11	30.0	2.6	0	47.0	Traces	79.6

Interestingly, both strains DN22 and 11Y showed unique recalcitrance towards HMX. In neither case we were able to observe any reduction in the initial concentration of HMX under similar conditions.

Molecular structure of RDX metabolite $C_2H_5N_3O_3$. Based on elemental analysis (Table 4) and LC/MS (ES-) data of the dead end metabolite $C_2H_5N_3O_3$, produced during RDX biodegradation by strains DN22, we tentatively identified the intermediate as either 4-nitro-2,4-diazabutanal (O_2NNHCH_2NHCHO) or 2-nitro-3-amino-2-azapropanal ($NH_2CH_2NNO_2CHO$) (Fournier et al., 2002).

Table 4. Elemental analysis of 4-nitro-2, 4-diazabutanal.

	Nitrogen % (SD)	Carbon % (SD)	Hydrogen % (SD)
Measured value	34.25 (0.028)	20.27 (0.021)	4.19 (0.005)
Calculated value	35.29	20.17	4.23

Suggested molecular formula is $C_2H_5N_3O_3$ (MW 119.08).

In the present study, NMR spectroscopy was used to elucidate further the structure of the metabolite. NMR spectra were collected in d_6-DMSO. The ^1H spectrum showed two broad signals at 12.45 (1H) and 8.93 (1H) ppm, assignable to exchangeable NH protons, and two duplet signals at 8.06 (1H) and 4.70 (2H) ppm, assignable to CHO and CH_2 groups, respectively, (Table 5).

A COSY experiment demonstrated that the splitting of these two latter signals was due to a coupling with the proton at 8.92 ppm (Table 5). Furthermore, saturation transfer at 323 K lead to the attenuation of the H (δ 8.06) signal by the H (δ 8.13), suggesting that the molecule exists as two isomers most probably as a keto-enol tautomer. When we repeated NMR in d_6-

DMSO we reproduced the C chemical shifts obtained in D_2O, but several new H chemical shifts were observed at 12.45, 8.92 and 8.41 ppm, in addition to the earlier two shifts seen a 4.70 and 8.13 ppm (Fig 5). After completion of this extensive analytical investigation on the true identity of the dead end product $C_2H_5N_3O_3$ we were able to obtain an authentic reference standard material of 4-nitro-2, 4-diazabutanal (SRI, Menlo Park, CA.) and thus were able to confirm the identity of RDX metabolite as 4-nitro-2, 4-diazabutanal.

Table 5. Molecular structure of 4-nitro-2, 4-diazabutanal as elucidated by NMR analysis in d_6-DMSO (dimethylsulfoxide).

Molecular structure of $C_2H_5N_3O_3$

O_2N—NH—CH_2—NH—CHO
d b c a

^{1}H signals	**^{13}C signals**
H^a : δ 8.06 (d, 1H, CHO)	C^a : δ 165.05 (CHO)
H^b : δ 4.70 (d, 2H, CH_2)	C^b : δ 47.73 (CH_2)
H^c : δ 8.93 (s, broad, 1H, NH)	
H^d : δ 12.45 (s, broad, 1H, NH)	

All above results and especially the two distinct NH signals are consistent with the structure of 4-nitro-2,4-diazabutanal (Table 2) rather than the alternative structure of 2-nitro-3-aminoazapropanal.

As we will describe below when we initiate denitration on either RDX or HMX using either base (pH 10) or light (350 nm) we obtained a similar product distribution (NO_2^-, NH_3, N_2O, HCHO and CO_2) most notably the dead end product 4-nitro-2,4-diazabutanal, detected during RDX biodegradation with DN22. Experimental findings suggested a resemblance in the degradation mechanisms of both reactions. RDX hydrolyzes in an alkaline solution (pH 12) *via* a bimolecular elimination of HNO_2 to initially produce 1,3,5-triaza-3,5-dinitrocyclohex-1-ene intermediate (I) (Croce and Okamoto, 1979). The later decomposes at a rate 10^5 times faster than the initial rate of RDX degradation by E2 (Hoffsommer et al., 1977). As Figure

3C shows we detected the product with MW 119 Da with the same retention time (3.6 min) as observed during incubation with *Rhodococcus*. It is possible that intermediate II was also formed by strain DN22, but its rapid decomposition would have prevented detection.

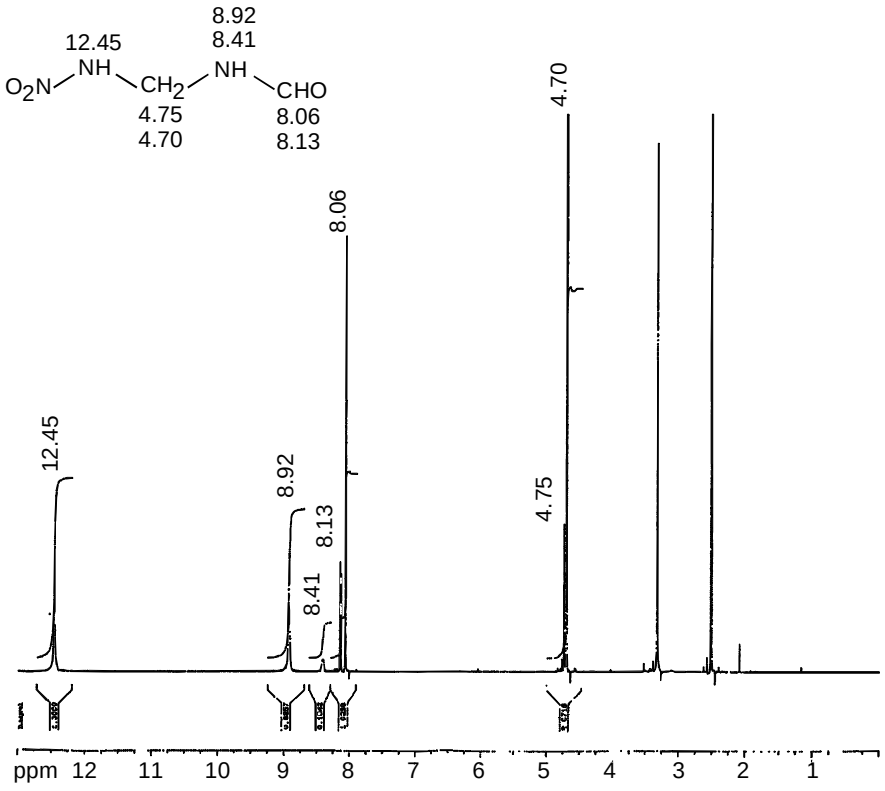

Figure 5. ^{1}H-NMR spectrum of 4-nitro-2,4-diazabutanal obtained in d_6-DMSO.

The nitrogen and carbon stoichiometry shown in Tables 1, 2 and 3 is consistent with the pathway in Figure 4 in which we assumed that both RDX denitration steps occurred prior to ring cleavage. Figure 4 thus represents the best explanation for the detected RDX degradation products, their time course of production and stoichiometry. Future work should focus on the actual enzymes involved in the initial attack on RDX and the role of enzymes vs. abiotic mechanisms in the subsequent complex reactions that take place following ring cleavage.

V.4.2 Biotransformation of hexahydro-1,3,5-trinitro-1,3,5-triazine (RDX) by a rabbit liver cytochrome P450: Insight into the mechanism of RDX biodegradation by **Rhodococcus** *sp. DN22.*

- Bhushan, B., Trott, S., Spain, J., Halasz, A. and J. Hawari. **2003.** Biotransformation of hexahydro-1,3,5-trinitro-1,3,5-triazine (RDX) by a rabbit liver Cytochrome P450: Insights into the mechanisms of RDX biodegradation by *Rhodococcus* sp. Strain DN22. Appl. Environ. Microbiol. 69: 1347-1351.

RDX biotransformation by rabbit liver cytochrome P450. A time course study of biotransformation of RDX catalyzed by cytochrome P450 2B4 showed the simultaneous release of nitrite and HCHO from RDX at expense of the electron donor NADPH (Fig 1). RDX was biotransformed at rates of 9.0 and 2.8 nmoles min^{-1} mg^{-1} protein at pH 7.2 and 37^{o}C under anaerobic and aerobic conditions, respectively. In comparison, the reaction rate of cytochrome P450 2B4 against the standard substrate, pentoxyresorufin, was 0.88 nmoles min^{-1} mg^{-1} protein under aerobic conditions which was about 3-fold lower than the RDX biotransformation rate. The metabolites produced during RDX biotransformation by P450 2B4 were 4-nitro-2,4-diazabutanal, nitrite, formaldehyde and ammonium (Table 1). In addition, traces of MNX and methylenedinitramine were also detected as transient metabolites, probably due to the presence of cytochrome P450 reductase activity in cytochrome P450 2B4 (as indicated in the product description from the manufacturer). For instance, when RDX was incubated with cytochrome P450 reductase and NADPH as an electron donor under anaerobic conditions at 37^{o}C, the compound was biotransformed at a rate of 0.42 μmoles min^{-1} mg^{-1} protein and produced MNX and methylenedinitramine as transient intermediates and N_2O, HCHO and NH_4^+ as end-products (data not shown).

In comparison, the reaction rate of cytochrome P450 reductase against cytochrome c was 32.50 μmoles min^{-1} mg^{-1} protein, which was about 77-fold higher than that of RDX biotransformation rate under similar reaction conditions.

As mentioned above, RDX biotransformation rate by P450 2B4 was about 3-fold higher

under anaerobic conditions compared to the aerobic conditions. Our experimental finding, that anaerobic conditions favored the RDX biotransformation by P450 2B4, can be explained on the basis of a single-electron transfer mechanism catalyzed by a cytochrome P450 (Guengerich, 2001).

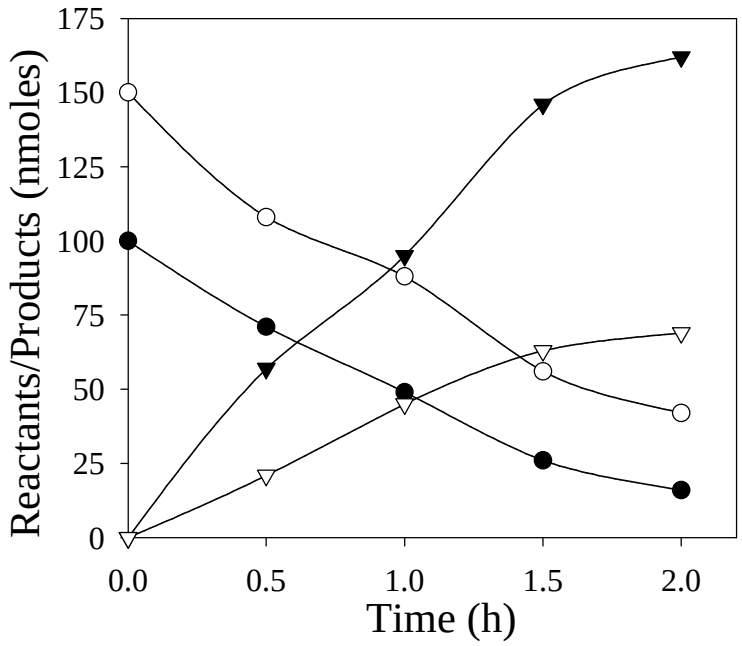

Figure 1. Time course study of biotransformation of RDX catalyzed by a rabbit liver cytochrome P450 2B4. The data are mean of duplicate experiments and SD were within 6 % of the mean absolute values (n = 2). Symbols, RDX (•), NADPH (?), NO_2^- (?), HCHO (∇).

According to this mechanism, the substrate either binds directly at the Fe^{2+} site of the prosthetic heme group or a nearby site (e.g. # 6 heme ligand position) and undergoes single electron reduction by oxidizing the Fe^{2+}. Besides substrate, the Fe^{2+} of the prosthetic heme is also a binding site for O_2. Therefore, O_2 competes with the substrate for binding at the same site and this provides a probable explanation for the inhibition of RDX biotransformation by cytochrome P450 2B4 under aerobic conditions. In case of *Rhodococcus* sp. DN22, although aerobic conditions were needed for bacterial growth, the RDX transformation does not

involve the incorporation of molecular oxygen. When RDX was incubated with strain DN22 in the presence of $^{18}O_2$ we detected the metabolite, 4-nitro-2, 4-diazabutanal, without ^{18}O incorporation (Fournier et al., 2002). In the presence of $H_2{}^{18}O$ we detected 4-nitro-2,4-diazabutanal (MW 121 [M+2]) with one ^{18}O atom. Similarly, in case of cytochrome P450 2B4, we observed that ^{18}O incorporation in 4-nitro-2, 4-diazabutanal was from $H_2{}^{18}O$ and not from $^{18}O_2$.

Table 1. Carbon and nitrogen mass balance and stoichiometry of reactants consumed and metabolites produced during RDX biotransformation catalyzed by rabbit liver cytochrome P450 2B4 (100 μg/ml) at pH 7.2 and 37°C for 2 h under anaerobic conditions.

Reactants/Metabolites	Amount of Reactants/Metabolites (nmoles)	% Carbon recovery[a]	% Nitrogen recovery[a]
Reactants consumed			
1. RDX	84	100	100
2. NADPH	108	NA	NA
Metabolites produced			
1. Nitrite (NO_2^-)	162	NA	32.0
2. 4-Nitro-2,4-diazabutanal	68	54	40
3. Formaldehyde (HCHO)	69	27	NA
4. Ammonium (NH_4^+)	65	NA	13
Total % mass recovery		81	85

[a] values calculated from the total carbon and nitrogen mass in the biotransformed RDX (84 nmoles); Initial RDX and NADPH conc. were 100 and 150 nmoles, respectively; NA, not applicable; The data are mean of duplicate experiments and SD were within 6 % of the mean absolute values (n = 2).

Inhibition study. A comparative inhibition study was carried out with cytochrome P450 2B4 and *Rhodococcus* sp. DN22 using various cytochrome P450 inhibitors. At a concentration of 200 μM, all tested inhibitors inhibited the RDX biotransformation activity of cytochrome P450 2B4 as well as *Rhodococcus* sp. DN22 (Table 2). These inhibitors act on the exposed prosthetic heme group of cytochrome P450 (Ortiz de Montellano and Correia, 1995). The inhibition study provided additional support for the hypothesis that the enzyme responsible for RDX biotransformation activity of *Rhodococcus* sp. DN22 is cytochrome P450. Coleman

et al. (2002) previously reported that metyrapone and menadione strongly inhibited the RDX biotransformation activity of *Rhodococcus* sp. DN22 which indicated the likely involvement of cytochrome P450 enzyme in RDX biotransformation by *Rhodococcus* sp. DN22. Seth-Smith et al. (2002) also reported a metyrapone mediated inhibition of RDX biotransformation by *Rhodococcus rhodochrous* strain 11Y expressing a cytochrome P450 gene.

Table 2**.** Effect of cytochrome P450 inhibitors on RDX biotransformation activity of rabbit liver cytochrome P450 2B4 (CYP 2B4) and *Rhodococcus* sp. DN22.

Inhibitors (200 μM)	% Inhibition	
	CYP 2B4 (100 μg/ml)	*Rhodococcus* sp. DN22 (5 mg wet biomass/ml)[a]
1. Control (no inhibitor)	0	0
2. Ellipticine	76 ± 4	76 ± 7
3. Metyrapone	68 ± 8	60 ± 6
4. Phenylhydrazine	70 ± 7	77 ± 5
5. 1-Aminobenzotriazole	55 ± 7	43 ± 7
6. Carbon monoxide[b]	82 ± 6	48 ± 5

RDX transformation activity without inhibitor was considered as 0 % inhibition. 100 % activities for CYP 2B4 and *Rhodococcus* sp. DN22 were 9.0 nmoles min^{-1} mg $protein^{-1}$ and 0.12 nmoles min^{-1} mg $biomass^{-1}$, respectively; [a] washed and centrifuged cell pellet was used as wet biomass. [b]Carbon monoxide was bubbled through aqueous phase and headspace for 60 seconds in sealed vials. Data are represented as % inhibition ± SD (*n*=3).

Stoichiometry and mass-balance of RDX biotransformation by cytochrome P450 2B4. We found that 84 nmoles of RDX were transformed at the expense of 108 nmoles of NADPH suggesting a 1:1 stoichiometry. The remaining 24 nmoles of NADPH were presumably consumed by cytochrome P450 reductase present in cytochrome P450 2B4 preparation (mentioned above) and/or a small fraction of NADPH can also react directly with RDX or its metabolites. The total recovered carbon mass-balance was 81 % and was distributed as 4-nitro-2,4-diazabutanal (54 %) and HCHO (27 %) (Table 3) and total nitrogen mass recovery

was 85 % and was distributed as nitrite (32 %), 4-nitro-2,4-diazabutanal (40 %) and ammonium (13 %) (Table 1).

Based on product distribution and mass-balance of RDX transformation by cytochrome P450 2B4, we concluded that of the 6 nitrogens and 3 carbons present in one RDX molecule, 2 nitrogens were recovered as nitrite ions. Whereas, 3 nitrogens and 2 carbons were recovered as a dead end metabolite, 4-nitro-2,4-diazabutanal. The remaining 1 nitrogen and 1 carbon were present in NH_4^+ and HCHO, respectively (Table 1).

Taken together, the above results provided several lines of evidence to propose that a cytochrome P450 type of enzyme is responsible for RDX transformation by *Rhodococcus* sp. DN22. Comparison of the biotransformation of RDX catalyzed by rabbit liver cytochrome P450 2B4 to that of *Rhodococcus* sp. DN22 (Fournier et al., 2002) revealed that the product distribution and stoichiometry were strikingly similar. In a previous report, cytochrome P450 from *Rhodococcus rhodochrous* participated in the degradation of 2-ethoxyphenol and 4-methoxybenzoate (Karlson et al., 1993). Our enzyme inhibition studies are consistent with those of Coleman et al. (2002) regarding involvement of cytochrome P450 in RDX degradation by *Rhodococcus* sp. DN22. Finally, Seth-Smith et al. (2002) have recently provided strong molecular evidence that a constitutively expressed cytochrome P450-like gene product *xplA* from *Rhodococcus rhodochrous* strain 11Y is responsible for RDX degradation.

Proposed mechanism. Based on stoichiometry and mass-balance studies and the key observation that ^{18}O incorporation into 4-nitro-2,4-diazabutanal was from $H_2{}^{18}O$ and not from $^{18}O_2$, we suggest a plausible mechanism for the initial biotransformation of RDX by cytochrome P450 2B4. According to this mechanism, cytochrome P450 2B4 catalyzed sequential transfer of two single electrons to RDX, the first electron would cause denitration to form product I (Fig. 2) and the second electron would cause a second denitration to produce II. The latter would be unstable in water and should hydrolyze by incorporating two ^{18}OH from two $H_2{}^{18}O$ molecules to give hypothetical compound III. The spontaneous decomposition of III would produce 4-nitro-2,4-diazabutanal (Fig. 2).

In conclusion, we provided here direct biochemical evidence that a rabbit liver cytochrome

P450 catalyzed the biotransformation of RDX. We proposed a plausible mechanism of initial enzymatic attack on RDX by cytochrome P450 which eventually produced the same products as those produced by *Rhodococcus* sp. DN22

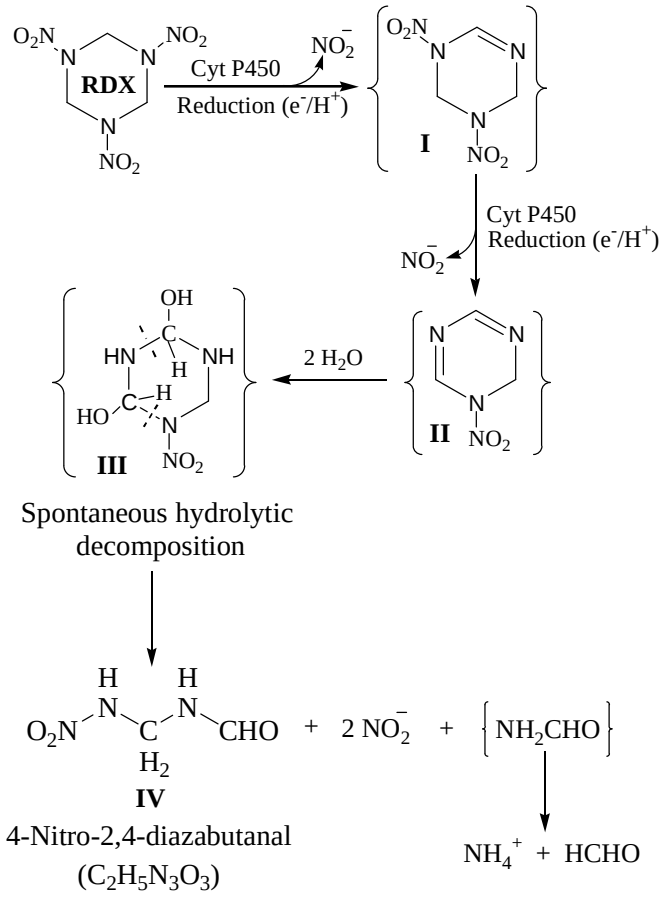

Figure 2. Proposed pathway of RDX biotransformation catalyzed by a rabbit liver cytochrome P450 2B4. Products shown inside brackets were not detected.

This mechanism is consistent with our observations that two electrons (~ 1 NADPH) were consumed and two nitrite ions were produced per reacted RDX molecule. Several lines of evidence in the present study and the results described in previous works (Coleman et al., 2002; Fournier et al., 2002; Seth-Smith et al., 2002) support the conclusion that an enzyme(s) belonging to the cytochrome P450 family is responsible for RDX biotransformation by *Rhodococcus* sp. DN22.

V.5 Abiotic Degradation of RDX and HMX: photolysis and hydrolysis

Hypothesis:

Initial microbial enzymatic denitration of RDX was found sufficient to cause spontaneous decomposition. We thus hypothesized that initial denitration of the energetic chemical via photolysis or bimolecular elimination of HNO_2 in alkaline medium should also lead to spontaneous decomposition of the compound. Denitration of RDX by the above abiotic processes is presumed to be more rapid than enzymatic denitration and therefore might lead to the formation of sufficient amounts of intermediate products to allow detection. Knowledge of intermediates and degradation products are the bottlenecks that hindered earlier attempts to understand the degradation pathways of this important family of energetic chemicals.

V.5.1 Photodegradation of RDX in aqueous solution: a mechanistic probe for biodegradation with **Rhodococcus** *sp.*

- Hawari, J., A. Halasz, C. Groom, S. Deschamps, L. Paquet, C. Beaulieu, and A. Corriveau. 2002. Photodegradation of RDX in aqueous solution: a mechanistic probe for biodegradation with *Rhodococcus* sp. strain DN22. Environ. Sci. Technol. 36: 5117-5123.

Previously we found that *Rhodococcus* sp. strain DN22 can degrade RDX effectively, but is unable to degrade HMX. We achieved 30 % mineralization, accounting for only one of the three C atoms in RDX leaving the remaining two carbons in a dead end product that was identified as 4-nitro-2,4-diaza-butanal, O_2NNHCH_2NHCHO. We suggested that initial enzymatic denitration of RDX during its incubation with strain DN22 was responsible for the destruction of the chemical in water. However, we were unable to detect the initial denitrated and other early intermediates considered important to the understanding of the degradation process.

Since initial enzymatic denitration of RDX was found sufficient to cause spontaneous decomposition we hypothesized that photodenitration of the compound in water should also lead to spontaneous decomposition. Denitration of RDX by photolysis is presumed to be more rapid than enzymatic denitration and therefore might lead to the formation of sufficient amounts of intermediate products to allow detection.

Several studies reported the successful photodegradation of RDX, mostly via the homolysis of the $N\text{-}NO_2$ bond, under several oxidation conditions (Kubose and Hoffsommer, 1977; Peyton et al., 1999). In most reported cases, photodecomposition of RDX produces common secondary products including HCHO, HCOOH, NH_2CHO, NH_3, NO_2^-, NO_3^-, and N_2O. Interestingly most of these secondary photoproducts resembled those observed during aerobic degradation of RDX with *Rhodococcus* sp. strain DN22 (Fournier et al., 2002) (Figure1).

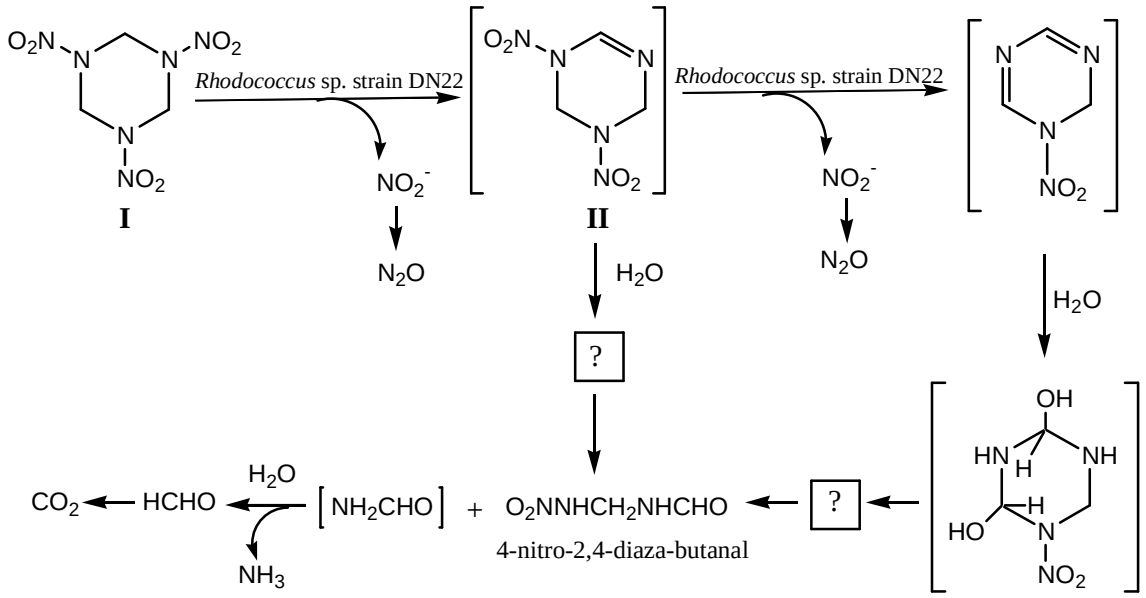

Figure 1. Proposed degradation routes of RDX by *Rhodococcus* sp. strain DN22 (Fournier et al. 2002).

The resemblance in product distribution between abiotic and biotic degradation of RDX indicates that once the molecule suffers a successful initial attack it undergoes rapid decomposition in water (Hawari, 2000). However, these initial attacks and their resulting intermediate products are not well known. We hope that the discovery of new RDX intermediates through a more rapid photodenitration technique can provide us with insight into the initial enzymatic degradation mechanism(s) of cyclic nitramine explosives. Understanding the degradation pathways of RDX would help in the development of optimized (bio)remediation strategies for their removal.

Our objective is thus to photodenitrate RDX in deionized water at 350 nm in an attempt to generate sufficient amounts of initial intermediate(s) that we were unable to detect previously with *Rhodococcus* sp. strain DN22. We will conduct the photolysis experiments in non degassed aqueous solutions at pH 5.5 and room temperature to mimic the conditions employed during RDX degradation with Strain DN22 (Fournier et al., 2002). The use of low energy wavelength light (350 nm) at neutral conditions was to minimize the formation of secondary photoproducts whose presence might interfere with other prime products considered important to the understanding of the degradation process. Some of the photolysis

experiments were conducted in the presence of acetone in an attempt to enhance denitration through the energetic acetone triplet ($T_1(n,\pi^*)$) whose excitation energy (326.04 $KJmole^{-1}$, Turro, 1978) is sufficient to break down the $N\text{-}NO_2$ bond (BDE 229.9 $KJmole^{-1}$) in RDX.

Photodegradation of RDX in aqueous solution at 350 nm. Figure 2A is a typical GC/MS (PCI) chromatogram of RDX after 2 h of photolysis at 350 nm showing a product with a retention time at 12.7 min and a protonated molecular mass ion [M + H] at 176 Da, matching a molecular formula of $C_3H_5N_5O_4$. The product also showed several other characteristic mass ions at 47, 102 and 149 Da representing $-HNO_2$, $CH_2NNO_2CH_2N$ and $O_2NHNCH_2NNO_2CH_2$, respectively (Figure 2B). The mass data of **II** matched exactly those of an earlier intermediate that was tentatively identified as pentahydro-3,5-dinitro-1,3,5-triaza-cyclohex-1-ene that we detected during hydrolysis of RDX in alkaline 2-propanol (Hawari et al., 1996). Therefore we tentatively identified the present RDX photoproduct also as pentahydro-3,5-dinitro-1,3,5-triazacyclohex-1-ene. However, when we injected a standard material of RDX on the same GC we observed a peak that had the same r.t. and $[M+H]^+$ as that obtained during RDX photolysis. RDX is thermally unstable and decomposes *via* HNO_2 elimination (Zhao et al., 1988), indicating that the energetic chemical might also undergo thermal decomposition at least partially during GC analysis. However, we found that the GC area of **II** generated during RDX photolysis was approximately twice as large as the area obtained from dark controls, suggesting its potential formation as a photoproduct.

Several reports indicated the formation of **II** during photolysis, thermolysis and hydrolysis of RDX (Bose et al., 1998; Peyton et al., 1999; Hawari et al., 1996; Hoffsommer et al., 1977), but as far as we are aware **II** has never been isolated. **II** is an enamine with a reactive -C=N bond that is expected to undergo rapid hydrolysis in water (March, 1985).

Therefore we conducted RDX photolysis in the presence of a sensitizer such as acetone in an attempt to enhance photodegradation and to generate sufficient amounts of **II** for detection. We were unable to see **II**, but more importantly we detected two LC/MS chromatographic peaks **III** and **IV** at 6.8 and 18.2 min respectively, (Figure 3B). Each showed the same $[M\text{-}H]^-$ at 192 Da, matching a molecular formula of $C_3H_7N_5O_5$ (MW 193 Da). The two products also showed several other characteristic mass ions at 46, 61 and 118 Da, representing $-NO_2$, -

$NHNO_2$ and -$OHCNCH_2NHNO_2$ (Figure 4).

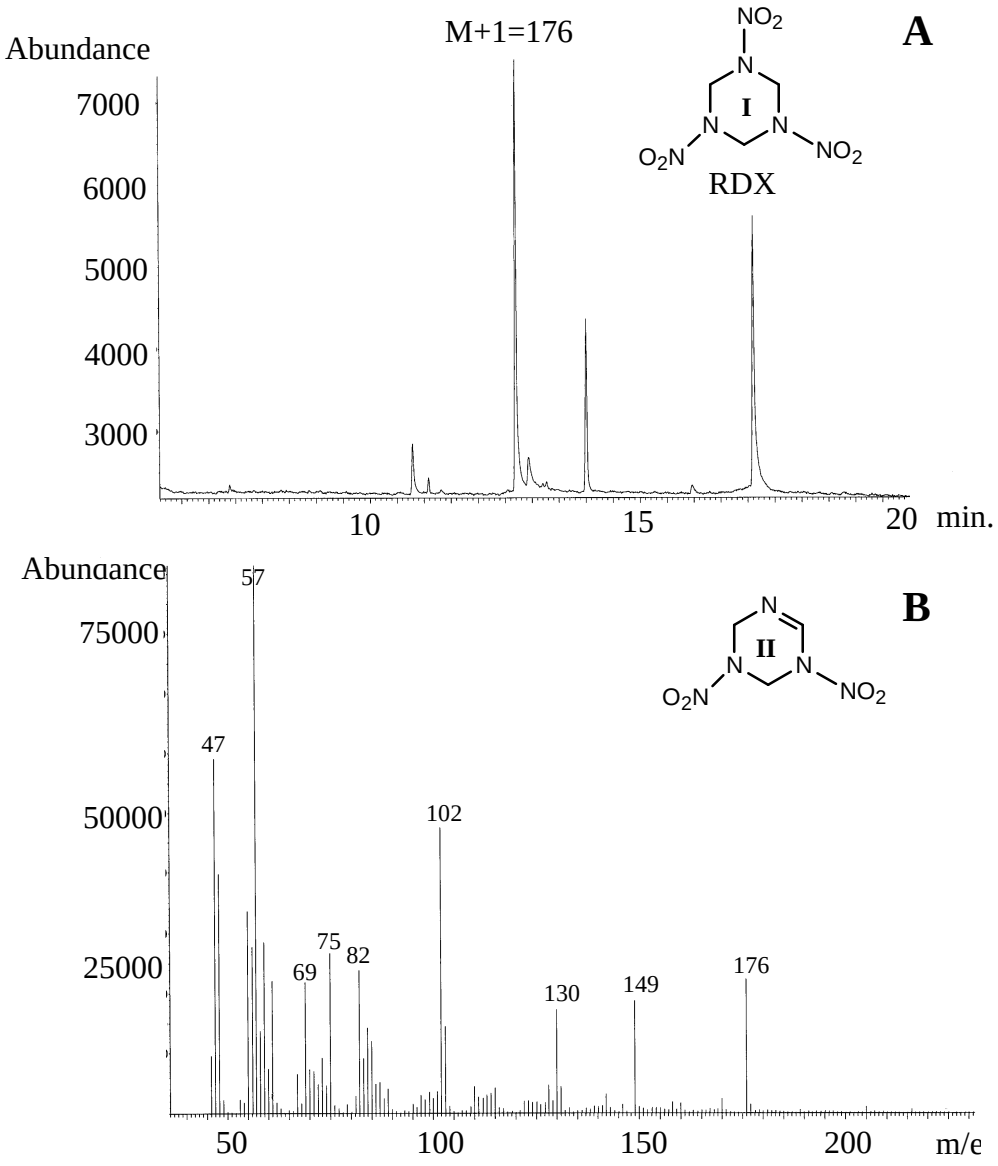

Figure 2. GC/MS (PCI) chromatogram of RDX after 2 h of photolysis at 350 nm (A) and mass spectrum of denitrated intermediate (**II**) at 12.7 min. (B).

Peak **III,** which appears next to RDX at a higher r.t. is presumed to be less polar and thus was tentatively identified as the cyclic carbinol pentahydro-1,3-dinitro-1,3,5-triaza-cyclohexanol (**III**) derivative of **II**. Whereas peak **IV**, which appears at a lower r.t was tentatively

identified as the ring cleaved product 4,6-dinitro-2,4,6-triaza-hexanal ($O_2NNHCH_2NNO_2CH_2NHCHO$) of **III** (Figure 4).

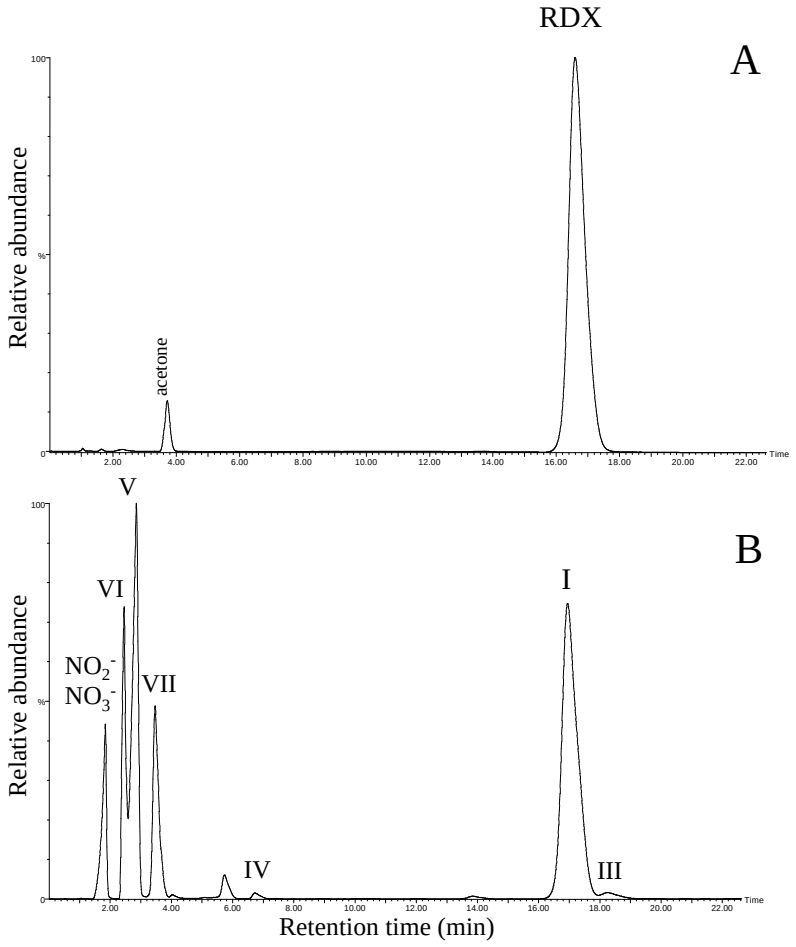

Figure 3. HPLC/UV chromatogram of RDX. A: before photolysis, B: after 3 h of photolysis at 350 nm.

We observed two other familiar intermediates, **V** at a r.t of 2.9 min with a $[M-H]^-$ at 118 Da, matching a molecular formula of $C_2H_5N_3O_3$ and **VI** at a r.t. of 2.3 min with a $[M-H]^-$ at 135 Da matching a molecular formula of $CH_4N_4O_4$ (Figures 3 and 4). **V** was identified as 4-nitro-2,4-diaza-butanal by comparing its chromatographic and mass data with those of a standard material of $OHCNHCH_2NHNO_2$ obtained by incubating RDX with strain DN22 (Fournier et

al., 2002). Whereas **VI** was identified as methylenedinitramine, $O_2NNHCH_2NHNO_2$, by comparison with a commercial reference standard (Figures 3 and 4).

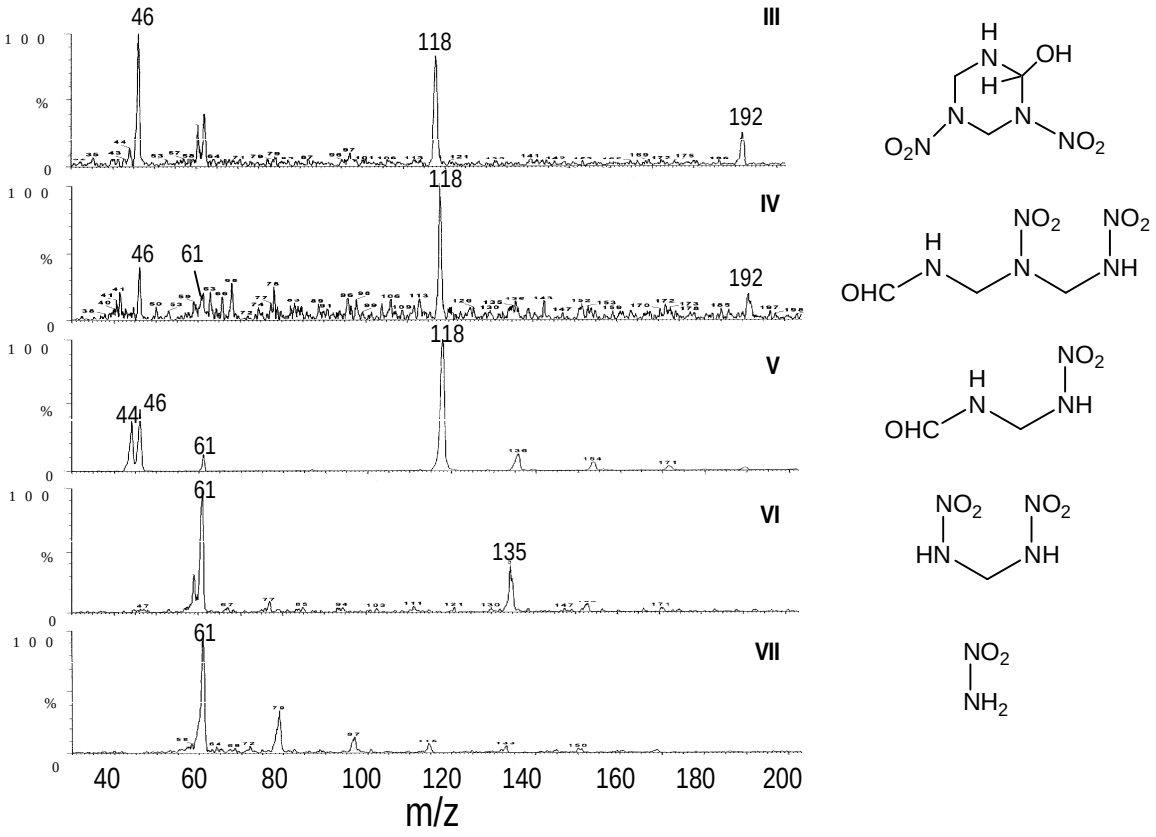

Figure 4. LC/MS (ES-) spectra of RDX degradation products **III**, **IV**, **V**, **VI** and **VII** observed during photolysis at 350 nm in aqueous solution (see Figure 2B).

Interestingly, the LC/MS(ES-) spectrum of **IV** was found to contain a strong mass ion at 118 Da (Figure 4), suggesting that this intermediate might act as a precursor to O_2NNHCH_2NHCHO (**V**) whose $[M-H]^-$ was also observed at 118 Da. Consequently, the dominant formation of **V** (66 %) during biodegradation of RDX with *Rhodococcus* might thus suggest the direct involvement of intermediate **IV** in its formation too.

The last LC/MS (ES-) peak **VII** appearing at 3.9 min showed mainly a strong mass ion at 61 Da and was tentatively identified as the nitramide H_2NNO_2 (**VII**) (Figure 4). Spontaneous decomposition of **VII** in water produces nitrous oxide, N_2O and formaldehyde, HCHO (Hawari, 2000).

The present mild photolysis (350 nm) of RDX in non degassed aqueous solution did not produce any of the RDX nitroso derivatives such as MNX, DNX and TNX. Interestingly none of the nitroso products was detected during RDX aerobic degradation with strain DN22 (Fournier et al., 2002; Coleman et al., 1998). Fenton reagent (Fe^{+2}/H_2O_2), which is known to be a powerful generator of the highly reactive hydroxyl radicals, $OH^{\cdot}$, mineralized both RDX and HMX to CO_2 and NO_3^- without producing the nitroso compounds (Zoh and Stenstrom, 2002). However, photolysis of RDX at shorter wavelengths (higher energy) produced the nitroso derivatives (Peyton et al., 1999). Nitroso products were frequently detected during biodegradation of RDX (Hawari, 2000; McCormick et al., 1981; Oh et al., 2001) under anaerobic conditions. Interestingly when we photolyzed RDX under a blanket of argon (anaerobic) at shorter wavelengths (254 nm) we detected all three nitroso products (unpublished data).

At the end of photolysis, which lasted 16 h we observed the accumulation of the following products NO_2^-, NO_3^-, NH_2CHO, HCHO, HCOOH, and N_2O. Most of these products were also detected during RDX incubation with the aerobic degrader DN22, emphasizing that once a successful initial attack takes place on RDX, denitration in the present case, the molecule undergoes spontaneous decomposition in water (Hawari, 2000).

The presence of acetone during RDX photolysis did not seem to drastically change product distribution. For instance, all products that were detected during RDX photolysis in the absence of acetone were also detected during its presence. Some slight variation in the relative distribution of these products was noted. For instance the yield of HCHO was almost two times higher in experiments containing acetone. Preliminary investigation with other photo sensitizers such, as phenothiazine and benzyl viologen also did not seem to drastically affect RDX product distribution. No RDX degradation was observed in dark aqueous controls with and without the sensitizer.

Kinetics and Stoichiometry – a comparative study with strain DN22. The removal of RDX during photolysis was accompanied by the concurrent formation of nitrite NO_2^- and nitrate NO_3^- ions (Figure 5A).

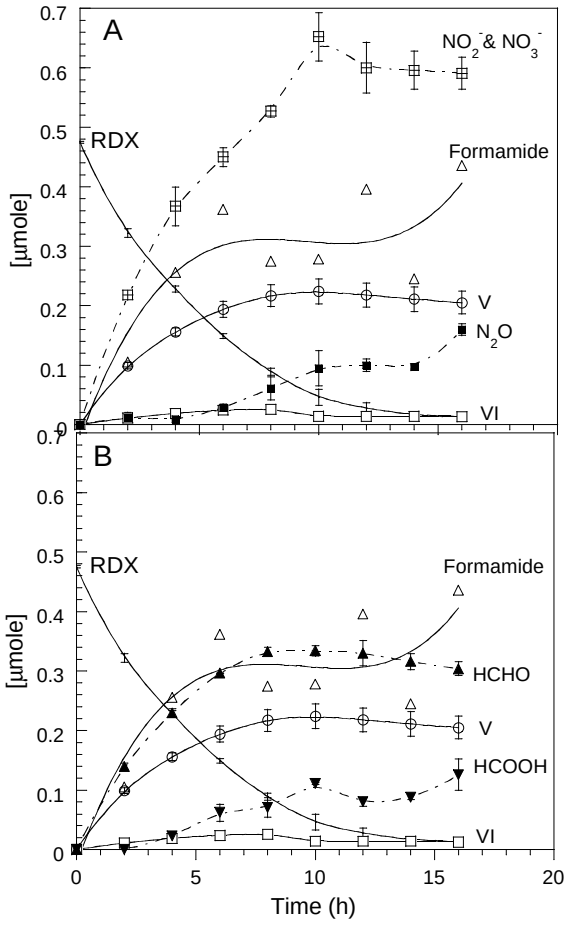

Figure 5. A time course of RDX photodegradation in aqueous solution at 350 nm.
A: N –containing products. B: C-containing products.

At the end of the experiment, which lasted 16 h almost all of the NO_2^- transformed to NO_3^-, suggesting that nitrate ion was produced from nitrite photo-oxidation. For instance when we

photolyzed $NaNO_2$ at 350 nm under the same conditions used to photolyze RDX we detected NO_3^-. Bose et al. (1998) reported that photo-oxidation of RDX with ozone at 230 nm also produced nitrate. In contrast, incubation of RDX with *Rhodococcus* strain DN22 produced NO_2^- without nitrate ion (Fournier et al., 2002). The microorganism initiated enzymatic denitration to get its own need of nitrogen for growth since RDX was used as the sole source for nitrogen.

Photodegradation of RDX was also accompanied by the accumulation of NH_2CHO, HCHO, and HCOOH (Figure 5B). In the previous RDX biodegradation study with *Rhodococcus* we detected HCHO which latter mineralized (liberated as $^{14}CO_2$), but NH_2CHO was inferred to exist by the detection of its degradation products ammonia and HCHO. For instance, when NH_2CHO was incubated with strain DN22 the amide degraded to ammonia and HCHO (Fournier et al., 2002).

Figure 5A also showed that the removal of RDX was accompanied by the accumulation of the ring cleavage product 4-nitro-2,4-diaza-butanal (**V**), which was also detected during RDX biodegradation with DN22. However, **V** was found to persist indefinitely in incubation mixtures with strain DN22 at pH 7, but degraded slowly with light.

Table 1 shows that the N mass balance of RDX removal is 73 % distributed as follows; NO_2^- and NO_3^- (21.4 %), NH_2CHO (15.7), N_2O (11.6 %), $CH_2(NHNO_2)_2$ (**VI**) (1.9 %) and O_2NNHCH_2NHCHO (**V**) (22.2 %). The C mass balance is 93 % distributed as follows: NH_2CHO (31.9 %), HCHO (22.0%), HCOOH (9.1 %), and O_2NNHCH_2NHCHO (**V**) (31.5 %) and $CH_2(NHNO_2)_2$ (**VI**) (0.9 %).

We were unable to detect N_2 or CO_2. In comparison, N- and C- mass balances of RDX biodegradation with strain DN22 were calculated as 90 and 94 %, respectively (Fournier et al., 2002). In the latter case approximately 30% of the C-content (1 atom) of RDX was found in $^{14}CO_2$ and 64% (2 C atoms) was incorporated in the dead end product **V**. The slight differences in product distribution and N and C mass balances between photolysis and biodegradation experiments were possibly caused by some variations in the relative reactivities of certain intermediates toward light and enzymes.

Table 1. Carbon and N- mass balance of RDX (0.46 μmole) after 16 h of photolysis at 350 nm in the absence of acetone in water

Products	μmole ± SD	C-content %	N-content %
O_2NNHCH_2NHCHO (V)	0.205 ±0.019	29.6	22.2
H_2NCHO	0.436 (nd)	31.5	15.7
$CH_2(NHNO_2)_2$ (VI)	0.013 (nd)	0.9	1.9
$NO_2^- + NO_3^-$	0.591 ±0.027	-	21.4
N_2O	0.160 ±0.009	-	11.6
HCHO	0.304 ±0.011	22.0	-
HCOOH	0.126 ±0.026	9.1	-
% mass balance		93.1	72.8

nd; no data

Insights into the photodecomposition mechanism of RDX: the parallel with Strain DN22.

- Initial denitration. Figure 5A shows that the removal of RDX was concurrent with the formation of nitrite, NO_2^- (and NO_3^-), indicating the occurrence of an important initial denitration step during degradation. The absence of RDX nitroso products MNX, DNX and TNX supported our belief that initial denitration was responsible for subsequent RDX degradation. Likewise, initial enzymatic denitration of RDX with *Rhodococcus* sp. strain DN22 was found sufficient to cause ring cleavage and subsequent decomposition in water (Fournier et al., 2002).

During RDX photolysis in the presence of acetone the ketone should produce a triplet $T_1(n,\pi^*)$ with excitation energy equal to 326.04 $KJmole^{-1}$ (Turro, 1978). Subsequent hydrogen atom abstraction from one of RDX methylene groups by acetone $T_1(n,\pi^*)$ would generate an RDX carbenyl radical $RDX^{\cdot}$. Elimination of NO_2 from $RDX^{\cdot}$ should lead to the formation of the enamine **II**. This reaction is exothermic because the bond dissociation energies (BDE) of the cleaved C-H (in RDX) and the generated O-H (in acetone) bonds are 376.2 and 418.0 $KJmole^{-1}$, respectively. However, the energy associated with acetone triplet

$T_1(n,\pi^*)$ is high (326.04 $KJmole^{-1}$) (11) and should be sufficient to cleave the N-NO_2 bond (BDE 229.9 $KJmole^{-1}$). Alternatively, direct homolytic cleavage of the N-NO_2 bond in RDX should not be excluded. For instance the energy associated with λ 350 nm is 342 $KJmole^{-1}$ and therefore should be sufficient to cleave the N-NO_2 bond (BDE 205 $KJmole^{-1}$) (Behrens and Bulusu, 1991). However, a synchronous bimolecular elimination (E_2) of one molecule of HNO_2 during RDX photolysis has been suggested to occur (Peyton et al., 1999, Melius; 1990). Nonetheless such an elimination would also lead to the formation of the enamine **II** (Figure 6).

As we mentioned previously, the presence of sensitizers such as acetone, phenothiazine and benzyl viologen during RDX photolysis did not seem to change product distribution drastically. Therefore it is difficult to determine which among the previous denitration routes was the most probable one.

- ***Secondary Decomposition.*** The potential involvement of the enamine **II** in the initial decomposition of RDX is supported by our observation of its carbinol derivative (**III**) and its subsequent ring cleavage product (**IV**) (Figure 6). As we mentioned previously enamines are unstable in water and therefore **II** should react through its -C=N bond with an H_2O molecule to produce the carbinol **III.** The latter is also expected to be unstable and should undergo rapid ring cleavage across its NNO_2-CH(OH) to produce **IV** (Figure 6). For instance**,** α-hydroxylation of dialkylnitrosamine by a mixed function oxidase produces unstable carbinol products that tend to cleave easily at the C(OH)-NNO_2 bond in water (Druckrey, 1973).

Intermediate **IV** with several labile C-NNO_2 bonds is thus expected to decompose in water to give several products depending on which bond is hydrolyzed first. For example 4,5 cleavage produces 4-nitro-2,4,-diaza-butanal (**V)** whereas 3,4 cleavage produces methylenedinitramine (**VI**) (Figure 6). Although we were unable to detect **III** and **IV** during RDX incubation with *Rhodococcus* (Fournier et al 2002) we now suggest their potential presence based on the predominant formation of their hydrolyzed product **V** (Figure 6). Our ability to detect both early intermediates **III** and **IV** during photolysis was possibly caused by higher initial rates of RDX denitration during photolysis as compared to biodegradation with strain DN 22, respectively.

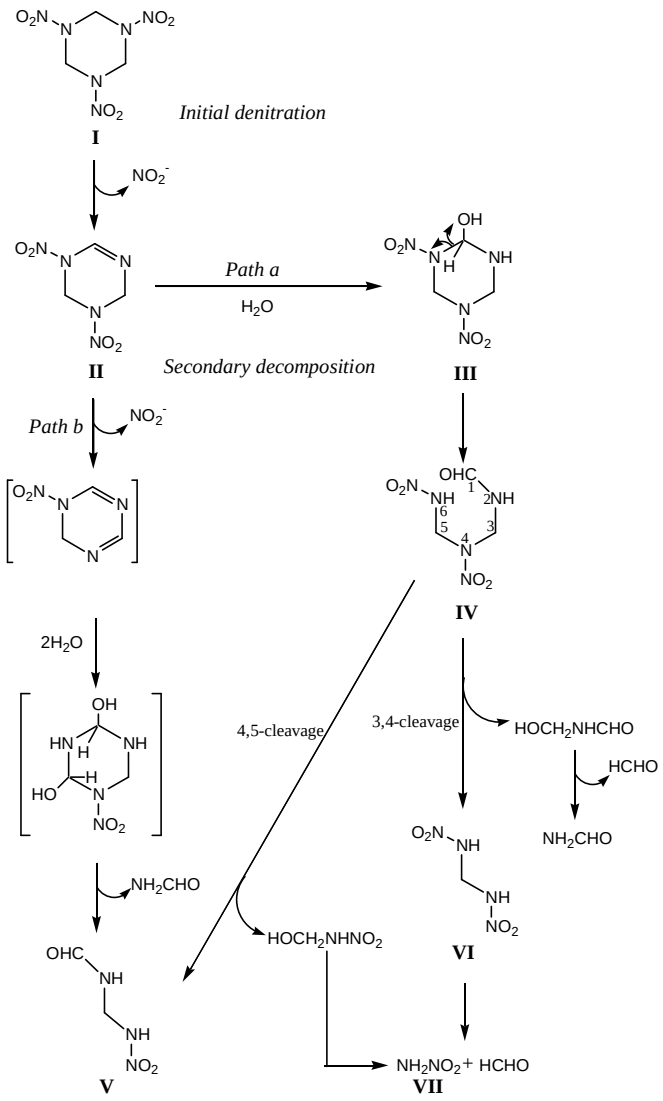

Figure 6. Postulated decomposition routes of RDX following its initial denitration by photolysis at 350 nm in an aqueous solution: a comparison with *Rhodococcus* sp. strain DN22 (Figure 1) (Fournier et al 2002). *Path a* cleavage following one denitration step and *path b*: cleavage following second denitration step.

A high denitration rate should result in the formation of sufficient amounts of these early intermediates to permit detection. Subsequent reactions of these early intermediates in water

are expected to be rapid and thus their product distribution will not be drastically influenced by light or enzyme.

After 16 h of photolysis we found that the disappearance of 0.46 μmole of RDX produced approximately 0.6 μmole of nitrite and nitrate ions, indicating that for every reacting molecule of RDX there was more than one N atom but less than two that were involved in the formation of nitrite (and nitrate) ion. Therefore we suggested the involvement of two denitration routes in the degradation of RDX; a mono denitration route leading to the formation of **II** (Figure 6, *path a*) and a second route which involved two denitration events prior to RDX ring cleavage (Figure 6, *path b*). In Figure 6, *route a* lead to the detected intermediates **IV**, **V**, **VI** and **VII** whereas *route b* leads to **V.** Previously we found that during RDX incubation with DN22 resting cells, there were two nitrite ions produced for each disappearing molecule of RDX, suggesting the involvement of the cyclic dicarbinol intermediate prior to ring cleavage (Figure 6, *path a*) (Fournier et al., 2002). Our earlier hypothesis on the potential involvement of **II**, **III** and **IV** as key intermediates during RDX incubation with DN22 is now supported by the direct observation of these intermediates during photodenitration of the energetic chemical (Figure 6).

In conclusion Figure 6 represents the best explanation for the detected RDX degradation products obtained during photolysis and incubation of the chemical with *Rhodococcus* sp. DN22. Figure 6 clearly shows that the reaction steps involved in the photodecomposition of RDX are replicates of those occurring during biodegradation of the energetic chemical under aerobic conditions with strain DN22. These findings are in accordance with our earlier hypothesis, which emphasizes that once a successful initial enzymatic or chemical attack, denitration in the present study, occurs on RDX (or HMX), the energetic chemical will decompose rapidly in water (Hawari, 2000). Our hypothesis is proven through the obtaining of a similar product distribution (NO_2^-, N_2O, NH_3, NH_2CHO, HCHO, HCOOH and O_2NNHCH_2NHCHO) in both cases.

V.5.2 Hydrolysis of RDX and HMX: bimolecular elimination of HNO_2 followed by ring cleavage and decomposition.

- Balakrishnan, V.K., Halasz, A. and J.Hawari. 2003. The alkaline hydrolysis of the cyclic nitramine explosives RDX, HMX and CL-20: New insights into degradation pathways obtained by the observation of novel intermediates. Environ. Sci. Technol. 37: 1838-1843.

To gain further understanding of the mechanisms of biodegradation of cyclic nitramines we initiated laboratory chemical experiments to denitrate RDX abiotically under alkaline conditions in an attempt to obtain sufficient amounts of degradation products first. Knowledge of degradation products can then be used to provide further insight into the biodegradation processes. Understanding these mechanisms is critical to optimize soil and groundwater decontamination schemes.

In the pervious chapters we showed that both *Rhodococcus* sp. strain DN22 (Fournier et al., 2002) and light (350 nm) (Hawari et al., 2002) can successfully decompose RDX in water *via* initial denitration to produce 4-nitro-2,4-diazabutanal (4-NDAB, O_2NNHCH_2NHCHO) as a major ring cleavage product in both cases. In addition the end product distributions that we found in the previous photochemical and enzymatic studies were basically similar and included NO_2^-, N_2O, NH_3, HCHO, CO_2, and H_2NCHO.

While many of the end products of RDX hydrolysis are known, intermediates and decomposition pathways are not well understood. Heilmann et al. (1996) suggested that RDX and HMX contaminated waters could be economically treated using granular activated carbon (GAC) to first adsorb the explosive, followed by off-line regeneration of the laden GAC through alkaline hydrolysis. However, for this technology to be optimized, knowledge of intermediates and the degradation pathways of these two monocyclic nitramines are critical both to predict their behavior and enhance their removal from the environment.

Since the end products of RDX decomposition during enzymatic biodegradation with strain DN22 (Fournier et al., 2002) were similar to those obtained *via* both alkaline hydrolysis (Hoffsommer et al., 1977; Croce and Okamoto, 1979; Heilmann et al., 1996) and photolysis (Hawari et al, 2002), we hypothesize that following initial denitration of the cyclic nitramine,

ring cleavage and subsequent decomposition is largely dictated by the aqueous chemistry of the resulting intermediates. Therefore, if other cyclic nitramines such as MNX and HMX produce end products similar to those of RDX, then their decomposition mechanisms should also be similar (Heilmann et al., 1996; Bishop et al., 1999). Hence, our objective in the present study was to provide additional insight into the degradation pathways of these cyclic nitramines by first determining whether RDX, HMX, or MNX hydrolyzed in aqueous, alkaline (pH 10) conditions to produce similar end products. We then selected RDX as a model cyclic nitramine compound and hydrolyzed it in aqueous acetonitrile solutions (pH 12.3) in the presence and absence of hydroxypropyl-β-cyclodextrin (HP-β-CD) in an attempt to explore other early intermediates in more detail.

Product distribution. Figure 1 shows that the disappearance of RDX during hydrolysis in water (pH 10) is concomitant with the formation and accumulation of NO_2^-, N_2O and formaldehyde (HCHO). Although we were unable to detect formamide, we detected its hydrolyzed products $HCOO^-$ (0.18 μmole) and NH_3 (0.20 μmole, detected as NH_4^+). Amides are known to undergo spontaneous hydrolysis under alkaline conditions (Brown et al., 1992) to produce the corresponding amines and acids. Figure 1 also shows that the disappearance of RDX was accompanied by the accumulation of the ring cleavage product 4-nitro-2,4-diaza-butanal (4-NDAB, O_2NNHCH_2NHCHO), which was also a key product during photo denitration (Hawari et al., 2002), microbial (Fournier et al., 2002) and enzymatic degradation (Bhushan et al., 2003a) of RDX. With the exception of our observation of 4-NDAB, the product distribution of the present RDX hydrolysis resembles that reported by Hoffsommer et al. (1977), Croce and Okamoto (1979), and Heilmann et al. (1996).

Table 1 summarizes the normalized molar yields for the products obtained at the end of the hydrolysis experiments for RDX, MNX, and HMX at pH 10. From this Table, it is apparent that each compound loses one equivalent of NO_2^- and forms O_2NNHCH_2NHCHO (4-NDAB) as a major product. This is the first time that 4-NDAB formation has been conclusively demonstrated as a common feature in the alkaline hydrolyses of RDX, MNX, and HMX (Figure 2).

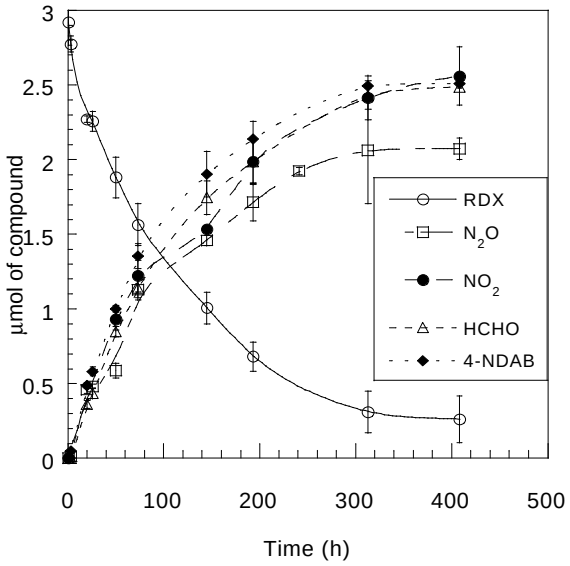

Figure 1. Time course of the alkaline hydrolysis of RDX at pH 10. Data points are the mean and error bars the standard deviation (n =3).

Table 1. Normalized molar yields of the end products obtained upon alkaline hydrolysis (pH 10) of the cyclic nitramines RDX, MNX, HMX.

Cyclic Nitramine	Observed Products					
	NO_2^-	N_2O	NH_4^+	4-NDAB	HCHO	$HCOO^-$
RDX[a]	0.972 ± 0.056	0.770 ± 0.130	0.075 ± 0.032	0.951 ± 0.005	0.939 ± 0.037	0.070 ± 0.005
MNX[a]	0.935 ± 0.005	0.008 ± 0.001	0.141 ± 0.035	0.842 ± 0.032	0.800 ± 0.027	0.152 ± 0.008
HMX[b]	1.15 ± 0.03	1.48 ± 0.06	n.d.[c]	0.859 ± 0.016	1.82 ± 0.04	n.d.[c]

[a] Values are the average of data from three replicate measurements, error values are the standard deviation.
[b] Values are the average of data from duplicate measurements, error values are the standard deviation.
[c] Due to its slow reaction rate, monitoring of HMX hydrolysis was stopped after 21 days. It is possible that NH_3 and $HCOO^-$ formed, but were at levels less than the detection limit of the capillary electrophoresis method.

In addition to forming NO_2^- and 4-NDAB, MNX hydrolysis (Figure 3) produced N_2O (trace quantities), HCHO, and small amounts of $HCOO^-$ (0.35 µmol) and NH_3 (0.33 µmol) (Table 1), which presumably formed from the hydrolysis of formamide as discussed above.

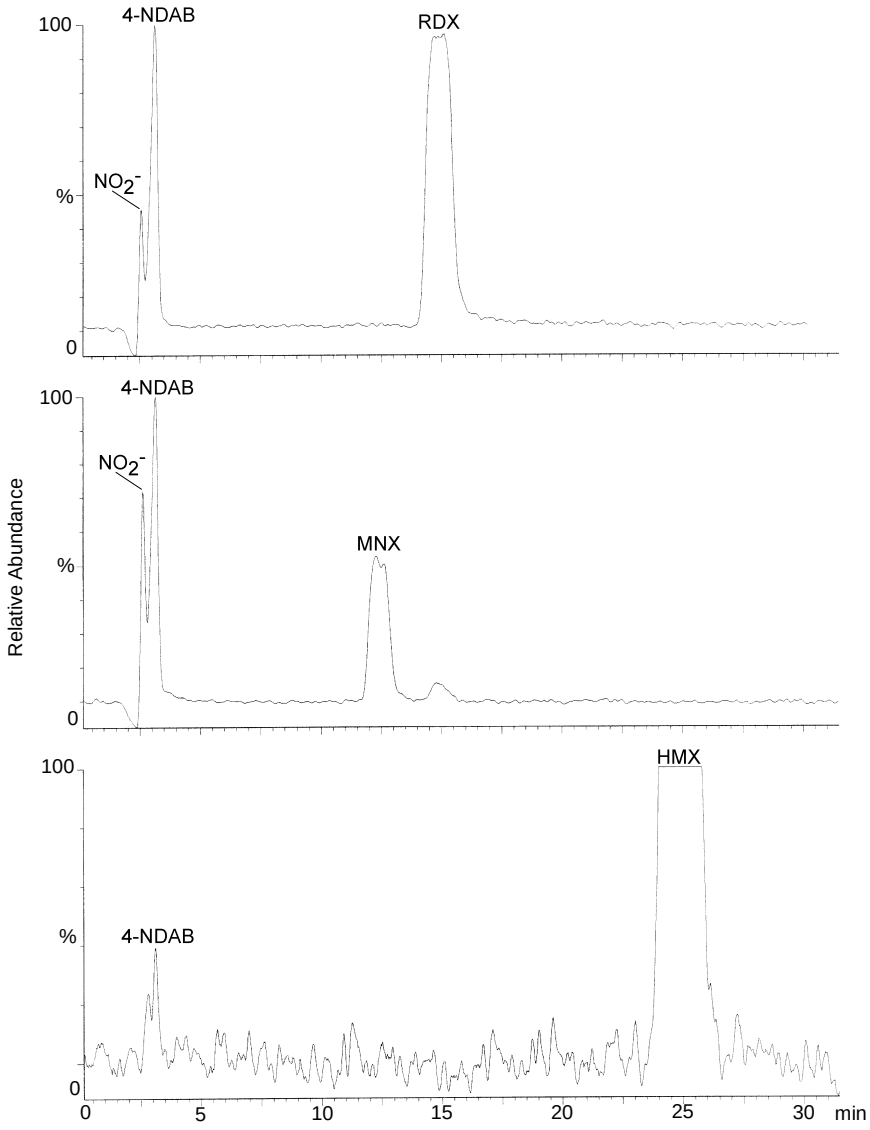

Figure 2. Typical LC/MS chromatograms of intermediates formed during hydrolysis of cyclic nitramines RDX, MNX and HMX in aqueous media at pH 10. Top: RDX after 8 days. Center: MNX after 1 day. Bottom: HMX after 15 days.

Likewise, HMX hydrolysis was accompanied by the release of 1 molar equivalent of NO_2^- with the formation of the end products N_2O, HCHO, and 4-NDAB (Table 1). Since HMX hydrolyzes an order of magnitude more slowly than RDX (Croce and Okamoto, 1979), we followed only the first 5 % of the reaction (i.e., 21 days) and were thus unable to

unequivocally confirm the presence of NH_3 and $HCOO^-$. However, when we increased the pH to accelerate the reaction, we detected NH_3 and $HCOO^-$. After 60 h at pH 12.3, HMX decomposed to produce NO_2^-, N_2O, HCHO, 4-NDAB, NH_3, and $HCOO^-$, just as we observed at pH 10 for RDX and MNX. Interestingly, after an additional 60 h at this elevated pH, 4-NDAB completely disappeared.

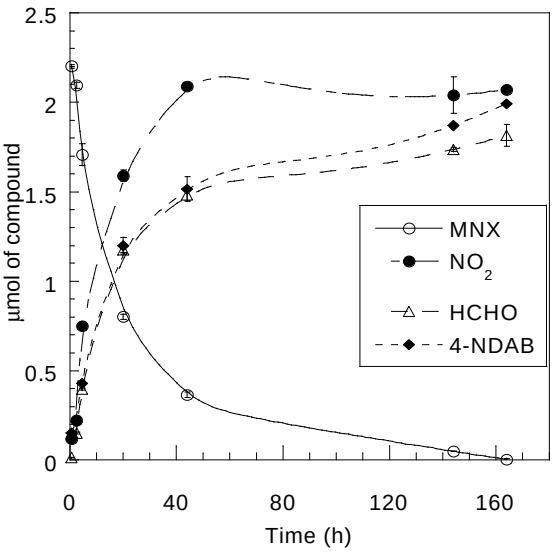

Figure 3. Hydrolysis of MNX at pH 10. Error bars; standard deviation (n =3).

This instability explains why 4-NDAB was not reported during earlier hydrolysis studies (Hoffsommer et al., 1977; Croce and Okamoto, 1979; Heilmann et al., 1996).

We were unable to observe any RDX nitroso products MNX, DNX, and TNX, which is also consistent with other reports on the alkaline hydrolysis of RDX (Hoffsommer et al., 1977; Croce and Okamoto, 1979; Heilmann et al., 1996). Indeed we found that hydrolysis on MNX under the same conditions failed to produce the dinitroso (DNX) or the trinitroso (TNX) compounds. Likewise, when we hydrolyzed HMX at pH 10, none of its corresponding nitroso products were observed. These results provide strong evidence that initial denitration is a key step responsible for the decomposition of cyclic nitramines in water.

For RDX, we found a C mass balance of 97 % distributed as follows: HCHO (31.3 %), HCOOH (2.3 %), and O_2NNHCH_2NHCHO (63.4 %) and a N mass balance of 90.7 %

distributed as follows: NO_2^- (16.2 %), N_2O (25.6 %), NH_3 measured as NH_4^+ (1.3 %), and O_2NNHCH_2NHCHO (47.6 %). For MNX, we found a C mass balance of 87.8 % in: HCHO (26.6 %), HCOOH (5.05 %), and O_2NNHCH_2NHCHO (56.1 %) and a N mass balance of 60.45 % distributed as follows: NO_2^- (15.6 %), N_2O (0.14 %), NH_3 measured as NH_4^+ (2.35 %), and O_2NNHCH_2NHCHO (42.1 %). Whereas for HMX, we found a C mass balance of 90 % distributed as follows: HCHO (46.2 %), O_2NNHCH_2NHCHO (43.8 %) and a N mass balance of 86 % distributed as follows: NO_2^- (14.7 %), N_2O (38.5 %), O_2NNHCH_2NHCHO (32.8 %).

Identification of early intermediates in RDX hydrolysis. In none of the LC/MS chromatograms shown (Figures 2 and 4) were we able to directly detect pentahydro-3,5-dinitro-1,3,5-triaza-1-ene (**II**). Since **II** is an enamine, it should react quite readily with water through its reactive -C=N bond (March, 1985), and in fact, it is known that **II** hydrolyzes at a rate 5 orders of magnitude higher than RDX (**I**) (Hoffsommer et al., 1977; Croce and Okamoto, 1979). Therefore, we hydrolyzed RDX in a MeCN:H_2O mixture in the presence and absence of HP-β-CD in an attempt to generate and stabilize sufficient amounts of **II** and other suspected key intermediates.

Figure 4A shows that RDX hydrolysis in a MeCN:H_2O mixture (70 % v/v) produced 4-NDAB (r.t. 3.6 min) and two additional peaks marked **III** (r. t. 6.7 min) and **IV** (r.t. 4.4 min). **III** was detected only in trace amounts, but as discussed below, the presence of HP-β-CD increased its yield (Figure 3B). Figure 5A shows **III** with a $[M–H]^-$ at 192 Da, matching a molecular mass formula of $C_3H_7N_5O_5$, and three other mass ion fragments at 46 Da, 61 Da and 118 Da, representing $-NO_2$, $-NHNO_2$, and the deprotonated mass ion of O_2NNHCH_2NHCHO (4-NDAB), respectively.

When ring-labeled [^{15}N]-RDX was used, the $[M-H]^-$ ion appeared at 195 Da, confirming that this intermediate contained all three ^{15}N atoms originally present in the ring structure of RDX. In addition, the mass ion fragments appearing at 118 and 61 Da were shifted to 120 Da ($O_2{}^{14}N{}^{15}NHCH_2{}^{15}NHCHO$) and 62 Da ($-{}^{15}NH{}^{14}NO_2$), respectively. We tentatively identified **III** as the ring cleavage intermediate 4,6-dinitro-2,4,6-triaza-hexanal

($O_2NNHCH_2NNO_2CH_2NHCHO$), considered as a hydrolyzed product of the presumably formed denitrated cyclohexene intermediate (**II**). Previously, we demonstrated that RDX photolysis in aqueous solution in a Rayonet photoreactor at 350 nm also produced intermediate $O_2NNHCH_2NNO_2CH_2NHCHO$, which was also attributed to the hydration of the initially formed denitrated intermediate **II** (Hawari et al., 2002). This, however, is the first report of the formation of intermediate $O_2NNHCH_2NNO_2CH_2NHCHO$ *via* the alkaline hydrolysis of RDX.

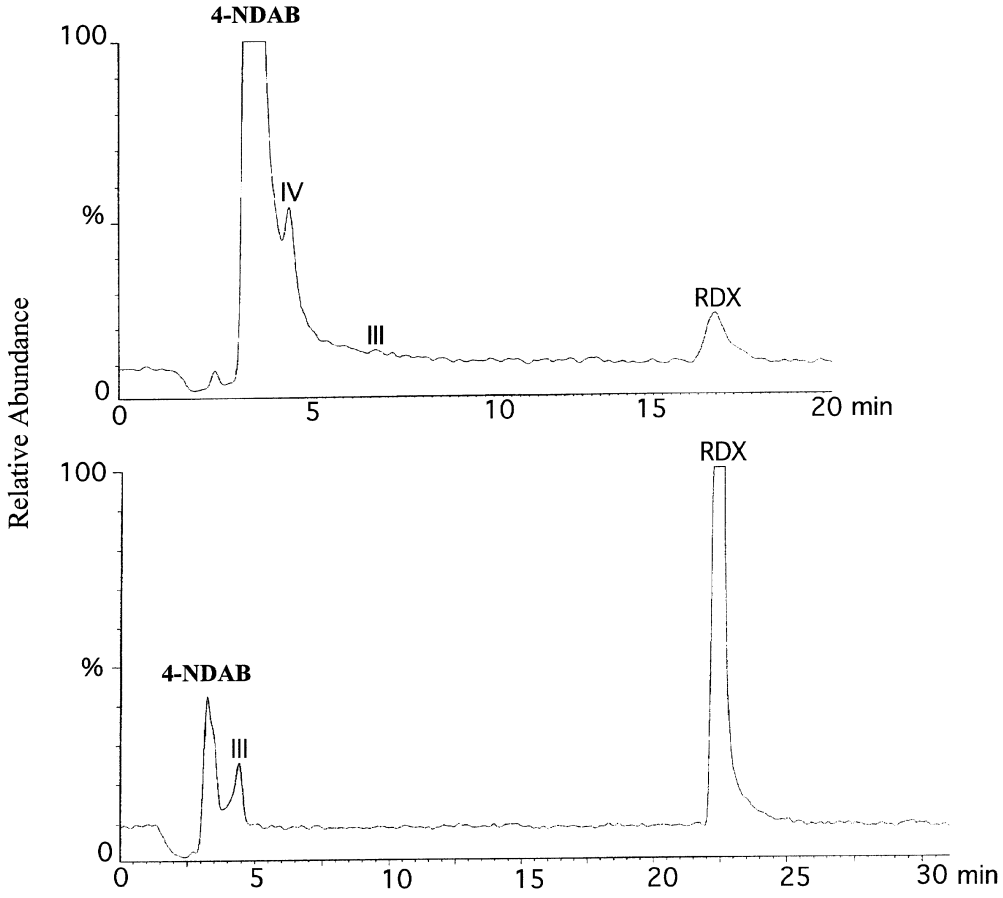

Figure 4. LC/MS chromatograms of RDX and the early intermediates formed during its degradation in acetonitrile: water (70:30 % v/v) at pH 12.3. Top: In the absence of HPβCD. Bottom: in the presence of HPβCD (3 % w/v), using a SynergiPolar-RP column (4.6 mm ID by 15 cm; Phenomenex, Torrance, Ca) at 25 ^{0}C, and eluted using a methanol:water gradient. **III**: 4,6-dinitro-2,4,6-triaza-hexanal, **IV**: 5-hydroxy-4-nitro-2,4-diaza-pentanal.

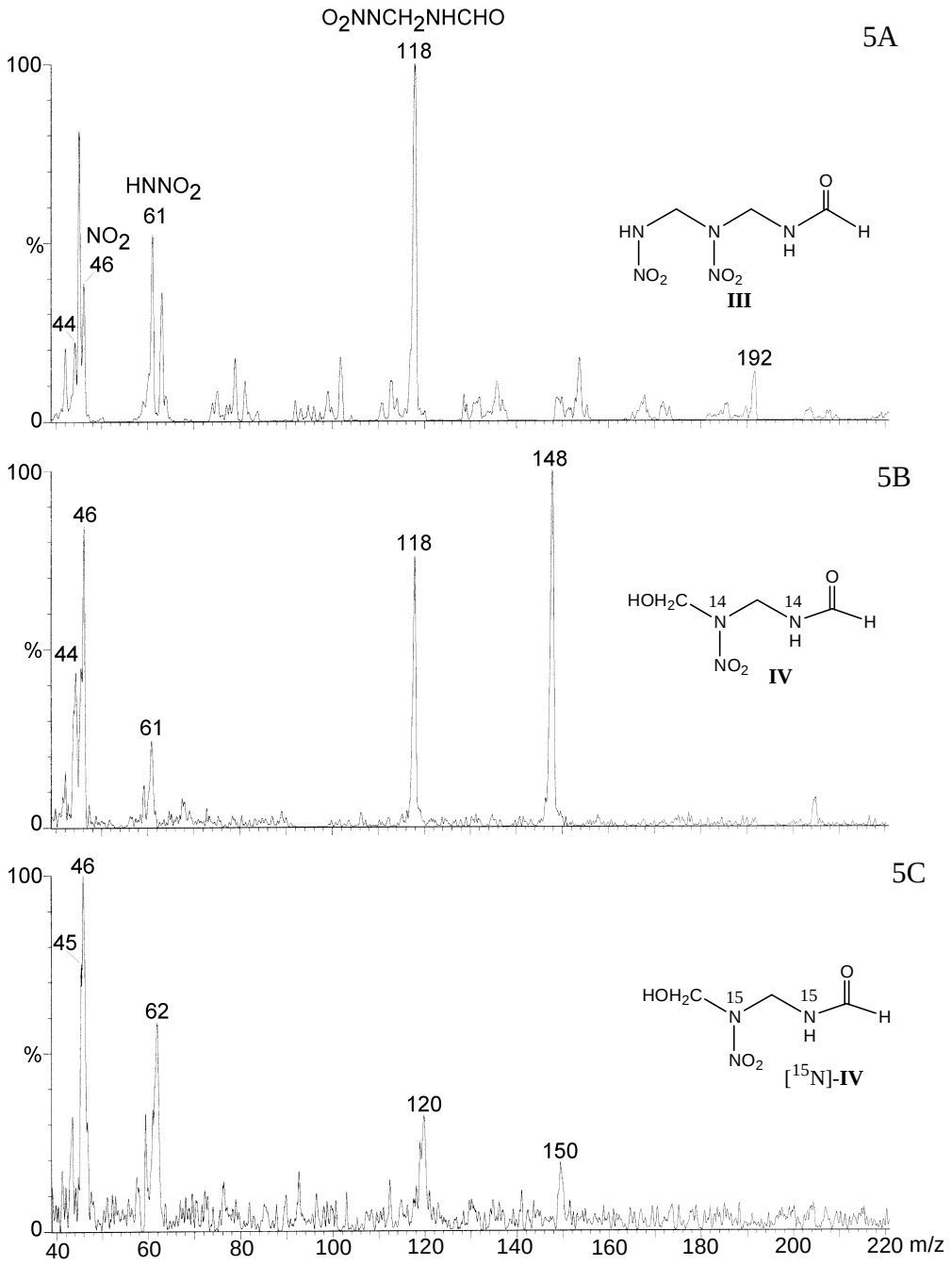

Figure 5. LC-MS (ES) mass spectra. Top: 4,6-dinitro-2,4,6-triaza-hexanal (**III**). Middle: 5-hydroxy-4-nitro-2,4-diaza-pentanal (**IV**). Bottom: ^{15}N-**IV** .

Meanwhile, the peak labeled **IV** exhibited a $[M–H]^-$ at 148 Da, matching a molecular mass formula of $C_3H_7N_3O_4$. **IV** showed three other mass ion fragments at 46, 61 and 118 Da, representing $-NO_2$, $-NHNO_2$, and the $[M-H]^-$ of O_2NNHCH_2NHCHO, respectively (Figure 5B). When ring-labeled [^{15}N]-RDX was used, the $[M-H]^-$ ion of **IV** shifted to 150 Da (Figure 5C), indicating that the intermediate contained only two of the three ring-labeled ^{15}N atoms in RDX. In addition, the [M-H] peaks that were detected at 118 and 61 Da shifted to 120 ($O_2{}^{14}N^{15}NHCH_2{}^{15}NHCHO$) and 62 Da ($-{}^{15}NH^{14}NO_2$) Da, respectively. Therefore, we suggested that the $[M-H]^-$ peak detected at 148 Da arose from the ring cleavage product 5-hydroxy-4-nitro-2,4-diaza-pentanal ($HOCH_2NNO_2CH_2NHCHO$, **IV**) that likely formed upon hydrolysis of $O_2NNHCH_2NNO_2CH_2NHCHO$ (**III**).

When we hydrolyzed RDX (1% w/v) in the presence of 3% HP-β-CD in a 65:35 (v/v) MeCN: H_2O mixture at pH 12.3, we only observed **III** and 4-NDAB (Fig 4B).

As indicated above, we used HP-β-CD during the hydrolysis of **I** to stabilize its initial denitrated intermediate (**II**) through the formation of an inclusion complex and thus facilitate its detection. Instead, it appears that the addition of HP-β-CD stabilized **III**, and allowed its unequivocal detection.

Decomposition pathways of RDX. Based on product distribution and mass balance studies (Table 1) and the critical observation that denitration was a key step responsible for degradation of cyclic nitramines we proposed a degradation pathway for RDX as shown in Figure 6. The novel input in the present study is the discovery of several ring cleavage products including **III**, **IV** and 4-NDAB (Figure 6). Although we were unable to detect the initially denitrated intermediate 3,5-dinitro-1,3,5-triazacyclohex-1-ene (**II**) due to its rapid hydrolysis in water (Hoffsommer et al., 1977), we were able to detect its hydrolyzed product **III**.

Figure 1 shows that for every mole of RDX that disappears, approximately one mole of 4-nitro-2,4-diaza-butanal (4-NDAB) is formed. However, we found that the disappearance of 0.14 μmol of RDX was accompanied by the formation of only 0.04 μmol of 4-NDAB during the first three hours, suggesting that there are intermediates *en route* to 4-NDAB. Also, both intermediates **III** and **IV** were found to contain a strong mass ion fragment at 118 Da (Figure

5) characteristic of the $[M–H]^-$ assigned to 4-NDAB, indicating that both **III** and **IV** act as precursors to the dead end product 4-NDAB.

Intermediates **III** and **IV** have different C-N bonds that are subject to hydrolytic cleavage. A plausible route for the formation of the novel intermediate observed with a $[M–H]^-$ at 148 Da (**IV**) could be *via* nucleophilic attack by OH^- at the C atom of the NH-C1 bond in **III**, accompanied by the loss of NH_2NO_2 (Figure 6).

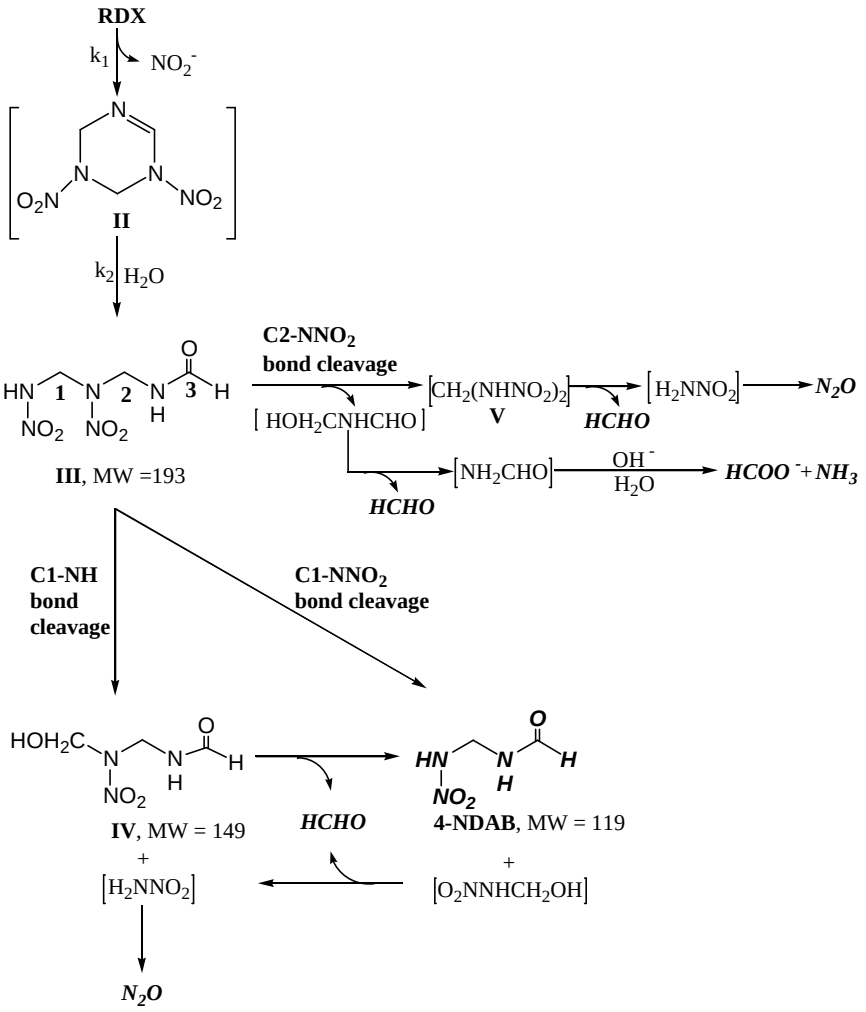

Figure 6. Major (attack at C1) and minor (attack at C2) pathways for the alkaline hydrolysis of RDX. Bracketed compounds were not observed.

IV could then decompose to form 4-NDAB and HCHO. Alternatively, cleavage of the C1-NNO_2 bond in **III** would directly give rise to 4-NDAB and hydroxymethyl nitramide, O_2NNHCH_2OH (Figure 6). However O_2NNHCH_2OH, being an α-hydroxyalkyl nitramine, is expected to be unstable in water and should thus decompose to HCHO and N_2O (Halasz et al., 2002).Finally, cleavage at the C2-NNO_2 bond in **III** would lead to the production of methylene dinitramine (**V**) and formamide, NH_2CHO (Figure 6). Although **V** was not detected, its presence cannot be excluded since it decomposes rapidly under alkaline conditions to produce HCHO and N_2O (Lamberton et al., 1949a,b).

Clearly, nucleophilic attack at the C1 position in **III** is favoured because C1, being surrounded on both sides by stronger electron-withdrawing nitramine groups, is more electrophilic than C2. Consequently, C1 is more susceptible to nucleophilic attack by OH^- than C2, explaining why attack at C2 (producing $HCOO^-$ and NH_4^+) is of only minor importance (Table 1). Interestingly, we observed **III** during both RDX photo denitration at 350 nm (Hawari et al., 2002) and the present alkaline hydrolysis, but were unable to observe **IV** prior to this work. However, the C1-NH bond cleavage that produces IV (Figure 6) is favoured only when the solution pH exceeds the nitramine pK_a of 6.55 (Arrowsmith et al., 1991), at which point nitramine can serve as a leaving group. Hence, we were able to observe intermediate **IV** during alkaline hydrolysis at pH 10 but not during photolysis at pH 5.5 (Hawari et al., 2002).

The pathway proposed previously for photodenitration (Hawari et al., 2002) is strikingly similar to the one proposed in the present study. However, in contrast to the single denitration event seen during either alkaline hydrolysis (present study) or photodenitration (Hawari et al., 2002), Fournier et al. (2002) reported the occurrence of two enzymatic denitration events en route to producing 4-NDAB. However, under extreme conditions ([NaOH] > 19 M), the occurrence of two denitration events has been reported for RDX (Hoffsommer et al., 1977).

Both MNX and HMX also hydrolyze *via* initial denitration to produce NO_2^-, followed by a ring cleavage and spontaneous decomposition to N_2O, HCHO, and 4-NDAB. These findings indicate that the mechanism postulated for the alkaline hydrolysis of RDX applies more broadly to other mono cyclic nitramine explosives. For MNX, the analogous intermediate to

III is $ONNHC^{1}H_2NNO_2C^{2}H_2NHCHO$ (4-nitro-6-nitroso-2,4,6-triaza-hexanal). Since the` C-2 position of this analog is expected to be more electrophilic than the C-2 position in **III** itself, it becomes more amenable for nucleophilic substitution by OH^-. As a result, the minor pathway producing NH_3 and $HCOO^-$ is of somewhat more importance with MNX than it is for RDX (see Table 1 for product distribution).

In conclusion, the present results confirm the hypothesis that a successful initial (primary) attack, denitration in this case, is detrimental in the degradation of monocyclic nitramines. Once denitration occurs, ring cleavage becomes spontaneous and is dictated by the chemistry of the ensuing intermediates in water. The similarities observed in the decomposition patterns of cyclic nitramines under various chemical (present study), photochemical (Hawari et al., 2002) and biochemical (Fournier et al., 2002) conditions suggest that the employment of a more rapid chemical denitration process might serve as a useful probe into the early stages of the enzymatic and microbial mechanisms responsible for their decomposition.

V.6 Biodegradation of RDX and HMX in soil

Knowledge of the products and transformation pathways from the anaerobic and aerobic biodegradation of RDX and HMX in liquid culture has provided us with information that is necessary in the design of effective remediation technologies. However, it is also necessary to assess the transformation, microbial degradation, and immobilization behavior of the two energetic chemicals in soil to assess the effectiveness of soil bioremediation. Therefore, the objective of the present study was first to determine the sorption-desorption behavior and the long-term fate of RDX and HMX in sterile and non-sterile soils and second to determine the effect of sorption on mineralization kinetics.

V.6.1 The Fate of the Cyclic Nitramine Explosives RDX and HMX in Natural Soil.

- Sheremata, T.W., A. Halasz, L. Paquet, S. Thiboutot, G. Ampleman, and J. Hawari. **2001**. The fate of the cyclic nitramine explosive RDX in natural soil. *Environ. Sci. Technol*. 35:1037-1040.
- Monteil-Rivera, F., C. Groom, and J. Hawari. **2003.** Sorption and Degradation of Octahydro-1,3,5,7-tetranitro-1,3,5,7-tetrazocine (HMX) in soil. *Environ. Sci. Technol*. 37: 3878-3884.

Sorption and Degradation of RDX in Soil. In a previous study we determined the sorption-desorption behaviour and long-term fate of RDX in natural soil in sterilized and non-sterilized topsoil (Sheremata et al., 2001). Results of this study indicate that although RDX is not extensively sorbed by the topsoil (K_d^s of 0.83 L/kg), sorption is nearly irreversible. Furthermore, there was no difference in the sorption behaviour for sterile and non-sterile topsoil. However, over the long-term, RDX completely disappeared within 5 weeks in non-sterile topsoil, and MNX, DNX, and TNX metabolites formed in the aqueous phase. Over the same period, recovery of RDX from sterile topsoil was high (55-99 %), and the nitroso metabolites were not detected. Only traces of RDX were mineralized to CO_2 and N_2O by the indigenous microorganisms in non-sterile topsoil. Of the RDX that was mineralized to N_2O, one N originated from the ring and the other from the nitro group substituent, as determined using N^{15} ring-labeled RDX. However, N_2O and CO_2 from RDX represented only 3 % of the total N_2O that formed from the process of nitrification/denitrification.

In contrast to biodegradation in liquid cultures, attempts to identify other ring cleavage products or metabolites by LC-MS were not successful. The absence of extensive mineralization in the present system may be due to the adsorption of ring cleavage products by soil, or binding with dissolved organic matter (Sheremata et al., 2001). The topsoil contained 8.4 % organic carbon, and the presence of dissolved organic matter was visible. Binding of organic contaminants by such solid soil particles and possibly by dissolved organic matter is known to reduce the availability of organic contaminants to microorganisms for biodegradation in soil (Apajalahti and Salkinoja-Salonen, 1984; Ogram et al., 1985.).

To further investigate this possibility, the radioactivity in the aqueous phase was measured at the end of the [^{14}C]-RDX mineralization experiments. Results indicate that although RDX had disappeared, and the nitroso metabolites were no longer present, 1.93 % (± 0.59) of radioactivity was recovered as $^{14}CO_2$ and 53.06 % (± 2.47) of the radioactivity was recovered from the aqueous phase. Therefore, by difference, approximately 45 % of the radioactivity partitioned with the solid-sorbed phase. Such partitioning may have rendered the sorbed phase as unavailable to the indigenous microorganisms for mineralization. However, at this point, the chemical structures of the breakdown products in the aqueous and solid-sorbed phases remain unknown. Based on the results of the present study, in contrast to what we observed in liquid culture (Hawari et al., 2000a, Sheremata and Hawari, 2000), N_2O formation in topsoil is slow and the yield is small.

Sorption and Degradation of HMX in Soil. Recently, soil samples were characterized from a NATO anti-tank firing range at Wainwright, Alberta (Groom et al., 2002), where past and present practices involve the extensive use of ammunitions containing the melt-cast explosive Octol. Although the latter is composed of HMX (70 wt. %), TNT (30 wt. %) and RDX (<1 wt. %) (Table 1), only HMX was detected as the principal soil contaminant. Similar observations were obtained at anti-tank firing ranges at Valcartier, Quebec (Dubé et al., 1999) and Ford Ord, California (Jenkins et al., 1998). The pattern of HMX distribution was similar at all three sites, as HMX concentrations were found to decrease greatly with distance from the targets, and to be confined to depths of 15 cm or less from the soil surface. Pennington et al. (2001) also observed that in field samples HMX persists in surface soil where oxygen is available, but is not typically observed in deep aquifers where an anaerobic environment is expected to prevail.

Although the water solubility of HMX is low (5 mg/L at 25 °C) as compared to that of TNT and RDX (145 and 60 mg/L, respectively, Talmage et al., 1999), HMX could migrate through subsurface soil and cause groundwater contamination. In this context, the extent and the reversibility of HMX sorption onto soil, and its ability to undergo (bio)transformation will be major factors determining the fate of HMX in natural environments. HMX was shown to

biodegrade only under anaerobic conditions in culture media (Adrian and Lowder, 1999), sludge (Hawari et al., 2001) and soil bioslurry amended with anaerobic sludge (Shen et al., 2000).

Table 1: Physico-chemical properties[a] of TNT, RDX, and HMX.

Name	TNT	RDX	HMX
Formula	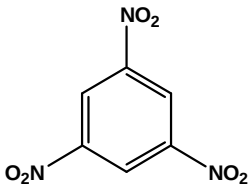	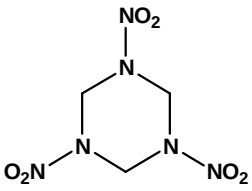	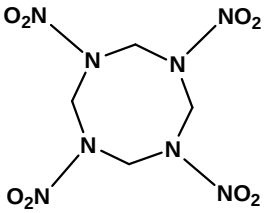
Log K_{ow}	1.6, 2.2, 2.7	0.87 (0.90)	0.13 (0.16)
Water Solubility at 20° C (mg L^{-1})	130	42.3 (42.6)	6.6 (3.3)
Vapor Pressure at 25 °C (mm Hg)	1.99×10^{-4}	4.03×10^{-9}	3.33×10^{-14}

[a] data from ref. (Hawari and Halasz, 2000,) and references cited therein; Values between brackets are from the present study.

Limited research has been conducted on HMX sorption in soil. Leggett studied the sorption of RDX and HMX on bentonite drilling muds in batch experiments and found that the sorption of both explosives was linear (Legget, 1985). The samples used in the above study consisted mainly of montmorillonite and no mention was made concerning the presence of organic matter. Myers et al. studied the sorption of HMX in soil column experiments and observed some HMX disappearance in the column effluents that was tentatively attributed to reductive transformation (Myers et al., 1996). No further details on sorption mechanisms were given. Recently, Brannon *et al.* studied the effects of changing the composition of simulated groundwater on adsorption of TNT, RDX, and HMX in low carbon aquifer soils (Brannon et al., 2002), and found that modifying the soil cation did not affect significantly the adsorption of HMX.

The fate of HMX in soil as determined by sorption and degradation is still inadequately

characterized. The objective of the present study was therefore to determine the sorption-desorption behavior and the disappearance of HMX in sterile and non-sterile soils. Two soils were investigated: i) an agricultural topsoil taken from Varennes, Quebec, which has been used earlier to determine the fate of TNT (Sheremata et al., 1999) and RDX (Sheremata et al., 2001); ii) a Sassafras sandy loam sampled at the Aberdeen Proving Ground, MD. Knowing the sorption-desorption behavior and the long-term fate of HMX in soil will help assess the effectiveness of natural attenuation for HMX removal. Also it will provide insight as to why only HMX persisted close to the soil surface (Jenkins et al., 1998) and accumulated in plant leaf tissues (Groom et al., 2002), at sites initially contaminated with TNT, RDX and HMX.

Experimental Section

Soils. We use two well-characterized soils in this study: an agricultural topsoil that has previously been used in sorption studies involving RDX and TNT and a sandy loam. The agricultural topsoil originated from Varennes, Quebec, Canada, while the sandy soil was sampled at the Aberdeen Proving Ground, MD. In the present study they will be referred to as VT (for Varennes Topsoil) and SSL (for Sassafras Sandy Loam), respectively. Properties of both soils are summarized in Table 2. Soil sterilization was accomplished by gamma irradiation from a cobalt-60 source at the Canadian Irradiation Center (Laval, Quebec) (Sheremata et al., 2001).

Table 2: Properties of soils used for sorption of HMX

Soil	Particle size distribution			Total Org. C (%)	pH	CEC[a] (mequiv./100g)
	% Clay (< 2 μm)	% Silt (2-53 μm)	% Sand (> 53 μm)			
VT	4	12	83	8.4	5.6	14.6
SSL	11	18	71	0.33	5.5	4.3

[a] CEC = Cationic Exchange Capacity.

General Sorption/Desorption Procedure. Batch sorption experiments were conducted at room temperature. A volume of HMX solution (15 mL) was added to 2 g of dried (left in desiccator until mass remains constant) soil in 16 mL borosilicate centrifuge

tubes fitted with Teflon coated screw caps, without degassing. The tubes were wrapped in aluminum foil and agitated on a Wrist Action® shaker (Burrell Corp., Pittsburgh, PA) for the desired contact time. They were then centrifuged for 30 min at 3500 rpm, and the supernatant was filtered through a Millex-HV 0.45 μm filter (Millipore Corp., Bedford, MA). The filtrate collected after discarding the first 3 mL was analyzed by HPLC, as described below.

Desorption experiments were conducted by adding 15 mL of distilled water to the pellet remaining in the tube after removing the supernatant, and agitating the suspensions for the required contact times. Samples were then centrifuged, filtered and analyzed as described for sorption experiments. The solution volume that remained with the soil at the end of sorption was estimated gravimetrically and corrections were made to take into account the amount of HMX present in this volume. In order to estimate the amount of HMX losses during the sorption and desorption experiments, sorbed HMX was extracted with CH_3CN from the solid recovered after sorption or desorption as described in the EPA SW-846 Method 8330 (EPA 1997). A percent recovery was then calculated.

Sorption Kinetics. Sorption kinetics experiments were carried out for both soils according to the above procedure. An aqueous stock solution of HMX (3 mg/L) was prepared by weighing the adequate amount of HMX and dissolving it in water. The solution was then contacted with soil over a period ranging from 1 h to 7 days. Resazurin was added under a CO_2 blanket to test for the presence of oxygen after 1 week of contact time. Triplicate experiments were performed for each contact time.

Desorption Kinetics. The soil was first contacted with a 3 mg/L HMX solution for 60 h. After centrifugation, the supernatant was removed and the pellet was contacted with 15 mL of fresh water during periods varying from 1 h to 7 days. Controls (n=3) containing an aqueous solution of HMX (3 mg L^{-1}) and no soil were allowed to shake from the beginning of sorption to the end of the longer desorption time. Recoveries of 100 % were obtained, demonstrating the absence of HMX degradation or adsorption to the container material (glass or Teflon) during sorption-desorption cycles.

Sorption/Desorption isotherms. Aqueous HMX solutions were prepared (*via* dilutions) from a saturated aqueous solution that has been filtered, to give initial HMX concentrations ranging from 0.5 to 4 mg/L. Sorption experiments were conducted over a period of 60 h, with 6 replicates for each concentration. Three of the 6 samples were extracted with acetonitrile while the three remaining samples were subjected to desorption in water (40 h). After desorption, samples were extracted with acetonitrile.

Long-term Fate. The long-term fate of HMX was monitored in sterile and non-sterile VT soil. A sterile aqueous solution (15 mL) of HMX (1.39 mg/L) was combined with 2 g of either sterile or non-sterile VT soil, in 16-mL vials keeping an empty headspace volume of 0.5 mL. The vials were kept statically, away from light at room temperature for 16 weeks. A sufficient number of vials were prepared to allow for sacrificial sampling. Soil suspensions were centrifuged and the resulting soil pellets were subjected to acetonitrile extraction. The supernatant aqueous phases and acetonitrile soil extracts were then analyzed for HMX, as described below. At termination of the study, sterile and non-sterile tubes were augmented with resazurin to test for the presence of oxygen.

HMX degradation products. Experiments to identify the degradation products of HMX in topsoil (VT) were performed with 1.28 µmol HMX per sample. Stock acetone solutions of HMX were added in 20 mL headspace vials and solvent was evaporated under aseptic conditions. The vials were then filled with 1 g of sterile or non-sterile VT soil and 7.5 mL of sterile deionized water before crimping with Teflon coated rubber septa. The vials were then sparged with argon for 20 minutes and incubated away from light at 37°C. After 35 weeks, the samples were sacrificed. The liquid and solid fractions were analyzed for HMX and possible metabolites. Mineralization experiments were performed at 35 °C in 120 mL serum bottles containing 3 g of VT soil and 15 mL of aqueous solutions of HMX (1.0 mg) spiked with UL-[^{14}C]-HMX (0.033 µCi). Liberated $^{14}CO_2$ was collected in KOH traps and measured as described in Sheremata et al. (2001).

HMX concentrations were determined by HPLC equipped with a photodiode array (PDA) detector as described in Hawari et al. (2001). Log K_{ow} values were measured for HMX and RDX using the Flask-shaking method as described in the OECD guideline 107 (OECD

1981). Solubility in water for both compounds was determined by stirring an excess amount of solid explosive in water at 20°C according to the procedure described in Lynch et al. (2001). A Micromass LC/MS was used to analyze HMX, its nitroso-derivatives and ring cleavage products such as methylene dinitramine. Analyte ionization was done in a negative electrospray ionization mode producing mainly the deprotonated molecular mass ions $[M - H]^-$. The instrumental operating conditions are reported elsewhere (Hawari et al., 2001, Halasz et al., 2002).

Results and Discussion

Sorption/Desorption kinetics. The minimum time required to reach sorption and desorption equilibrium for both VT and SSL soil is shown in Figures 1a and 1b, respectively. The results indicated that HMX retention was rapid and appeared to reach equilibrium within approximately 1 day. Likewise, the desorption of HMX in water was rapid and showed little time dependence after 1 day of contact time. Analogous results were obtained with SSL soil (results not shown). To our knowledge, no data have been reported on the sorption kinetics for HMX, but for RDX, a rapid sorption was reported to occur in less than 24 h for different soils (Myers et al., 1996; Sheremata et al., 2001; Xue et al., 1995; Singh et al., 1998). Analysis of the acetonitrile extracts of both soils led to recoveries higher than 96 %, indicating that no significant HMX transformation occurred during the time frame of the present experiments. The addition of resazurin after 1 week of contact time indicated that oxygen was still present in the samples.

Sorption/desorption mechanisms. The isotherms of the sorption and desorption of HMX in soils are presented in Figures 2 and 3 for VT and SSL soils, respectively. Sorption was measured after 60 h of contact time, while desorption was measured after contacting the sorbed solid with fresh water for 40 h. It is common to estimate the amount of sorbed contaminants by difference from the aqueous concentration, but in the case where contaminants are partially degraded this can lead to an overestimation of the adsorbed fraction. We thus analyzed HMX in both the aqueous phase and the sorbed soil and used data to construct the sorption isotherms presented in Figures 2 and 3.

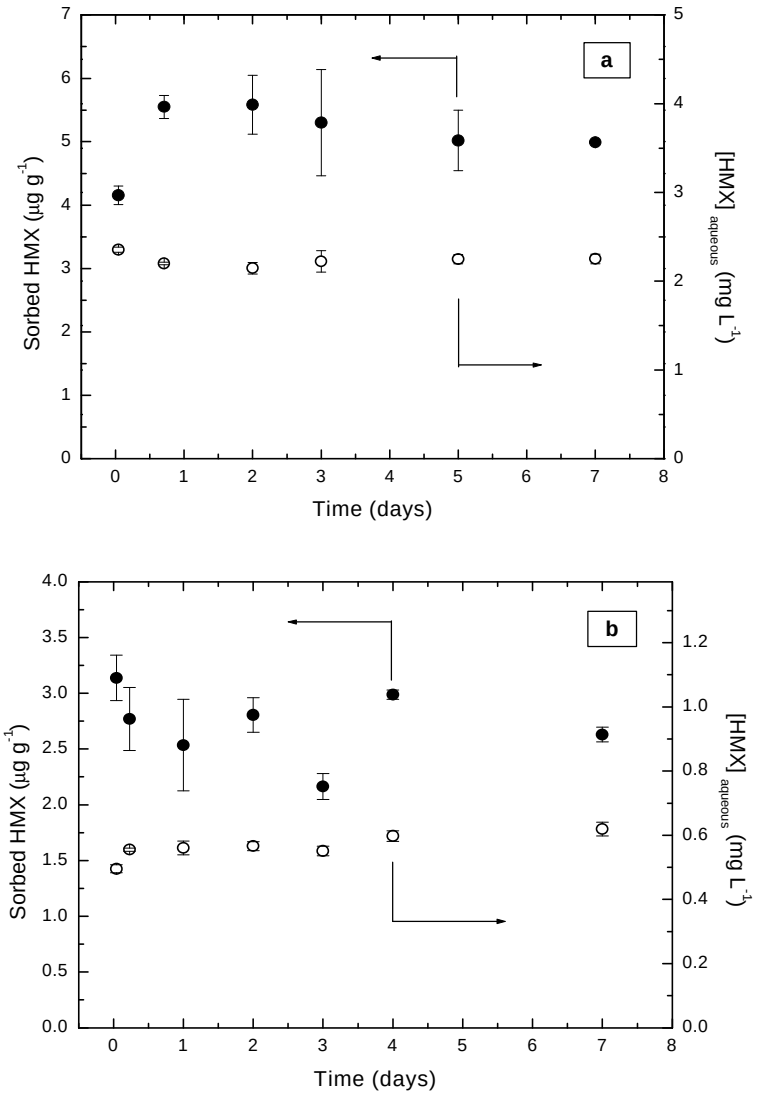

Figure 1: Kinetics results for sorption (a) and desorption (b) of HMX on VT soil (○, sorbed HMX determined by extraction from the solid; ○, aqueous concentration of HMX; error bars represent standard deviations of 3 replicates).

Linear, Freundlich, or Langmuir equations are frequently used to describe the distribution of solute at equilibrium. Based on visual observation of the experimental data obtained for HMX, the isotherms appear to follow a linear trend. Legget also reported linear sorption of

RDX and HMX onto drilling muds (Leggett, 1985), and Townsend *et al.* found that RDX and HMX column elution curves could be adequately described using a linear equilibrium model (Townsend et al., 1996). The linear equation [1] was thus used to describe the equilibrium sorption and desorption of HMX in soil:

$$\frac{x}{m} = K_d C \qquad [1]$$

where *x/m* is the mass of solute sorbed per unit mass of dried soil at equilibrium (μg g^{-1}), K_d is the distribution coefficient (L kg^{-1}) and *C* is the aqueous equilibrium phase solute concentration (mg L^{-1}). The distribution coefficient for sorption will be denoted as K_d^S, while for desorption it will be denoted as K_d^D. The K_d^S and K_d^D values for HMX are reported for both soils in Table 3, along with the corresponding K_{oc} (= K_d^S/f_{oc}, where f_{oc} corresponds to the weight fraction of organic carbon).

Table 3: Sorption and desorption distribution coefficients for HMX and sterile and non-sterile VT and SSL soils.

Parameters	VT	Sterile VT	SSL	Sterile SSL
K_d^S (L/kg)	2.47	2.52	0.67	0.69
r^2	0.983	0.964	0.992	0.960
K_d^D (L/kg)	5.04	4.50	0.615	n.d.[a]
r^2	0.966	0.936	0.876	n.d.[a]
log K_{oc} [b]	1.47	1.48	2.31	2.32

[a] n.d.: Non determined; [b] based on measured K_d^S values and f_{oc} = 0.084 and 0.0033 for VT and SSL, respectively.

The linearity of the adsorption isotherm implies that HMX binding to soil is not strongly concentration-dependent, suggesting that HMX is adsorbed onto soil mainly by non-specific interactions. However, only a narrow concentration range could be used, as a result of the low solubility of HMX in water (3.3 mg/L at 20°C). At low surface coverage, linear isotherms have also been observed for nitroaromatic compounds whose adsorption isotherms are usually curved and converge to a saturation level (Haderlein et al., 1996).

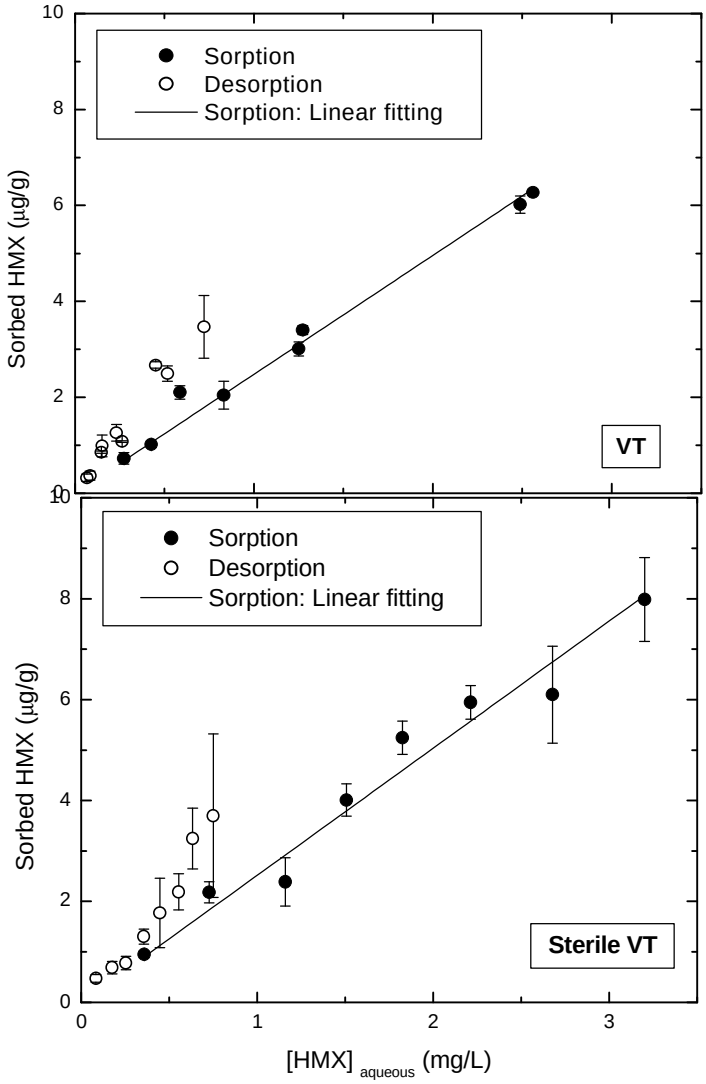

Figure 2: Sorption and desorption isotherms of HMX on sterile and non-sterile VT soil (Error bars represent the standard deviation of 3 replicates; fitting parameters are given in Table 3).

Therefore, specific interactions between HMX and soils are not excluded. Desorption experiments were thus performed using both VT and SSL soils to provide more insight into the strength of HMX binding onto the soil matrix. Data obtained using VT soil (K_d^D = 4.5 – 5.0 L kg^{-1} > K_d^S = 2.5 L kg^{-1}) (Figure 2) clearly indicate a sorption-desorption hysteresis, which implies the occurrence of specific interactions between HMX and VT soil.

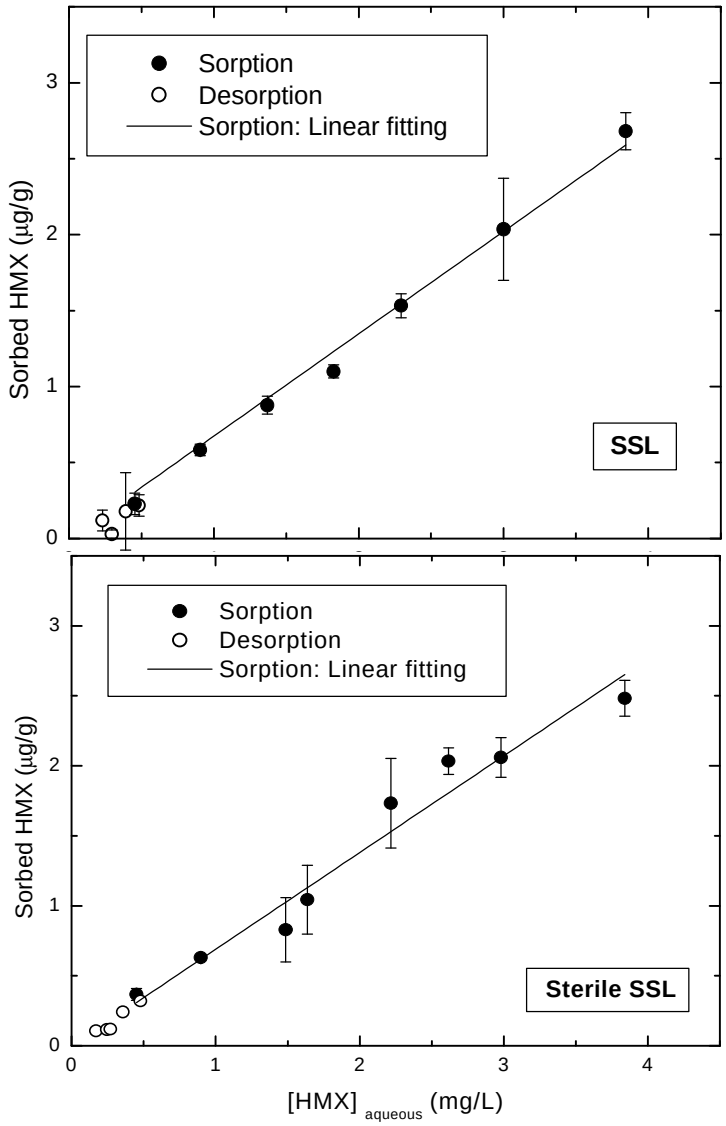

Figure 3: Sorption and desorption isotherms of HMX on sterile and non-sterile SSL soil (Error bars represent the standard deviation of 3 replicates; fitting parameters are given in Table 3).

As for SSL soil (Figure 3), the low extent of sorption led to desorption data points that are all gathered at the bottom left of the isotherm, making it difficult to determine the reversibility of HMX sorption.

The hysteresis observed with VT soil is not due to the formation of covalent bonds between HMX and the organic matter present in the soil since the nitramine was fully recovered when extracting the sorbed matrix with acetonitrile.

Table 4 gives a comparison of sorption parameters for TNT, RDX and HMX obtained by our group and by others (Leggett, 1985; Brannon et al., 2002; Sheremata et al., 1999, 2001). Several trends appear from this table that can also be seen in Figure 4: i) the sorption distribution coefficients K_d^S for HMX are slightly higher than those for RDX, but significantly lower than those of TNT for the same soil; ii) the percentage of organic matter does not govern the sorption of HMX and iii) HMX sorption grows exponentially with the amount of clay.

Table 4: K_d^S values obtained when sorbing TNT, RDX, and HMX onto different matrices.

Soil	Sand %	Silt %	Clay %	TOC[a] %	K_d^S		
					TNT	RDX	HMX
LAAP A[b]	89	5	6	0.31	26	-	1
LAAP C[b]	77	11	12	0.08	64	0.3	-
LAAP D[b]	27	41	32	0.20	167	0.7	2
Montmorillonite[b]	n.a.[c]	n.a.[c]	n.a.[c]	n.d.[d]	416	3.2	22.5
Aqua-Gel[e]	>5		> 87	n.d.[d]	131	6.6	8.0
VT	83	12	4	8.4	4.2[f]	1.9[g]	2.5[h]
SSL	71	18	11	0.33	-	-	0.7[h]

[a] Total Organic Carbon in wt. %; [b] data from ref. (16): LAAP = Louisiana Army Ammunition Plant; K_d^S values obtained with montmorillonite saturated with K^+; [c] n.a. = Not applicable; [d] n.d. = Not determined; [e] data from ref. Leggett (1985); [f] data from ref. Sheremata et al. (1999); [g] data from ref. (Sheremata et al. (2001); [h] data from the present study.

The higher K_d^S values obtained for TNT are consistent with the non-linear shape observed for its sorption isotherms (Leggett, 1985; Haderlein et al;, 1996; Townsend et al., 1996). TNT is a nitroaromatic compound that can interact with soil through the formation of electron-donor acceptor complex between the oxygen atoms present at the mineral surface (e^- donor) and the π–system of the electronic ring in TNT (e^- acceptor) (Haderlein et al., 1996). Also, TNT can transform quite readily under both abiotic and biotic conditions, leading to the formation of amines, which can irreversibly bind onto soil through amide linkages (Bruns-Nagel et al.,

2000) or be intercalated between negative clay plates by cationic exchange when protonated.

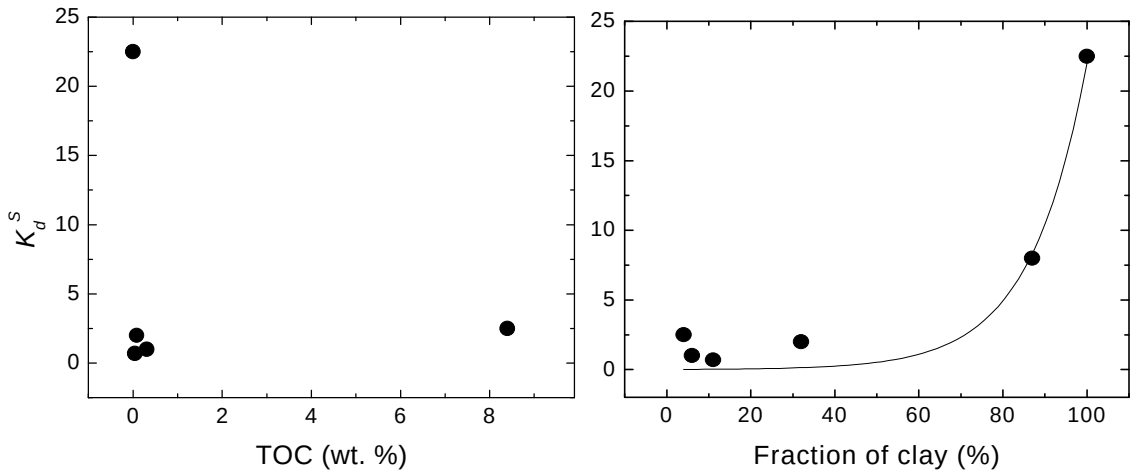

Figure 4: Effect of TOC and clay content on HMX sorption on soils (data from Boopathy, 2001; Myers et al., 1996; and from the present study).

This last assumption is consistent with the good correlation observed between TNT K_d^S values and Cation Exchange Capacities (Brannon et al., 2002) or pH (Sheremata et al., 1999). Such interactions cannot exist with RDX and HMX because cyclic nitramines are non-aromatic (no π–system) and do not form stable amine (-NH_2) derivatives. However, as seen in Figure 4, the presence of clay in the soil plays a significant role in the sorption of HMX. Hydrogen bonds between surface hydroxyl groups in soil and nitro groups of nitramines have been reported as a possible sorption mechanism (Leggett, 1985). The higher K_d^S values obtained for HMX, which contains one extra -NO_2 group, as compared to that obtained with RDX, and the positive effect of clay both support the possible interaction of -NO_2 groups with hydroxyl surface groups of clay.

The absence of correlation between the TOC and HMX K_d^S values (Figure 4) shows that organic carbon does not govern HMX sorption, as substantiated also by the different K_{oc} values calculated from sorption of HMX on VT and SSL soils (Table 3). Moreover, the relative K_{ow} values for RDX and HMX (Table 1) fail to explain the difference of sorption between both compounds (K_d^S (HMX) > K_d^S (RDX)), thus reinforcing the limited role of hydrophobicity on HMX sorption to soils. Pennington and Brannon reported that in contrast

to TNT, only small amounts of RDX were actually associated with soil organic matter (Pennington and Brannon, 2002).

Finally, data shown in Figures 2 and 3 and the corresponding K_d values reported in Table 3 indicate that there is no difference in the sorption-desorption behavior of HMX using sterile or non-sterile soils. Also more than 96 % recoveries were measured for HMX, indicating the absence of biotic or abiotic losses of the chemical within the time course of sorption/desorption cycles (1 wk in total).

Long-term Fate. The fate of HMX in sterile and non-sterile topsoil systems was subsequently studied in static experiments over a period of 16 wks. Following the first 3 weeks, almost all HMX was recovered from both sterile and non-sterile systems (Figure 5a). After 16 weeks, the percentage of HMX recovery for sterile and non-sterile soils was 95 % and 40 %, respectively, indicating the occurrence of biotransformation in the later case. The addition of resazurin at the end of the experiment confirmed the presence of an anaerobic environment in the soil samples. RDX was also found to degrade in non-sterile VT soil but at a much faster rate since total disappearance was observed after 4 wks (Sheremata et al., 2001).

The K_d^S values were determined for each time interval of the fate study (Figure 5b). K_d^S values measured with sterile and non-sterile soils were in agreement with each other during the first three weeks but past this time, K_d^S values became higher with non-sterile soil. HMX sorption/desorption on VT soil is faster than its biotransformation, therefore if sorption was fully reversible, K_d^S values would remain unchanged whatever the total amount of HMX in the medium. The increase in K_d^S when using non-sterile VT soil supports the occurrence of hysteresis with this soil and suggests that biotransformation takes place in the aqueous phase. LC/MS analysis of separate experiments containing a higher concentration of HMX (1.38 μmol / 7.5 mL) with non-sterile VT soil showed after 35 wks the disappearance of HMX and the formation of the four nitroso-derivatives octahydro-1-nitroso-3,5,7-trinitro-1,3,5,7-tetrazocine (**2**), octahydro-1,5-dinitroso-3,7-dinitro-1,3,5,7-tetrazocine (**3**), octahydro-1,3,5-trinitroso-7-nitro-1,3,5,7-tetrazocine (**4**) and octahydro-1,3,5,7-tetranitroso-1,3,5,7-tetrazocine (**5**) (Figure 6).

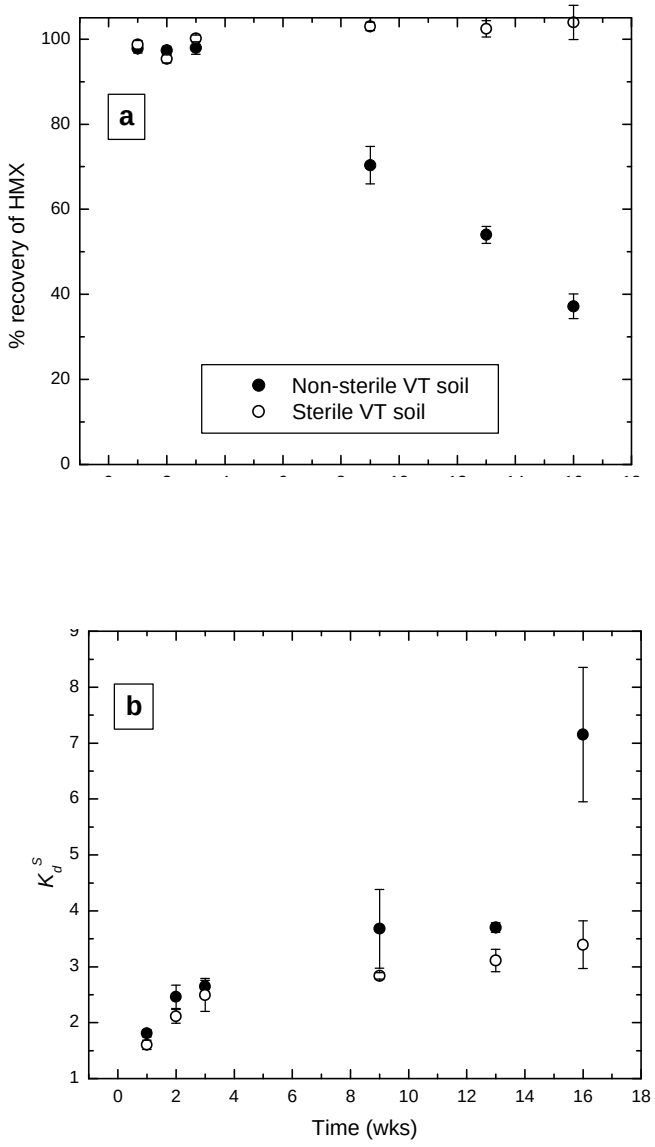

Figure 5: Long-term static sorption experiments on sterile (open circles) and non-sterile (solid circle) VT soil (Error bars represent the standard deviation of 3 replicates): (a) total HMX recovered from the aqueous and soil-sorbed phases; (b) K_d^S values.

The transformation of HMX to its corresponding nitroso-derivatives at contaminated sites has also been reported (Spanggord et al., 1985). We were unable to detect the ring cleavage product, methylenedinitramine, that has been previously observed in sludge (Hawari et al., 2001). However, when methylenedinitramine was added to a VT soil slurry, it disappeared

rapidly to form N_2O and HCHO, demonstrating that methylenedinitramine cannot be used as a marker to follow the fate of nitramines in soil. At the end of the mineralization experiment, which lasted 35 wks, we obtained 14 % mineralization (evolved $^{14}CO_2$). The remaining radioactivity was found in soil (15 %) and in the aqueous phase (63 %) accounting for a carbon balance of 92 %.

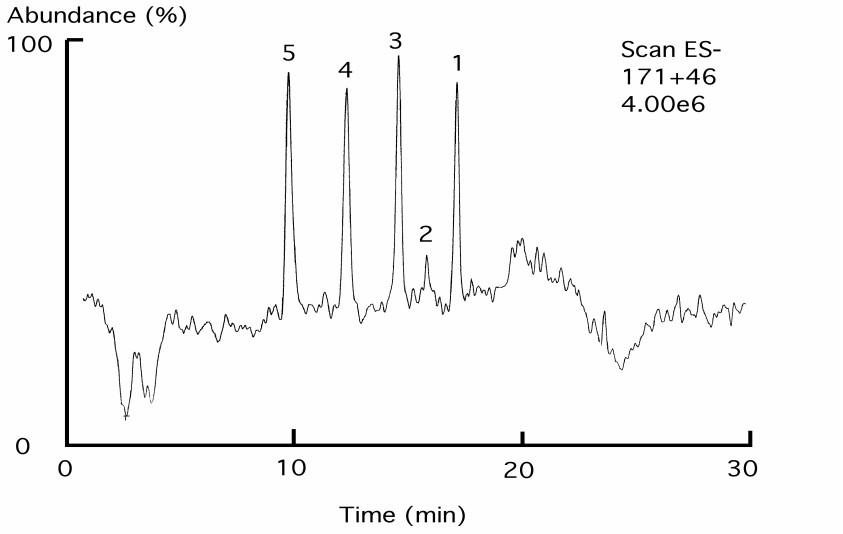

Figure 6: LC-MS chromatogram (negative electrospray ionization; extracted ions m/z 171 and 46) for supernatant of non-sterile VT soil microcosm after 35 weeks at 37°C. The numerated peaks correspond to **1**: Octahydro-1,3,5,7-tetranitro-1,3,5,7-tetrazocine, **2**: Octahydro-1-nitroso-3,5,7-trinitro-1,3,5,7-tetrazocine, **3**: Octahydro-1,5-dinitroso-3,7-dinitro-1,3,5,7-tetrazocine, **4**: Octahydro-1,3,5-trinitroso-7-nitro-1,3,5,7-tetrazocine, **5**: Octahydro-1,3,5,7-tetranitroso-1,3,5,7-tetrazocine.

The results of the present data suggest that HMX will persist at active anti-tank firing ranges, as its low volatility (Hawari and Halasz, 2000), low aqueous solubility (Talmage et al., 1999), and slow (bio)chemical reactivity in aerobic environments (Hawari et Halasz, 2000) do not allow for natural attenuation to effectively compete with constant soil loading. However, at abandoned sites, the compound's poor soil affinity (K_d^S 0.7-2.5 L kg^{-1}, Table 3) will permit its slow migration to subsurface soil where anaerobic conditions prevail thus allowing anaerobic degradation to take place. HMX degradation should proceed through the formation of

nitroso-derivatives and be accompanied by partial mineralization. These experimental findings are promising for the natural attenuation of HMX at contaminated sites.

Fate of the two key intermediates methylenedinitramine and 4-nitro-2,4-diazabutanal in soil. Methylenedinitramine (MEDINA) and 4-nitro-2,4-diazabutanal (NDAB) were previously identified as ring cleavage products of both RDX and HMX during biodegradation (Halasz et al., 2002; Hawari et al., 2001; Fournier et al., 2002; Bushan et al., 2003a). MEDINA is known to undergo rapid abiotic hydrolysis with the production of nitrous oxide (N_2O). The aqueous concentrations of methylenedinitramine and the production of N_2O were monitored in agitated aseptic methylenedinitramine solutions with and without topsoil to detect the inhibition of hydrolysis by soil components. Under both conditions methylenedinitramine was observed to degrade rapidly, with equivalent rates of N_2O production for samples with or without soil. Methylenedinitramine was also not detected in soil extracts. The results suggest that methylenedinitramine does not interact with topsoil and hydrolyzes rapidly in solution. In contrast 4-nitro-2,4-diazabutanal is very soluble in water and does not hydrolyze. Instead it was found to poorly sorb onto soil and water was sufficient to mobilize the chemical towards migration. Interestingly, analysis of soil samples collected from a contaminated area showed the presence of NDAB, thus providing the first experimental evidence for the occurrence of natural attenuation.

V.6.2 Anaerobic Degradation of RDX and HMX in Soil by Indigenous Bacteria.

We found that regardless of the growth conditions, all tested soil microcosms (Table 1) displayed an average two day lag period before any disappearance of RDX or HMX was observed. The rate of RDX disappearance was found to be most rapid in the presence of glucose or nutrient broth (NB) (Table 2). The disappearance of RDX was accompanied by the formation of MNX, DNX and TNX as shown in Fig. 1. Likewise HMX degraded and lead to the formation of its four nitroso derivatives (H1-4, Fig 2). Only traces of N_2O were detected when no extraneous degraders, apart from indigenous degraders, were used.

Table 1: Anaerobic soil slurry microcosms for the degradation of cyclic nitramins RDX (1035 mg/kg) and HMX (385 mg/kg) at 37^{o}C.

	Soil and Water		Soil and 0.2% Glucose	
Day	E_h (mV)	pH	E_h (mV)	pH
0	235	7,01	249	7,07
2	-146	6,68	-361	5,82
3	-89	6,72	-182	6,03
7	-87	6,65	-140	6,24
9	-54	6,65	-106	6,09

RDX disappearance was more rapid than HMX and the transformation of HMX appeared to have only commenced after near complete removal of RDX.

In general we found that TNX (from RDX) is less reactive than its lower nitroso counterparts MNX and DNX (Fig 2 E). However, after 16 days of incubation all the nitroso derivatives of RDX disappeared and only the tetra isomer of HMX remained undegraded until 27 days. Interestingly, the redox potential (E_h) dropped from 235 mV to low negative values during degradation, although much variation in E_h was noted in microcosms supplemented with glucose (Table 1). The pH also seemed to turn slightly acidic during degradation (Table 1).

Table 2. Biodegradation of RDX (1075 mg/kg) and HMX (385 mg/kg) in soil slurry (20% w/v) after 5 days of incubation at 37°C with anaerobic sludge.

Additives	RDX remained (%)	HMX remained (%)
N/A	26.7	100.0
2 g/l Glucose w/o sludge	17.6	47.7
8 g/l Nutrient Broth (NB) w/o sludge	7.5	24.4
2 g/l Glucose with Sludge	8.6	32.9
8 g/l NB with Sludge	8.0	30.3

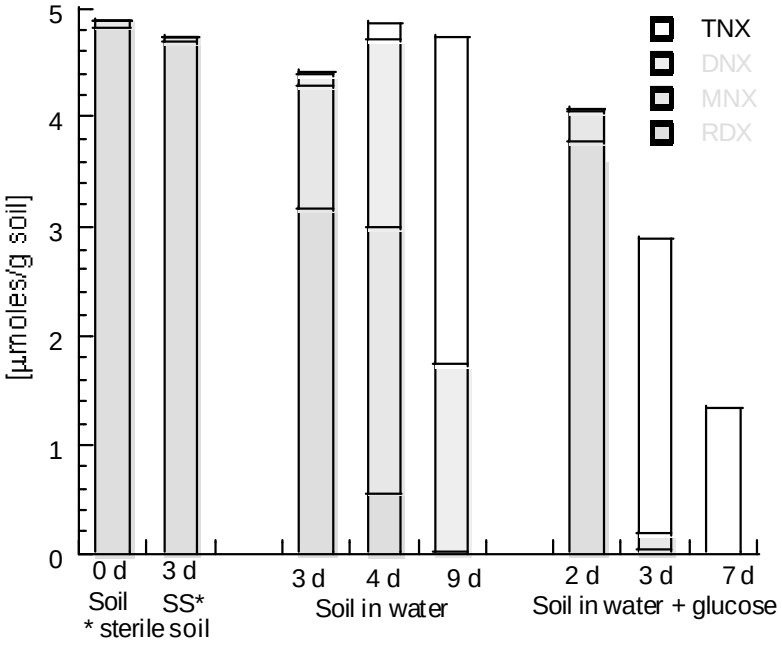

Figure 1. RDX transformation to nitroso products by indigenous soil bacteria at 37°C

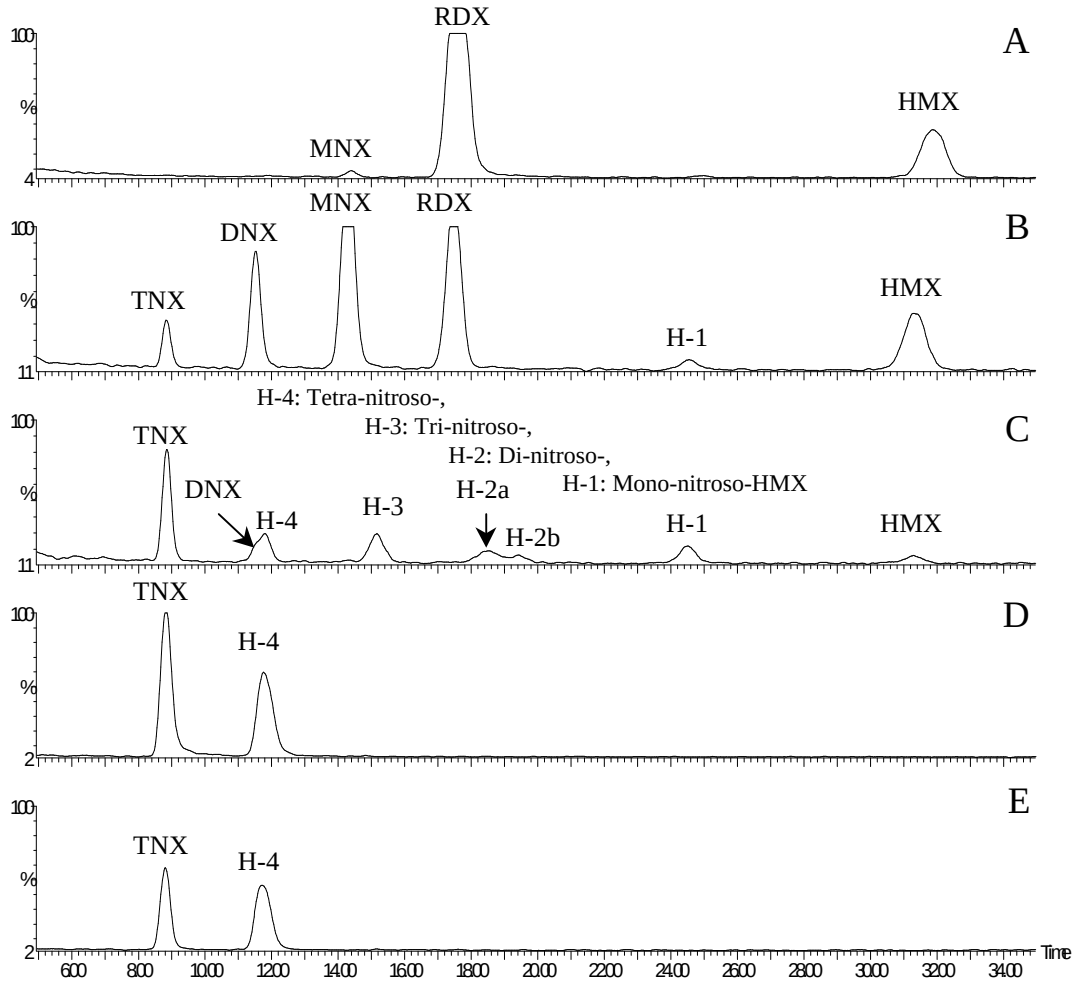

Figure 2. Biodegradation of RDX and HMX in field contaminated soil supplemented with domestic anaerobic sludge at pH 7. A: 0 h; B: 40 h without sludge; C: 40 h in presence of sludge; D: 90 h without sludge, and E: 90 h in presence of sludge.

Sterile soil controls did not show appreciable degradation of RDX or HMX after three days of incubation regardless of the liquid media used, indicating that RDX and HMX transformation in soil is a microbial rather than abiotic. In addition, the pH (7.0) and E_h (235 mV) remained unchanged in the sterilized controls.

Anaerobic Sludge. When the soil slurry microcosms were amended with anaerobic sludge,

degradation was rapid and all RDX in the liquid phase was transformed after 16 hours of incubation. The redox potential (E_h) dropped to –300 mV after 2 hours of incubation. The removal of RDX was accompanied by the formation and accumulation of N_2O (50 % of total N content of reacted RDX). In the case of HMX, only trace amounts of N_2O were detected in the absence of sludge. On the other hand the amounts of the nitroso derivatives seemed to be less in soil microcosms that were amended with sludge (Figure 2). These research findings suggested the occurrence of a significant change, in the degradation pathway of RDX and HMX in the presence of sludge.

In general, biodegradation of RDX and HMX in soil produces more nitroso products (a 2e-transfer process that is O_2-tolerant) than ring cleavage products originating from initial denitration (a 1e-transfer process that is O_2-sensitive). Since soil in known to contain spin traps, the latter pathway (the one -e transfer process) is expected to be partially or totally quenched in soil.

V.6.3 Biodegradation of the RDX Ring Cleavage Product 4-Nitro-2,4-Diazabutanal (NDAB) by **Phanerochaete chrysosporium.**

KEY FINDINGS:

Initial denitration of RDX by *Rhodococcus sp*. strain DN22 produces CO_2 and the dead-end product 4-nitro-2,4-diazabutanal, $OHCNHCH_2NHNO_2$, (NDAB) in high yield. Here we describe experiments to determine the biodegradability of NDAB in liquid culture and soils containing *Phanerochaete chrysosporium*. A soil sample taken from an ammunition plant contained RDX (342 μmol kg^{-1}), HMX (3057 μmol kg^{-1}), MNX (155 μmol kg^{-1}) and traces of NDAB (3.8 μmol kg^{-1}). The detection of the latter in real soil provided the first experimental evidence for the occurrence of natural attenuation that involved ring cleavage of RDX. When we incubated the soil with strain DN22 both RDX and MNX (but not HMX) degraded and NDAB appared (388 ± 22 μmol kg^{-1}) in 5 days. Subsequent incubation of the soil with the fungus led to the removal of NDAB and the liberation of nitrous oxide (N_2O). In cultures with the fungus alone NDAB degraded to give a stoichiometric amount of N_2O. To determine C stoichiometry we first generated [^{14}C]-NDAB in-situ by incubating [^{14}C]-RDX with strain DN22 followed by incubation with the fungus. The production of $^{14}CO_2$ increased from 30 % (DN22 only) to 76 % (fungus). Experiments with pure enzymes revealed that manganese peroxidase (MnP) rather than lignin peroxidase (LiP) was responsible for NDAB degradation. The detection of NDAB in contaminated soil and its effective mineralization by the fungus *P. chrysosporium* may constitute the basis for the development of bioremediation technologies.

***Organisms and growth conditions*.** Three *Rhodococcus* sp. strains (DN22 (Coleman et al., 1998), 11Y (Seth-Smith et al., 2002) and A (Jones et al., 1995) were employed in the present study. The three strains were isolated from aerobic enrichments prepared from soils contaminated with explosives. In this study, each of the three strains (DN22, 11Y and A) was cultivated in the M-succinate medium as previously described (Coleman et al., 1998).

P. chrysosporium ATCC 24725 was provided by Ian Reid (Paprican, Canada, Montreal) and

was maintained on YPD (per liter: yeast extract, 5 g; peptone, 10 g; dextrose, 20 g; agar, 20 g; at pH 5.5 adjusted with H_2SO_4) at 37 ºC. Conidiospores were harvested from 10 day-old cultures in a sterile aqueous solution with 0.2% Tween 80 and kept at 4 ºC. Degradation assays were performed in 120-ml sealed serum bottles with 10 ml of ligninolytic *P. chrysosporium* cultures. The ligninolytic cultures are referred to as 7-day-old cultures incubated in a medium deficient in nitrogen (1.2 mM ammonium). The composition of the low nitrogen MC1 medium was modified from Capdevila et al. (1990). Glycerol was replaced by glucose (10 g l^{-1}). Yeast extract and veratryl alcohol were omitted and diammonium tartrate was added at 0.22 g l^{-1}. The cultures were inoculated at a concentration of 2 x 10^5 conidiospores/ml and then they were incubated in the dark at 37 °C under static condition. The head-space of the microcosms was flushed 30 sec. with air each 3 to 5 days. Unless specified NDAB was added after 7 days of incubation. A similar procedure was used for the degradation experiments performed in soils. *P. chrysosporium* conidiospores were inoculated to 20% wt/vol soil slurries prepared in MC1 medium (2 g of soil and 10 ml of MC1). After a pre-incubation period of 7 days, NDAB (126 µmol l^{-1}) was added to the slurries.

Microtox assay of NDAB. The toxicity of NDAB was assessed using the 15-min Microtox (*Vibrio fisheri*) test for acute microbial toxicity (Microbics, 1992). Reconstituted cells of *V. fisheri* were exposed in triplicate to different dilutions of NDAB. The detailed procedure is described in Sunahara et al. (1998) and the relative toxicity was expressed as IC (inhibition concentration) 20 values, which represent the concentrations that inhibit 20% of bioluminescence.

Soil characteristics. Three soils were used in the present study: 1) an agricultural topsoil (VT) originating from Varennes, Quebec, Canada, 2) a Sassafras Sandy Loam (SSL) obtained from Aberdeen Proving Ground, MD, and 3) a soil sample collected from an ammunition plant in Valleyfield, Quebec, Canada. The latter soil was analyzed according to the EPA Method 8330 (1997) and found to contain RDX (342 µmol kg^{-1}), MNX (155 µmol kg^{-1}), and HMX (3057 µmol kg^{-1}). Other characteristics of the soils are presented in Table 1. Prior to

usage, each soil was passed through a 2 mm sieve and residual moisture was removed by air-drying in a fume-hood.

Biodegradation of NDAB in Soil. In order to distinguish the role of *P. chrysosporium* from that of the soil microorganisms, the soils were sterilized by gamma irradiation from a cobalt-60 source at the Canadian Irradiation Center (Laval, Quebec) with a dose of 50 kGy over 2 h. Twenty percent (wt/vol) soil slurries were prepared using 2 g of soil and 10 ml of MC1 medium in 120-ml serum bottles. Spores of *P. chrysosporium* were added and cultures were grown as mentioned above. On the seventh day of incubation, NDAB (126 µmol l^{-1}) was added to the soil slurries. Uninoculated soil slurries served as controls.

Table 1. Characteristics of soils used during this study.

Characteristics	Agricultural topsoil (VT)	Sassafras Sandy loam (SSL)	Ammunition soil
Granulometry (%)			
Sand	83	71	14
Silt	12	18	44
Clay	4	11	42
Tot. Org. C (%)	8.4	0.3	0.8
Total N ($mg.kg^{-1}$)	1100	420	1100
Total P ($mg.kg^{-1}$)	400	100	400
pH	5.6	5.1	6.5
Nitramines (µmol kg^{-1})	none	none	RDX : 342 MNX : 155 HMX : 3057 NDAB : 3.8

Mineralization assay. We prepared [^{14}C]-NDAB in-situ by incubating [^{14}C]-RDX with strain DN22 as previously described (Fournier et al., 2002). When the mineralization reached a plateau of 30%, representing maximum mineralization by DN22 (Fournier et al., 2002), the culture medium containing NDAB (10 ml) was directly transferred to 10 ml of a 7-day-old culture of *P. chrysosporium*. A KOH trap was placed in the serum bottle to capture generated $^{14}CO_2$.

Enzyme assays. Manganese-dependent peroxidase (MnP) (provided by M. Paice from Paprican, Canada) assays were performed as previously described by Hofrichter et al. (1998). Briefly, the MnP enzyme was added to 50 mM sodium malonate buffer (pH 4.5) containing 1mM $MnCl_2$ (1mM), 15 mM glucose, 0.04 U of glucose oxidase (from *Aspergillus niger*, low in catalase activity) (Sigma-Aldrich) and 1 U of MnP. The reaction was conducted following the addition of NDAB (30 mg l^{-1}) in the dark at 37°C under agitation. Lignin peroxidase (LiP) (Sigma-Aldrich) assays were performed as described previously by Stahl et al. (2001). Briefly, NDAB (30 mg l^{-1}) was incubated in 15 mM sodium tartrate buffer (pH 4.5) containing 15 mM glucose, 0.033 U of glucose oxidase, 2.5 mM of veratryl alcohol and 1 U of LiP. The reaction was performed as mentioned for MnP.

The concentration of NDAB and nitramide (H_2NNO_2) in the supernatant of centrifuged samples (16,000 g) was determined using an HPLC system (Waters Associates, Milford, MA) consisted of a W600 pump, a 717 plus Auto-Sampler, a 996 Photodiode Array (PDA) detector and Millenium data acquisition software. The samples were injected into an AnionSep Ice-Ion-310 Fast organic acids column 6.5 x 150 mm (Cobert associates chromatography products, St-Louis, Missouri) kept at 35°C. The mobile phase was composed of 1.73 mM sulfuric acid with a flow rate of 0.6 ml/min. Under these conditions NDAB eluted at 8 min. The detection was at 225 nm. NDAB in soil was extracted by washing with deionized water for 1 h. Soil extract was filtered through a 3-amino-propyl-functionalized silica gel (Aldrich) column to remove interfering ions. NDAB was also analyzed using a Bruker bench-top ion trap mass detector attached to a Hewlett Packard 1100 Series HPLC system equipped with a PDA detector. The samples were injected into a 5 µm-pore size Zorbax SB-C18 capillary column (0.5 mm ID x 150 mm; Germany) at 25°C. The solvent system was composed of acetonitrile/water isocratic (20% vol/vol acetonitrile) at a flow rate of 12 µl min^{-1}. For mass analysis, ionization was performed in a negative electrospray ionization mode, ES(-), producing mainly the deprotonated molecule mass ions [M-H]. The mass range was scanned from 40 to 400 Da. Analyses of nitrite (NO_2^-), nitrate (NO_3^-), formaldehyde (HCHO), formic acid (HCOOH), nitrous oxide (N_2O), ammonium (NH_4^+) were performed as described previously in the report and in Hawari et al. (2002).

Detection of NDAB in contaminated soil: evidence of natural attenuation. Analysis of a field soil sample from the ammunition plant showed the presence of traces of NDAB (3.8 µmol kg^{-1}) in addition to RDX (342 µmol kg^{-1}), MNX (155 µmol kg^{-1}), and HMX (3057 µmol kg^{-1}) (Fig. 2).

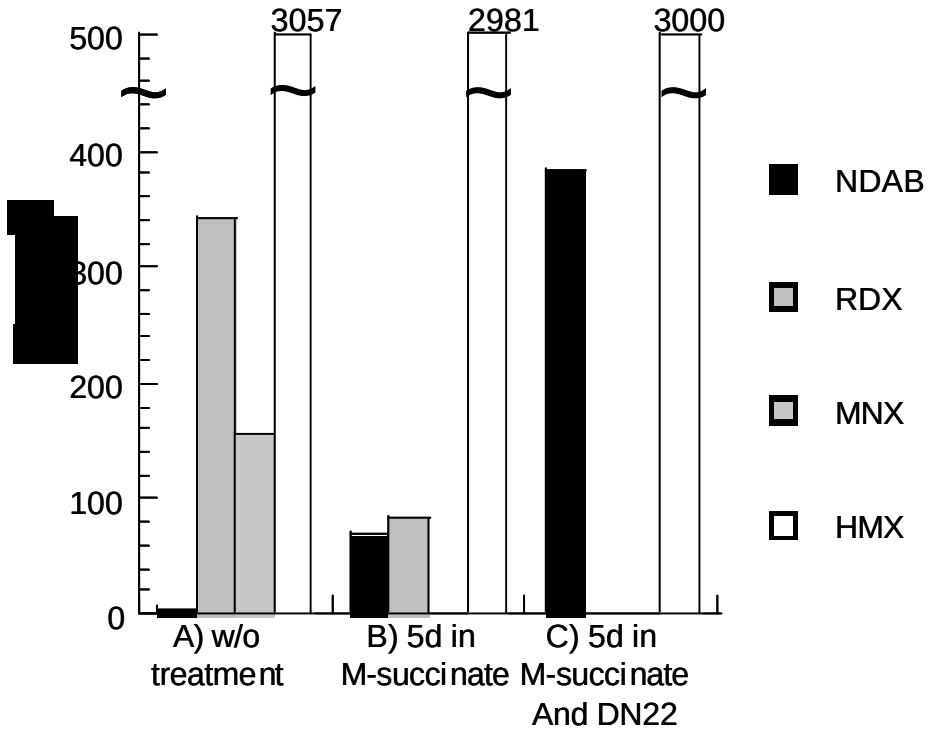

Figure 2. Distribution of cyclic nitramines and products in soil collected from an ammunition plant containing RDX (342 µmol kg^{-1}), HMX (3057 µmol kg^{-1}), MNX (155 µmol kg^{-1}) and traces of NDAB (3.8 µmol kg^{-1}). A) No added reagents; B) After 5 days incubation in M-succinate medium (20% wt/vol); and C) After 5 days incubation in M-succinate medium and RDX-induced DN22 strain (20% wt/vol).
(DN22 was induced with RDX, harvested at mid-log phase and concentrated to an OD_{530} of approx 4.0. The bacterial suspension (0.6 ml) was used to inoculate the slurries. Incubation was performed at 30°C with agitation at 180 rpm).

The detection of the ring cleavage product, NDAB, represents the first experimental evidence of the occurrence of natural attenuation of cyclic nitramines. LC-MS analysis confirmed that the mass spectrum of the compound was similar to that obtained with strain DN22 (Fournier

et al., 2002). Previously only the nitroso derivatives of RDX (and HMX) were reported to coexist with the cyclic nitramines at contaminated sites (Spanggord et al., 1983; Pennington and Brannon, 2002). However, RDX and HMX are often contaminated with their nitroso derivatives, making the use of the latter as markers for natural attenuation uncertain. In contrast, NDAB can only be formed from the degradation of the cyclic nitramines and has never been detected during the synthesis of RDX or HMX. For instance, we detected NDAB in sterilized controls during the degradation of MNX with *Clostridium bifermentans* strain HAW-1 (Zhao et al., 2003a), during hydrolysis (Balakrishnan et al., 2003) and photolysis (Hawari et al., 2002) of RDX.

The above observations are in sharp contrast to the ring cleavage product, methylenedinitramine (MEDINA), that we detected earlier during degradation of RDX (and HMX) with anaerobic sludge (Halasz et al., 2002; Hawari et al., 2001), anerobic culture (Oh et al., 2001), *Klebsiella pneumoniae* SCZ-1 (Zhao et al., 2002) or nitrate reductase (Bhushan et al., 2002b). MEDINA was unstable in water at pH 7 and decomposes to N_2O and HCHO. Beller and Tiemeier (2002) searched for MEDINA in ground water contaminated with RDX, but were unable to detect it.

Biotransformation of RDX and MNX to NDAB. Figure 2 shows the formation of NDAB as a major product during incubation of the non-sterilized ammunition soil with and without the inoculation of RDX-induced DN22. In the absence of DN22, all of MNX and 76 % of RDX in the soil degraded with the concurrent formation NDAB (69 μmol kg^{-1}). In contrast, HMX did not degrade.

When the three *Rhodococcus* strains (DN22, A and 11Y) were added separately to the soil described above, similar amounts (388 ± 22, 426 ± 39, and 384 ± 21 μmol kg^{-1}) of NDAB were produced (Fig. 3).

Although Seth-Smith et al. (2002) were unable to detect NDAB from the degradation of RDX by 11Y, we were able to observe the accumulation of the dead-end product. As was the case with the two other rhodococci strains A and DN22, the addition of supplementary carbon and nitrogen sources to 11Y culture did not promote any further degradation of NDAB. In addition, when we incubated MNX (200 μmol) with any of the three *Rhodococcus* in M-

succinate liquid culture medium, MNX degraded rapidly to produce NDAB (90 µmol) that persisted. Once again, HMX was found to be recalcitrant under these conditions.

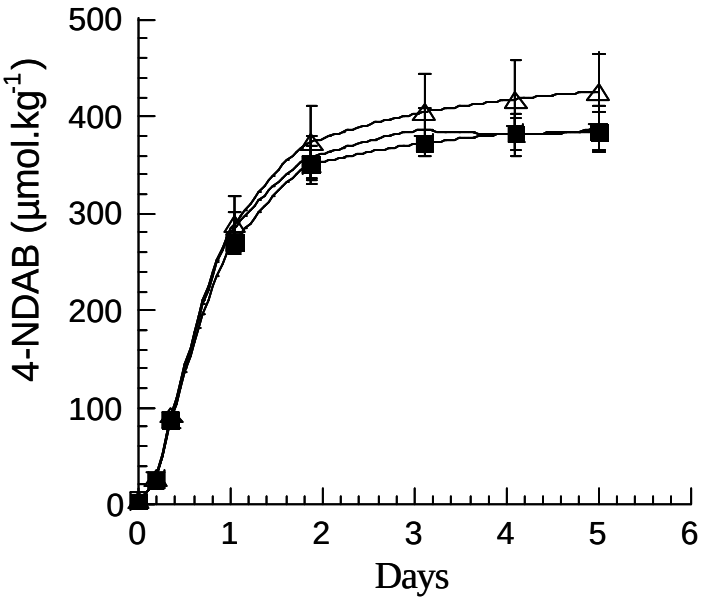

Figure 3. Formation of 4-nitro-2, 4-diazabutanal (NDAB) in aerobic soil slurries (20% wt/vol) prepared with an ammunition soil contaminated with RDX (342 µmol kg^{-1}), HMX (3057 µmol kg^{-1}), MNX (155 µmol kg^{-1}) and traces of NDAB (3.8 µmol kg^{-1}), in M-succinate medium inoculated with either RDX-induced *Rhodococcus sp*. DN22 (■) *Rhodococcus sp*. strain A (○) or *R. rhodochrous* 11Y (?). (The strains were induced with RDX, harvested at mid-log phase and concentrated to an OD_{530} of approx. 4.0. The bacterial suspensions (0.6 ml) were used to inoculate the slurries. Incubation was performed at 30°C with agitation at 180 rpm. Values represent the average and standard deviation of triplicate experiments).

Biodegradation of NDAB. Experimental evidence gathered thus far indicated that aerobic bacteria are able to bio-transform RDX to NDAB which resisted further degradation. To assess the toxicity of NDAB we choose the rapid and simple Microtox assay. The results showed NDAB (IC_{20} 191.0 µM) to be toxic, but less so than previously reported for RDX (IC_{20} 104.6 µM), HMX (IC_{20} 21.7 µM) or TNT (IC_{20} 0.5 µM) (Sunahara et al., 1998). Standard Microtox tests can be performed on aqueous solutions and soil leachates. In this

work, the NDAB toxicity was assessed using a pure solution, which cannot be compared directly with NDAB toxicity assessment in soil. Several factors may interact in the soil medium, such as sorption, or the synergistic and antagonistic effects of other compounds present in the soil. Because of its extreme solubility in water, NDAB can migrate through subsurface soil and cause groundwater contamination. Therefore, its degradability should be investigated using a well-studied microorganism such as *P. chrysosporium.* The fungus has already been found to effectively mineralize RDX (Stahl et al., 2001; Sheremata and Hawari, 2000) without the detection of NDAB. We were unable to detect NDAB during RDX incubation with *P. chrysosporium* because of its potential degradation. For instance, when we incubated RDX with a crude extract obtained from the culture supernatant of the fungus, only trace amounts of NDAB were observed which did not accumulate, indicating that the extracellular enzymes degraded NDAB.

We tested the degradation of NDAB with *P. chrysosporium* in an artificially contaminated liquid culture and in soil slurries (Fig. 4). The ligninolytic cultures of *P. chrysosporium* in MC1 medium began to degrade NDAB after 3 to 4 days of incubation. More than 80% of the initial concentration of NDAB (118 μmol l^{-1}) was degraded within 29 days of incubation at a rate of 3.4 μmol d^{-1}. In the uninoculated control NDAB did not degrade. Using ligninolytic cultures of *P. chrysosporium,* Stahl et al. (2001) demonstrated that RDX began to degrade after 3 to 4 days of incubation and attributed degradation to the presence of both MnP and LiP. The concentrations of both enzymes reached optimal values after 5 days of incubation and persisted until RDX ceased to degrade. However when they used pure peroxidase, only MnP was able to degrade RDX. In the present study, the incubation of NDAB (252 μmol l^{-1}) with pure MnP resulted in 18% (46 μmol l^{-1}) degradation of the nitramine after 18 hours of incubation. In control mixtures prepared without MnP or without glucose oxidase, no degradation of NDAB occurred. Pure LiP did not catalyze the degradation of NDAB, but *in vivo,* the enzyme could play an indirect catalytic role in the degradation of the compound (Kirk and Farrell, 1987).

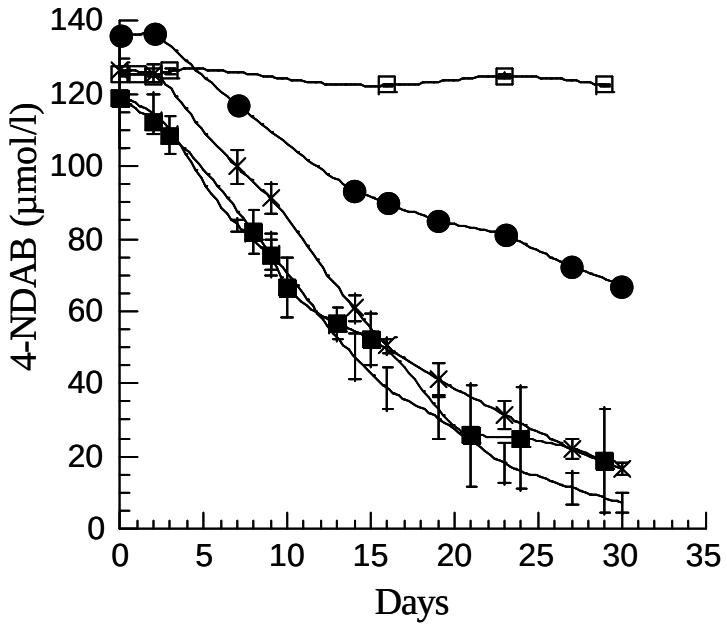

Figure 4. Degradation of 4-nitro-2, 4-diazabutanal (NDAB) added to uninoculated MC1 medium (□), to ligninolytic *P. chrysosporium* in MC1 (■), and to *P. chrysosporium* grown in 20% (w/v) slurries prepared with agricultural topsoil (VT) (-), with Sassafras sandy loam (SSL) (x), and with an ammunition soil contaminated with RDX, MNX, HMX and traces of NDAB (●). Values represent the average and standard deviation of triplicate experiments.

The degradation of NDAB by *P. chrysosporium* cultures in MC1 medium led to the production of trace amounts of H_2NNO_2 and N_2O. Previously we demonstrated that the production of N_2O during RDX degradation with DN22 (Fournier et al., 2002) and the fungus (Sheremata and Hawari, 2000) originated from the ring cleavage product, H_2NNO_2. We calculated that the molar ratio of N_2O produced per NDAB degraded was 0.89 ± 0.10.

P. chrysosporium was incubated in gamma-irradiated soils to determine its ability to degrade NDAB. Degradation rates of NDAB in VT and SSL soils and in MC1 cultures were closely similar (Fig. 4) despite the fact that SSL and VT contained different amounts of C and N (Table 1).

The fungus degraded NDAB added to the ammunition soil but at a rate (2.0 µmol d^{-1}) about 55 % less than the rates in the two artificially contaminated soils. The above results suggest that, although not all forms of organic matter are repressive for the production of ligninolytic enzymes (Kirk and Farrell, 1987), the high nitrogen content of VT soil did not repress the

enzyme(s) responsible for NDAB degradation.

Mineralization of [^{14}C]-RDX in liquid medium took place in two distinct phases (Fig. 5).

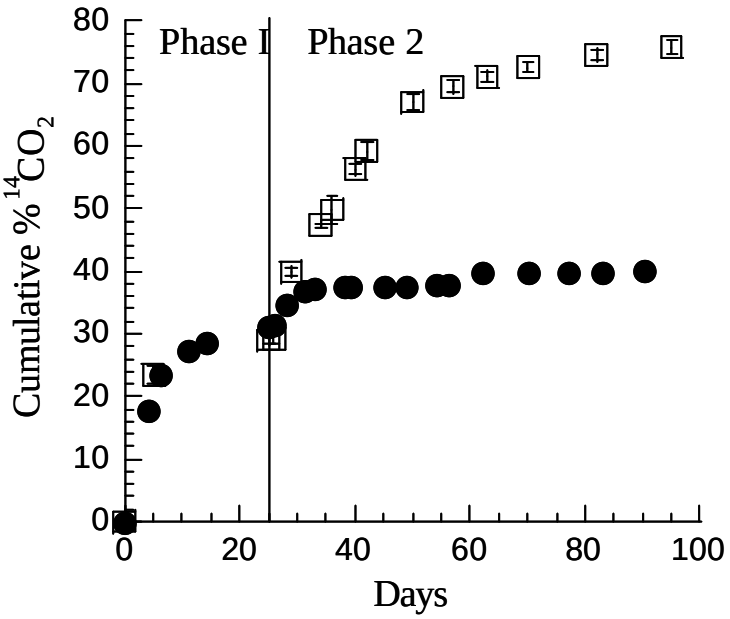

Figure 5. Sequential biodegradation of [^{14}C]-RDX (40 ppm). Phase 1: with *Rhodococcus sp.* DN22 in 10 ml M-succinate medium (for in-situ production of [^{14}C]-NDAB). Phase 2: after the addition of MC1 medium (10 ml) to 10 ml of DN22 culture (●), after the addition of *P. chrysosporium* culture (10 mL) to 10 ml of DN22 culture (□). Values represent the average and standard deviation of triplicate experiments.

The first phase, which lasted from 0 to 26 days, involved incubation with DN22. In the second phase, the 26 day-old DN22 cultures were added to *P. chrysosporium* pre-grown in MC1 medium. In phase I, approximately 30 % of the RDX was converted to CO_2 and the remainder of the energetic chemical accumulated as NDAB (see above). In phase II, the [^{14}C]-NDAB generated in-situ was mineralized to $^{14}CO_2$ (75.8 ± 1.0 %) in 95 days (Fig. 5). The addition of the acidic MC1 medium (pH 4.5) alone following DN22 treatment (phase I) led to a slight increase (from 30 to 37 %) in the concentration of $^{14}CO_2$ due to the reduction in the solubility of carbon dioxide. Since no other products were detected we assumed that the 76 % accumulated mineralization in 100 days also represents the C mass balance.

In conclusion, the detection of the ring cleavage product, NDAB, in RDX contaminated soil

provides clear evidence of RDX natural attenuation. It is not clear whether the low concentrations of NDAB indicate low rates of RDX degradation, or subsequent transformation of the NDAB. Because abiotic and biological transformation of RDX both yield NDAB, it is not possible to judge the relative contributions of the processes in the soil collected from the contaminated site. It is clear, however, from our results that aerobic biodegradation in soil produces NDAB almost exclusively and that the metabolite is biodegradable by fungi. Future research should thus focus on the determination of the relative contributions of biodegradation and abiotic processes during natural attenuation of RDX taking advantage of the novel discovery of NDAB in natural contaminated soil.

VI APPENDIX 1: OUTPUTS

VI.1 Publications

1. Zhao, J.-S; D. Fournier, S. Thiboutot, G, Ampleman, and J. Hawari et al (**In press**) Biodegradation and Bioremediation of Explosives. In ¨Soil Biology¨, Bioremediation, Phytoremediation and Natural Attenuation, Ed A. Singh and O. Ward. Vol. 1, Springer-Verlag (Book chapter)
2. Bonin, P.M.L., D. Bejan, L. Schutt, J. Hawari, and N.J. Bunce. **(2004)** Electrochemical reduction of RDX in aqueous solution. Environ. Sci. Technol. 38(5): 1595-1599.
3. Fournier, D., A. Halasz, J. Spain, R. J. Spanggord, J. C. Bottaro, and J. Hawari. **(2004)** Biodegradation of the RDX Ring Cleavage Product 4-Nitro-2,4-Diazabutanal (NDAB) by *Phanerochaete chrysosporium.* Appl. Environ. Microbiol. 70(2):1123-1128.
4. Monteil-Rivera, F., L. Paquet, S. Deschamps, V. K. Balakrishnan, C. Beaulieu, J. Hawari **(2004)** Physico-chemical measurements of CL-20 towards environmental applications: comparison with RDX and HMX. J. Chromataogr. A. 125-132.
5. Zhao, J. -S., C. W. Greer. S. Thiboutot, G. Ampleman and J. Hawari. (**2004)** Biodegradation of the nitramime explosive hexahydro-1,3-5-trinitro-1,3,5-triazine and octahydro-1, 3,5,7-tetranitro-1,3,5,7-tetrazocine in cold marine sediment under anaerobobic and oligottrophic conditions. Can. J. Microbiol. 50: 91-96.
6. Balakrishnan, V., A. Halasz and J. Hawari**. (2003)** The alkaline hydrolysis of the cyclic nitramine explosives RDX, HMX and CL-20: New insights into degradation pathways obtained by the observation of novel intermediates. Environ. Sci. Tech.37: 1838-1843.
7. Bhushan, B., L. Paquet, A. Halasz, J.C. Spain, and J. Hawari. **(2003)** Mechanism of xanthine oxidase catalyzed biotransformation of HMX under anaerobic conditions. Biochem. Biophys. Res. Commun. 306: 509-515.
8. Bhushan, B., S. Trott, J. Spain, A. Halasz, and J. Hawari. **(2003)** Biotransformation of RDX by Cytochrome P450 2B4: Insights into the mechanisms of RDX biodegradation by *Rhodococcus* sp. Strain DN22. Appl. Environ. Microbiol. 69: 1347-1351.
9. Groom, C, A. Halasz, L. Paquet, P. Dcruz and J. Hawari. **(2003)** Cyclodextrin-assisted capillary electrophoresis for determination of the cyclic nitramine explosives RDX, HMX and CL-20 a comparison with high-performance liquid chromatography. J. Chromatography A. 999:17-22.
10. Zhao, J.-S., Halasz, A., Paquet, L. and J. Hawari. **(2003)** Metabolism of hexahydro-1,3,5-trinitro-1,3,5-triazine through initial reduction to hexahydro-1-nitroso-3,5-dinitro-1,3,5-triazine followed by denitration in *Clostridium bifermentans* HAW-1. Appl. Microbiol. Biotech. 63 : 187-193.
11. Monteil-Rivera, F., C. Groom, and J. Hawari. **(2003)** Sorption and Degradation of Octahydro-1,3,5,7-tetranitro-1,3,5,7-tetrazocine (HMX) in Soil. Environ. Sci. Technol. 37: 3878-3884.
12. Zhao, J.-S., J. Spain, and J. Hawari**. (2003)** Phylogenetic and metabolic diversity of hexahydro-1,3,5-trinitro-1,3,5-triazine (RDX)-transforming bacteria in strictly anaerobic mixed cultures enriched on RDX as nitrogen source. FEMS Microbiol. Ecol. **46**: 189-196.

13. Bhushan, B., Halasz, A., Spain, J., Thiboutot, S., Ampleman G. and J. Hawari. **(2002).** Diaphorase catalyzed biotransformation of RDX *via* N-denitration mechanism. Biochem. Biophys. Res. Commun. **296**: 779-784.

14. Bhushan, B., Halasz, A., Spain, J., Thiboutot, S., Ampleman G. and J. Hawari. **(2002)** Biotransformation of Hexahydro-1,3,5-trinitro-1,3,5-triazine Catalyzed by a NAD(P)H: Nitrate Oxidoreductase from *Aspergillus niger*. Environ. Sci. Technol **36**: 3104-3108

15. Fournier, D., A. Halasz, J. Spain, P. Fiurasek, and J. Hawari **(2002)** Determination of key metabolites during biodegradation of hexahydro-1,3,5-trinitro-1,3,5-triazine (RDX) with *Rhodococcus* sp. Strain DN22. Appl. Environ. Microbiol. **68**(1): 166-172.

16. Halasz, A., C. Groom, E. Zhou, L. Paquet, C. Beaulieu, S. Deschamps, A. Corriveau, S. Thiboutot, G. Ampleman, C. Dubois and J. Hawari. (**2002**) Detection of explosives and their degradation products in soil environments. J. Chromatography A. **963**: 411-418.

17. Halasz, A., Spain J., Paquet L., Beaulieu C. and Hawari J. (**2002)** Insights into the Formation and Degradation Mechanisms of Methylenedinitramine during the Incubation of RDX with Anaerobic Sludge. Environ. Sci. Technol., **36**: 633-638.

18. Hawari JA and A. Halasz. **(2002)** Microbial Degradation of Explosives, pp. 1979-1993. In The Encyclopedia of Environmental Microbiology, (Ed) G. Bitton, John Wiley & Sons ltd, N.Y. (Book Chapter)

19. Hawari, J., A. Halasz, C. Groom, S. Deschamps, L. Paquet, C. Beaulieu, and A. Corriveau. **(2002)** Photodegradation of RDX in aqueous solution: a mechanistic probe for biodegradation with *Rhodococcus* sp. Environ. Sci. Technol. 36: 5117-5123.

20. Zhao, J.-S., Halasz, A., Paquet, L., Beaulieu, C., J. Hawari. **(2002)** Biodegradation of RDX and its Mononitroso Derivative MNX by *Klebsiella* sp. Strain SCZ-1 Isolated from an Anaerobic Sludge Appl. Environ. Microbiol, 68: 5336-5341.

21. Halasz, A., Bayona, J.M. and J. Hawari. **(2002)** Sample preparation techniques for soil analysis, ch. 26, pp. 895-918. In Sampling and Sample Preparation for Field and Laboratory: fundamental and new directions in sample preparation, (Ed) J. Pawlyszin, (Comprehensive Analytical Chemistry Vol. XXXVII, ed. D. Barceló) Elsevier Science, Amsterdam, The Netherlands

22. Hawari JA, Halasz A, Beaudet S, Paquet L, Ampleman G, and Thiboutot S. **(2001)** Biotransformation Routes of Octahydro-1,3,5,7-tetranitro-1,3,5,7-tetrazine by Municipal Anaerobic Sludge. Environ. Sci. Technol., **35**: 70-75.

23. Sheremata T, Halasz A, Paquet L, Thiboutot S, Ampleman G and Hawari JA. **(2001)** The fate of cyclic nitramine explosive RDX in natural soil. Environ. Sci. Technol. **35**: 1037-1040

VI.2 Symposia and conferences

- Biodegradation of Explosives: Environmental fate, 18th Eastern Canadian Sym. of the Can. Assoc. on Water quality Research (CAWQ), Ecole Polytechnique, Montreal, Oct 18, 2002.
- Environmental Biotechnology of Explosives as part of an award reception ceremony outstanding people outstanding achievements, NRC, Ottawa (Feb 21, 2002)
- Cyclodextrins for desorption, solubilization and hydrolysis of the cyclic nitramine explosives RDX and HMX from soils, 18th Eastern Canadian Symposium of the Canadian Association on Water Quality (CAWQ), Ecole Polytechnique, Montreal, Oct 18, 2002.
- Microbial Degradation of RDX and HMX at Partners in Environmental Technology Tech. Sym. & Workshop; W.D.C., sponsored by SERDP/ESTCP, US Army (Dec 2002)
- Microbial Degradation of RDX and HMX, Partners in Environmental Technology, Technical Symposium & Workshop sponsored by SERDP and ESTCP, Nov 27-29, 2001, Washington, D.C.
- Enzymatic Mechanisms of hexahydro-1,3,5-trinitro-1,3,5-triazine (RDX) Degradation under Anaerobic Conditions, Technology, Technical Symposium & Workshop sponsored by SERDP and ESTCP, Nov 27-29, 2001, Washington, D.C

VI.3 Patents

Processes for the selective biotransformation of cyclic nitramine explosives, Provisional US Patent (60/404,147).

VI.4 Public Impact/Awards

- SERDP project of the year award on Cleaup, Washington, D.C., Dec 2003
- NRC external recognition award for being a recipient of US SERDP cleanup project of the year award, Feb, 2004
- A Director General (BRI) Meritorious Award for international visibility, Dec 2003
- NRC Press release: 1st Canadian to receive US SERDP Award (Dec 23, 2003 Montreal).

- A medal commemorating the Golden Jubilee of Her Majesty Queen Elizabeth II accession to the throne (Dec 13, 2002) (see: SERDP inf. Bulletin Winter 2003, # 15, pp 2 & 8).
- A Corporate Outstanding Achievement Award "Outstanding People, Outstanding achievement" for the Collaboration with US-ARL through SERDP support (Feb. 2002 pending) (see: SERDP inf. Bulletin Spring 2000, # 12, pp 7).
- A Director General (BRI) Meritorious Award in industrial entrepreneurship (in recognition of the collaboration with US-ARL through SERDP support, Dec. 14, 2001).
- A press release by NRC, Nov. 7, 2001, NRC's Biotechnology Research Institute collaborates with US Air Force Research Laboratory on Biodegradation of Explosives (www2.cdn-news.com/script/ccn-release.pi? current/1107012N.html)
- A press release by the daily Le Soleil, Quebec City, QC, Canada, Thursday, Nov. 8, 2001, À la recherche d'un moyen pour dépolluer les sites d'entraînement et les zones de combat, (by Annie Morin: Amorin@lesoleil.com).
- Insights for the Life Science Industry, BRI Collaborates with US Air Force, Biotechnology Focus, Vol. 5, Nov 1, 2001

VI.5 Collaborations

Since the inception date of project (CU1213), which involved collaboration with US Air Force Research Laboratory and DRDC, DND-Canada, we increased our collaboration to include:

1. Dr. Neil Bruce, Institute of Environmental Biotechnology, Cambridge University,

   Present address: York University, York, UK.

   Enzymatic role in the degradation of RDX by Rhodococcus
2. Professor Owen Ward, Department of Microbiology, Waterloo University.

   Degradation of aromatic and cyclic nitramine explosives by isolated strains capable of degrading hydrocarbons.
3. Professor Nigel Bunce, Chemistry Department, University of Guelph

   Electrochemical destruction of RDX and HMX: a mechanistic probe for reduction by nitroreductase enzymes.

VII TRANSITION PLAN

Our results are providing the scientific community with the knowledge needed to further develop and improve bioremediation and natural attenuation technologies for RDX and HMX. The discovery of key intermediates and the enzymes that form them coupled with new knowledge of the degradation pathways of RDX and HMX will enable engineers to optimize pilot tests and field applications to remediate RDX- and HMX-contaminated soils and groundwater effectively. Initiatives are already under way with U.S. and other Canadian firms to seek opportunities for field applications. In the US, we have been in direct contact with Shaw Environmental (Princeton Research Center, Lawrenceville, NJ) who received ESTCP funding for a field demonstration of in situ bioremediation of an RDX- and TNT-contaminated aquifer at the Picatinny Arsenal in NJ. and with IAAP (c/o Kevin Howe), MAAP (c/o Chris Lutes: ARCHADIS, G&M Inc NC) and US Army, ERDC (c/o Neal Adrian) to provide understanding of in-situ bioremediation processes of RDX and HMX in ground water. Meanwhile, in Canada we are working with BioGenie (Ste Foy, Quebec, Canada) on the scale up and application of a soil biopile technology for the remediation of soil contaminated with RDX and HMX. As part of the project we will measure breakdown products during the demonstration. Further, through the extrapolation of microcosm data to sediments and marine estuaries, the tools and the science generated from the SERDP CU1213 project has provided similar insight into the fate and biodegradation of RDX/HMX at Navy bases. Presently, we are collaborating with the Office of Naval research, US Navy and the Canadian Navy to determine the microbial degradation of RDX and HMX in sediments and then to determine the potential for the occurrence of natural attenuation (in situ remediation). Finally we collaborated with several Universities and institutions in the US (SRI, Menlo Park, CA; Rice University, TX; Iowa University, Iowa), Canada (Guelph University) and the UK (Cambridge University and University of York).

VIII ACKNOWLEDGMENTS

The authors would like to thank Stéphane Deschamps, Chantale Beaulieu, Alain Corriveau, and Dominic Manno for their technical assistance, Claude Masson for soil sampling, and Sylvie Rocheleau for providing the toxicity data on NDAB. We are grateful to Drs. Charles W. Greer, Nicholas V. Coleman, and Neil C. Bruce for providing the *Rhodococcus* strains. We would also like to thank Defence Research and Development Canada (DRDC), Valcartier, Canada, for providing samples of RDX and HMX, Dr R. Spanggord (SRI, Menlo Park, CA) for providing samples of NDAB and MEDINA, and the Strategic Environmental Research and Development Program (SERDP), USA (CU-1213) for financial support.

IX REFERENCES

Adrian, N.R., and T. Chow. **2001.** Identification of hydroxylaminodinitroso-1,3,5-triazine as a transient intermediate formed during the anaerobic biodegradation of RDX. *Environ. Toxicol. Chem*. 20, 1874-1877.

Adrian, N.R., and A. Lowder. **1999.** Biodegradation of RDX and HMX by a methanogenic enrichment culture, p. 1-6. *In*. B. C. Alleman and A. Leeson (ed.), Bioremediation of nitroaromatic and haloaromatic compounds, vol. 7. Battelle Press, Columbus, OH.

Adrian, N.R., and K. Sutherland. **1998**. RDX biodegradation by a methanogenic enrichment culture obtained from an explosives manufacturing wastewater treatment plant. Technical report 99-15. US Army Construction Engineering Research Laboratories, Champaign, IL.

Akhavan, J. **1998**. The Chemistry of Explosives. The Royal Society of Chemistry, Cambridge, U.K.

Ampleman, G., A. Marois, S. Thiboutot, J. Hawari, C.W. Greer, J. Godbout, G.I. Sunahara, C.F. Shen, and S.R. Guiot. **1999a**. Synthesis of ^{14}C-labelled octahydro-1,3,5,7-tetranitro-1,3,5,7-tetrazocine (HMX), and ^{15}N-isotopically labeled hexahydro-1,3,5-trinitro-1,3,5-triazine (RDX) for use in microcosm experiments. DREV-TR-1999-99. Defense Research Establishment Valcartier, Val Bélair, Québec, Canada.

Ampleman, G.; A. Marois, S. Thiboutot, J. Hawari, C.W. Greer, J. Godbout, G.I. Sunahara, C.F. Shen, S. R. Guiot. **1999b**. Synthesis of ^{14}C-labelled octahydro-1,3,5,7-tetranitro-1,3,5,7-tetrazocine (HMX), for use in microcosm experiments. *J. Label. Compd. Radiopharm*. 42, 1251-1264.

Ampleman, G., S. Thiboutot, J. Lavigne, A. Marois, J. Hawari, A.M. Jones, and D. Rho**. 1995.** Synthesis of ^{14}C-labelled hexahydro-1,3,5-trinitro-1,3,5-triazine (RDX), 2,4,6-trinitrotoluene (TNT), nitrocellulose (NC) and glycidylazide polymer (GAP) for use in assessing the biodegradation potential of these energetic compounds. *J. Label. Compd. Radiopharm*. 36, 559-577.

Anusevicius, Z., J. Sarlauskas, H. Nivinskas, J. Segura-Aguilar, N. Cenas. **1998**. DT-diaphorase catalyzes N-denitration and redox cycling of tetryl. *FEBS Lett*. 436, 144-148.

Apajalahti, J.H.A. and M.S. Salkinoja-Salonen. **1984**. Absorption of pentachlorophenol (PCP) by bark chips and its role in microbial PCP degradation. *Microb. Ecol*. 10, 359-367.

Arrowsmith, C.H.; A. Awwal, B.A. Euser, A.J. Kresge, P.P.T. Lau, D.P. Onwood, Y.C. Tang, E.C. Young. **1991**. The base-catalyzed decomposition of nitramide: a new look at an old reaction. *J. Am. Chem. Soc.*, 113, 172-179.

Averill, B. A. **1995**. Transformation of Inorganic N-Oxides by Denitrifying and Nitrifying Bacteria: Pathways, mechanisms, and Relevance to Biotransformation of Nitroaromatic Compounds; In *Biodegradation of Nitroaromatic Compounds,* Spain, J. C. Ed.; Plenum Press, New York, p. 183-197.

Babu, G.R.V., O.K. Vijaya, V.L. Ross, J.H. Wolfram, and K.D. Cahpatwala. **1996**. Cell free extract(s) of *Pseudomonas putida* catalyzes the conversion of cyanides, cyanates, thiocyanates, formamide, and cynide-containing mine waters into ammonia. *Appl. Microbiol. Biotechnol*. 45, 273-277.

Balakrishnan, V.K., A. Halasz, and J. Hawari. **2003**. Alkaline hydrolysis of the cyclic nitramine explosives RDX, HMX, and CL-20: New insights into degradation pathways obtained by the observation of novel intermediates. *Environ. Sci. Technol*. 37, 1838-1843.

Beller, H.R. **2002.** Anaerobic biotransformation of RDX (hexahydro-1,3,5-trinitro-1,3,5-triazine) by aquifer bacteria using hydrogen as the sole electron donor. *Wat. Res.* 36, 2533-2540.

Beller, H.R., and K. Tiemeier. **2002**. Use of liquid chromatography/tandem mass spectrometry to detect distinctive indicators of in situ RDX transformation in contaminated groundwater. *Environ. Sci. Technol*. 36, 2060-2066.

Behrens, Jr, R., and S. Bulusu. **1991.** Thermal decomposition of energetic materials. 2. Deuterium isotope effects and isotopic scrambling in the condensed phase decomposition of octahydro-1,3,5,7-tetranitro-1,3,5,7-tetrazocine. *J. Phys. Chem*. 95, 5838-5845.

Bhushan, B., A. Halasz, J.C. Spain, S. Thiboutot, G. Ampleman, and J. Hawari. **2002a.** Biotransformation of hexahydro-1,3,5-trinitro-1,3,5-triazine catalyzed by a NAD(P)H: nitrate oxidoreductase from *Aspergillus niger*. *Environ. Sci. Technol***.** 36, 3104-3108.

Bhushan, B., A. Halasz, J.C. Spain, and J. Hawari. **2002b**. Diaphorase catalyzed biotransformation of RDX via N-denitration mechanism. *Biochem. Biophys. Res. Commun.* 296, 779-784.

Bhushan, B., S. Trott, J.C. Spain, A. Halasz, L. Paquet, and J. Hawari. **2003a.** Biotransformation of hexahydro-1,3,5-trinitro-1,3,5-triazine (RDX) by a rabbit liver cytochrome P450: Insight into the mechanism of RDX biodegradation by *Rhodococcus sp*. strain DN22. *Appl. Environ. Microbiol.* 69, 1347-1351.

Bhushan, B., L. Paquet, A. Halasz, J.C. Spain, and J. Hawari. **2003b**. Mechanism of xanthine oxidase catalyzed biotransformation of HMX under anaerobic conditions. *Biochem. Biophys. Res. Commun*. 306, 509-515.

Binks, P.R., S. Nicklin, and N.C. Bruce. **1995.** Degradation of hexahydro-1,3,5-trinitro-1,3,5-

triazine (RDX) by *Stenotrophomonas maltophila* PB1. *Appl. Environ. Microbiol*. 61, 1318-1322.

Bishop, R.L., R.L. Flesner, P.C. Dell'Orco, T. Spontarelli, and S.A. Larson. **1999.** Base hydrolysis of HMX and HMX-Based Plastic Bonded Explosives with Sodium Hydroxide between 100 and 155 °C. *Ind. Eng. Chem. Res.* 38, 2254-2259.

Boopathy, R., M. Gurgas, J. Ullian, and J.F. Manning. **1998**. Metabolism of explosive compounds by sulfate-reducing bacteria, *Curr. Microbiol*. 37, 127-131.

Boopathy, R. **2001**. Bioremediation of HMX-contaminated soil using soil slurry reactors. *Soil Sediment Contam*. 10, 269-283.

Bose, P., W.H. Glaze, and S. Maddox. **1998**. Degradation of RDX by various advanced oxidation processes: II. Organic byproducts. *Wat. Res.* 32, 1005-1018.

Brannon, J.M., C.B. Price, C. Hayes, and S.L. Yost. **2002**. Aquifer soil cation substitution and adsorption of TNT, RDX, and HMX. *Soil Sediment Contam.* 11, 327-338.

Brian R.C., and A.H. Lamberton. **1949.** Studies on Nitroamines. Part II. The Nitration of some Methylenebisamides and Related Compounds. *J. Chem. Soc.* 1633-1635.

Brockman, F.J., D.C. Downing, and G.F. Wright. **1949.** Nitrolysis of hexamethylenetetramine. *Can. J. Res*. 27B, 469-474.

Brown, R.S., A.J. Bennet, H. Slebocka-Tilk, and A. Jodhan. **1992**. Base catalyzed hydrolysis and carbonyl ^{18}O exchange kinetics for toluamides containing amine portions of reduced basicity. N-Toluoyl-3,3,4,4-tetrafluoropyrrolidine and N-toluoylpyrrole. *J. Am. Chem. Soc*. 114, 3092-3098.

Bruns-Nagel, D., S. Scheffer, B. Casper, H. Garn, O. Drzyzga, E. von Löw, and D. Gemsa. **1999**. Effects of 2,4,6-trinitrotoluene and its metabolites on human monocytes. *Environ. Sci. Technol*. 33, 2566-2570.

Bruns-Nagel, D., K. Steinbach, D. Gemsa, E. von Löw. **2000**. In: *Biodegradation of nitroaromatic compounds and explosives*, Spain, J.C.; Hughes, J.B.; Knackmuss, H.-J. Eds., CRC Press, Boca Raton FL., p.357-394.

Bryant, C., M. DeLuca, **1991.** Purification and characterization of an oxygen-insensitive NAD(P)H nitroreductase from *Enterobacter cloacae*. *J. Biol. Chem*. 266, 4119-4125.

Campbell, W.H. **1999.** Nitrate reductase structure, function and regulation: bridging the gap between biochemistry and physiology. *Annu. Rev. Plant Physiol. Plant Mol. Biol.* 50, 277-303.

Campbell, W.H. **2001**. Structure and function of eukaryotic NAD(P)H:nitrate reductase. *Cell. Mol. Life Sci.* 58, 194-204.

Capdevila, C., S. Moukha, M. Ghyczy, J. Theilleux, B. Gelie, M. Delattre, G. Corrieu, and M. Asther. **1990**. Characterization of peroxidase secretion and subcellular organization of *Phanerochaete chrysosporium* INA-12 in the presence of various soybean phospholipid fractions. *Appl. Environ. Microbiol*. 56, 3811-3816.

Chapman, R.D., R.A. O'Brien, P.A. Kondracki. **1996**. N-denitration of nitramines by dihydronicotinamides. *Tetrahedron* 52, 9655-9664.

Chen, J., B.P. Preston, M.J. Zimmermann. **1997**. Analysis of organic acids in industrial samples: comparison of capillary electrophoresis and ion chromatography. *J. Chromatogr. A* 781, 205-213.

Coleman, N.V., D.R. Nelson, and T. Duxbury. **1998**. Aerobic degradation of hexahydro-1,3,5-trinitro-1,3,5-triazine (RDX) as a nitrogen source by a *Rhodococcus* sp., strain DN22. *Soil Biol. Biochem*. 30, 1159-1167.

Coleman, N.V., J.C. Spain, and T. Duxbury. **2002**. Evidence that RDX biodegradation by *Rhodococcus* strain DN22 is plasmid-borne and involves a cytochrome p-450. *J. Appl. Microbiol.* 93, 463-472.

Collins, M.D., P.A. Lawson, A. Willems, J.J. Cordoba, J. Fernandez-Garayzabal, P. Garcia, J. Cai, H. Hippe, and J.A.E. Farrow. **1994**. The phylogeny of the genus *Clostridium*: proposal of five new genera and eleven new species combinations. *Int. J. Syst. Bacteriol.* 44: 812-826.

Corbett, M. D., B. R. Corbett. **1995**. Bioorganic chemistry of the arylhydroxylamine and nitrosoarene functional groups. In *Biodegradation of Nitroaromatic Compounds:* Spain, J. C. Ed.; Plenum Press, NY. p. 151-182.

Croce, M. and Y. Okamoto. **1979**. Cationic micellar catalysis of the aqueous alkaline hydrolyses of 1,3,5-triaza-1,3,5-trinitrocyclohexane and 1,3,5,7-tetraaza-1,3,5,7-tetranitrocyclooctane. *J. Org. Chem*. 44, 2100-2103.

Doel, J. J., B. L. J. Godber, R. Eisenthal, R. Harrison. **2001.** Reduction of organic nitrates catalysed by xanthine oxidoreductase under anaerobic conditions, *Biochim. Biophys. Acta*. 1527: 81-87.

Druckrey, H**. 1973.** Specific carcinogenic and teratogenic effects on "indirect" alkylating methyl and ethyl compounds, and their dependency on stages of ontogenic development. *Xenobiotica*, 3, 271-303.

Dubé, P., G.;Ampleman, S. Thiboutot, A. Gagnon, A. Marois. **1999**. Report DREV –TR-1999-13. Defence Research Establishment Valcartier. Department of National Defence

Canada,

Ecker, S., T. Widmann, H. Lenke, O. Dickel, P. Fischer, C. Bruhn, and H.-J. Knackmuss. **1992**. Catabolism of 2,6-dinitrophenol by *Alcaligenes eutrophus* JMP 134 and JMP 222. *Arch. Microbiol.* 158, 149-154.

EPA, US Environmental Protection Agency**.** Method 8330 SW-846 update III Part 4: 1 (B), Nitroaromatics and nitramines by high performance liquid chromatography (HPLC). Office of Solid Waste, Washington, DC, **1997.**

Fournier, D., A. Halasz, J. C. Spain, P. Fiurasek, and J. Hawari. **2002**. Determination of key metabolites during biodegradation of hexahydro-1,3,5-trinitro-1,3,5-triazine with *Rhodococcus* sp. strain DN22. *Appl. Environ. Microbiol*. 68:166-172.

Fournier, D., A. Halasz, J. Spain, R.J. Spanggord, J.C. Bottaro, and J. Hawari. **2004.** Biodegradation of the RDX Ring Cleavage Product 4-Nitro-2,4-Diazabutanal (NDAB) by *Phanerochaete chrysosporium. Appl. Environ. Microbiol*. **In press.**

Fritz, G., D. Griesshaber, O. Seth, and P.M. Kroneck. H. Nonaheme. **2001**. Cytochrome c, a New Physiological Electron Acceptor for [Ni,Fe] hydrogenase in the sulfate-reducing bacterium *Desulfovibrio desulfuricans* Essex: primary sequence, molecular parameters, and redox properties. *Biochemistry.* 40: 1317-1324.

Funk, S.B., D.J. Roberts, D.L. Crawford, and R.L. Crawford. **1993**. Initial-phase optimization for bioremediation of munition compound-contaminated soils. *Appl. Environ. Microbiol*. 59: 2171-2177.

Garber, E.A.E., and T.C. Hollocher. **1982**. Positional isotopic equivalence of nitrogen in N_2O produced by the denitrifying bacetrium *Pseudomonas stutzeri*. *J. Biol Chem*. 257: 4705-4708.

Godber, B.L.J., J.J. Doel, G.P. Sapkota, D.R. Blake, C.R. Stevens, R. Eisenthal, R. Harrison. **2000**. Reduction of nitrite to nitric oxide catalysed by xanthine oxidoreductase, *J. Biol. Chem*. 275, 7757-7763.

Groom, C. A., A. Halasz, L. Paquet, N. Morris, L. Olivier, C. Dubois, J. Hawari. **2002.** Accumulation of HMX (octahydro-1,3,5,7-tetranitro-1,3,5,7-tetrazocine) in indigenous and agricultural plants grown in HMX-contaminated anti-tank firing-range soil. *Environ Sci. Technol.* 36, 112-118.

Groom, C. A., A. Halasz, L. Paquet, P. D'Cruz, J. Hawari. **2003.** Cyclodextrin-assisted capillary electrophoresis for determination of the cyclic nitramine explosives RDX, HMX and CL-20: Comparison with high-performance liquid chromatography, *J. Chromatogr. A* 999: 17-22.

Guengerich, P.F. **2001**. Common and uncommon cytochrome P450 reactions related to

metabolism and chemical toxicity. *Chem. Res. Toxicol*. 14, 611-650.

Guiot, S. R., B. Safi, J. C. Frigon, P. Mercier, C. Mulligan, R. Tremblay, R. Samson. **1995.** *Biotechnology Bioengineering* 45: 398-405.

Haderlein, S.B., K.W. Weissmahr, R.P. Schwarzenbach. **1996.** Specific adsorption of nitroaromatic explosives and pesticides to clay minerals. *Environ. Sci. Technol.* 30: 612-622.

Halasz, A., J. Spain, L. Paquet, C. Beaulieu, and J. Hawari. **2002**. Insights into the formation and degradation mechanisms of methylenedinitramine during the incubation of RDX with anaerobic sludge. *Environ. Sci. Technol*. 36: 633-638.

Hawari, J. **2000**. Biodegradation of RDX and HMX: from basic research to field application. *In* J.C. Spain, J.B. Hughes, and H.-J. Knackmuss (ed.) Biodegradation of nitroaromatic compounds and explosives. CRC Press, Boca Raton, p. 277-310. Chapter 11.

Hawari, J., and A. Halasz. **2002**. Microbial degradation of explosives. In: *Encyclopedia of Environmental Microbiology*, Bitton, G. (Ed.), John Wiley & Sons Ltd, Amsterdam, Netherlands, p. 1979-1993.

Hawari, J., A. Halasz, C. Groom, S. Deschamps, L. Paquet, C. Beaulieu, and A. Corriveau. **2002**. Photodegradation of RDX in aqueous solution: a mechanistic probe for biodegradation with *Rhodococcus* sp. *Environ. Sci. Technol*. 36: 5117-5123.

Hawari, J., A. Halasz, S. Beaudet, L. Paquet, G. Ampleman, and S. Thiboutot. **2001**. Biotransformation routes of octahydro-1,3,5,7-tetranitro-1,3,5,7-tetrazocine by municipal anaerobic sludge. *Environ. Sci. Technol.* 35: 70-75.

Hawari, J., A. Halasz, T. Sheremata, S. Beaudet, C. Groom, L. Paquet, C. Rhofir, G. Ampleman, and S. Thiboutot. **2000a**. Characterization of metabolites during biodegradation of hexahydro-1,3,5-trinitro-1,3,5-triazine (RDX) with municipal sludge. *Appl. Environ. Microbiol*. 66: 2652-2657.

Hawari, J., S. Beaudet, A. Halasz, S. Thiboutot and G. Ampleman. **2000b.** Microbial degradation of explosives: biotransformation versus mineralization. *Appl. Microbiol. Biotechnol.* 54: 605-618.

Hawari, J., L. Paquet, E. Zhou, A. Halasz, B. Zilber. **1996.** Enhanced recovery of the explosive hexahydro-1,3,5-trinitro-1,3,5-triazine (RDX) from soil: cyclodextrin versus anionic surfactants. *Chemosphere***,** 32, 1929-1936.

Heilmann, H.M., Wiesmann, U. and M.K. Stenstrom. **1996**. Kinetics of the alkaline hydrolysis of high explosives RDX and HMX in Aqueous Solution and Adsorbed to Activated Carbon. *Environ. Sci. Technol.* 30: 1485-1492.

Hille, R., and T. Nishino. **1995.** Flavoprotein structure and mechanism. 4. Xanthine oxidase and xanthine dehydrogenase. *FASEB J*. 9, 995-1003.

Hoffsommer, J.C., D.A. Kubose, and D.J. Glover. **1977**. Kinetic isotope effects and intermediate formation for the aqueous alkaline homogeneous hydrolysis of 1,3,5-triaza-1,3,5-trinitrocyclohexane (RDX). *J. Phys. Chem*. 81, 380-385.

Hofrichter, M., K. Scheibner, I. Schneegaß, and W. Fritsche. **1998.** Enzymatic combustion of aromatic and aliphatic compounds by manganese peroxidase from *Nematoloma frowardii*. *Appl. Environ. Microbiol*. 64: 399-404.

Holdeman L.V., E.P. Cato, W.E.C. Moore. **1977**. Anaerobic laboratory annual, 4th ed. Virginia Polytechnic Institute and State University, Blacksburg, Virginia .

Ichimori, K., M. Fukahori, H. Nakazawa, K. Okamoto, T. Nishino. **1999**. Inhibition of xanthine oxidase and xanthine dehydrogenase by nitric oxide. *J. Biol. Chem*. 274, 7763-7768.

Jenkins, T.F., M.E. Walsh, P.T. Thorne, P.H. Miyares, T.A. Ranney, C.L. Grant, J.R. Esparza. **1998**. CRREL Special Report 98-9. Cold Regions Research and Engineering Laboratory, US Army Corps of Engineers, Office of the Chief of Engineers

Johnson, J.L **1994**. Similarity analysis of rRNAs. In: Methods for General and Molecular Bacteriology (Gerhardt, P., Murry, R.G.E, Wood, W.A, Krieg, N.R, Eds), pp. 683-700. American Society for Microbiology, Washington D.C.

Jones, A.M., C.W. Greer, G. Ampleman, S. Thiboutot, J. Lavigne, and J. Hawari. **1995**. Biodegradability of selected highly energetic pollutants under aerobic conditions. *In* R. E. Hinchee, D. B. Anderson, and R. E. Hoeppel (ed.), Bioremediation of recalcitrant organics, Symp. Battelle Press, Columbus. 251-257.

Jones W.H. **1954.** Mechanisms of the homogeneous alkaline decomposition of cyclotrimethylenetrinitramine: kinetics of consecutive second-and first-order reactions. A polarographic analysis for cyclotrimethylenenitramine. *J. Am. Chem. Soc*. 76, 829-835.

Kamachi, M., S. Murahashi. **1974.** The polymerization of formaldazine. I. The nature of formaldazine. *Polymer J.* 6, 295-301.

Kaplan, F., P. Setlow, N.O. Kaplan. **1969**. Purification and properties of a DPNH-TPNH diaphorase from *Clostridium kluyveri*. *Arch. Biochem. Biophys*. 132, 91-98.

Karlson, U., D.F. Dwyer, S.W. Hooper, E.R.B. Moore, K.N. Timmis, and L.D. Eltis. **1993**. Two independently regulated cytochromes P-450 in a *Rhodococcus rhodochrous* strain that degrades 2-ethoxyphenol and 4-methoxybenzoate. *J. Bacteriol*. 175, 1467-1474.

Khan, H., R.J. Harris, T. Barna, D.H. Craig, N.C. Bruce, A.W. Munro, P.C.E. Moody, N.S. Scrutton. **2002**. Pentaerythritol tetranitrate reductase: kinetic and structural basis of reactivity with NADPH, 2-cyclohexenone, nitroesters and nitroaromatic explosives. *J. Biol. Chem*. 277, 21906-21912.

Kinouchi, T., and Y. Ohnishi. **1983.** Purification and characterization of 1-nitropyrene nitroreductases from *Bacteroides fragilis*. *Appl. Environ. Microbiol.* 46, 596-604.

Kirk, T. K., and R. L. Farrell. **1987**. Enzymatic "combustion" the microbial degradation of lignin. *Ann. Rev. Microbiol*. 41, 465-505.

Kitts, C.L., D.P. Cunningham and P.J. Unkefer. **1994**. Isolation of three hexahydro-1,3,5-trinitro-1,3,5-triazine degrading species of the family *Enterobacteriaceae* from nitramine explosive-contaminated soil. *Appl. Environ. Microbiol*. 60, 4608-4711.

Kitts, C.L., C.E. Green, R.A. Otley, M.A. Alvarez, and P.J. Unkefer. **2000.** Type I nitroreductase in soil enterobacteria reduce TNT (2,4,6-trinitrotoluene) and RDX (hexahydro-1,3,5-trinitro-1,3,5-triazine). *Can. J. Microbiol*. 46, 278-282.

Knox, R. J., F. Friedlos, M. P. Bolland. **1993**. The bioactivation of CB 1954 and its use as prodrug in antibody-directed enzyme prodrug therapy (ADEPT). *Cancer Metastasis Rev*. 12, 195-212.

Koder, R. L., A.-F. Miller. **1998.** Steady-state kinetic mechanism, stereospecificity, substrate and inhibitor specificity of *Enterobacter cloacae* nitroreductase. *Biochim. Biophys. Acta*, 1387, 395-405.

Komai, H., V. Massey, G. Palmer. **1969.** The preparation and properties of deflavo xanthine oxidase, *J. Biol. Chem*. 244, 1692-1700.

Kubose, D. A. and J. C. Hoffsommer. 1977. *Technical Report 77-20*, ADA 042199, Naval Surface Weapons Center, White Oak Laboratory, Silver Spring, MD.

Kumar, S., K. Tamura, I.B. Jakobsen, and M. Nei. **2001**. MEGA2: molecular evolutionary genetics analysis software. *Bioinformatics*. 17: 1244-1245.

Lamberton, A.H., C. Lindley, P.G. Owston, J.**C**. Speakman. **1949.** Studies of nitroamines. Part V. Some properties of hydroxymethyl- and aminomethyl-nitroamines. *J. Chem. Soc.* 355, 1641-1646.

Lamberton, A.H., C. Lindley, J.C. Speakman. **1949.** Studies on Nitroamines. Part VII. The decomposition of methylenedinitramine in aqueous solutions. *J. Chem. Soc.*, 357, 1650-1656.

Larson, S.L., and A.B. Strong. **1996.** Ion chromatography with electrochemical detection for hydrazine quantification in environmental samples. Technical Report IRRP-96-3. U.S. Army

Corps of Engineers, Waterways Experiment Station, Viksbourg, Miss.

Leggett, D.C. **1985**. CRREL Report 85-18. US Army Cold Regions Research and Engineering Laboratory, Hanover, NH.

Li, H., A. Samouilov, X. Liu, J.L. Zweier. **2001**. Characterization of the magnitude and kinetics of xanthine oxidase-catalyzed nitrate reduction: evaluation of its role in nitrite and nitric oxide generation in anoxic tissues. *J. Biol. Chem*. 276, 24482-24489.

Li, H., A. Samouilov, X. Liu, J.L. Zweier. **2003**. Characterization of the magnitude and kinetics of xanthine oxidase-catalyzed nitrate reduction: evaluation of its role in nitrite and nitric oxide generation in anoxic tissues. *Biochem.* 42, 1150-1159.

Lindsay, H., E. Beaumont, S.D. Richards, S.M. Kelly, S.J. Sanderson, N.C. Price, J.G. Lindsay. **2000**. FAD insertion is essential for attaining the assembly competence of the dihydrolipoamide dehydrogenase (E3) monomer from *Escherichia coli*. *J. Biol. Chem*. 275, 36665-36670.

Lynch, J.C., Myers, K.F., Brannon, J.M. and J.J. Delfino. **2001**. Effect of pH and temperature on the aqueous solubility and dissolution rate of 2,4,6-trinitrotoluene (TNT), hexahydro-1,3,5-trinitro-1,3,5-triazine (RDX), and octahydro-1,3,5,7-tetranitro-1,3,5,7-tetrazocine (HMX). *J. Chem. Eng. Data* 46**:** 1549-1555.

Madigan, R.A. and S.G. Mayhew. **1993**. Preparation of the apoenzyme of the FMN-dependent *Clostridium kluyveri* diaphorase by extraction with apoflavodoxin, *Biochemical Soc. Trans.* 22, 57S.

March, J. **1985**. *Advanced Organic Chemistry*. Third ed., Wiley-Interscience Publication, John Wiley & Sons, New York, US, p. 784-785.

Martos, P.A. and J. Pawliszyn. **1998.** Sampling and determination of formaldehyde using solid-phase microextraction with on-fiber derivatization. *Anal. Chem*. 70, 2311-2320.

Mashima, M. **1966.** The infra red absorption spectra of the condensation products with hydrazines. *Bull. Chem. Soc. Jpn.*, 39, 504-506.

Massey, V., and D. Edmondson. **1970**. On the mechanism of inactivation of xanthine oxidase by cyanide. *J. Biol. Chem*. 245, 6595-6598.

Matsubara, T., and T. Mori. **1968.** Studies on the denitrification. IX. Nitrous oxide, its production and reduction to nitrogen. *J. Biochem. (Tokyo)* 64**,** 863-871.

McCormick, N.G., J.H. Cornell and A.M. Kaplan. **1981**. Biodegradation of hexahydro-1,3,5-trinitro-1,3,5-triazine. *Appl. Environ. Microbiol*. 42, 817-823.

McDonnell, C.H. **1978**. In *Encyclopedia of explosives and related items.* Fedoroff, B.T., Kaye, S.M., and O.E. Sheffield, Eds., Picatinny Arsenal, Dover, NJ. Vol 8, M 49-54.

Melius, C.F. **1990.** In Chemistry and Physics of Energetic Materials: Thermochemical Modeling: I Applications to Decomposition of Energetic Materials; Bulusu, S. N., Ed; Kluwer Academic Publishers: Dordrecht, Netherlands, pp 21-49.

Microbics Corp. **1992**. *Microtox manual: Microtox basic test procedures*. Carlsbad, CA.

Miksovsky, D., J. Korinek, and A. Vojtech. **1993.** An Optimized Process for Making MEDINA. *Propellants, explosives, pyrotechnics*. 18, 51.

Myers, T.E.; Brannon, J.M.; Pennington, W.M.; Myers, K.F.; Townsend, D.M.; Ochman, M.K.; Hayes, C.A. Technical Report IRRP-96-1. US Army Corps of Engineers, Waterways Experiment Station, Vicksburg, MS, 1996.

Nivinskas, H. R.L. Koder, Z. Anusevicius, J. Sarlauskas, A-F. Miller, N. Cenas. **2001**. Quantitative structure-activity relationships in two-electron reduction of nitroaromatic compounds by *Enterobacter cloacae* NAD(P)H:nitroreductase. *Arch. Biochem. Biophys* 385, 170-178.

OECD Guideline for Testing of Chemicals 107: Partition Coefficient (n-octanol/water) (Flask-shaking method). Adopted on 12 May **1981.**

Oh, B.-T., C.L. Just, and P.J.J. Alvarez. **2001**. Hexahydro-1,3,5-trinitro-1,3,5-triazine mineralization by zero valent iron and mixed anaerobic cultures. *Environ. Sci. Technol.* 35, 4341-4346.

Okada, M., M. Mochizuki, T. Anjo, T. Stone, Y. Wakabayashi, and E. Suzuki. **1980**. Formation, deoxygenation, and mutagenicity of α-hydroperoxydialkylnitrosamine. pp 71-79, *In* N-Nitroso Compounds: Analysis, Formation and Occurrence, Walker, E. A. et al. Eds.; Int. Agency for Research on Cancer, Lyon (IARC Scientific Publication, No 31)

Okemgbo, A.A., H.H. Hill, S.G. Metcalf, and M.A. Bachelor. **1999**. Determination of nitrate and nitrite in Hanford defense waste by reverse-polarity capillary zone electrophoresis. *J. Chromatogr. A* 844, 387-394.

Ogram, A.V., R.E. Jessup, L.T. Ou, and P.S. Rao. **1985**. Effect of sorption on biological degradation rates of (2,4-dichlorophenoxy)acetic acid in soils. *Appl. Environ. Microbiol.*, 49, 582-587.

Ortiz de Montellano, P.R., and M.A. Correia. **1995**. Inhibition of cytochrome P450 enzymes, In : Cytochrome P450 : Structure, mechanism and biochemistry, 2nd Ed. P. R. Ortiz de Montellano Ed., Plenum Press, NY and London, pp. 305-366.

Owens, J.D., and R.M. Keddie. **1969**. The nitrogen nutrition of soil and herbage coryneform bacteria. *J. Appl. Bacteriol.* 32, 338-347.

Pennington, J., J.M., Brannon, D. Gunnison, D.W. Herrelson, M. Zakikhani, P. Miyares, T.F. Jenkins, J. Clarke, C. Hayes, D. Ribgleberg, E. Perkins, H. Fredrickson. **2001.** *Soil Sediment Contam*. 10, 45.

Pennington, J.C., and J.M. Brannon. **2002**. Environmental fate of explosives. *Thermochimica Acta.* 384, 163-172.

Peterson, F.J., R.P. Mason, J. Hovesepian, and J.L. Holtzman, **1979**. Oxygen-sensitive and –insensitive nitroreduction by *Escherichia coli* and rat hepatic microcosms. *J. Biol. Chem.* 254, 4009-4014.

Peyton, G.R., M.H. LeFaivre, S.W. Maloney. **1999.** Verification of RDX photolysis mechanism. CERL Technical Report 99/93, 40161102B25, Environmental Research, Engineer Research and Development Center, Champaign, IL.

Pudge, I.B., A.J. Daugulis, and C. Dubois. **2003.** The use of *Enterobacter cloacae* ATCC 43560 in the development of a two-phase partitioning bioreactor for the destruction of hexahydro-1,3,5-trinitro-1,3,5-triazine (RDX). *J. Biotechnol.* 100, 65-75.

Regan, K.M., and R.L. Crawford. **1994.** Characterization of *Clostridium bifermentans* and its biotransformation of 2,4,6-trinitrotoluene (TNT) and 1,3,5-triaza-1,3,5- trinitrocyclohexane (RDX). *Biotechnol. Lett.* 16, 1081-1086.

Riley, R.J., P.Workman. **1992**. DT-diaphorase and cancer chemotherapy. *Biochem. Pharmacol.* 43, 1657-1669.

Ritter, C.L. and D. Malejka-Giganti. **1998**. Nitroreduction of nitrated and C-9 oxidized fluorenes *in vitro*. *Chem. Res. Toxicol.* 11, 1361-1367.

Robidoux, P.Y., J. Hawari, S. Thiboutot, G. Ampleman, and G.I. Sunahara. **2001.** Chronic toxicity of octahydro-1,3,5,7-tetranitro-1,3,5,7-tetrazocine (HMX) in soil determined using the earthworm (*Eisenia andrei*) reproduction test. *Environ. Pollut*. 111, 283-292.

Robidoux, P.Y, C. Svendsen, J. Caumartin, J. Hawari, G. Ampleman, S. Thiboutot, J.M. Weeks, and G.I. Sunahara. **2000**. Chronic toxicity of energetic compounds in soil determined using the earthworm (*Eisenia Andrei*) reproduction test. *Environ. Toxicol. Chem*. 19, 1764-1773.

Rocheleau, S., R. Cimpoia, L. Paquet, I. van Koppen, S. Guiot, J. Hawari, G. Ampleman, S. Thiboutot and G.I. Sunahara. **1999.** Ecotoxicological Evaluation of a Bench–Scale Bioslurry Treating Explosives – Spiked Soil. *Bioremediation J*. 3(3), 233-245.

Roller, P., D.R. Shimp, and L.K. Keefer. **1975**. Synthesis and solvolysis of methyl(acetoxymethyl)nitrosamine. Solution chemistry of the presumed carcinogenic metabolite of dimethylnitrosamine. *Tetrahedron Lett.* 25, 2065-2068.

Rowland, R**. 1988**. The toxicology of *N*-nitroso compounds. p. 117-141. *In* Nitrosamines: toxicology and microbiology. M.J. Hill (ed.) Ellis Horwood Ltd., Chichester, England and VCH, Weinheim, Germany and New York.

Sambrook, J. and D.W. Russell. **2001**. Molecular cloning: a laboratory manual, 3rd ed. Cold Spring Harbor Laboratory Press, New York.

Sauer, C.W., and R.P. Follett. **1955.** Nitramines. I. Methylenedinitramine. *J. Am. Chem. Soc*. 77, 2560-2561.

Schlegel, H.G. and K. Schneider. **1978.** Hydrogenase: their catalytic activity, structure and function. Erich Goltze KG, Göttingen.

Seth-Smith, H.M.B., S.J. Rosser, A. Basran, E.R. Travis, E.R. Dabbs, S. Nicklin, and N.C. Bruce. **2002.** Cloning, sequencing, and characterization of the hexahydro-1,3,5-trinitro-1,3,5-triazine degradation gene cluster from *Rhodococcus rhodochrous. Appl. Environ. Microbiol.* 68, 4764-4771.

Shah, M.M. and J.C. Spain. **1996.** Elimination of nitrite from the explosive 2,4,6-trinitrophenylmethylnitramine (tetryl) catalyzed by ferredoxin NADP oxidoreductase from spinach. *Biochem. Biophys. Res. Commun.* 220, 563-568.

Shen, C.F., J. Hawari, G. Ampleman, S. Thiboutot, S.R. Guiot. **2000.** Enhanced biodegradation and fate of hexahydro-1,3,5-trinitro-1,3,5-triazine (RDX) and octahydro-1,3,5,7-tetranitro-1,3,5,7-tetrazocine (HMX) in anaerobic soil slurry bioprocess. *Bioremediation J*. 4, 27-39.

Sheremata, T.W., and J. Hawari. **2000**. Mineralization of RDX by the white rot fungus *Phanerochaete chryso*sp*orium* to carbon dioxide and nitrous oxide. *Environ. Sci. Technol*. 34, 3384-3388.

Sheremata, T.W., A. Halasz, L. Paquet, S. Thiboutot, G. Ampleman, and J. Hawari. **2001**. The fate of the cyclic nitramine explosive RDX in natural soil. *Environ. Sci. Technol*. 35, 1037-1040.

Sheremata, T.W., S. Thiboutot, G. Ampleman, L. Paquet, A. Halasz and J. Hawari. **1999**. Fate of 2,4,6-Trinitrotoluene and its metabolites in natural and model soil systems. *Environ. Sci. Technol*. 33, 4002-4008.

Singh, J., S.D. Comfort, L.S. Hundal, P.J. Shea. Long-term RDX sorption and fate in soil. *J. Environ. Qual*. **1998**, 27, 572.

Smibert, R.M. and N.R. Krieg. **1981.** General Characterization. In: Manual of methods for general bacteriology (Gerhardt, P., Eds), p436. Ammerican Society For Microbiology, Washington, D. C.

Sneath P.A. **1986**. Endospore-forming gram-positive rods and cocci. In Sneath P.A., Mair N.S., Sharpe M.E., Holt J.G. (eds) Bergey's manual of systematic bacteriology, Vol 2. Williams & Wilkins, Baltimore, pp1104-1200.

Sorensen, J., J. M. Tiedje, R.B. Firestone. **1980.** Inhibition by sulfide of nitrite and nitrous oxide reduction by *Pseudomonas fluorencens*. *Appl. Environ. Microbiol.* 39, 105-108.

Spanggord, R. J., W. R. Mabey, T.-W. Chou, S. Lee, P. L. Alferness, and T. Mill. **1983**. *Environmental fate studies of HMX; Phase II- Detailed studies, Final Report.* U.S. Army Medical Research and Development Command Contract DAMD17-82-C-2100, SRI International, Menlo Park, CA. AD-A145122.

Spanggord, R.J., W.R. Mabey, T.W. Chou. **1985.** In: *Chemical industry institute of toxicology series. Toxicity of nitroaromatic compounds.*, Rickert, D.E. Ed. Hemisphere publishing corp., Washington, DC, 15.

Stahl, J.D., B. Van Aken, M.D. Cameron, and S.D. Aust. **2001**. Hexahydro-1,3,5-trinitro-1,3,5-triazine (RDX) biodegradation in liquid and solid-state matrices by *Phanerochaete chrysosporium*. *Bioremediation Journal.* 5, 13-25.

St. John, R.T., and T.C. Hollocher. **1977**. Nitrogen-15 tracer studies on the pathway of denitrification in *Pseudomonas aeruginosa*. *J. Biol. Chem*. *252*, 212-218.

Summers W.R. **1990.** Characterization of formaldehyde and formaldehyde releasing preservatives by combined reversed phase cation-exchange high performance liquid chromatography with postcolumn derivatization using Nash's reagent. *Anal. Chem*. 62, 1397-1402.

Sunahara, G.I., S. Dodard, M. Sarrazin, L. Paquet, G. Ampleman, S. Thiboutot, J. Hawari, and A.Y. Renoux. **1998**. Development of a soil extraction procedure for ecotoxicity characterization of energetic compounds. *Ecotoxicol. Environ. Safety*. 39, 185-194.

Sunahara, G.I., Dodard, S., Sarrazin, M., Paquet, L., Ampleman, G., Thiboutot, S., Hawari. J., A.-Y. Renoux. **1999**. Ecotoxicological characterization of energetic substances using a soil extraction procedure. *Ecotoxicol. Environ. Safety* 43, 138-148.

Talmage, S.S., D.M. Opresko, C.J. Maxwel, C.J.E. Welsh, F.M. Cretella, P.H. Reno, and F.B. Daniel. **1999**. Nitroaromatic munition compounds: environmental effects and screening values. *Rev. Environ. Contam. Toxicol*. 161, 1-156.

Tam, T.-Y., and R. Knowles. **1979**. Effect of sulfide and acetylene on nitrous oxide reduction by soil and by *Pseudomonas aerukginosa*. *Can. J. Microbiol.* 25, 1133-1138.

Tedeschi, G., S. Chen, and V. Massey. **1995**. Active site studies of DT-diaphorase employing artificial flavins. *J. Biol. Chem.* 270, 2512-2516.

Townsend, D.M., T.E. Myers, D.D. Adrian. **1996.** Technical Report IRRP-96-8, U.S. Army Engineer Waterways Experiment Station, Vicksburg, MS.

Turro, N. J. Modern Molecular Photochemistry, Benjamin Cumming Publishing Co., 1978, ch10, pp 362.

Urbanski, T. **1967**. *Chemistry and Technology of Explosives*, Jurecki, M. (trans), Laverton, S. Ed.; Pergamon Press, Oxford, Vol. III, Ch II, pp 17-47.

Weiss, R. F., and B. A. Price. **1980**. *Marine Chemistry* 8, 347-359.

Weimer, P.J. **1984**. Control of product formation during glucose fermentation by *Bacillus macerans*. *J. Gen. Microbiol*. 130, 103-111.

Wenzhong, L., Y. Ping, Y. Uanxi. **1987**. Properties of TNT-degrading enzymes in intact cells of *Citrobacter freundii*. *ACTA Microbiol. Sin.* 27, 257-263.

Widdel, F. and T.A. Hanson. **1991.** The dissimilatory sulfate and sulfur-reducing bacteria. In: The Prokaryotes (2^{nd}) (Balows, A., Trüper, H.G., Dworkin, M., Harder, W., and Schleifer, K.-H., Eds), 1, p583-624. Springer-Verlag, New York.

Wolin, E.A., M.J. Wolin, and R.S. Wolfe. **1963**. Formation of methane by bacterial extracts. *J. Biol. Chem*. 238, 2882-2886.

Wu, L.-F. and M.A. Mandrand. **1993**. Microbial hydrogenase: primary structure, classification, significance and phylogeny. *FEMS Microbiol. Rev.* 104, 243-270.

Xia, L., M. Bjornstedt, T. Nordman, L.C. Eriksson, and J.M. Olsson. **2001**. Reduction of ubiquinone by lipoamide dehydrogenase: An antioxidant regenerating pathway. *Eur. J. Biochem.* 268, 1486-1490.

Xue, S.K., I.K. Iskandar, and H.M. Selim. **1995.** Adsorption-desorption of 2,4,6-trinitrotoluene and hexahydro-1,3,5-trinitro-1,3,5-triazine in soil. *Soil. Sci.*, 160, 317-327.

Young, D.M., P.J. Unkefer, and K.L. Ogden. **1997a**. Biotransformation of Hexahydro-1,3,5-trinitro-1,3,5-triazine (RDX) by a prospective consortium and its most effective isolate *Serratia marcescens*. *Biotechnol. Bioeng*. 53, 515-522.

Young, D.M., C.L. Kitts, P.J. Unkefer, and K.L. Ogden. **1997b**. Biological breakdown of

RDX in slurry reactors proceeds with multiple kinetically distinguishable paths. *Biotechnol. Bioeng.* 56, 258-267.

Zehnder, A.J.B. **1988**. Biology of anaerobic microorganisms. John Wiley & Sons, New York.

Zhang, C. and J.B. Hughes. **2003**. Biodegradation pathways of hexahydra-1,3,5-trinitro-1,3,5-triazine (RDX) by *Clostridium acetobutylicum* cell-free extract. *Chemosphere*. 50, 665-671.

Zhao, X., E.J. Hintsa, and Y.T. Lee, **1988**. Infrared multiphoton dissociation of RDX in a molecular beam. *J. Chem. Phys.* 88, 801-810.

Zhao, J.-S., A. Singh, X.D. Huang, and O.P. Ward. **2000**. Biotransformation of hydroxylaminobenzene and aminophenol by *Pseudomonas putida* 2NP8 cells grown in the presence of 3-nitrophenol. *Appl. Environ. Microbiol*. 66, 2336-2342.

Zhao, J.-S., A. Halasz, L. Paquet, C. Beaulieu, and J. Hawari. **2002**. Biodegradation of hexahydro-1,3,5-trinitro-1,3,5-triazine and its mononitroso derivative hexahydro-1-nitroso-3,5-dinitro-1,3,5-triazine by *Klebsiella pneumoniae* strain SCZ-1 isolated from an anaerobic sludge. *Appl. Environ. Microbiol.* 68, 5336-5341.

Zhao, J.-S., L. Paquet, A. Halasz, and J. Hawari. **2003a**. Metabolism of hexahydro-1,3,5-trinitro-1,3,5-triazine through initial reduction to hexahydro-1-nitroso-3,5-dinitro-1,3,5-triazine followed by denitration in *Clostridium bifermentans* HAW-1. *Appl. Microbiol. Biotechnol*. 63, 187-193.

Zhao, J.-S., J. Spain, and J. Hawari. **2003b**. Phylogenetic and metabolic diversity of hexahydro-1,3,5-trinitro-1,3,5-triazine (RDX)-transforming bacteria in strictly anaerobic mixed cultures enriched on RDX as nitrogen source. *FEMS Microbiol. Ecol*. 46, 189-196.

Zoh, K.; and M.K. Stenstrom. **2002.** Fenton oxidation of hexahydro-1,3,5-trinitro-1,3,5-triazine (RDX) and octahydro-1,3,5,7-tetranitro-1,3,5,7-tetrazocine (HMX). *Wat. Res.* 36, 1331-1341.

Zumft, W.G. **1997**. Cell biology and molecular basis of denitrification. *Microbiol. Mol. Biol. Rev*. 61, 533-616.

X APPENDIX 2: PUBLICATION FROM THE PROJECT

In addition to the comprehensive list provided in pages 200-202 in this report we have downloaded the pdf.files **of published papers separately**.